Tumour-selective apoptosis : identification of NMHCIIa as novel death receptor interactor regulating the response to TRAIL

Cathrin Müller Schulz

UNIVERSITÉ DE STRASBOURG

ÉCOLE DOCTORALE des Sciences de la Vie et de la Santé

THÈSE présentée par :

Cathrin SCHULZ

soutenue le : **26 Septembre 2012**

pour obtenir le grade de : **Docteur de l'Université de Strasbourg**

Discipline/ Spécialité : Aspects Moléculaires et Cellulaires de la Biologie

Tumour-Selective Apoptosis

Identification of NMHCIIa as Novel Death Receptor Interactor Regulating the Response to TRAIL

THÈSE dirigée par :

M. GRONEMEYER Hinrich	Dr., Université de Strasbourg
M. MICHEAU Olivier	Dr., Université de Dijon

RAPPORTEURS :

M. VANDENABEELE Peter	Prof., Université de Gent
M. VICENTE-MANZANARES Miguel	Dr., Université Autonome de Madrid

---

AUTRES MEMBRES DU JURY :

M. LABOUESSE Michel	Dr., Université de Strasbourg

Meiner Familie in Dankbarkeit

“Does a real interaction mean that two proteins interact if they are placed next to each other in a test tube, or that they must interact in a cell? Or does real mean that the interaction should have a biological function?” - Trey Ideker

[Bonetta, L. (2010) Nature 468, 851-854]

TABLE OF CONTENTS

TABLE OF FIGURES

SUPPLEMENTARY

WORK IN PROGRESS

DISCUSSION & PERSPECTIVES

LIST OF ABBREVIATIONS

A

AB	antibody
ADP	adenosine diphosphate
AKT	RAC-alpha serine/threonine-protein kinase
APAF1	apoptotic protease-activating factor 1
APC	adenomatous polyposis coli
APL	acute promyelocytic leukemia
APS	ammonium persulfate
ASK1	apoptosis signal-regulating kinase 1
ATP	adenosine triphosphate

B

(B)	IP-antibody coupled beads
βACT	beta actin
BID	BH3-interacting domain death agonist
BJ	normal foreskin fibroblasts
BJAB	Burkitt's lymphoma cells
BJELR	HTERT, SV40ER and HRASG12V-transformed foreskin fibroblasts
BSA	bovine serum albumin

C

$CaCl_2$	calcium chloride
CALD	caldesmon
CALM	calmodulin
CAPS	cyclohexylamino propanesulfonic acid
CASP	caspase
cFLIP	cellular FLICE-like inhibitory protein
cFLIP(R)	short cFLIP isoform cloned from the Raji B-cell line
CHOP	CCAAT/enhancer-binding protein–homologous protein
CK	citron kinase
CK2	casein kinase 2
CPI17	inhibitory subunit of PP1
CRD	cystein-rich domain
CUL3	cullin-based E3 ligase

D

DcR1	decoy receptor 1
DcR2	decoy receptor 2
DAPK3	death-associated protein kinase 3
DD	death domain
ddH_2O	double-distilled water
DED	death-effector domain
DIABLO	direct IAP binding protein with low pI
DIC	differential interference contrast
DISC	death inducing signalling complex
DMEM	Dulbecco's Modified Eagle medium
DMSO	dimethyl sulfoxide
DN	dominant-negative
DR4	death receptor 4
DR5	death receptor 5
DTT	dithiothreitol

E

ECL	enhanced chemiluminescence
EDTA	ethylenediaminetetraacetic acid
EGFR	epidermal growth factor receptors
ELC	essential light chain
ERK	extracellular-signal regulated kinase
ERM	ezrin, radixin, moesin

F

F-actin	actin filaments
FACS	fluorescence-activated cell sorting
FADD	FAS-associated death domain
FAS	FAS receptor
FASL	FAS ligand
FDA	US Food and Drug Administration

G

GPI	glycosylphosphatidylinositol
GRB2	growth factor receptor-bound protein 2

H

HA1ER	HTERT, SV40ER and HRASG12-transformed human embryonic kidney cells
HAMLET	human alpha-lactalbumin made lethal to tumour cells
HCl	hydrochloride
HEK	human embryonic kidney
HER2	tyrosine kinase-type cell surface receptor
HIS	histidine

H

HGFR hepatocyte growth factor receptor
HMEC human mammary epithelial cells
HRASG12V constitutively active mutant of GTPase HRAS
HTERT human telomerase catalytic subunit
HTRA2 high temperature requirement protein A2

I

IAP inhibitor of apoptosis
IEF isoelectric focusing
IgG immuneglobulin G
IKB inhibitor of kappa B
IKK I kappa B kinase
ILK integrin-linked protein kinase
IP immunoprecipitation
IPTG isopropyl β-D-1 thiogalactopyranoside

J

JNK stress-activated protein kinase

K

KCl potassium chloride
KD knockdown
K_{off} dissociation constant
K_{on} association constant

L

(L) long isoform
IL24 interleukin 24
LPS lipopolysaccharide
LT large T

M

MADD MAP kinase-activating death domain protein
MAPK mitogen-activated protein kinases
MCA methylcholanthrene
MDA7 melanoma differentiation-associated gene 7
MDCK Madin-Darby canine kidney
MDM2 E3 ubiquitin-protein ligase Mdm2
MEKK MAPK/ERK kinase kinases
MFI mean (or median) fluorescence intensities
$MgCl_2$ magnesium chloride
$MgSO_4$ magnesium sulfite
MLCK myosin light chain kinase
MLCP myosin phosphatase
MLC2 regulatory myosin light chain 2

M

MOMP mitochondrial outer membrane permeabilisation
MRCK myotonic dystrophy kinase-related CDC42-binding kinase
MS mass spectrometry
MST2 mammalian STE20-like protein kinase 2
MW molecular weight
MYC proto-oncogene cMYC
MYPT1 regulatory subunit of MLCP

N

NaH_2PO_4*H2O monobasic sodium phosphate monohydrate
NaCl sodium chloride
NFKB nuclear factor kappa B
NH_4HCO_3 ammonium bicarbonate
Ni nickel
NK natural killer
nm non-muscle
nml non-muscle like
NMII non-muscle myosin II
NMHCII non-muscle myosin heavy chain II
NSCLC non-squamous non–small-cell lung cancer
NTA nitriloacetic acid

O

OD optical density
OMI omi stress-regulated endoprotease
ON over night
OPG osteoprotegerin

P

PAGE polyacrylamide gel electrophoresis
PAK p21-activated kinase
PARA pro-apoptotic receptor agonists
PARP poly ADP-ribose polymerase
PBS phosphate buffered saline
PE phycoerythrin
PEG polyethylene glycol
PFA paraformaldehyde
Pi inorganic phosphate
PI3K phosphoinositol-3-kinase
PLAD pre-ligand assembly domain
PML promyelocytic leukemia
PP1 protein phosphatase 1
PP2A protein phosphatase 2A
pRB retinoblastoma protein
p53 tumour suppressor protein 53

R

RA	retinoic acid
RANK	receptor activator of NFKB
RARα	retinoic acid receptor alpha
RBX1	ring-box 1
rh	recombinant human
RHO-GDI	RHO-GDP dissociation inhibitors
RIPK	receptor interacting serine/threonine protein kinase
ROCK	RHO-associated kinase
RPMI	Roswell Park Memorial Institute medium
RT	room temperature
RU	resonance units

S

(S)	short isoform
SCID	severe combined immunodeficiency
SCR	scramble
SDS	sodium dodecyl sulfate
Ser	serine
SPR	surface plasmon resonance
SRC	proto-oncogene tyrosine protein kinase
ST	small T
sTRAIL	soluble TRAIL
sm	smooth-muscle
SMAC	second mitochondria–derived activator of caspase
SOS1	son of sevenless homolog 1
SV40	Simian virus 40

S

SV40ER	Simian virus 40 early region
S100A4	S100 calcium-binding protein A4
S6K	S6 kinase

T

tBID	truncated BID
TBS	Tris-buffered saline
TBST	TBS supplemented with Tween 20
TCR	T cell receptor
Thr	threonine
TM	tropomyosin
TNFα	tumour-necrosis factor alpha
TNFR1	tumour-necrosis factor receptor 1
TRADD	TNFR1-associated death domain protein
TRAF2	TNF receptor-associated factor 2
TRAIL	tumour-necrosis factor alpha-related apoptosis inducing ligand
TRAIL-R	murine TRAIL receptor

V

VEGF	vascular endothelial growth factor

W

WCL	whole cell lysate

Z

Zn^{2+}	zinc
$ZnSO_4$	zinc sulfate

PREAMBLE

Several main strategies to therapeutically approach cancer exist (Figure 1) and their variety, operation mode and effectiveness have been extensively reviewed, some with special regard to a certain type of cancer. Aiming to give a general overview about the difficulties of existing cancer therapies, the major problems shall be briefly summarised. Surgery as the first applied cancer therapy is suitable only for non-hematological tumours and if cancer has metastasised, the complete surgical excision is impossible. Radiation therapy and chemotherapy lack tumour cell-specificity. Whilst radiation therapy damages the genetic material of both normal and transformed cells, chemotherapy interferes with cell division of all rapidly dividing cells and thus affects amongst others cells of the intestinal lining. Since normal cells, unlike their transformed counterparts, usually are able to repair their DNA, normal cells recover after treatment. However, this recovery phase for the patient is associated with inconceivable suffering from side effects or, if repair mechanisms in normal cells fail, secondary cancer can derive from the therapy itself. In targeted therapies, mutated, overexpressed or otherwise critical proteins in cancer cells are in the focus. If the cause for cancer is based on a single mutational event, like it is the case for acute promyelocytic leukemia (APL) where a part of the *promyelocytic leukemia* (*PML*) gene has fused with the *retinoic acid receptor alpha* (*RARa*) gene and the maintenance of the leukemic phenotype depends on the presence of the PML-RARa fusion protein, addition of a single agent that induces the degradation of the PML-RARa protein (*here:* all-trans retinoic acid) can suffice to achieve

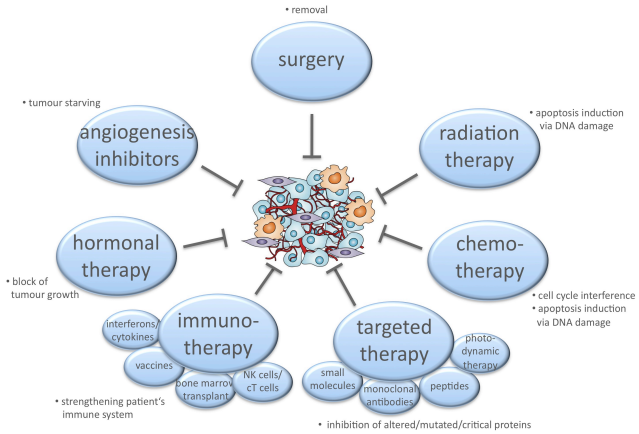

Figure 1: Main strategies of cancer treatment and their method of action. Various strategies in the fight of cancer are being followed, but to date no single strategy has proven efficient and tumour cell-specific. The tumour mass in the middle was taken from [Bode and Dong 2009].

complete remission in human patients [as reviewed by de Thé and Chen et al 2010]. Unfortunately, the vast majority of human cancers display multiple genetic changes, which even increase in number with tumour progression. Not always these changes are associated with alterations in the DNA sequence, but can be linked to inherited modifications in DNA methylation states of CpG dinucleotides that are referred to as 'epigenetic' alterations. Cancer cells show global genomic hypomethylation leading to chromosomal instability and gene-specific promoter hypermethylation resulting in the silencing of for instance tumour suppressor genes. Administration of epigenetic drugs such as inhibitors of DNA methlation can revert aberrant DNA methylation and histone modification, thus providing another approach in targeted cancer therapy [reviewed in Rodriguez-Paredes and Esteller 2011]. In turn, other therapeutic tactics use monoclonal antibodies or peptides that bind to a cancer cell-specific surface protein, delivering coupled cytotoxic agents into the vicinity of the tumour cell. Major drawbacks using these approaches include the stability of the targeting protein as well as the circumstance that cancer cells constantly change the repertoir of expressed cell surface proteins and can downregulate or loose the targeted antigen. In immunotherapy, one of the major drawback is time, which is one one hand required to generate the vaccine or antibody and on the other hand is needed by the immune cells to react upon the boost, so that immunotherapy usually demands longer periods to observe effects on the tumour. Therefore, immunotherapy for most cancers is used as an adjuvant cancer treatment [reviewed by Sharma et al 2011, Gerritsen and Sharma 2012]. Depending on the modality used (vaccine, antibody), strong or immediate passive immune responses can be observed, including flu-like symptoms. Usually only a limited number of tumour-associated antigens are present to be targeted and there is currently no experience with long-term effects of immunotherapy. Hormone therapy does not lead to cure, but keeps tumour growth under control until cancer cells become hormone resistant or refractory, which then will require a different set of therapy. The use of angiogenesis inhibitors to prevent blood vessel growth required for tumour nutrition is complicated by the fact that normal and transformed tissues require several, but the same angiogenic factors. Usually, only one factor is targeted in therapy which is not sufficient for a full tumour remission or even could lead to the activation of compensatory pathways augmenting tumour invasion and metastasis [Benest and Augustin 2009, Ellis and Reardon 2009].

Moreover, the administration route of agents and the maintenance of stability and activity of agent are difficult.

The variety of possible targeted cancer therapies becomes evident, if pathological characteristics are considered that are common to all human malignancies [reviewed by Hanahan and Weinberg 2000, Hanahan and Weinberg 2011]. These include self-sufficiency in growth signalling, insensitivity to growth inhibitory signals, evasion from apoptosis, limitedless replicative potential, sustained angiogenesis and tissue invasion and metastasis (Figure 2). Recently, the addition of a seventh feature called 'inflammatory microenvironment' was postulated, since tumour cells are capable to increase cytokine production of surrounding matrix cells enabling metastasis [Mantovani et al 2009, Cavallo et al 2011]. Many novel therapies constantly arise immediately attacking these so-called 'hallmarks of cancer', some of which are approved by the US Food and Drug Administration (FDA) or are currently tested in clinical trials (Table 1) [http://fda.gov, http://clinicaltrials.gov]. One example targeting for instance cancer cells self-sufficiency in growth signals is the development of monoclonal antibodies promoting internalisation and degradation of epidermal growth factor receptors (EGFR), which are transmembrane tyrosine kinase receptors regulating cell proliferation and survival. In cancer cells EGFR are commonly overexpressed and either signal autonomously via ligand secretion through the cancer cell itself, or they even signal in absence of the ligand. Inactivating EGFR signalling thus inhibits proliferative signals required by the cancer cell and induces its apoptosis [reviewed by Shawver et al 2002, Hynes and Lane 2005].

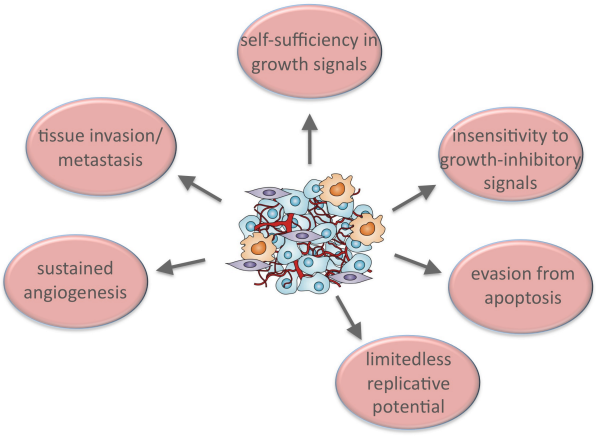

Figure 2: Hallmarks of cancer as defined by Hanahan and Weinberg 2000. Targeted strategies for cancer therapy are under development that specifically aim at one or several of these features. The tumour mass in the middle was taken from [Bode and Dong 2009].

Table 1: Examples for targeted cancer therapies directed against cancer hallmarks. Indicated are small molecule inhibitors and monoclonal antibodies, which are FDA-approved or currently tested in clinical trials [http://fda.gov, http://clinicaltrials.gov]. The primary mode of anti-estrogen ICI 182780 action is the rapid MYC expression [Carroll et al 2002, reviewed by Hermeking 2003].

cancer hallmark	cellular target	agent	name	product/company
self-sufficiency in growth signalling	epidermal growth factor receptor (EGFR)	inhibitor	gefitinib	Iressa/AstraZeneca
	tyrosine kinase-type cell surface receptor (HER2)	monoclonal antibody	trastuzumab	Herceptin/Genentech
insensitivity to growth inhibitory signals	proto-oncogene MYC (via estrogen receptor)	inhibitor	ICI 182780	Fulvestrand/ AstraZeneca
evasion from apoptosis	tumour suppressor p53/ E3 ubiquitin-protein ligase MDM2 interaction	inhibitor	JNJ-26854165, RG7112	JNJ-26854165/Janssen Research & Development, RG7112/Hoffmann-La Roche
limitedless replicative potential	telomerase	inhibitor	imetelstat	GRN163/Geron
sustained angiogenesis	vascular endothelial growth factor (VEGF)	monoclonal antibody	bevacizumab	Avastin/Genentech/ Roche
		inhibitor	/	Axitinib/Pfizer, Inc
tissue invasion and metastasis	hepatocyte growth factor receptor (HGFR) cMET	inhibitor	tivantinib	ARQ197/ArQule

Whichever route might be taken, only tumour-specific therapies leading to cancer cell death-driven removal of all transformed cells from a patients body ultimately will lead to cure from cancer. Of note, agents of different origin are described selectively inducing tumour cell death. These comprise viruses that specifically replicate in cancer cells leading to their lysis, virus-derived proteins (E4ORF4, NS1, apoptin [reviewed by Noteborn 2009]) that induce cytotoxicity in transformed but not normal cells if overexpressed, as well as human endogenous proteins with tumouricidal activity such as human alpha-lactalbumin made lethal to tumour cells (HAMLET), melanoma differentiation-associated gene 7 (MDA7)-encoded interleukin 24 (IL24) and tumour-necrosis factor alpha-related apoptosis inducing ligand (TRAIL). Whilst potential cancer therapies based on virus-derived tumouricidal proteins require an appropriate non-toxic vehicle allowing the inward transfer of the gene [Peng et al 2007] or protein [Sun et al 2009] into target cells, HAMLET, IL24 and TRAIL mediate their cancer-cell specific and cytotoxic action from outside the cell, binding to their own receptors. However, in contrast to TRAIL, to date only little is known about the cell death mechanisms executed by HAMLET and IL24 and receptors have so far only been identified for latter. Secondly,

whilst TRAIL can execute its tumouricidal function systemically with good tolerability, *in vivo* studies demonstrating HAMLET's therapeutic potential applied this agent only locally [Gustafsson et al 2004, Mossberg et al 2007]. Thus, future HAMLET-based cancer therapies might be restricted to a limited spectrum of cancer types. Finally, tumour-selective apoptosis observed for IL24 appears to result from IL24-mediated activation of the FAS ligand (FASL) and TRAIL pathways [Ekmekcioglu et al 2008]. Whilst FASL or antibodies targeting its receptor displayed severe liver toxicity in mice eventually leading to the death of animals within a few hours [Ogasawara et al 1993, Ni et al 1994], TRAIL was proven safe in diverse animal models [Kelley et al 2001]. Because of its practicability, systemic action and safety, our team focused its work on understanding the signaling of TRAIL and not of other endogenous proteins inducing tumour-selective apoptosis.

Indeed, the therapeutic promise of TRAIL is reflected in the large number of ongoing clinical trials [Yerbes et al 2011, http://clinicaltrials.gov] applying either the recombinant human protein (rhTRAIL), humanised antibodies targeting the TRAIL death receptors (DR5: lexatumumab=HGS-ETR2, AMG655, PRO95780; DR4: mapatumumab=HGS-ETR1), or adenoviral delivery of TRAIL coding sequences in monotherapy or in combination with chemotherapeutic drugs. Initial phase I clinical trials using rhTRAIL, HGS-ETR1, HGS-ETR2 or PRO95780 in monotherapy confirmed good tolerance for all agents and no dose-limiting toxicity in patients, partial response in 3% and stable disease in 53% of patients with advanced cancer for rhTRAIL [Ashkenazi 2008, Herbst et al 2010, Tolcher et al 2007, Plummer et al 2007, Camidge et al 2010]. Thereby, the most common adverse effects were nausea, fatigue, constipation and leucopenia in 10-20% of patients. Phase Ib clinical studies of rhTRAIL in combination with paclitaxel, carboplatin and bevacizumab revealed tumour progression-free survival of patients with advanced non-squamous non–small-cell lung cancer (NSCLC) [Soria et al 2010]. However, phase II clinical trials using rhTRAIL in combination with bevacizumab in patients with advanced NSCLC [Soria et al 2011], HGS-ETR1 in patients with refractory colorectal cancer [Trarbach et al 2010] or HGS-ETR1 or PRO95780 in combination with paclitaxel or carboplatin in patients with advanced cancer [reviewed by Bellail and Cho 2012] did not reveal improvements of response rates. Thus, human cancers display resistance to TRAIL targeting agents in mono- and combination therapy, a difficulty that was known from early stage. Even before clinical trials were conducted,

in vitro studies demonstrated that some cancer cell lines and many patient-derived primary cultures [Nguyen et al 2001, Wuchter et al 2001, MacFarlane 2002, Koschny et al 2007, Todaro et al 2008] escape from TRAIL-apoptosis and thus resist TRAIL treatment. Understanding the molecular mechanisms of TRAIL resistance is therefore vital for the development of TRAIL-based cancer therapies. At least *in vitro*, a multitude of TRAIL-resistance mechanisms in tumour cells have been identified [reviewed by Mahalingam et al 2008, Roth 2009, Mellier et al 2010, Khaider et al 2011] and likewise, many sensitising agents to TRAIL-apoptosis were explored *in vitro* and in preclinical studies [reviewed by Ashkenazi and Herbst 2008, Johnstone et al 2008]. It should be noted that cancer cell resistance to TRAIL-apoptosis can be acquired upon TRAIL treatment or it can be inherent. Since most patient-derived primary tumour cells seem to be resistant to TRAIL [Nguyen et al 2001, MacFarlane 2002, Koschny et al 2007, Todaro et al 2008], one has to assume that in most cases escape from TRAIL-apoptosis is inherent. If TRAIL-resistance in a given cancer cell was inherent, one has to question whether resistance accompanied the process of neoplastic transformation, or whether it was kept from the normal, TRAIL-resistant ancestor cell. Since studies of TRAIL-apoptosis signalling and/or resistance almost exclusively were conducted in transformed cells, there is nothing known about the mechanism(s) of TRAIL-apoptosis resistance in normal cells. Consequently, the mechanism(s) for TRAIL's tumour-selective apoptosis-induction in tumourigenic but not normal cells is (are) unknown. We are convinced that before further investments are done in clinical studies, we first need to comprehend resistance to TRAIL-apoptosis signalling in normal cells and to clarify how TRAIL exerts its cancer-specific apoptosis action. We assume this could either uncover (not acquired but) inherent cancer cell resistance mechanisms towards TRAIL-apoptosis and/or highlight key cellular differences between normal and cancer cells that might be exploitable for potential TRAIL-based therapies. Only if these mechanisms and diversities are understood, we have a chance to progress the development of TRAIL for cancer therapies. Attempting to contribute to the understanding of normal cell resistance to TRAIL-apoptosis, to the mechanism(s) for resistance-loss through the process of transformation and thus the molecular basis for tumour-selective apoptosis, this study focuses on the identification of substantial differences in the initial phase of the TRAIL apoptotic signalling pathway in TRAIL-resistant normal and TRAIL-sensitive transformed cells.

INTRODUCTION

Tumour-specific cell-death is the ultimate goal of cancer therapy and eradication of all malignant cells from a human body is the only way for long-term cure. Endogenous mechanisms of programmed cell death exist [Lockshin and Zakeri 1994], distinguished mainly by morphological criteria. One discriminates between apoptosis [Kerr et al 1072], autophagy and necrosis, but also other types and somehow intermediate forms have been described [reviewed by Kroemer et al 2005, Galluzzi et al 2012].

Apoptosis

Morphologically, apoptosis features cell membrane blebbing, cell shrinkage, chromatin condensation, nucleosomal fragmentation and the breaking up of cells into fragments called apoptotic bodies. Contrary to the other forms of programmed cell death that do not involve membrane blebbing of dying cells, the dynamic plasma membrane alterations of apoptotic cells are thought to attract innate immune cells that facilitate their rapid removal from tissues before rupture and release of their cytoplasmic contents [Savill and Fadok 2000]. In the body, apoptosis serves to remove irreparably damaged, surplus or infected cells. Apoptosis is accomplished via two different routes, the extrinsic and the intrinsic pathways (Figure 3), which are triggered by pro-apoptotic receptors and intracellular BCL2 proteins, respectively.

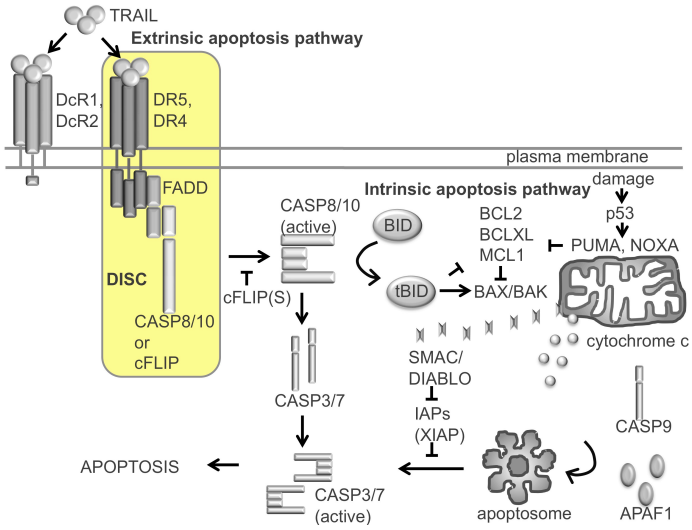

Figure 3: Extrinsic and intrinsic apoptosis pathways. The extrinsic pathway is activated by binding of TNF cytokine family members (*here:* TRAIL) to their death receptors (*here:* DR5, DR4), leading to the formation of the death inducing signalling complex (DISC) (yellow). The intrinsic apoptosis pathway is stimulated by severe cell stress, such as DNA or cytoskeletal damage. Unlike the intrinsic pathway, the extrinsic pathway operates independently of tumour suppressor p53 and can activate the mitochondrial pathway to amplify the apoptotic signal. The figure is based on the idea of [White-Gilbertson et al 2008, Newsom-Davis et al 2009].

The extrinsic apoptosis pathway and type I versus type II signalling cells. The extrinsic apoptosis pathway is activated by death domain (DD) containing cell surface receptors, the so-called death receptors [for activation by dependence receptors please see review Goldschneider and Mehlen 2010] and formation of the death inducing signalling complex (DISC) (Figure 3) [Kischkel et al 1995]. The most extensively studied death receptors are TNF receptor 1 (TNFR1), FAS receptor (FAS), death receptor 5 (DR5) and death receptor 4 (DR4), whereby 2 DR5 isoforms, a long (DR5(L)) and a short one (DR5(S)) exist. Common to these receptors are highly homologous cystein-rich domains (CRD) in their extracellular part, defining their ligand specificity. The membrane-distal first CRD is also referred to as pre-ligand assembly domain (PLAD) enabling TNFR1, FAS, DR5 or DR4 interactions amongst each receptor type, independent of their ligands [Chan et al 2000, Siegel et al 2000, Clancy et al 2005]. Extracellular ligand binding to death receptors oligomerises the receptors, which, at least in case of FAS, stabilises the intracellular receptor-DD in such a conformation that DD-containing adaptor molecules can bind (Figure 3) [Scott et al 2009]. While different DD-containing adaptor molecules exist, only FAS-associated death domain (FADD) additionally houses a death-effector domain (DED) [reviewed by Park et al 2007, Wu and Lo 2009, deathdomain.org]. Via its DED, FADD interacts with tandem DED-comprising proteolytic enzymes, the initiator caspases procaspase-8a, -8b (CASP8) or procaspase-10 (CASP10) or with the proteolytically inactive protein cellular FLICE-like inhibitory protein (cFLIP) [Irmler et al 1997]. The entity comprising at least the receptor, FADD, the initiator caspase(s) and/or cFLIP is called the death inducing signalling complex (DISC) (Figure 3). DISC formation results in the autocatalytic cleavage-stimulated activation of CASP8 and/or CASP10, which can be regulated by cFLIP. Out of 10 different cFLIP mRNA splice isoforms, only a long cFLIP (cFLIP(L)), a short cFLIP (cFLIP(S)), and a short isoform cloned from the Raji B-cell line (cFLIP(R)) are expressed at protein level [Golks et al 2005]. Moreover, 2 cleavage products of cFLIP(L) exist, cFLIP(L)p43 resulting from FASL-stimulated CASP cleavage at residue D376 inside the DISC [Scaffidi et al 1999] and cFLIP(L)p22 resulting from ligand-independent CASP cleavage at amino acid D196 within the cytosol of malignant B and T lymphoblastoma cell lines [Golks et al 2006]. Whilst cFLIP(S) blocks CASP activation at the DISC, probably competing with CASP for FADD binding, and cFLIP(R) due to its structural similarity with cFLIP(S) might act similarly, the role of cFLIP(L) at the FAS-DISC is controversial [Chang et al 2002]. Some

reports stated an anti-apoptotic cFLIP(L) function at the FAS-DISC due to its ability to block CASP8 activation [Irmler et al 1997, Rasper et al 1998], or to activate pro-survival pathways via adaptor protein recruitment to the TNFR1- and FAS-DISC [Hu et al 2000, Kataoka et al 2000]. Studies on the cFLIP(L) cleavage products demonstrated that upon its generation, cFLIP(L)p43 stays bound to the FAS-DISC, blocking CASP8 processing [Scaffidi et al 1999]. Or, after FASL treatment, cFLIP(L)p43 forms a complex with CASP8 and the E3 ubiquitin-protein ligase TNF receptor-associated factor 2 (TRAF2) to activate the transcription factor nuclear factor kappa B (NFKB) [Kataoka and Tschopp 2004]. Contrary, cFLIP(L)p22 found in nonapoptotic malignant cells, primary phytohaemaglutinin-activated T and B cells, and mature lipopolysaccharide (LPS)-activated dendritic cells induced NFKB activity, which prevented these cells from FASL- and TRAIL-induced apoptosis [Golks et al 2006, reviewed by Lavrik and Krammer 2012]. Other studies described a pro-apoptotic cFLIP(L) activity based on its ability to activate CASP8 cleavage at the FAS-DISC [Micheau et al 2002, Dohrman et al 2005]. Apparently, at the DR5/DR4-DISC, cFLIP(L) causes a likewise double-edged effect, as certain Jurkat clones expressing cFLIP(L) display reduced cell viability upon TRAIL treatment [Irmler et al 1997]. A recent report expressing different cFLIP variants in human HACAT keratinocytes demonstrated that all forms protected from FASL- and TRAIL-apoptosis, but the CASP8 cleavage pattern was changed in such a way that cFLIP(L) induced CASP8 processing to its active CASP8 p43/41 fragments irrespective of cFLIP cleavage and that cFLIP(S) or cFLIP(L)p43 blocked CASP8 cleavage [Kavuri et al 2011]. Importantly, cFLIP knockout in mice causes the same embryonic lethality than FADD- or CASP8-deficient mice and cFLIP-depleted mouse fibroblasts are highly sensitive to TNFα- and FAS-apoptosis [Yeh et al 2000]. Remarkably, the substrate-range of initiator CASP8 depends on its state of maturity. Using recombinant proteins in *in vitro* assays, the CASP8 substrate-range was shown to be limited to CASP8 itself and cFLIP [Chang et al 2003, Hughes et al 2009]. In contrast, cleaved CASP8 does not process inactive CASP8 molecules, but efficiently processes effector caspases (like 3, 6, 7) thus triggering the apoptotic signal [Lavrik et al 2003].

Downstream of DISC formation and signalling events, the pro-apoptotic signal is propagated via 2 different pathways, dependent on the cell type (Figure 3). In type I cells the activation of effector procaspases-3 (CASP3), -6 (CASP6) and -7 (CASP7) by CASP8 and/or CASP10 suffices to induce apoptosis [Scaffidi et al 1998], and no cleavage

of BH3-interacting domain death agonist (BID) to activate the intrinsic apoptosis pathway is required (Figure 3) [Yin et al 1999, Ozoren and El-Deiry 2002, Kandasamy et al 2003, Rathmell et al 2003]. In type II cells, apoptosis requires the release of apoptogenic factors from the mitochondria, which is mediated by CASP8 and/or CASP10 cleaving BID [Luo et al 1998, Milhas et al 2005, Fischer et al 2006] that connects the extrinsic apoptosis pathway to the mitochondria. Truncated BID (tBID) translocates to the mitochondrial membrane where it promotes aggregation of the BCL2 protein family members BAX and BAK leading to mitochondrial outer membrane permeabilisation (MOMP), as described in the following section.

The intrinsic apoptosis pathway. The signal triggering the intrinsic apoptosis pathway is elicited inside the cell and comprises stimuli such as DNA or cytoskeletal damage caused by agents such as ionising radiation, heat shock, toxins, cell detachment, bacterial or viral infection and oncogenic transformation. Other stimuli triggering this cascade during development, such as growth factor deprivation or decline in tissue morphogen concentrations as well as during prolonged stress of the endoplasmatic reticulum due to accumulation and aggregation of unfolded proteins [reviewed by Ashkenazi 2008]. The efflux of effector proteins during MOMP represents a crucial step in the intrinsic apoptosis pathway that is mainly regulated by members of the BCL2 protein family, which are divided into anti-apoptotic (e.g. A1, BCL2, BCLW, BCLXL, MCL1, promote survival) pro-apoptotic (e.g. BAX, BAK, BCLXS, BOK, activate apoptotic effector pathway) and BH3-only death proteins (e.g. BAD, BID, BIK, BIM, BMF, HRK, NOXA, PUMA, initiate apoptosis) [reviewed by Kelly and Strasser 2011]. Whilst anti-apoptotic and BH3-only BCL2 proteins regulate the interaction of BCL2 proteins amongst each other, the pro-apoptotic BCL2 family members BAX and BAK insert into the mitochondrial membrane to form pores, leading to MOMP. This enables the release of apoptogenic factors such as cytochrome c, inhibitor of apoptosis (IAP), second mitochondria–derived activator of caspase/direct IAP binding protein with low pI (SMAC/DIABLO) and omi stress-regulated endoprotease/high temperature requirement protein A2 (OMI/HTRA2). After its release, cytochrome c binds to apoptotic protease-activating factor 1 (APAF1) to form the apoptosome, which recruits initiator procaspase-9 (CASP9) promoting its self-activation. Activated CASP9 cleaves the

downstream effector proteases CASP3 and CASP7, which cleave various intracellular substrates leading to cell death. Notably, CASP9, CASP3 and CASP7 can be inhibited by direct binding of IAP family members (XIAP, cIAP1, cIAP2, IAP2, MLIAP, NAIP, survivin and apollon) to their active site or by enhancement of CASP proteasome degradation. In turn, IAP proteins can be inactivated intrinsically by SMAC/DIABLO and OMI/HTRA2 binding (Figure 3) [Du et al 2000, Verhagen et al 2000, Suzuki et al 2001]. This inhibtion has biological significance as during FASL- and TRAIL-apoptosis, depletion of IAP family members such as XIAP renders cells independent to BID cleavage and hence directs them from type-II to type-I signalling cells [Jost et al 2009, Varfolomeev et al 2009].

The medical relevance of apoptosis in cancer therapy. Control over apoptosis is of immense therapeutic importance for many human health conditions, be it the inhibition of cell death in heart cells in cardiac ischaemia [Hayakawa et al 2002], of neurons in Alzheimer's [Rohn et al 2001] and Huntington's disease [Sanchez-Mejia and Friedlander 2001] or the augmentation of apoptosis in self-reactive T cells in autoimmune diseases [reviewed by Prasad and Prabhakar 2003] and in malignant cells in cancer [reviewed by Gerl and Vaux 2005, Ashkenazi 2008]. Since the human body on average generates 60 billion cells per day, an equal number of cells must die to maintain cell homeostasis [reviewed by Cotter 2009]. Defective or inefficient apoptosis is therefore disastrous and represents one out of six acquired hallmarks of cancer cells (Preamble Figure 2) [Hanahan and Weinberg 2000]. Many cancers that evade from apoptosis carry inactivating mutations in genes such as the transcription factor *tumour suppressor protein 53* (*p53*) [reviewed by Kinzler and Vogelstein 1996], which is instrumental in the activation of the intrinsic apoptosis pathway. For instance, upon DNA damage, p53 accumulates, leading to the expression of cell cycle arresting proteins. During this arrest, repair mechanisms can act in the cell. However, if the repair fails, p53 stimulates the expression of pro-apoptotic factors (PUMA, NOXA, BAX, APAF1) and inhibits anti-apoptotic protein expression (BCL2, BCLXL) (Figure 3) [reviewed by Brosh and Rotter 2009]. In tumours that escape apoptosis, either p53 itself is inactivated, or p53-regulating proteins are uncontrolled such as the hyperactivation of the E3 ubiquitin protein-ligase MDM2, which promotes p53 degradation [reviewed by Hahn and Weinberg 2002]. Alternatively, anti-apoptotic proteins are frequently upregulated in many cancers, such as BCL2 and IAP family members [Beroukhim et al 2010, Smolewski

and Robak 2011]. Many tumour cells rely on the deregulation of these proteins to survive, so that cells transformed with the oncogenic transcription factor MYC highly proliferate, but undergo apoptosis if survival factors like BCL2 are withdrawn [Askew et al 1991, Shi et al 1992, Evan et al 1992]. This way, tumour cells are more prone to apoptosis than normal cells, but can counterbalance detriments increasing pro-survival factors. Certain cancer cells master the balancing act between apoptosis and survival so well that they survive although displaying elevated levels of active effector caspases [Yang et al 2003]. Generally, evasion from apoptosis is thought to promote and enable metastasis [reviewed by Mehlen and Puisieux 2006]. Potential future cancer therapies currently tested in clinical trials target both the extrinsic and intrinsic apoptosis pathways, whereby pro-apoptotic receptor agonists (PARA) and antagonists of the anti-apoptotic BCL2 family are in focus [reviewed by Ashkenazi 2008, Pavet et al 2011]. Contrary to the intrinsic pathway, targeting the extrinsic pathway has the advantage that it triggers tumour cell apoptosis independent of p53 and that mutations inactivating the extrinsic pathway occur less frequent [reviewed by Ashkenazi 2008]. Most importantly, DR5- and/or DR4-activating PARA, unlike other pro-apoptotic agents can discriminate between malignant and normal cells and thus carry a significant lower risk of side effects.

The pro-apoptotic subset of TNF cytokines and its most prominent member(s)

The extrinsic apoptotis pathway is elicited by endogenous proteins [reviewed by Noteborn 2009, Pavet et al 2011] such as cytokines of the tumour necrosis factor (TNF) superfamily. Cytokines are immunomodulatory proteins that alter the interaction between cells, the communication between cells, or the behavior of cells. The TNF superfamily of cytokines for example can induce inflammation, apoptosis, proliferation, invasion, angiogenesis, metastasis and morphogenesis [reviewed by Aggarwal et al 2012]. Whilst all TNF cytokines are pro-inflammatory, TRAIL, the ligand of DR5 and DR4, is additionally classified into the pro-morphogenic and pro-apoptotic subsets of TNF cytokines (Figure 4, A) [reviewed by Gonzalvez and Ashkenazi 2010, Aggarwal et al

2012], even though TRAIL's affiliation to the pro-apoptotic subclass is most renown and hitherto characterised best. Of all other pro-apoptotic TNF members, TRAIL shares highest protein sequence homology with FAS ligand (FASL), which binds and activates the FAS death receptor (Figure 4, B). The most well-known TNF superfamily member however is the activator of death receptor TNFR1, tumour necrosis factor alpha (TNFα), which presumably was the first representative of this class of proteins to be identified [Aggarwal et al 2012]. Today, most of what is accepted in TRAIL signalling was originally identified in TNFα- or FASL-signalling and only later proven to account also for TRAIL. However, it shall be stated clearly that TNFα, FASL and TRAIL are different signalling systems and many aspects that have been substantiated for TNFα or FASL lack demonstration for TRAIL. The variety of human TNF cytokine genes (18 in total) arose from duplication events [reviewed by Ware 2003, Wiens and Glenney 2011]. When duplicated genes are preserved in evolution, this is because a higher dosage of the gene product is advantageous, because the copies have distinct functions or the copies share the same function [as reviewed by Innan 2009]. As TRAIL is unique for its tumour cell-specific induction of apoptosis, it clearly differs in its functionality as compared to TNFα or FASL. Thus, major differences in signalling pathways must exist.

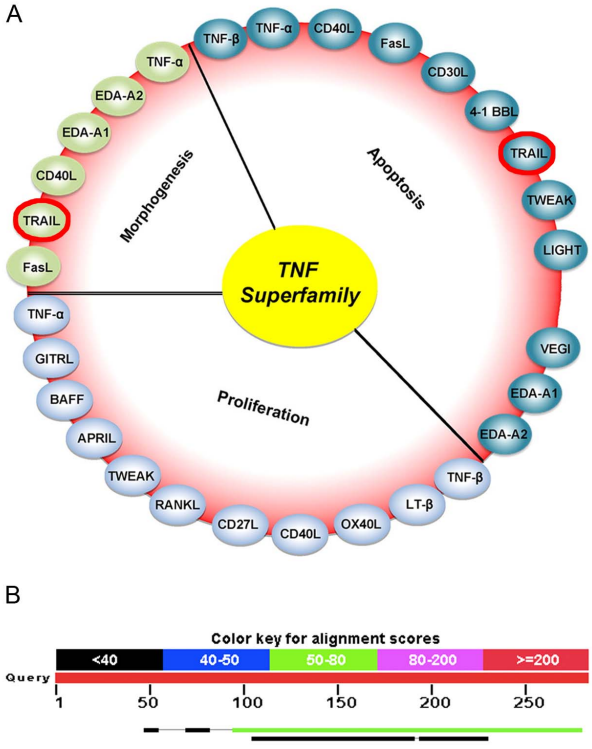

Figure 4: Classification of TNF superfamily members and protein sequence homologies of TRAIL versus FASL and TNFα, respectively. **(A)** Overview of TNF superfamily members classified according o their roles in inflammation, cellular proliferation, apoptosis and morphogenesis. All TNF superfamily members exhibit pro-inflammatory activity initiating the transcription factor nuclear factor kappa-B (NFKB) (red circle). Certain members display proliferative activity on hematopoietic cells triggering various mitogen-activated kinases (MAPK) (light blue). Other representatives, such as tumour necrosis factor alpha (TNFα), FAS ligand (FASL), and TNFα-related apoptosis inducing ligand (TRAIL, encircled in red) control apoptosis (dark blue) and regulate morphogenesis and differentiation (green). The figure is taken and modified from [Aggarwal et al 2012]. **(B)** Graphic summary for the protein sequence alignments of human TRAIL and FASL (upper black and green lane) and human TRAIL and TNFα (lower black lane) using NCBI-BLAST Align [Altschul et al 1990].

TRAIL structure. Expressed as type II transmembrane glycoprotein (mTRAIL) with a short cytoplasmic N-terminal domain and a long C-terminal extracellular receptor-binding domain, the carboxyl-terminal extracellular part of TRAIL can be cleaved off to form a soluble molecule (sTRAIL). Thus, TRAIL signalling can occur via cell-cell contact or systemic in an autocrine or paracrine fashion. Whilst soluble TNFα and FASL are shed from cell membranes by metalloproteases *in vivo* [Moss et al 1997, Tanaka et al 1998, Schneider et al 1998], metalloprotease inhibitors did not increase TRAIL surface levels in any cell-type tested [Mariani and Krammer 1998]. Instead, sTRAIL *in vitro* was generated by cysteine proteases [Mariani and Krammer 1998], but the identity of the critical enzyme(s) is still unclear. It has been demonstrated that the membrane-bound and not the soluble form of FASL is critical for apoptosis [Schneider et al 1998, O'Reilly et al 2009] and likewise, a higher pro-apototic activity of mTRAIL than of sTRAIL was observed [Schneider et al 1998, Wajant et al 2001]. However, whilst Schneider et al do not obtain apoptosis induction at 5μg mL^{-1} (!) sTRAIL in otherwise highly TRAIL-sensitive BJAB cells and they do not demonstrate that single M2-antibody treatment does not induce apoptosis, one cannot exclude that the sTRAIL preparation utilised in that study was biologically inactive. Moreover, reports by Schneider and Wajant investigated TRAIL's cytotoxic action only on transformed cells, so that a higher apoptosis-inducing potential, procured by crosslinking, might be detrimental for TRAIL's tumour-cell specificity, like it was concluded for FASL [Schneider et al 1998]. Compared to other TNF members, TRAIL is unique as it contains an unpaired cysteine residue (Cys^{230}) in its extracellular TNF homology domain, which coordinates a zinc (Zn^{2+})-ion that stabilises TRAIL's homotrimeric, bell-shaped structure [Hymowitz et al 2000, Bodmer et al 2000]. It was the first example of metal binding-mediated trimerisation of a cytokine [Hymowitz et al 2000] and mutation of this residue or interchain disulfide bond formation on Cys^{230} lead to TRAIL's dissociation into dimeric and/or monomeric subunits, a decline in TRAIL's binding affinity to its receptor and hence a decrease in its pro-apoptotic activity [Bodmer et al 2000]. At physiologic pH TRAIL specifically exerts its pro-apoptotic action by binding to its receptors, whilst at pH-values smaller than 4.5 TRAIL changes its conformation, which increases its binding ability with membranes, induces pore formation and membrane permeabilisation and thus enforces TRAIL's unspecific cytotoxicity to cells [Nam and Choi 2002]. Moreover, at a pH-value of 6.5 TRAIL-induced cell death in tumour cells adopted necrotic and

apoptotic features [Meurette et al 2005]. Thus, the extracellular pH seems critical for the tumour-specificity and mode of cell death induction by TRAIL. The importance of TRAIL's protein structure for its specific action became evident when initial indications for a certain susceptibility of human normal cells towards TRAIL-apoptosis *in vitro* [Jo et al 2000, Leverkus et al 2000, Nitsch et al 2000, Nesterov et al 2002, Lane et al 2004, Steele et al 2006] were associated to amine (polyhistidine, FLAG, leucine zippers) tags attached to the TRAIL sequence [Lawrence et al 2001] aiming to enhance TRAIL's biological activity [reviewed by Schneider and Tschopp 2000]. Thus, the structure of TRAIL is essential for TRAIL's selectivity to tumour versus normal cells. The indispensability of a native and untagged TRAIL structure for TRAILs tumour-selectivity and safety has also been proven *in vivo* during preclinical studies. Initially observed TRAIL-toxicity towards mice xenografted with human hepatocytes was clearly related to exogenously added TRAIL amine tags [Hao et al 2004, reviewed by Ashkenazi et al 2008]. Therefore, next to humanised antibodies specifically targeting DR5 or DR4, only one rhTRAIL variant is accepted and tested in clinical trials. This version is based on the human protein's natural sequence (extracellular amino acid residues 114-281) and does not carry an exogenous tag. The exact same untagged rhTRAIL version is used in this study.

TRAIL expression in health and disease. In non-pathologic conditions TRAIL is expressed on human immune effector cells, such as interleukin 12-stimulated natural killer (NK) cells [Zhang et al 2008], peripheral blood T and B lymphocytes [Kayagaki et al 1999, Ehrlich et al 2003], interferon-activated monocytes [Griffith et al 1999], LPS-induced monocytes and macrophages [Halaas et al 2000], neutrophils [Tecchio et al 2004] and dendritic cells. Even if its pioneering and several following reports denoted that TRAIL mRNA in contrast to TNFα and FASL mRNA is expressed in many normal human tissues [Wiley et al 1995, Pitti et al 1996], one should consider that TRAIL detection in tissues might originate from immune cells that permanently reside in the different tissues analysed [Lohmann-Matthes et al 1994, Berent-Maoz et al 2010].

Elevated mTRAIL expression on immune effector cells, increased sTRAIL levels in body fluids and the enhanced TRAIL expression on normal cells was reported in connection with many human diseases leading to tissue-damage and cell death.

Examples are autoimmune disorders (multiple sclerosis [Wandinger et al 2003], rheumatoid arthritis [Ichikawa et al 2003, Audo et al 2011], systemic lupus erythematosus [Lub-De Hooge et al 2005], systemic sclerosis [Azab et al 2012]), cardiovascular diseases (myocardial infarction [Nakajima et al 2003]), viral infections (hepatitis C [Mundt et al 2003], HIV-1 [Herbeuval et al 2005]), neurologic diseases (Alzheimer's disease [Cantarella et al 2003, Uberti et al 2004]), metabolic diseases (obesity [Bernardi et al 2012], type I diabetes [Lamhamedi-Cherradi et al 2003a]), pulmonary diseases (asthma [Collison et al 2009]), bacterial infections (periodontal disease [Mori et al 2009]), hematologic diseases (myelodysplastic syndromes [Campioni et al 2005]) and further degenerating diseases like intervertebral disk degeneration in scoliosis or vertebrae fracture [Bertram et al 2009]. Since TRAIL-stimulated apoptosis requires a functional DR5 and/or DR4-mediated extrinsic apoptosis pathway within the target cell, the origins for each of these conditions are apparently potent sensitisers of (normal) cells to TRAIL-apoptosis.

Contrary to above mentioned conditions, cancer does not cause tissue-damage by dying but through hyperproliferating cells. TRAIL expression in certain transformed cells has therefore been related to their resistance to TRAIL-apoptosis [Frank et al 1999, Rieger et al 1999, Zhao et al 1999, Inoue et al 2002, Koyama et al 2002]. Although TRAIL induces apoptosis in transformed cells *in vitro* [Wiley et al 1995] and *in vivo* [Wiley et al 1995, Walczak et al 1999], some cancer cell lines and many patient-derived primary cultures *in vitro* are resistant to TRAIL treatment [Nguyen et al 2001, MacFarlane 2002, Koschny et al 2007, Todaro et al 2008]. Cancer cells thus might have to escape from TRAIL-apoptosis to be able to grow at all *in vivo*.

TRAIL function *in vivo*. Based on its expression on immune effector cells and its feature to induce apoptosis selectively in tumour cells *in vitro* and in human tumour xenografts implanted in SCID mice [Wiley et al 1995, Walczak et al 1999], TRAIL is thought to function in tumour surveillance. In support of this assumption, treatment of wildtype mice with TRAIL-neutralising antibodies promoted tumour initiation if mice were challenged with the chemical carcinogen methylcholanthrene (MCA) [Takeda et al 2002] and increased liver metastases if mice were inoculated with murine cancer cells [Takeda et al 2001, Seki et al 2003]. Likewise, TRAIL knockout increased

tumourigenesis in response to MCA [Cretney et al 2002] and augmented metastases if mice were inoculated with murine lymphoma cells [Sedger et al 2002], renal carcinoma or mammary carcinoma cells [Cretney et al 2002]. Overexpression of TRAIL in skin keratinocytes prevented from experimentally induced skin carcinogenesis [Kedinger et al 2011]. Contradictorily, mice deficient in TRAIL or their single TRAIL death receptor and DR5 homologue (TRAIL-R) [Wu et al 1999] did not spontaneously develop tumours [Yue et al 2005]. Moreover, although detachment of tumour cells from the extracellular matrix was suggested to increase sensitivity to exogenously added TRAIL [reviewed by Grosse-Wilde and Kemp 2008], TRAIL did not inhibit metastasis of TRAIL-sensitive cancer cells to all organs equally well [Seki et al 2003]. Finally, TRAIL-deficient mice developed hematologic malignancies only at late stage of life [Zerafa et al 2005], if then to a larger extend than control cells. The role of TRAIL in tumour surveillance therefore has not been fully resolved.

Even more controversial are results from studies investigating TRAILs putative function in the negative selection of premature T lymphocytes in the thymus and the development of autoimmunity, which was suggested based on TRAIL expression on dendritic and epithelial cells. Whilst some studies reported more severe and accelerated experimentally induced autoimmune diseases in TRAIL deficient or TRAIL inhibited mice [Hilliard et al 2001, Lamhamedi-Cherradi et al 2003a, Lamhamedi-Cherradi et al 2003b, Mi et al 2003, Cretney et al 2005], others could not experimentally elicit accelerated diseases at all [Simon et al 2001, Cretney et al 2003]. Moreover, TRAIL- or TRAIL-R knockout mice did not spontaneously develop autoimmunity [Cretney et al 2003], even not with prolonged age [Cretney et al 2003, reviewed in Cretney et al 2006] and TRAIL-R knockout mice demonstrated normal negative selection [Diehl et al 2004]. Thus, TRAIL may not have a direct role in negative selection and prevention of spontaneous autoimmunity. Instead, it is currently postulated that TRAIL may act on autoreactive T cells by inhibiting cytokine and antibody production and in this way inhibit proliferation of autoreactive T lymphocytes causing inflammation [reviewed by Shepard and Badley 2009].

Finally, adapted from the finding that many cells of the innate immune system increase their TRAIL expression upon their activation by a variety of pro-inflammatory cytokines (IFNα, IFNβ, IFNγ, IL2, TNFα) [Kayagaki et al 1999, Ehrlich et al 2003, Kemp et al 2003, Liu et al 2001, Takeda et al 2001, Johnsen et al 1999, Kashii et al 1999] and that

the TRAIL gene promoter is induced by interferons [Gong et al 2000, Sato et al 2001, Clarke et al 2004], TRAIL-apoptosis is suggested to function in the clearance of virus-infected cells [reviewed by Shepard and Badley 2009, Cummins and Badley 2009]. It appears that on one hand, TRAIL-mediated apoptosis of virus-infected cells is protective to the host. On the other hand, some viruses may activate TRAIL-apoptosis and use the TRAIL system to release and disseminate the virus. Furthermore, TRAIL-apoptosis can negatively contribute to virus pathogenesis as certain virus proteins induce TRAIL-expression on uninfected macrophages, which subsequently facilitate TRAIL-apoptosis in uninfected T lymphocytes, a process referred to as 'bystander killing' [Miura et al 2001, Zhang et al 2001].

In conclusion, even though further studies are required to tailor TRAIL's exact function in immune surveillance, its potential to induce apoptosis in transformed, virus-infected or diseased cells *in vivo* is doubtless. Especially in light of TRAIL's anti-tumour function it must not be forgotten that spontaneous tumour-development usually requires the accumulation of several genetic alterations over time. If instead tumour formation is accelerated challenging a system with mutagenic substances, TRAIL's tumour-surveillance activity became evident. Since not all metastasising cells are more susceptible to TRAIL-apoptosis than their primary tumour cells [Vigneswaran et al 2005] and most probably not all tissues display equal abundances of resident immune effector cells, clarification of general TRAIL sensitivities of metastatic cells and as well as tissue-distribution of resident immune effector cells may allow us to understand current gaps and inconsistencies in TRAIL's *in vivo* anti-tumour function.

Potential therapeutic advantages of TRAIL

Several features make TRAIL a promising cancer therapeutic agent. First and foremost, in contrast to conventional therapies that lead to systemic toxicity, TRAIL induces apoptosis in human cancer cells, whilst sparing healthy normal ones. This tumour-selectivity is the key therapeutic trait of TRAIL, which separates TRAIL from other pro-apoptotic TNF cytokines. In support of this, whilst TNFα proved unsuccessful in preclinical studies causing deadly inflammatory response, liver- and kidney toxicity [Leist et al 1996] and intravenous injection of FASL into severe combined immunodeficiency (SCID) mice caused apoptosis of xenografted human hepatocytes [Hao et al 2004], preclinical and finally clinical studies have shown that rhTRAIL was well tolerated. Particularly, rhTRAIL did not cause undesired accumulation of the recombinant protein or immune response in patients [reviewed by Ashkenazi et al 2008]. Apart from its safety, further therapeutic advantages of TRAIL are its activation of the extrinsic apoptosis pathway independent of the p53 status in tumour cells [Galligan et al 2005] and the circumstance that common oncogenes like MYC and RAS sensitise cells to TRAIL (see 'TRAIL-apoptosis and the stepwise transformation model') [Nesterov et al 2004, Wang et al 2005]. In preclinical trials rhTRAIL demonstrated growth inhibitory and cytotoxic activity against a wide variety of tumours originating from solid and hematologic human malignancies xenografted into SCID or athymic mice. Thereby, rhTRAIL showed anti-tumour activity as single agent or in combination with several chemotherapeutics [reviewed by Ashkenazi et al 2008]. Confirmed tumouricidal in preclinical studies, rhTRAIL was tested in human studies for the treatment of solid malignancies and currently has reached phase III clinical trials. As already outlined in the preamble, hitherto achieved response rates in phase II clinical trials with patients obtaining PARA and chemotherapeutics in combination therapy were low, which supports the notion that further preclinical research on the mechanistics of TRAIL apoptosis signalling is required. On the basis of TRAILs non-controversial selectivity towards tumour cells, research on TRAIL apoptosis signalling has pivotal importance.

Trail apoptotic signalling and DISC formation

Generally, TRAIL-induced apoptosis follows the extrinsic pathway common to the pro-apoptotic TNF cytokines described above. However, compared to other TNF members, there are considerable differences and uncertainties in the membrane-localisation of DISC proteins, the proteomic composition of the native DISC and the subsequent intracellular fate of the DISC components (Figure 5), which all impact on the signalling outcome and therefore are important to highlight.

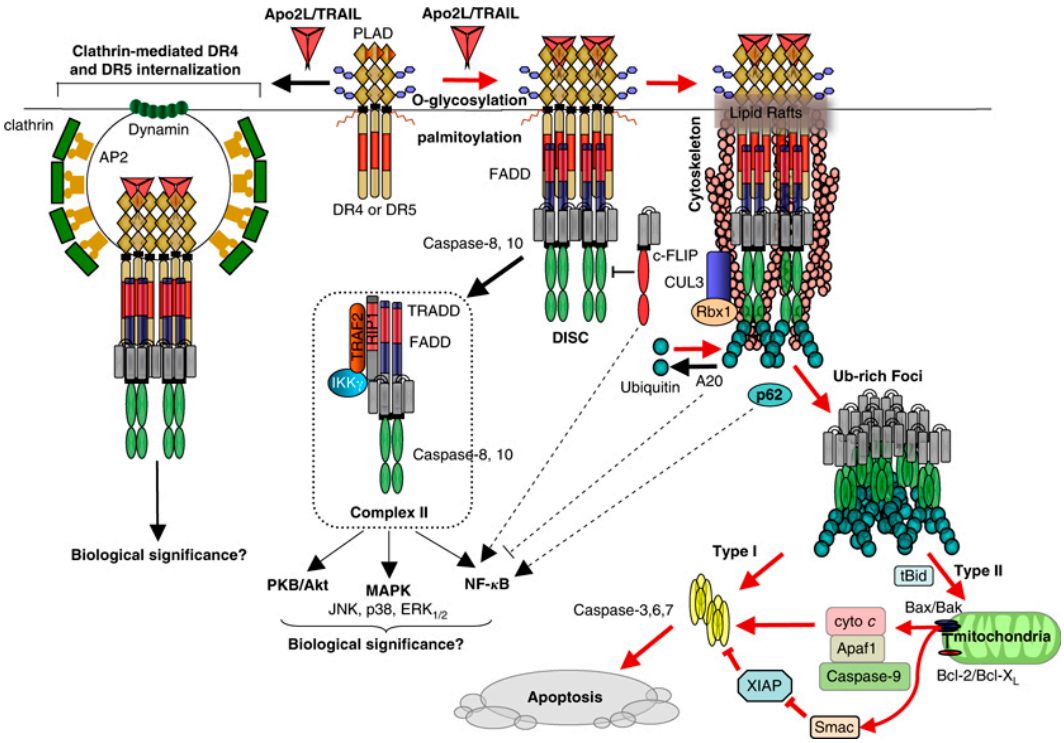

Figure 5: Current model for TRAIL signalling. For details see text. Reprinted by permission from Macmillan Publishers Ltd: [Oncogene] (Gonzalvez and Ashkenazi 2010), copyright (2010).

TRAIL-DISC. Altogether, TRAIL binds to 5 different receptors (see 'TRAIL Non-Apoptotic Signalling'), but only 2, the death receptors 5 and 4 (DR5, DR4) contain a cytoplasmic DD allowing homotypic interaction with the DD within FADD. There are 2 DR5 isoforms, DR5(L) and DR5(S), expressed, but their functional difference is unclear. Contrary to the TNFα receptor TNFR1, FADD binding to DR5 or DR4 does not require the adaptor molecule TNFR1-associated death domain protein (TRADD). Via its DED, FADD co-recruits CASP8 and/or CASP10 to DR5 and DR4 and thus enables their activation, a process that was shown to require both proximity-induced dimerisation

and proteolytic cleavage in FASL and TNFα signalling [Boatright et al 2003, Donepudi et al 2003, Hughes et al 2009, Oberst et al 2010, Lavrik and Krammer 2012] and that generally got accepted for TRAIL-signalling as well. Whilst CASP8 is essential for TRAIL-apoptosis, the role of CASP10 in the DISC is controversial [Kischkel et al 2001, Sprick et al 2002].

Notably, PLAD-mediated and ligand-independent heterotypic receptor interactions between TRAIL receptors (Figure 5) [Clancy et al 2005] have not been confirmed with endogenously expressed receptors [reviewed by Gonzalvez and Ashkenazi 2010]. Therefore, it is assumed that TRAIL binding to the receptors induces DR5 and DR4 microaggregates. Whilst DR4 becomes activated by both mTRAIL and sTRAIL, DR5 activation requires mTRAIL or crosslinked sTRAIL [Mühlenbeck et al 2000, Wajant et al 2001]. As it appears that DR5 is the major apoptosis-inducing receptor [Kelley et al 2005], these findings are in line with previous notion that mTRAIL is the more potent apoptosis activator. However, it shall be noted that the capacity of sTRAIL or mTRAIL to activate DR5 or DR4 most probably depends on the utilised TRAIL variant as well as on the batch of purification. Moreover, a final prove for a differential function of DR5 and DR4 is still missing.

Both, DR5 and DR4 are subjected to posttranslational modifications, which are thought to positively stimulate their pro-apoptotic activity via different means. For instance O-glycosylation (binding of glycosyl groups to serine and threonine residues) of DR5 and DR4 enhanced DISC formation and CASP8 activation by facilitating receptor aggregation (Figure 5). Thereby, O-glycosyltransferases were found overexpressed in cancer tissues and correlated with TRAIL sensitivity [Wagner et al 2007]. Furthermore, S- nitrosylation (covalent binding of a nitrogen monoxide to a reactive thiol cysteine) of DR4 but not DR5 stimulated CASP8 cleavage via a not further defined mechanism [Tang et al 2006]. Finally, S-palmitoylation (the reversible attachment of palmitate to a cysteine residue) of DR4 and not DR5 promoted receptor oligomerisation, DISC formation and TRAIL-apoptosis localising receptors to lipid rafts (Figure 5) [Rossin et al 2009], which are detergent-resistant membrane domains rich in sphingomyelin, sphingolipids and cholesterol. However, whilst S-nitrosylation was only observed upon nitrosylcobalamin treatment and endogenous S-nitrosylation could not be determined in 3 cancer cell lines [Tang et al 2006], oligomerisation-promoting effects of S-

palmitoylation was only demonstrated in an overexpression system [Rossin et al 2009]. The biological significance of S-nitrosylation and S-palmitoylation thus remain unclear.

The requirement of death receptor recruitment into lipid rafts for effective apoptosis signalling originally has been reported for FAS signalling [Gajate and Mollinedo 2005] and was suggested for DR5 and DR4 by 2 studies working with NSCLC and HeLa cells, respectively (Figure 5) [Song et al 2007, Rossin et al 2009]. This notion recently got challenged by findings where no association of the full, native TRAIL DISC with lipid rafts was found in hematopoietic (BJAB, Jurkat, Z138), nor in HeLa cells [Dickens et al 2012]. Whilst the HeLa cell study [Rossin et al 2009] did not demonstrate a co-localisation of FADD and CASP8 with lipid rafts, the NSCLC study [Song et al 2007] did, so that it was suggested that raft structures might play a greater role in in epithelial (NSCLC) tumour cells [Dickens et al 2012]. The biological sinificance of lipid rafts in TRAIL apoptosis signalling thus appears to be limited to only few cell types and requires clarification.

One of the most striking differences between TRAIL-induced and TNFα- or FASL-stimulated apoptosis is the requirement of ligand-induced receptor internalisation for apoptosis to occur (Figure 5). Whilst receptor internalisation is crucial for TNFR1- and FAS-apoptosis [Schneider-Brachert et al 2004, Lee et al 2006] and TRAIL binding induces rapid internalisation of both DR5 and DR4 via clathrin-dependent [Austin et al 2006] and independent [Kohlhaas et al 2007] pathways, inhibition of endocytosis does not prevent FADD or CASP8 recruitment in various type I signalling cells [Austin et al 2006, Kohlhaas et al 2007]. Thus, unlike TNFR1 and FAS, DR5 and DR4 do not require TRAIL-induced internalisation for DISC formation and apoptosis at least in type I cells [Austin et al 2006, Kohlhaas et al 2007]. If receptor internalisation is required in type II signalling cells is unknown. Apart from TRAIL-induced internalisation, DR5 and DR4 can undergo constitutive clathrin-dependent endocytosis as part of a desensitising mechanism in leukemia, colon and breast cancer cells [Jin et al 2004, Cheng et al 2006, Zhang and Zhang 2008].

Another level of complexity is added to the regulation DISC formation by the fact that next to DR5 and DR4, also the activity of CASP8 and cFLIP can be modulated by posttranslational modifications. For instance, CASP8 phosphorylation at tyrosine 380 by the focal adhesion kinase and proto-oncogene tyrosine protein kinase (SRC) was reported, which prevented CASP8 cleavage at the DISC. Expression of a non-

phosphorylatable CASP8 mutant or SRC inhibition sensitised TRAIL-resistant human colon cancer DLD1 cells to TRAIL-apoptosis [Cursi et al 2006, De Toni et al 2007]. Increased phosphorylation of cFLIP(L) and cFLIP(S) was observed upon bile acid GCDCA treatment of hepatocellular cancer cells, which lowered their affinity for FADD and thus lead to an increased recruitment of CASP8 and CASP10 to the TRAIL-DISC. Bile acid effects could be prevented by PKC inhibition (chelerythrine) [Higuchi et al 2003]. Notably, endogenous cFLIP phosphorylation has not been reported yet. Finally, ubiquitinylation of DR5 [Johnson et al 2003], CASP8 and CASP10 [McDonald et al 2004] and cFLIP [Poukkula et al 2005, Chen et al 2007, Kim et al 2002], which labels proteins for proteosomal degradation, negatively influences the pro-apoptotic DISC and thus TRAIL-apoptosis. Interestingly, ubiquitinylation of CASP8 either can lead to protein degradation and apoptosis resistance, or to CASP8 aggregation in high molecular weight structures promoting CASP8 autoactivation and apoptosis sensitivity [Jin et al 2009]. In the latter case CASP8 ubiquitinylation was mediated by a lipid raft localised cullin-based E3 ligase (CUL3), depended on ring-box 1 (RBX1) and triggered the recruitment of the ubiquitin binding protein p62, which in turn localised DISC CASP8 to ubiquitin-rich foci, where CASP8 cleavage was promoted. Overexpression of an additionally identified CASP8-bound deubiquitinase called A20 prevented CUL3-mediated effects (Figure 5) [Jin et al 2009].

Previous FAS and consequently DR5- and DR4-signalling models suggested that the receptor, FADD and CASP8, CASP10 or cFLIP are assembled in a 3:3:3 ratio, meaning that one FADD molecule binds to one receptor recruiting one molecule of CASP8, CASP10 or cFLIP and that single DISCs are clustered by receptor [(FAS) Scott et al 2009] and/or FADD interactions (Figure 5) [(FAS) Carrington et al 2006]. Now, this model appears to require a complete reassessment, since recent quantitative mass spectrometrical analyses have shown that FADD is consistently substoichiometric relative to FAS, DR5 and DR4 or DED-only proteins [Schleich et al 2012, Dickens et al 2012]. Strikingly, there was up to 9-fold more CASP8 than FADD in the TRAIL-DISC and on average only 1 FADD molecule per 3 receptors detected. Therefore, a DISC structure has been proposed, which relies on the formation of CASP8 chains (Figure 6). Indeed, CASP8, CASP10 and cFLIP can interact with each other via their second DED domain (DED2) [Irmler et al 1997, Wang et al 2001] and mutating a specific motif within the

CASP8 DED2 prevented chain formation, CASP8 activation and TRAIL-apoptosis [Dickens et al 2012].

Interestingly, Dickens et al could not detect any CUL3 in the native DISC of type I (BJAB) or type II signalling (Z138, Jurkat) cells and detected only very low CUL3 ratios in the DISC of type II HeLa cells. Therefore, the relevance of CUL3-mediated CASP8 ubiquitinylation and subsequent DISC localisation into ubiquitin-rich foci remains to be established (Figure 5). Moreover, mass-spectrometry analysis of the TRAIL DISC identified CASP10 only in type I signalling BJAB at much lower abundance than CASP8, from Dickens et al concluded that CASP10 does not have an obligatory role in TRAIL-DISC signalling. Nonetheless, one has to consider that the timepoint or target of the immunoprecipitaton was inappropriate to detect CUL3 and CASP10 or that DISC composition simply depends on the kind of stimulus applied to the receptors, as it was indicated for FAS signalling [Chaigne-Delalande et al 2009]. Finally, Dickens et al noted that a structural CASP8 rearrangement would be required to unmask CASP8 DED2 to facilitate CASP8 chain formation at DR5 and DR4. Amongst the options for how this structural rearrangement could be accomplished, it was hypothesised that also the cytoskeleton might play a role, which was not further specified [Dickens et al 2012].

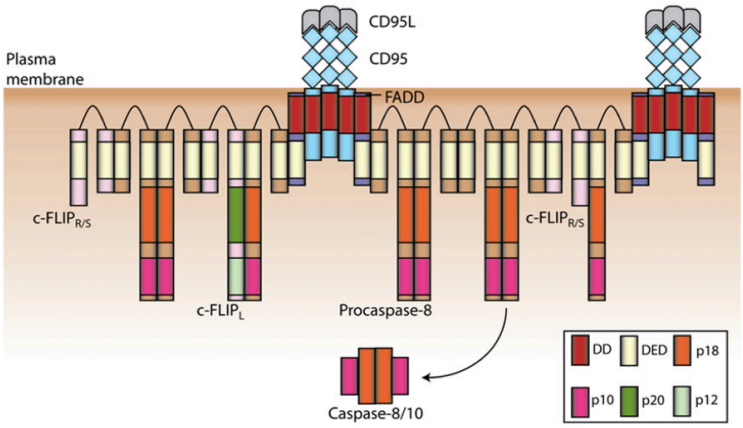

Figure 6: Refined model of the TRAIL and FAS DISC. Upon ligand stimulation, FADD is recruited first to FAS or DR5 and DR4. Subsequently, CASP8, CASP10 or cFLIP are recruited and form chains via DED interactions. Chain formation enables dimerization of CASP and efficient activation. Chains might form between neighboring death receptors. The figure is taken from [Schleich et al 2012] and refers to work of [Dickens et al 2012] and [Schleich et al 2012]. Reprinted with permission from Elsevier.

TRAIL-DISC and non-apoptotic forms of programmed cell death. Recently, the death receptors of TNFα and FASL were shown to induce necrotic cell death, a process dependent on the kinase activity of receptor interacting serine/threonine protein kinase 1 and 3 (RIPK1, RIPK3) [Cho et al, 2009, He et al 2009, Zhang et al 2009, summarised by Vandenabeele and Melino 2012]. A similar necrotic activity has been

proposed for TRAIL [Holler et al 2000], but the interaction of DR5 and DR4 with RIPK1 has been questioned early on [Kischkel et al 2000]. In fact, only 1 publication so far has demonstrated an interaction between DR5 or DR4 with RIPK1 by co-immunoprecipitation in an endogenous system [Harper et al 2001]. This finding recently was challenged by a study coming from the same team, which failed to detect RIPK1 in mass spectrometric analyses of the native DISC immunoprecipited targeting TRAIL from BJAB, Jurkat, Z138 and HeLa cells [Dickens et al 2012]. It could however be possible that the detection of RIPK1 requires the immunoprecipitation of proteins downstream the receptors, such as FADD or CASP8.

Anti-apoptotic TRAIL-DISC components. Several proteins oppose TRAIL-apoptotis signalling at the level of the DISC, interfering with efficient initiator CASP activation in the DISC and/or activating pro-survival pathways (see also 'TRAIL non-apoptotic signalling and complex II formation'). Amongst those proteins are 3 further TRAIL receptors, decoy receptor 1 and 2 (DcR1, DcR2) [Degli-Esposti et al 1997a, Degli-Esposti et al 1997b] and soluble osteoprotegerin (OPG), to which TRAIL binds besides DR5 and DR4. Structurally DcR1 and DcR2 resemble DR5 and DR4, but whilst DcR1 is a glycosylphosphatidylinositol (GPI)-linked receptor that lacks the entire intracellular domain inclusively the DD, DcR2 possesses a truncated, dysfunctional DD (Figure 3). Therefore, TRAIL binding to DcR1 or DcR2 fails to elicit apoptosis. The mode of how DcR1 and DcR2 interfere with DR5- and DR4-stimulated apoptosis in the DISC appears to differ. Whilst DcR1 localises to lipid rafts where it captures TRAIL away from the DISC, DcR2 competes with DR4 for DR5 binding upon TRAIL stimulus inhibiting efficient recruitment, cleavage and activation of initiator CASP at the DISC [Merino et al 2006]. Notably, the decoy function of DcR1 and DcR2 has so far been shown in overexpression studies only [Degli-Esposti et al 1997a, Degli-Esposti et al 1997b, Merino et al 2006]. Compared to other TNF family members, TRAIL has the lowest affinity to OPG at physiological temperature [Truneh et al 2000]. Therefore, even though binding of TNF family members to OPG contributes to bone remodelling [Emery et al 1998], the physiologic role if TRAIL/OPG binding remains unclear.

Probably the most potent inhibitors of CASP8 activation in the DISC are the DISC-binding cFLIP proteins cFLIP(L), cFLIP(L)p43 and cFLIP(S). Contrary to the FAS-DISC

[Chang et al 2002, Micheau et al 2002, Dohrman et al 2005] (see 'The extrinsic pathway and type I versus type II signalling cells'), no pro-apoptotic activity of ectopically expressed cFLIP(L) has yet been demonstrated for the TRAIL-DISC. However, evidence that overexpression of cFLIP(L) protects from TRAIL-apoptosis is weak, as ectopic expression of cFLIP(L) in type II signalling Jurkat cells that only express cFLIP(L) but no cFLIP(S), lead to controversial outcomes if stimulated with TRAIL. Whilst one clone appears to be fully protected from TRAIL-treatment, another clone was only partially protected, whilst a third clone was as sensitive to TRAIL as the wildtype cells [Irmler et al 1997]. Moreover, downregulation of cFLIP(L) by adenomatous polyposis coli (APC)/ß-catenin mediated activation of MYC left colorectal cancer cells resistant to TRAIL [Zhang et al 2010, reviewed by Gonzalvez and Ashkenazi 2010]. Irrespective of that, the protective role of cFLIP(L) in TRAIL-apoptosis was demonstrated by knockdown-experiments in several cancer cell lines, which lead to an enhanced CASP8 activation upon TRAIL-challenge [Sharp et al 2005]. In line with this, expression of cFLIP(L), cFLIP(L)p43 and cFLIP(S) in FLAG-TRAIL sensitive normal human HACAT keratinocytes, blocked CASP8 cleavage [Kavuri et al 2011]. Unfortunately, most studies describing the (anti-)apoptotic cFLIP function of cFLIP proteins at the DISC were conducted focusing on the FAS-DISC, and the outcomes might not be automatically translatable to the TRAIL-DISC.

Further non-canonical DISC-binding proteins have been identified in cancer cells to negatively impact on initiator CASP activation in the TRAIL-DISC (PED/PEA15, the DDX3/GSK3/cIAP1 capping complex, PRMT5) [reviewed by Pennarun et al 2010, Shirley et al 2011]. For reasons of space these will not be further described.

TRAIL non-apoptotic signalling and complex II formation

Even though much less efficient than TNFα, TRAIL can activate pro-survival signalling pathways such as nuclear factor B (NFKB), the mitogen-activated protein kinases (MAPK) stress-activated protein kinase (JNK), p38 and extracellular-signal regulated kinase (ERK), as well as RAC-alpha serine/threonine-protein kinase (AKT)

(Figure 5). This is thought to depend on the formation of spatially and temporally distinct receptor/adaptor complexes, as described in the following.

TRAIL-induced NFKB, MAPK (JNK, p38, ERK) and AKT activation via complex II formation. Studies utilising overexpression systems [Schneider et al 1997, Degli-Esposti et al 1997a] revealed that DR5, DR4 and DcR2 activated NFKB, a transcription factor involved in pro-survival signalling activating genes like *cFLIP*, *cIAP1*, *cIAP2*, *XIAP* and *BCLXL*. Subsequently, TRAIL-induced NFKB activation was observed in TRAIL-resistant human embryonic kidney 293 (HEK293) cells, pan-CASP inhibited HeLa cells [Harper et al 2001], TRAIL-resistant Jurkat [Ehrhardt et al 2003] and cholangiocarcinoma cell lines [Ishimura et al 2006], in which TRAIL-stimulated NFKB activation promoted cell survival, proliferation [Ehrhardt et al 2003] or migration [Ishimura et al 2006]. Generally, NFKB is activated via the I kappa B kinase (IKK) complex consisting of 3 kinases IKKα, IKKβ and IKKγ whose activation leads to phosphorylation and degradation of the inhibitor of kappa B (IKB). This degradation in turn permits NFKB translocation to the nucleus where it stimulates transcription [reviewed by Li and Lin 2008]. Since death receptor signalling appears to be influenced by the formation of spatially and temporally distinct receptor/adaptor complexes, in this context the formation of a secondary complex (complex II) has been proposed (Figure 5). Complex II is suggested to form subsequent to DISC formation and requires recruitment of the DD-containing RIPK1 for IKK activation [Lin et al 2000]. Via a yet unspecified mechanism FADD and activated CASP8 are described to dissociate from DR5 and DR4 to then bind multiple proteins (the adaptor TRADD, RIPK1, IKKγ and the E3 ubiquitin-protein ligase (TRAF2)) forming complex II [Varfolomeev et al 2005, Jin and El-Deiry 2006]. Besides activating NFKB, complex II was reported to signal to JNK and p38 in TRAIL-resistant HT1080 fibrosarcoma cells [Varfolomeev et al 2005], as well as to ERK in normal human vascular smooth muscle cells fostering survival and migration [Secchiero et al 2004a], and in normal human endothelial cells promoting migration, invasion, proliferation and differentiation [Secchiero et al 2004b]. Finally, complex II also activated AKT in normal human endothelial cells (Figure 5) [Secchiero et al 2003]. Complex II-mediated activation of NFKB depended on the presence of FADD, RIPK1 and IKKγ, whilst activation of JNK demanded TRAF2 [Lin et al 2000] and triggering of p38 required RIPK1 and TRAF2 [Varfolomeev et al 2005]. The detailed mechanisms for how this DR5 and/or DR4-derived complex II activates either NFKB, MAPK or AKT signalling

pathway is not known and intermediate signalling components are not yet defined, but studies of the TNFR1-derived complex II reported that complex II signalling is altered in dependence of the ubiquitinylation and/or phosphorylation state of RIPK1. Intriguingly, a recent study could not detect RIPK1 being associated with the TRAIL DISC in several hematopoetic tumor cell lines [Dickens et al 2012], which challenges their own previous findings [Harper et al 2001]. Regardless of whether a DR5/DR4-derived complex II exists, cFLIP(L)p22 was capable to interact with IKKγ and activate NFKB in TRAIL-resistant tumour cells in absence of a ligand [Golks et al 2006]. The molecular pathway for a complex II-mediated activation of ERK has only been outlined in its basic features for FASL signalling and was proposed to involve FASL-induced and cFLIP(L)p43-dependent recruitment of TRAF2, RIPK1 and the proto-oncogene serine/threonine-protein kinase RAF1 [Kataoka et al 2000]. About the mechanism of DR5/DR4-derived AKT activation even less is known, so far only its dependence on the phosphoinositol-3-kinase (PI3K) has been described [Secchiero et al 2003]. Although the molecular players for the activation of TRAIL's non-apoptotic signalling cascades have not been elucidated yet, evidence for the regulation of TRAIL's pro-survival signalling via events such as exclusion from lipid rafts [Song et al 2007] already exist. Possibly, the TRAIL-induced activation of pro-survival pathways occurs independent of a complex II, but involves yet unidentified adaptor and effector molecules recruited to the TRAIL-receptors. Evidence supporting this hypothesis comes, for instance, from overexpression studies suggesting a ligand-independent activation of AKT through DcR2 [Lalaoui et al 2011], or from studies on endogenous systems indicating that AKT-phosphorylated MAP kinase-activating death domain protein (MADD) binds to DR4 [Li et al 2010]. Remarkably, in case of TNFα-signalling endogenous MADD was required to recruit the adaptor protein growth factor receptor-bound protein 2 (GRB2) and son of sevenless homolog 1 (SOS1) to TNFR1 and to subsequently activate RAS and the MAPK/ERK kinase kinases 1 and 2 (MEKK1/2) [Kurada et al 2009]. Thus, at least JNK and ERK might be activated by TRAIL via additional and/or other routes than a TRAIL receptor-derived complex II. Enlightenment about how TRAIL and its receptors activate pro-survival signalling pathways is essential, since TRAIL-induced CASP activation occurs rapidly, and complex II generation takes place subsequent to the formation of the DISC. Therefore it was hypothesised that (apart from CASP activation itself) the level of pro-survival signal activity prior to ligand stimulation sets the threshold of cells to undergo TRAIL-

apoptosis and not pro-survival pathways activated downstream of DISC formation [as suggested for NFKB by Gonzalvez and Ashkenazi 2010]. However, this assumption has to be redefined if TRAIL would activate pro-survival pathways via faster routes than complex II, especially if these pathways negatively feedback on CASP8 activation in the DISC.

The stepwise system cells and transformation-associated changes in the actin cytoskeleton

Cancer development in humans involves a sequence of events. As cancer incidence increases with age, these events appear to occur over many decades. Since patient-derived cancer cell lines conserve the status of a tumour the time the biopsy was taken, these cell lines contain already a multitude of alterations. The decisive and minimally required events that lead to neoplastic transformation thus are hard to trace back. A huge step towards understanding the cancer progress was achieved, when Hahn and Weinberg succeeded to systematically transform human cells *in vitro* (Figure 7) [Hahn et al 1999]. The generation of their stepwise transformation model aided to limit the pathogenesis of human cancers to a set of genetic and biochemical rules, as summarised in the following [and reviewed by Hahn and Weinberg 2002].

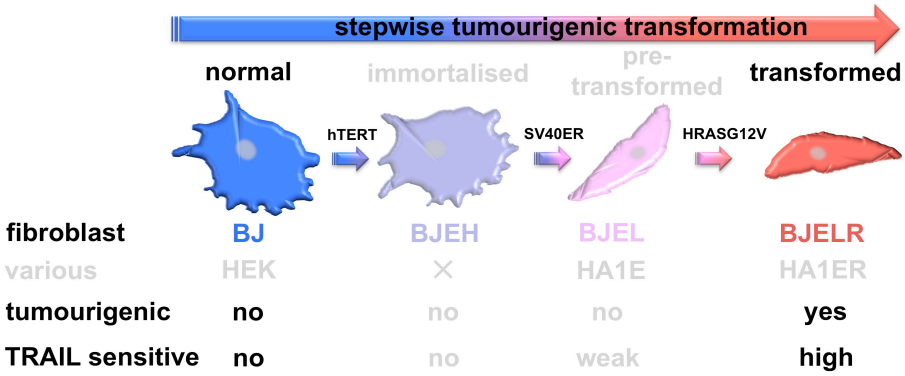

Figure 7: Scheme of Hahn and Weinberg's stepwise transformation model. Normal cells (*here:* human foreskin fibroblasts (BJ) or human embryonic kidney cells (HEK)) were gradually transformed by introducing the human telomerase catalytic subunit (HTERT), simian virus 40 early region (SV40ER) and a constitutively active HRAS mutant (HRASG12V). Whilst HTERT maintains telomere length and confers replicative immortality to BJ cells, HEK cells require additional SV40ER-encoded elements to reach immortality. Obtained transformed cells (*here:* BJELR or HA1ER) display cancer cell features like unlimited proliferation, anchorage-independent growth and tumour formation in vivo and are sensitive to TRAIL-induced apoptosis.

The stepwise transformation model. *In vitro*, neoplastic transformation of normal human fibroblasts (BJ), embryonic kidney cells (HEK) or mammary epithelial cells (HMEC) is achieved by the introduction of 3 genetic elements, the telomerase catalytic subunit (HTERT), the Simian virus early region (SV40ER) and a constitutively active mutant of HRAS (HRASG12V) (Figure 7) [Hahn et al 1999]. Thereby, cell transfection with HTERT serves to immortalise the otherwise growth-limited normal cells via maintenance of the telomeres. Interestingly, a reactivation of telomerases is often observed in cancers. Although SV40ER encodes large T (LT), small T (ST) and 17KT proteins, subsequent experiments utilising only the LT and ST viral oncoproteins and oncogenic RAS demonstrated that the disruption of intracellular pathways regulated by LT, ST and RAS is sufficient for the carcinogenic conversion of human cells [Hahn et al 1999, Yu et al 2001, Hahn et al 2002, Rangarajan et al 2004]. Whilst LT localises to the cells nucleus, it inhibits the transcription factor retinoblastoma protein (pRB), which determines whether or not a cell proceeds through G1 phase. Indeed, the pRB is commonly inactivated in cancers. In addition, LT blocks the pRB-related p107 and p130 proteins, which are repressors of E2F transcription factors that, in turn, are promoters of cell cycle entry and progression genes. Most importantly, LT restrains p53, the promoter of cell cycle arrest or apoptosis inducing genes that is inactivated in 50% of all tumours [reviewed by Cheng et al 2009]. Through its inhibition of pRB and p53, LT prevents HTERT-immortalised cells to undergo senescence.

Contrary to LT, the ST protein is localised in the cytoplasm where it binds and inhibits one or more isoforms of the tumour suppressor protein phosphatase 2A (PP2A), which dephosphorylates a wide variety of substrates. The introduction of an oncogene such as hyperactive RAS serves to generate a constitutive mitogenic signal, which reduces the dependence of transformed cells on external mitogenic stimulation. Importantly, fully transformed stepwise system cells (BJELR, HA1ER, HMLER) display cancer cell-characteristic features defined as anchorage-independent growth, loss of contact inhibition and tumourigenicity *in vivo*, which were assessed by colony formation/growth in soft agar, BrdU-incorporation upon confluency and tumour formation capacity in immunocompromised mice, respectively. Tumours obtained from injecting fully transformed cells in mice are anaplastic, strongly angiogenic and non-metastatic. The principal benefit that the stepwise transformation system holds, is that it provides tumourigenic cells for which their normal counterparts of isogenic

background are available. This milestone cannot be achieved with patient-derived cancer cells. Secondly, contrary to cancer cells originating from tumour explants, the genetic alterations that induced neoplastic transformation are clearly defined in the *in vitro* transformed tumour cells. Therefore, a targeted dissection of the cellular pathways that are modulated by LT, ST and HRAS is enabled, which will help to understand the etiology of transformation or transformation-associated features.

TRAIL-apoptosis and the stepwise transformation model. One feature connected to transformation is the gain of sensitivity to TRAIL-apoptosis. Whilst normal and HTERT-immortalised cells of the stepwise tumourigenesis model are resistant to rhTRAIL-apoptosis, HTERT/SV40ER-pretransformed cells are weakly sensitive and HTERT/SV40ER/HRASG12V-transformed cells are highly sensitive (unpublished observations from our laboratory). Hitherto, 2 studies used the stepwise tumourigenesis model to explore the causal mechanism(s) for TRAIL sensitivity of fully transformed cells (BJELR, HA1ER). These reported that constitutively active RAS, via the RAF1/MEK1/ERK pathway, stabilises the MYC protein (Figure 8). In turn, MYC transcriptionally upregulates DR4 and DR5, thus leading to a sensitisation of BJELR and HA1ER cells to TRAIL-apoptosis [Nesterov et al 2004, Wang et al 2004, Wang et al 2005]. Indeed, like pharmacological MEK1 inhibition [Nesterov et al 2004], siRNA-mediated MYC depletion diminishes TRAIL-apoptosis in BJELR (unpublished observations from our laboratory), which implies that MYC is one of the main drivers of TRAIL sensitivity in these cells. The importance of RAF1/MEK1/ERK pathway and MYC for TRAIL sensitivity has also been reported in other transformed cells, where the

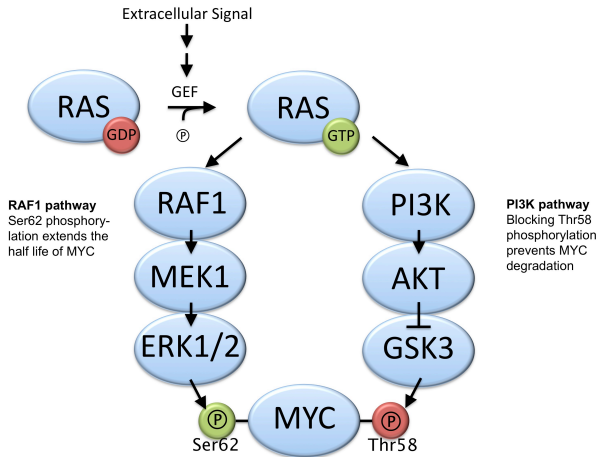

Figure 8: RAS-mediated stabilisation of MYC protein. Active RAS elevates MYC protein levels via two routes. On one hand activation of RAF1/MEK1/ERK phosphorylates MYC at Ser62, which extends the proteins half-life. Via ativation of PI3K/AKT, GSK3 is blocked and thus phosphorylation of MYC at Thr58, which prevents MYC degradation. The figure is based on the idea of [Bachireddy et al 2005].

dependence of TRAIL apoptosis on MEK1 activity [Drosopoulos et al 2005] or MYC's ability to repress cFLIP was shown [Ricci et al 2004, Amanullah et al 2002]. Contrary to these studies, APC/ß-catenin mediated activation of MYC in colorectal cancer cells was associated with a downregulation of cFLIP(L), but left cells resistant to TRAIL. Only upon retinoic acid (RA) treatment of MYC-activated cells, an upregulation of DR5 and DR4 and a sensitisation to TRAIL was observed [Zhang et al 2010]. Thus, MYC upregulation in malignant cells appears to have different effects on TRAIL sensitivity. Regarding MYC effects in normal cells, findings of Wang et al confirmed previous reports, which showed that ectopic MYC expression in normal fibroblasts sensitises to many different apoptotic stimuli [reviewed by Pelengaris et al 2002] such as FASL- [Hueber et al 1997] or TNFα-induced apoptosis [Klefstrom et al 1997]. Not only the death receptors, but also CASP8 and CASP9 might be MYC target genes, as indicated by a large-scale analyses of MYC binding to E-box consensus element CACGTG-containing promoters in live human cells [Fernandez et al 2003]. Indeed, an increase of full-length CASP8 protein levels can be seen upon exogenous MYC expression in BJ cells [Wang et al 2004]. Since overexpression of MYC occurs in a variety of human cancers, sensitivity to (TRAIL-) apoptosis is a physiological consequence of transformation. Whilst the mechanism(s) eliciting elevated MYC expression levels has (have) not been established in human cancer, in normal human epithelial cells MYC expression is activated upon cell adhesion to fibronectin and requires cytoskeletal rearrangements [Benaud and Dickson 2001]. Interestingly, advanced differentiation and epithelial cell organisation represses endogenous MYC expression [Simpson et al 2011].

Transformation-associated changes in the actin cytoskeleton. Morphological alterations linked to transformation are reminiscent to cytoskeletal changes of cells at the onset of mitosis. Cells round up, matrix adhesion is lost, a contractile actin–myosin ring is formed and cortical rigidity increases. Moreover, transformed cells display motile blebs and bulging pseudopodia, loose contact inhibition and stress fibers. All these events involve actin remodelling mediated by signalling pathways that implicate RHO family GTPases. Primarily the RHO-GTPases CDC42, RAC1 and RHOA have been associated with actin cytoskeleton rearrangements, whereby CDC42 induces filopodia [Nobes and Hall 1995, Kozma et al 1995], RAC1 regulates lamellipodia formation and

membrane ruffling [Ridley et al 1992] and RHOA regulates stress fiber and focal adhesion assembly (Figure 9) [Ridley and Hall 1992].

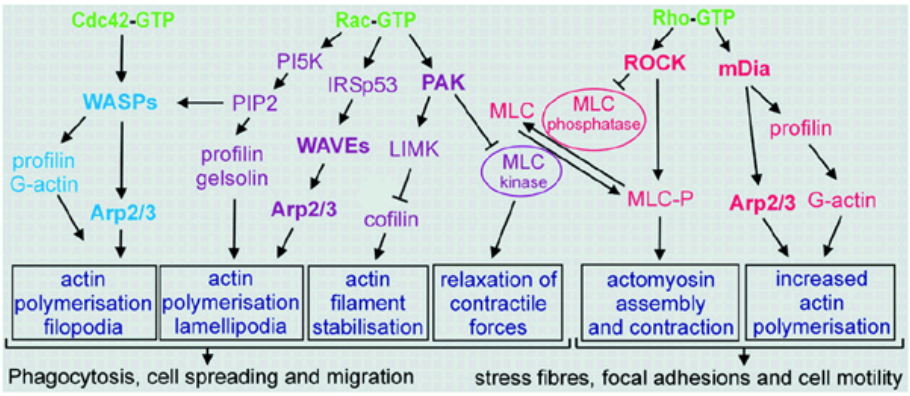

Figure 9: Regulation of the actin cytoskeleton motility by RHO-family GTPases. For details see text. Reprinted by permission from Macmillan Publishers Ltd: [EMBO Reports] (Ahmadian et al 2002), copyright (2002).

The actin cytoskeleton represents only one constituent of the mammalian cell cytoskeleton, which is composed of actin filaments, intermediate filaments (keratins, lamins, neurofilaments and vimentins), microtubules (consisting of alpha and beta tubulin) and microtubule motors (kinesins and dyneins). The actin cytoskeleton has essential functions in diverse cellular processes including endocytosis, motility, organelle and vesicle trafficking, cytokinesis and signal–response coupling. Within the actin cytoskeleton one discriminates between the cortical actin network that lies just beneath the plasma membrane and plays a profound role in cell surface growth and shape definition, actin stress fibers that traverse the cell, and actin that is involved in cell surface protrusions, including membrane ruffles (Figure 10).

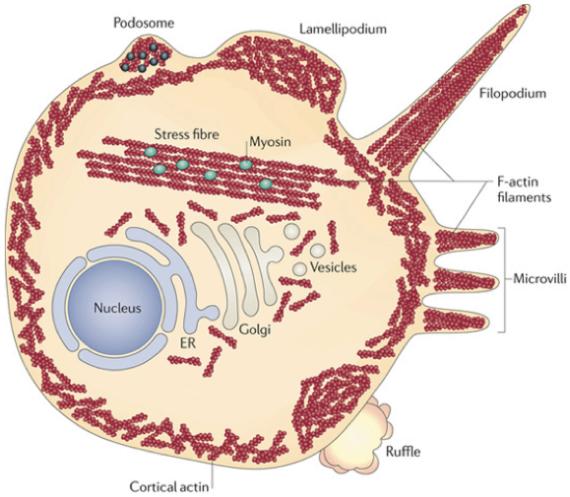

Figure 10: Localisation of actin filaments within the cell. The cortical actin is a loosely organised network of actin filaments underneath the plasma membrane. Actin stress fibers can span the whole cell. Actin filaments can also be organised to form cell extensions such as podosomes, lamellipodia, filopodia, microvilli and membrane ruffles. Myosins (green) confer contractability to the actin fibers and regulate their assembly. Reprinted by permission from Macmillan Publishers Ltd: [Nature Reviews Microbiology] (Taylor et al 2011), copyright (2011).

Cortical actin is primarily composed of actin, actin-bundling proteins and myosin II [reviewed by Bray and White 1988]. It is connected to the plasma membrane by proteins of the ezrin, radixin and moesin (ERM) family, which bind both actin and integral membrane proteins [reviewed by Bretscher et al 2002]. Finally, cortical actin is predominantly regulated by the RHO-GTPase RHOA [reviewed by Etienne-Manneville and Hall 2002], which, if RHOA is activated, leads to actin polymerisation and myosin II recruitment [Lee et al 2004, Bement et al 2005, Kamijo et al 2006]. Stress fibers are filament bundles emanating from the plasma membrane at focal adhesions, where clusters of integrin receptors bind to extracellular matrix proteins such as fibronectin and collagen. Stress fibers consist of actin and myosin filaments containing several non-muscle myosin II (NMII) isoforms, as well as proteins that stabilise (e.g. tropomyosin) or destabilise (gelsolin and cofilin) actin filaments, that control actin filament bundling (e.g. α-actinin, filamin and pallidin) or myosin contractility (e.g. myosin light chain kinase (MLCK), calmodulin (CALM), caldesmon (CALD)), as well as others [reviewed by Naumanen et al 2008]. Actin filaments are connected to the cells plasma membrane either via direct binding to integral membrane proteins, or indirectly through peripheral membrane proteins such as adducin, ankyrin, band 4.1 protein, tropomyosin, tropomodulin, CH domain proteins or proteins of the ezrin, radixin and moesin (ERM) family [summarised in Lodish et al 2012]. Importantly, the formation of actin stress fibers requires the assembly of myosin molecules into bipolar filaments [Wei and Adelstein 2000] and is mainly regulated by RHOA. In its entirety the actin cytoskeleton is a complex, highly dynamic and adaptive structure, which assembles in response to environmental cues. Thereby, the assembly of actin into higher-order structures like networks, fibers or protrusions in normal and transformed cells is regulated by the RHO-GTPases RHOA, CDC42 and RAC1, whereby actin fiber-dependent processes such as adhesion and motility are primarily regulated by RHOA [reviewed by Hall 1998, Schoenwaelder and Burridge 1999, Hernandez-Alcoceba et al 2000, Evers et al 2000, Parsons et al 2010, Rottner and Stradal 2011, Spiering and Hodgson 2011].

LT and ST-induced actin cytoskeleton changes. More than 2 decades ago it was demonstrated that the actin cytoskeleton is rearranged rapidly when normal

fibroblasts or epithelial cells are transformed with simian virus 40 (SV40) [Weber et al 1974]. Obvious morphological alterations of SV40-transformed cells included a disorganised actin cytoskeleton and an increased filopodial and lamellipodial production enhancing cellular motility and contributing to the loss of contact inhibition. In the following, the expression level of several actin cytoskeleton proteins was found deregulated upon SV40-transformation. For instance, SV40-transformed cells exhibited decreased levels of a subset of the tropomyosin family of proteins [Hendricks et al 1981, Matsumura et al 1983], which stabilise and protect stress fibers from disassembly by binding to F-actin [Bernstein et al 1982, summarised by Ostap 2008]. Another study revealed an SV40-mediated decline in α-actinin expression levels [Glück et al 1993], a protein that cross-links and anchors actin fibers to a variety of intracellular structures. Interestingly, recent studies compared the proteomes of BJ stepwise system cells at each step of the genetic modification towards full transformation [Pütz et al 2010, Pütz et al 2012]. Most drastic alterations in protein expression levels were revealed upon SV40ER introduction. Surprisingly, in the first study only 6 cytoskeletal proteins were found deregulated, of which in turn only one (ßACT) is an actin cytoskeleton protein [Pütz et al 2010]. In a consecutive study the same authors applied a more powerful SILAC-based 2D-DIGE approach and found the actin filament destabilising gelsolin and CALD (next to 3 further actin cytoskeleton proteins) downregulated upon SV40 introduction [Pütz et al 2012]. The contribution of the single SV40ER proteins to the drop in tropomyosin, gelsolin or CALD expression is not clarified. Since SV40 LT localises to the cells nucleus to inhibit pRB, p107, p130 and p53, one could speculate that SV40-associated downregulation of tropomyosin, gelsolin or CALD is mediated by LT. However, only little is known about LT action on the actin cytoskeleton or actin-related proteins and the introduction of LT alone did not induce alterations in actin fibers of rat embryo fibroblasts [Graessmann et al 1980]. Contrary, SV40 ST immediately engaged the actin cytoskeleton during cell transformation and its single expression sufficed to induce loss of actin filaments [Graessmann et al 1980]. Via the inhibition of PP2A, ST protein expression resulted in the rearrangement of F-actin networks in epithelial MDCK cells [Nunbhakti-Craig et al 2003]. Actin cytoskeleton rearrangements in ST expressing cells included RAC1-induced membrane ruffling and formation of lamellipodia, CDC42-initiated formation of filopodia, and loss of RHOA-dependent stress fibres, which coincided with increased RAC1 and CDC42 expression levels and decreased RHOA levels

in those cells (Figure 11) [Nunbhakdi-Craig et al 2003]. Importantly, expression of an ST mutant unable to interact with PP2A failed to induce the marked disorganization of F-actin observed in MDCK cells expressing wildtype ST [Nunbhakdi-Craig et al 2003]. Likewise, ST mutants that could not bind PP2A also failed to transform human cells expressing LT, hTERT and HRAS [Mungre et al 1994, Porras et al 1996, Yu et al 2001, Hahn et al 2002, Chen et al 2004, reviewed by Westermarck and Hahn 2008]. Thus, the ST/PP2 interaction is required for rearrangements of the actin cytoskeleton as well as for ST-mediated transformation. Summarising the role of PP2A inhibition in actin disassembly, decrease of cell adhesion and anchorage-independent growth would extend the scope of this paragraph and has been extensively reviewed elsewhere [Arroyo and Hahn 2005, Sontag and Sontag 2006, Virshup and Shenolikar 2009, Basu et al 2011]. It should nevertheless be noted that MYC is directly dephosphorylated by PP2A, and inhibition of PP2A activity by ST stabilised MYC [Yeh et al 2004]. Although a recent publication using less differentiated, human mammosphere-derived epithelial cells indicated that the introduction of only hTERT and SV40ER was sufficient for tumourigenic conversion [Paranjape et al 2012], cancerous transformation of differentiated human mammary epithelial cells usually requires additional activation of strong oncogenic signalling.

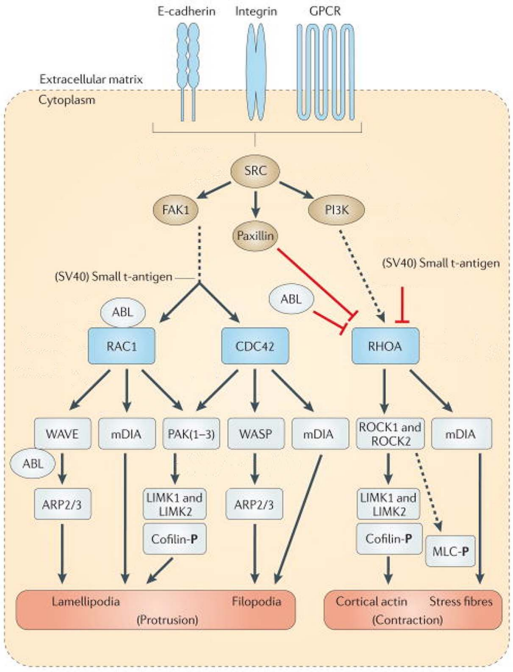

Figure 11: Influence of SV40 ST on RHO-family GTPase-mediated modelling of the actin cytoskeleton. SV40 ST upregulates the RHO-GTPases RAC1 and CDC42 and blocks RHOA-mediated signalling. Reprinted (with modifications) by permission from Macmillan Publishers Ltd: [Nature Reviews Microbiology] (Taylor et al 2011), copyright (2011).

HRASG12V-induced actin cytoskeleton changes. RAS controls at least 2 signal transduction pathways, one regulating gene transcription and translation, the other controlling cytoskeleton organisation. Since HRASG12V-transformation associated deregulations of cytoskeleton protein expression has been reported, both pathways shall be described in very brief. Generally, oncogenes stimulate growth-promoting translational processes to upregulate the synthesis of proteins critical for transformation. Transformation with HRASG12V stimulates growth-promoting translation at least in 2 ways. First, RAS directly activates PI3K, leading to PTEN/AKT/mTOR-stimulated translation by activation of EIF4E and the S6 kinase (S6K). Second, RAS activates the RAF1/MEK1/ERK pathway, which stimulates translation via MNK-mediated phosphorylation of EIF4E [reviewed by Steelman et al 2011]. As they support growth, oncogenes at the same time also activate transcriptional processes that render cancer cells sensitive to apoptosis. Again, RAS stimulates apoptosis-promoting transcription via at least two routes. First, RAS-mediated activation of RAF1 induces p16/ARF expression indirectly activating the tumour suppressor proteins RB and/or p53. This way, high RAS levels induce growth arrest, unless both RB and p53 pathways are inactivated [Peeper et al 2001, Serrano et al 1997]. Second, RAS-stimulated activation of the RAF1/MEK1/ERK pathway stabilises MYC protein (Figure 8), which leads to the transcriptional upregulation of pro-apoptotic genes, as described in a previous paragraph. Apart from its effects on transcription and translation, RAS has immediate influence on the actin cytoskeleton. Similar to SV40 transformation, microinjection of oncogenic HRAS typically disrupts RHOA-dependent stress fibers followed by the induction of RAC1-mediated membrane ruffling and loss of focal adhesions [Bar-Sagi and Feramisco 1986, Izawa et al 1998]. RHO-GTPases get activated by RAS along two different routes. On one hand, RAS signals via RAL-GDS/RAL/RALBP1/CDC42 to regulate the nucleation and polymerisation of actin, on the other hand it directly activates the PI3K/RAC1/RHOA pathway to regulate stress fiber contraction and focal adhesion formation (Figure 12). Whether RAS-induced alterations of the actin cytoskeleton are primarily brought by transcriptional, translational or direct events is unknown and most probably it involves multiple paths, as single RAS effectors play a role in all of these processes. For instance RAS-activated ERK does not only account for transcriptional events in the nucleus, but likewise signals at focal adhesions. There, in absence of fibronectin, ERK regulates the disassembly of focal adhesions in

migrating cells, in part through the activation of calpain proteases [Glading et al 2000, Glading et al 2004]. Inhibition of ERK signaling increased focal adhesion size and retarded disassembly of focal adhesions in adherent cells [Nobes and Hall 1999, Webb et al 2004, Pullikuth et al 2005, Vomastek et al 2007]. In line with this, stress fiber and focal contact disruption, that was observed in normal rat kidney cells transfected with a RAS mutant specifically activating the RAF1/MEK1/ERK pathway, could be reverted by chemical inhibition of MEK1 [Pawlak and Helfman 2002]. Only during adhesion to fibronectin, which is repressed by MYC [Coller et al 2000], ERK was proposed to promote focal adhesion formation by activating MLCK [Cheresh et al 1999, Fincham et al 2000, Klemke et al 2007] and this required RHOA or RAC1 activation [Chrzanowska-Wodnicka et al 1996, Machesky and Hall 1997]. In addition to the assumption that RAS-induced actin cytoskeleton modulation results from several events influenced by single RAS-effectors, most likely the activation of several RAS-effector molecules is involved to obtain the full morphological picture seen upon HRASG12V-transformation. Latter notion is supported by the finding that downstream of HRASG12V, the activation of the RAS effector pathways RAF1 and RAL-GEF were required for the transformation of human fibroblasts and activation of RAF1, RAL-GEF and PI3K was required for transformation of HMEC [Rangarajan et al 2004]. Similar to SV40- transformation, plain

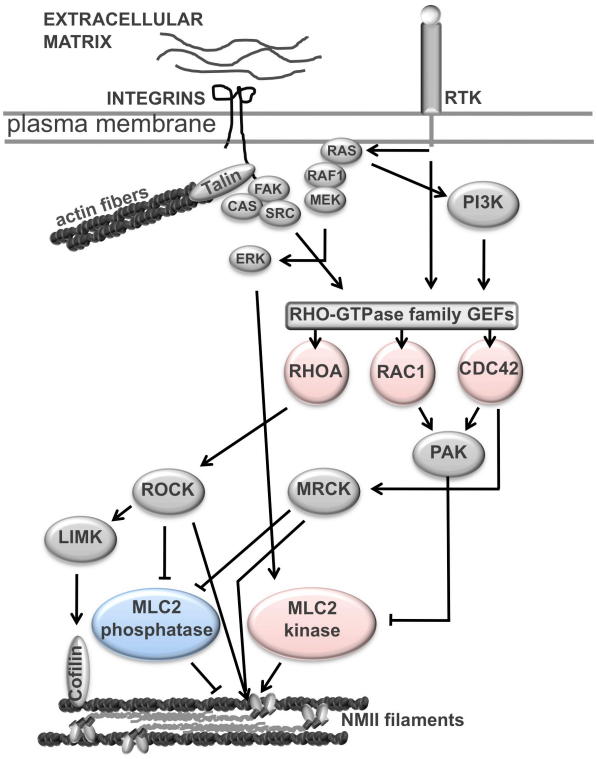

Figure 12: Signalling pathways converging on RHO-GTPases and their effect on the actin cytoskeleton during cell migration. Cofilin regulates actin depolymerization and NMII organizes and remodels actin. ERK-mediated MLCK occurs in presence of fibronectin and requires activation of RHOA and RAC1. The figure idea was based on [Vicente-Manzanares et al 2005].

transfection with oncogenic HRAS [Kumar et al 1991, Janssen et al 1998] or RAS effectors [Coller et al 2000] provoked repression of cytoskeleton protein expression such as tropomyosin [Janssen et al 1998, Coller et al 2000] and regulatory myosin light chain 2 (MLC2) [Kumar et al 1991, Gerrits et al 2012], or it leads to inactivation of actin cytoskeleton regulating kinases such as ROCK1 [Izawa et al 1998]. Moreover, in cancers, RAS mutations lead to overexpression and/or hyperactivation of p21-activated kinase 1 (PAK1), which dissolves stress fibers and reorganises focal adhesions (Figure 12) [reviewed by Dummler et al 2009]. Enforced expression of cytoskeleton proteins can revert the oncogenic HRAS-induced tumourigenic phenotype back to normal [reviewed by Pawlak and Helfman 2002]. Unfortunately, most of what is known about transformation-induced cytoskeleton changes originates from studies looking at either SV40- or oncogenic HRAS-transformation, but not at the alterations that occur if transforming cells with both oncogenes. One could argue that only cytoskeleton alterations induced by HRASG12V are relevant, as it is required to convey all cancer cell-specific features and to fully transform cells such as BJELR or HA1ER. However, one has to consider, that alterations observed with single HRASG12V- transformation might necessitate a normal cellular backbone. These alterations may not fully develop, or could differentially develop if the normal backbone has been disrupted by a previous transformation step with SV40ER. For instance, as ST-transformation is associated with an increase of RAC1 and CDC42 and a decline in RHOA expression levels, HRAS most probably will not impact on stress fiber contraction and focal adhesion formation via the PI3K/RAC1/RHOA pathway in ST-transformed cells (Figure 12). Moreover, as transformation with ST upregulates MYC levels, probably other signalling pathways than MYC-stabilisation by HRASG12V might be of importance. Therefore, studying HRASG12V-induced effects in an SV40ER-pretransformed backbone is essential to manifest differences in the cytoskeleton structure that are critical for features displayed by fully transformed cells.

Actin cytoskeleton and cancer cell apoptosis

For a while it has become clear that the actin cytoskeleton is not only a support giving structure that tents up cells, but that it actively influences incoming signalling pathways such as growth signals and that it controls cell adhesion and migration. In the past 20 years evidence accumulated that the actin cytoskeleton initiates or inhibits apoptosis, which is critical with regard to the disrupted cytoskeletal architecture of transformed cells.

The actin cytoskeleton regulates the intrinsic apoptosis pathway. Evidence for an active role of the actin cytoskeleton to induce or to inhibit apoptosis are manifold and refer to actin itself as well as to actin-binding proteins. Initially it was observed that stabilisation of actin filaments (F-actin) by drug-mediated inhibition of actin depolymerisation (jasplakinolide) induced increased CASP3 activation and mitochondria-dependent apoptosis in different transformed and normal human cells [Suria et al 1999, reviewed by Franklin-Tong and Gourlay 2008]. Accordingly, disruption of the actin cytoskeleton (cytochalasin D) inhibited nitric oxide-induced apoptosis in articular chondrocytes [Kim et al 2003], indicating that stabilisation of F-actin filaments initiated apoptosis. However, partially in the same cell types apoptosis could also be triggered by the destabilisation of F-actin structures using actin-depolymerising agents (cytochalasin D, latrunculin B, sphinxolide) [reviewed by Franklin-Tong and Gourlay 2008], which in some cases was shown to involve mitochondrial cytochrome c release [Suria et al 1999, Paul et al 2006]. It is not known under which conditions F-actin stabilisation or depolymerisation influences entry into apoptosis and there is only one mechanistic explanation for actin alteration-stimulated activation of BCL2 proteins available. A pro-apoptotic BCL2 member (BMF) was found to be sequestered with actin-associated myosin V motors and was released from the actin cytoskeleton upon cell detachment or cytochalasin D treatment resulting in mitochondrial-dependent apoptosis [Puthalakhat et al 2001]. In addition to its apparent 'reservoir' function for pro-apoptotic proteins, nuclear translocation of actin upon treatment of mast cells with actin depolymerising latrunculin A was observed, but did not induce apoptosis [Pendleton et al 2003]. Similarly, it was shown that caspase-generated actin fragments

were targeted to mitochondria after they have undergone N-myristoylation [Utsumi et al 2003]. Moreover, these fragments induced morphological changes resembling apoptotic cells if ectopically expressed in normal 3T3 fibroblasts [Mashima et al 1999]. However, this did not cause caspase activation or cleavage of the caspase substrate and apoptosis marker poly ADP-ribose polymerase (PARP) [Mashima et al 1999]. Thus, nuclear or mitochondrially translocated actin does not seem to have apoptosis-inducing function, but might regulate the progression of apoptosis in a way that has yet to be defined.

In addition to actin itself, several actin-binding proteins have been studied in their relation to mammalian cell apoptosis. These include cofilin (F-actin depolymerising), thymosin β (globular actin sequestering), coronin 1 (F-actin branching), filamin (F-actin branching), gelsolin (actin severing and F-actin capping), tropomyosin (actin stabilising) and myosin II (actin filament contraction or bundling) [reviewed by Franklin-Tong and Gourlay 2008, Leadsham et al 2010, Desouza et al 2012]. For reasons of complexity, the role of actin-branching proteins (coronin, filamin) in apoptosis is not introduced here and can be read elsewhere [Desouza et al 2012].

Likewise it is unknown at which cell state F-actin stabilisation or depolymerisation induces apoptosis, data for certain actin filament severing, capping and depolymerising proteins (cofilin) exist that support both, a protective as well as an apoptosis-promoting function [reviewed by Desouza et al 2012]. Interestingly however, is that actin depolymerising cofilin was shown to translocate to the mitochondrial membrane in response to the kinase inhibitor staurosporin, which resulted in cytochrome c release. Expression of a phosphorylated and inactive cofilin mutant abolished this mitochondrial targeting of cofilin and apoptosis, emphasising the requirement for active de-phosphorylated cofilin in apoptosis [Chua et al 2003]. Cofilin is dephosphorylated by PP2A, which lead to decreased F-actin depolymerisation rates inhibited of actin dynamics and reduced migration of human adenocarcinoma A549 cells, whilst chemical PP2A inhibition (calyculin) restored motility [Oleinik et al 2010]. Thus, cofilin phosphorylation status regulates a ‘flee or die’ situation and provides one explanation for how ST-transformed cells might be protected from apoptosis.

Thymosin ß, which prevents actin polymerisation, disrupted stress fibers and induced apoptosis if overexpressed in fibroblasts [Hall et al 1995], or ovarian cancer cell lines [Lee et al 2001]. Strikingly, overexpression of F-actin stabilising tropomodulin 1 inhibited thymosin ß-apoptosis competing for actin binding [Rho et al 2004]. Whilst

thymosin ß proteins appear to be upregulated in HRASG12V-transformed cells [Nummela et al 2006, reviewed by Sribenja et al 2009], no direct information about tropomodulin 1 expression in SV40 or oncogenic HRAS transformation exists. However, recent studies indicate that certain tropomodulins are downregulated in tissues of oncogenic KRAS-transgenic mice [Lee et al 2009]. These data suggest that HRASG12V-transformed cells might be sensitised to apoptosis via a deregulation of tropomodulin and thymosin ß proteins. If so, neither the mode of protein deregulation, nor the mechanism of pre-sensitisation to apoptosis is known.

Another actin-depolymerising protein that was shown to be downregulated in cells harboring activating KRAS-mutations in colorectal cancer cell lines and primary tumours is gelsolin. Interfering with gelsolin expression using siRNA enhanced CASP9 and CASP7 activation upon butyrate-induced apoptosis [Klampfer et al 2004]. Moreover, overexpression of full-length gelsolin protected Jurkat cells from apoptosis induced via the mitochondrial pathway (ceramide, dexamethasone, staurosporine, thapsigargin and protoporphyrin IX) [Ohtsu et al 1997, Koya et al 2000] and prevented apoptosis in neuronal cells [Harms et al 2004]. Gelsolins protective role has been associtated to its ability to control the closure of mitochondrial ion channels to prevent cytochrome c efflux [Kusano et al 2000]. At the same time, downstream of mitochondrial activation, CASP3-generated gelsolin fragments with high actin severing capacity [Kothakota et al 1997] were capable to induce apoptosis via the nuclear localization and activation of DNAse I [Chhabara et al 2005].

Finally, also several tropomyosin isoforms were evidenced to regulate apoptosis, mainly by coordinating the interaction of other actin-binding proteins with actin [reviewed by Desouza et al 2012]. Notably, tropomyosin 5 (TM5) expression in neuroepithelial cells was found to induce the recruitment of non-muscle myosin IIa (NMIIa) to stress fibers, resulting in reduced cell migration [Bryce et al 2003]. Downregulation of another isoform, tropomyosin 1 (TM1), in mammary epithelial carcinomas was correlated with an increased resistance to detachment-induced apoptosis (anoikis) [Raval et al 2003]. Restoring Tm1 expression in cultured mammary carcinoma cell lines (MCF7 and MBAMB231) led to the generation of distinct actin stress fibers and re-sensitised cells to anoikis [Bharadwaj et al 2005]. Therefore, TM1 represents an important mediator of anoikis, whereby the role of NMII in this process in undetermined.

Generally, involvement of myosin II has mainly been described for TNF-apoptosis and therefore will be introduced in the next paragraph. In essence, actin and actin-binding proteins take a central role in apoptosis, whereby both actin fiber dynamics as well as the intracellular localization of the actin cytoskeleton proteins are of apparent importance in the regulation of BCL2 protein storage, mitochondrial membrane permeabilisation and the intracellular localization of pro-apoptotic factors.

The actin cytoskeleton regulates the extrinsic apoptosis pathway. In addition to their impact on the intrinsic apoptosis pathway described in the previous section, actin cytoskeleton proteins also regulate apoptosis induced by cytokines of the TNF family. Especially the role of actin and ezrin has been analysed, since an interaction of actin mediated by ezrin [Lozupone et al 2004] and moesin [Hebert et al 2008] was demonstrated for FAS. The current FAS signalling model proposes that the interaction of actin and ezrin with FAS is required to localise FAS into lipid rafts and to mediate ligand-stimulated FAS internalisation, which is required for DISC formation and thus FAS-apoptosis. However, regarding the contradictory data in literature, the actual role of actin or ezrin in FAS-apoptosis is far from being understood, as it will be outlined in this paragraph.

Initially it was indicated that actin filament disruption with jasplakinolide treatment of normal epithelial cells induced apoptosis and DISC formation at the FAS receptor in the absence of FASL [White et al 2001]. Contrary, in type I SKW6.4 and H9 lymphoblastoma cells FADD recruitment to FAS, as well as FAS internalization was concluded to require intact actin fibers [Algeciras-Schimnich et al 2002], although the applied disruption of actin fibers with latrunculin A at least in H9 cells lead to reduced FADD expression and total FAS expression was not controlled. Evidence for an actin cytoskeleton-dependent regulation of TNF (and –related?) protein expression exists, since F-actin disruption using cytochalasin D blocked LPS-induced expression of TNFα in monocytes [Rosengart et al 2002] and RAC1 siRNA depletion reduced FASL mRNA levels in Jurkat cells [Ramaswamy et al 2007]. In line with Algeciras-Schimnich study, in FASL-sensitive, type-I activated CD4+ T lymphocytes [Parlato et al 2000] and HIV-specific CD8+ T-cells [Petrovas et al 2007a] actin filament disruption with cytochalasin D and/or latrunculin A reduced percentages of FAS-induced annexin V-positive cells

[Parlato et al 2000, Petrovas et al 2007a] and disordered the polarised FAS distribution observed prior to FASL stimulation [Parlato et al 2000]. Again, both studies did not exclude that actin cytoskeleton rupture was not associated with a decline in FAS or DISC protein expression levels. Finally, in type II cells actin filament disruption using cytochalasin increased TRAIL-apoptosis, which was not associated with an enhancement of CASP8 activation [Gasparian et al 2008]. As this study did not demonstrate that CASP8 expression levels upon cytochalasin D were unaltered, it remains unclear whether an intact actin cytoskeleton is required for the expression of FAS and DISC components, and/or whether it is required for the DISC formation process itself.

Ezrin originally was found to colocalise with FAS in FAS-sensitive, activated CD4+ T lymphocytes, as evidenced in cell fractionation assays and immunocytochemistry, latter demonstrating a polarised ezrin/FAS distribution. Ezrin depletion resulted in reduced FAS-stimulated percentages of annexin V positive cells and a scattered FAS distribution [Parlato et al 2000], which implied that the ezrin-mediated polarisation of FAS in activated CD4+ T lymphocytes is required to sensitise cells to FAS-apoptosis. Congruently, ezrin was co-immunoprecipitated with FAS from FAS-sensitive, but not from FAS-resistant T lymphocytes [Luciani et al 2004]. However, one should note that this study neither proved comparable FAS expression levels in the investigated cells nor comparable FAS immunoprecipitation levels. Regarding these missing but essential informations it therefore does not seem surprising that contradictory data for the role of the ezrin/FAS interaction in FAS-apoptosis exist. Namely, in type I signalling H9 T lymphoblastoma cells ezrin knockdown increased the percentages of FASL- or TRAIL-induced annexin V-positive cells. Moreover, ezrin knockdown in activated peripheral blood T lymphocytes or expression of dominant negative ezrin mutants in type I H9 lymphoblastoma cells increased percentages of FASL-induced annexin V-positivity. Finally, ezrin depletion enforced the FASL-stimulated activation of the CASP cascade in whole cell lysates [Kuo et al 2010]. However, the proapoptotic effect of ezrin loss regarding DISC formation remains unclear, as apparently more FAS was immunopurified from ezrin knockdown H9 lymphoblastoma cells, which puts the reported increased DISC formation into question [Kuo et al 2010]. Contrary to a report that indicated actin as an important constitutent of the endocytotic machinery that internalises FAS after induction in type I signalling SKW6.4 and H9 lymphoblastoma

cells [Algeciras-Schimnich et al 2003], this study denoted that FASL-induced internalization of FAS was unaffected by ezrin knockdown in exactly the same cell type (H9 lymphocytes) [Kuo et al 2010]. Thus, either actin does not play a role in FAS internalisation, or ezrin alone does not mediate binding of actin to FAS. Apparently, latter situation is the case, as also moesin (but not radixin) was reported to bind FAS [Hebert et al 2008]. Finally, the question of whether in type II signalling cells ezrin loss influences FAS-apoptosis or not was not convincingly solved by the Kuo study, as ezrin knockdown efficiencies in type II cells appear lower than in type I cell and loading controls seem to fluctuate. Interestingly, in type I signalling H9 lymphoblastoma cells time-course analysis of the FAS-DISC demonstrated that with increasing time of FASL-stimulation and DISC formation, ezrin was lost from FAS. In addition, ezrin KD enhanced FAS-apoptosis [Kuo et al 2010]. Contrary, in type II Jurkat cells the interaction of ezrin (and moesin) with FAS and ezrin and moesin phosphorylation levels increased over time of FASL treatment. Knockdown of either ezrin or moesin did not inhibit FADD or CASP8 association with FADD, but decreased CASP8 cleavage and FAS-mediated apoptosis [Hebert et al 2008]. These results indicate that the FASL-induced ezrin regulation and maybe even basal ezrin activity seem to fundamentally differ in type I and type II signalling cells. ERM proteins and their interaction with other proteins are regulated by phosphorylation/dephosphorylation events. ERM proteins are activated by RHOA/ROCK-mediated phosphorylation, whilst they are inactivated via constitutively active RAC1-stimulated dephosphorylation. Treatment of type II signalling Jurkat cells with aplidin, an actin cytoskeleton reorganising agent that acts via the activation of RAC1 [Gonzalez-Santiago et al 2006], lead to the clustering of FAS, DR5, FADD, CASP8, CASP10, ezrin, moesin, RHOA and RHO-GDP dissociation inhibitors (RHO-GDI) into lipid rafts and FAS-dependent apoptosis. Pretreatment of cells with actin cytoskeleton disrupting cytochalasin B or jasplakinolide in turn prevented aplidin-induced apoptosis and FAS-clustering into ‘caps’ [Gajate and Mollinedo 2005]. Similarly, in type I signalling T cell receptor (TCR)-stimulated CD4+ T cells were sensitive to FASL-apoptosis, which correlated with TCR-induced FAS translocation to lipid rafts and ERM protein dephosphorylation. RAC1 knockdown reduced FAS antibody-induced apoptosis in TCR-activated T cells [Ramaswamy et al 2007]. Thus, actin and actin-linking proteins regulate aplidin- or TCR- induced translocation of DISC components into lipid rafts via the activation of RAC1 and in this way it might prone cells for FAS-apoptosis. Of note,

also RHOA signalling and the actin-remodelling proteins filamin and cofilin are used in actin-dependent receptor clustering processes [Jimenez-Baranda et al 2007, Yoder et al 2008]. One model for FAS resistance was proposed based on the lack of FAS internalisation as a result of a defect in in the regulation of ezrin. In fibroblasts and fetal liver cells it was shown that FAS stimulation induced RAF1/ROCK2 clusters. Thereby, RAF1 which interacts directly with cFLIP [Kataoka et al 2000], restrained ROCK2 activity and therefore ezrin phosphorylation required for FAS/actin interaction, FAS internalisation and hence FAS-DISC formation [Piazzolla et al 2005]. Since RAF1, which plays an essential role in maintaining the cytoskeleton organisation and thus in cell polarity and migration [Ehrenreiter et al 2005], counteracts apoptosis additionally through inhibition of the proapoptotic kinases ASK1 and MST2 [reviewed by Matallanas et al 2011], it will be interesting to decipher the contribution of each these kinases in FASL-apoptosis. Concludingly, it remains to point out that even though no co-immunoprecipitation data of actin or ezrin for the other TNF death receptors TNFR1, DR5 and DR4 exist, an association of DR5 and DR4 with the cytoskeleton in general or with actin and ezrin is often described in literature. Given the current unclear picture for the actual role of actin and ezrin in FAS-signalling, the role of these proteins in TRAIL-signalling remains to be elucidated.

Less contradictory, probably because not as much studied examples for the regulation of TNF cytokine-induced apoptosis by cytoskeletal proteins are for instance thymosin ß, which enhanced TNFα-induced apoptosis when overexpressed in normal fibroblasts [Hall et al 1995], or gelsolin which inhibited FAS-mediated apoptosis of overexpressed in type II Jurkat cells [Ohtsu et al 1997]. Importantly, the actin-binding and crosslinking non-muscle myosin II (NMII), which conveys contractile properties to F-actin, has been marginally implicated in the extrinsic apoptosis regulation. In case of TNFα-signalling, NMII activity, measured at the level of MLC2 phosphorylation, was linked to the transport of TNFR1 from the trans-Golgi-network to the plasma membrane. If NMII were activated overexpressing the NMII regulatory kinase MLCK in normal epithelial Madin-Darby canine kidney (MDCK) cells, or treating cells with ionomycin or endotoxin, cell surface levels of TNFR1 transport was increased. Moreover, MLCK overexpression accelerated TNFα-induced apoptosis, whilst a dominant-negative (DN) MLCK version delayed apoptosis [Jin et al 2001]. Notably, apoptosis was quantified as the number of viable cells still attached after TNFα-treatment and total apoptosis

outcomes were not reduced by DN-MLCK expression. Another study conducted in normal pulmonary endothelial cells reported that NMII activity promoted TNFα-apoptosis and observed a TNFα-induced increase in MLC2 phosphorylation levels. Inhibition of MLCK (ML7) or ROCK (Y-27632) attenuated TNFα-induced stress fiber formation as well as relative percentages of apoptotic cells positive for annexin V and percentages of CASP8 activity [Petrache et al 2001]. Distinguishing between the two NMII isoforms NMIIa and NMIIb in HeLa cells, immunoprecipitation of NMIIb revealed co-purification of clathrin. Moreover, siRNA-mediated NMIIb depletetion resulted in consistent TNFR1 surface levels upon TNFα-stimulus as well as impaired CASP8 cleavage. Therefore, NMIIb was concluded to function in TNFR1 internalisation. Protein depletion of NMIIa neither reduced levels of TNFR1 internalisation nor CASP8 activation. The apoptosis-promoting function of NMIIb was deduced to occur independent of the actin myosin contractility, as neither NMII (blebbistatin) nor actin depolymerisation (cytochalasin D) inhibited CASP8 or CASP3 cleavage. Even though it was attempted, TNFR1 could not be co-immunoprecipitated with NMIIb [Flynn and Helfman 2010]. Similar to TNFα signalling, FAS-receptor clustering appeared to be actin- but not NMII-dependent, as the myosin inhibitor 2-3-butanedione monoxime showed no effect in suspension cells (SKW6.4 B cell lymphoma) [Algeciras-Schimnich et al 2002].

Non-muscle myosins II (NMII)

Myosins are actin-based ATP-driven motor proteins of which there are as yet 12 classes identified in humans (Figure 13). Most of what is known about myosin function and regulation was studied on class II myosins, which are unique compared to other myosins for their capacity to form filaments [reviewed by Sellers 2000]. Members of the myosin II family are hexameric proteins consisting of 2 heavy chains, 2 essential (ELC) and 2 regulatory light chains (MLC2). Myosins II are distinguished in dependence of their heavy chain, encoded by 13 different genes. The sequence of the motor domain, located in the head domain of the heavy chain, subdivides myosins II into skeletal/cardiac and muscle/non-muscle isoforms. With few exceptions, the single muscle and the 3 different non-muscle heavy chains are ubiquitously expressed in

muscle and non-muscle cells, although to varying concentration levels [reviewed by Eddinger and Meer 2007]. Contrary to the heavy chains, nothing is known about a functional difference of the 3 distinct MLC2 isoforms expressed in non-muscle cells. The 3 human MLC2 genes *MYL9*, *MYL12A* and *MYL12B* encode smooth muscle MLC2 (smMLC2), non-muscle-like MLC2 (nmlMLC2) and non-muscle MLC2 (nmMLC2), whose protein sequences are highly homologue, so that no antibody exists that can distinguish between these isoforms [Gerrits et al 2012]. The non-muscle myosins II (NMII), which are implicated in such diverse processes as adhesion, migration, vesicle transport from the Golgi, receptor capping [Jimenez-Baranda et al 2007, Yoder et al 2008, reviewed by Maravillas-Montero and Santos-Argumedo 2012], endocytosis [Rey et al 2007], apoptosis (as described in a previous section) and virus entry [Arii et al 2010, reviewed by Taylor et al 2011] and egress [van Leeuwen et al 2002], will be described in more detail in this chapter.

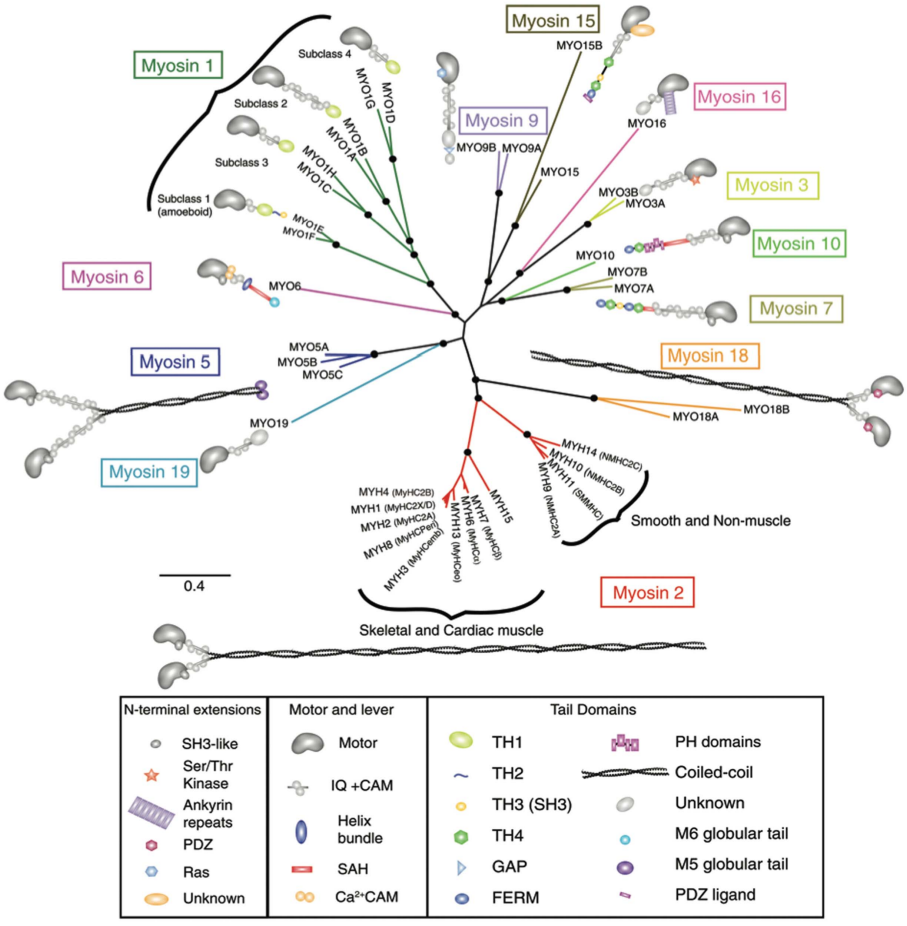

Figure 13: Phylogenetic tree of the human myosin family. Structural features of the single myosin domains are indicated as illustrated in the legend below the tree. Class II myosins are unique for their filament formation capacity and are subdivided into muscle and non-muscle forms according to their motor domain sequence. The figure is taken from [Peckham and Knight 2009].

NMII structure and function. Like all class II myosins, NMII molecules are composed of 2 heavy chains (NMHCII), have a globular adenosine triphosphate (ATP)- and actin-binding head which is capable of independent force generation, and an elongated coiled coil tail that allows NMHCII to dimerise (Figure 14, A) and then aggregate to form bipolar myosin filaments (Figure 14, B). The NMHCII have a flexible neck region, which comprises the ELC and MLC2 binding sites. Whilst ELC binding stabilises the NMHCII structure, MLC2 regulates NMII activity [reviewed by Vicente-Manzanares et al 2009]. Mammalian muscle and non-muscle cells express 3 different NMHCII genes, *MYH9*, *MYH10* and *MYH14* encoding the NMHCII isoforms NMHCIIa, IIb and IIc. NMHCIIa is most abundant compared to other NMHC isoforms in human lung, spleen, thymus, uterus, and colon, whereas neurons are enriched in NMHCIIb [Golomb et al 2004]. Only few examples exist where cells do not express all 3 protein isoforms (NMHCIIa-only cells: T cells [Jacobelli et al 2004], HeLa cells [Wei and Adelstein 2000], basophilic leukemia cell line RBL2H3 [Sellers 2000], mouse megakaryocytic and granulocytic lineages [Marigo et al 2004]; NMHCIIb-only cells: Cos-7 cells [Helfman et al 1999, Bao et al 2005]). Notably, no comparative expression study of all 3 NMHCII isoforms in human cells or tissues is available. So far, only mutations in NMHCIIa have been associated to human disease, causing kidney and platelet defects [Golomb et al 2004]. The NMHCII protein isoforms are highly homologous in their amino acid sequence (Figure 14, B & C).

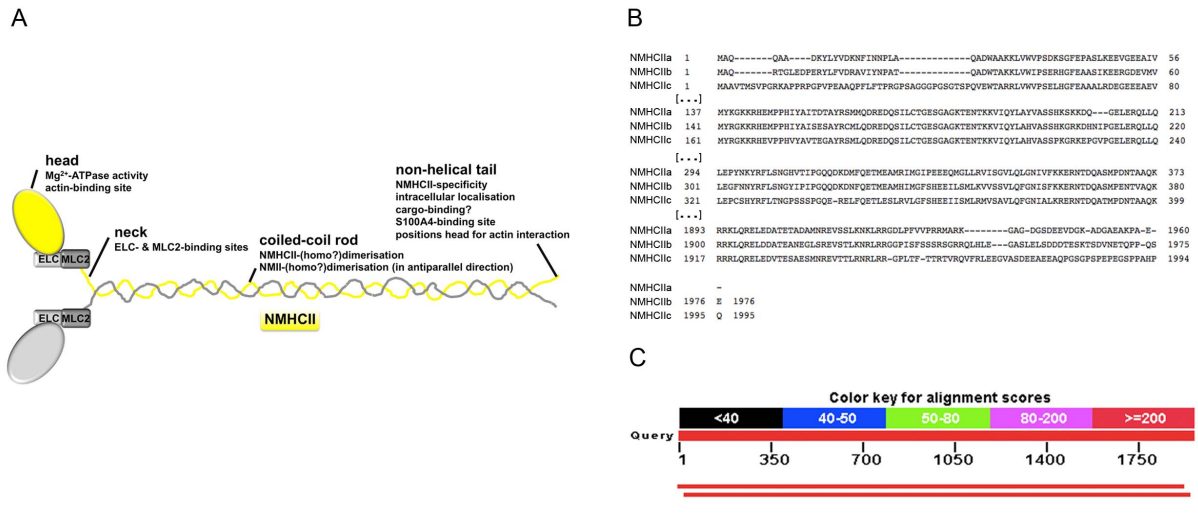

Figure 14: Non-muscle myosin II (NMII) molecule structure and heavy chain (NMHCII) protein homology. **(A)** Schematic structure of an NMII molecule indicating the main NMHCII (yellow) domains. **(B)** Protein sequence alignment of the human heavy chain isoforms NMHCIIa, IIb and IIc. **(C)** Graphical summary of the protein sequence alignments of human NMHCIIa versus IIb (upper red lane) and human NMHCIIa versus IIc (lower red lane). For alignments in (B) and (C) NCBI-BLAST Align [Altschul et al 1990] was used.

Whilst NMHCIIc differs from NMHCIIa and IIb in the N-terminal motor domain sequence, NMHCIIa and IIb are distinguished by only a few amino acids in their C-terminal tail region. Owing to the location of their amino acid sequence variance in their N- or C-terminal part, NMII isoforms display different Mg^{2+}-ATPase activity, which is the ability to hydrolyse ATP to adenosine diphosphate (ADP) and inorganic phosphate (Pi), and intracellular localisation. Importantly, NMII binding to actin is ADP-dependent and is thus influenced by the ATP hydrolysis speed (Figure 15, A). If ATP binds to the NMII head, the head takes on a conformation, which cannot bind actin (Figure 15, A, 1). When ATP gets hydrolysed, the NMII head swings into a cocked position, whereby ADP and Pi remain bound (Figure 15, A, 2). As soon as Pi leaves the NMII molecule, the head binds actin and a power stroke is released (Figure 15, A, 3). Finally, ADP is liberated to continue the cycle, a stage at which the NMII head is tightly bound to actin (Figure 15, A, 4). Whilst at steady-state NMII Mg^{2+}-ATPase activity is low, it is drastically induced in the presence of actin [Ramamurthy et al 2004] and can be enhanced by MLC2 phosphorylation [reviewed by Vicente-Manzanares et al 2009]. Amongst the NMII isoforms, NMIIa has the highest ATP hydrolysis rate and thus attaches and detaches more rapidly from F-actin than NMIIb and NMIIc, which hydrolyse ATP at the same speed [Golomb et al 2004]. As NMIIb hydrolyses ATP slower than NMIIa, it consumes less energy and the tension durations of NMIIb on actin fibers are longer. Apparently, only in motile cells a distinction between the subcellular distrubution of NMIIA and NMIIB can be made. Particularly, NMIIA is commonly found to enrich in the front of migrating cells relative to IIB, whereas NMIIB generally accumulates in the cell rear

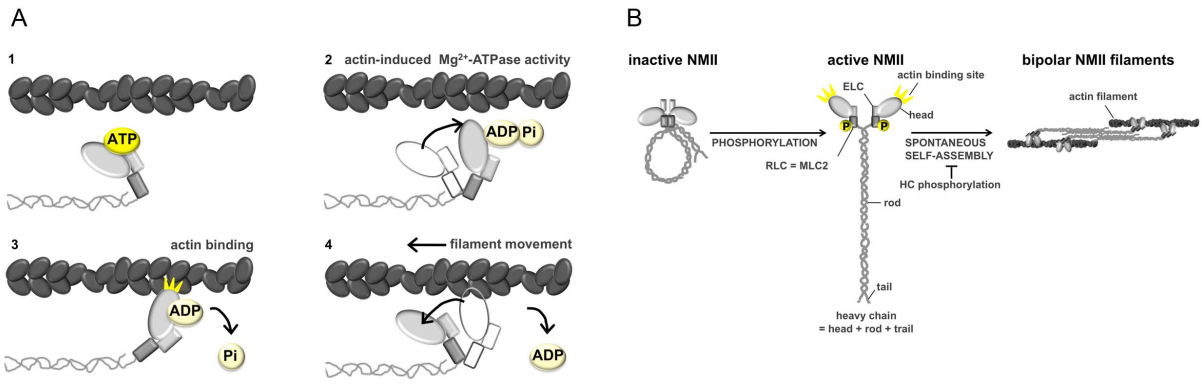

Figure 15: The Mg^{2+}-ATPase cycle and non-muscle myosin II (NMII) activation by regulatory myosin light (MLC2) phosphorylation. **(A)** Schematic representation of the Mg^{2+}-ATPase cycle conducted by the NMII head domain, which regulates the binding to actin and generation of tension on actin fibers. For details see text. **(B)** Regulation of NMII Mg^{2+}-ATPase activity and filament formation capacity by phosphorylation of MLC2.

[Kolega 1998, Saitoh et al 2001, Kolega 2003, Vicente-Manzanares et al 2008]. Using protein chimeras with exchanged C-terminal tails of NMHCIIa and NMHCIIb, it was demonstrated that the C-terminal tails determine the intracellular localisation of NMII isoforms [Sandquist and Means 2008]. NMII localise to actin fibers, whereby all 3 NMII isoforms are thought to perform the same two basic functions at the molecular level, namely, assembly into bipolar filaments and contraction of F-actin in an ATP-dependent manner [reviewed by Conti and Adelstein, 2008]. Although NMII isoforms colocalise in actin filaments, there is so far no indication for heterodimer formation between the three NMHCII isoforms. Contrary, each of the 3 MLC2 isoforms optimally bind to all NMHCII isoforms and are suggested to fine-tune NMII action [Park et al 2011]. Since NMII convey contractility to actin fibers, NMII function in cell migration. Moreover, active NMII mediate the maturation of integrin-mediated cell adhesions (Figure 16) [Choi et al 2008, reviewed by Vicente-Manzanares et al 2009]. Mechanistically, it is thought that adhesion maturation involves NMII-facilitated bundling of actin fibers, in turn leading to the clustering of adhesion proteins at the end of actin fiber. Another hypothesis suggests that NMII generate force on tension-sensitive adhesion proteins (e.g. fibronectin, talin, p130CAS), resulting in the uncovering of otherwise buried protein modification sites that represent new docking sites for signalling molecules promoting adhesion maturation. Latter theory refers to the principle of mechanotransduction, the

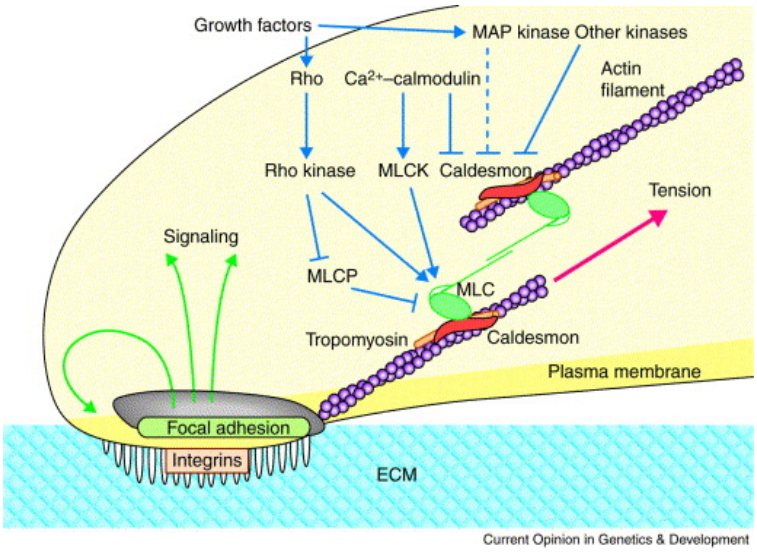

Figure 16: Actin cytoskeleton proteins regulate cell contractility and adhesion-dependent signaling. NMII (green) and actin filaments (purple) exert tension on integrins at focal adhesions, which affects adhesion-dependent signaling. This signaling, in turn, promotes further assembly of the focal adhesions and also induces downstream events such as cell proliferation and suppression of apoptosis. Whilst MLCK and the RHOA/ROCK pathway positively regulate tension, CALD negatively impacts on tension. Reprinted from [Pawlak and Helfman 2001], with permission from Elsevier.

perception of and reaction to a mechanical force, whereby a mechanical stimulus is converted into into a chemical signal [reviewed by Jaalouk and Lammerding 2009, Wang et al 2009]. On the basis of mechanotransduction, exposure of normal endothelial cells to stretching can activate RAS, ERK, JNK, RHO-GTPases and tyrosine kinases, processes that depend on integrin-mediated adhesion. *In vivo,* NMHCIIa knockout in mice lead to lethality at embryonic day 6.5. Since mice displayed severe defects in cell-cell adhesions, death preceded organogenesis. Depletion of NMHCIIb caused embryonic lethality at day 14.5, associated with brain and heart defects based on failures in cell adhesion and migration [Ma et al 2007]. Gene substitution of NMIIb by NMIIa did not rescue the lethal phenotype, but brain defects that were not associated to defects in migration [Bao et al 2007]. Thus, in addition to their function in the maturation of cell-substratum adhesions, NMII maintain the integrity of cell-cell adhesions required for epithelial cell polarisation and morphogenesis [Zhang et al 2011]. Whilst in the preservation of cell-cell adhesion integrity NMIIa and NMIIb can functionally substitute each other, in the promotion of cell migration they cannot as this process is dependent on ATPase activity. Unfortunately there is not much known about the function of NMHCIIc, but NMHCIIc knockout mice are vital and show no obvious defects [reviewed by Vicente-Manzanares et al 2009].

Regulation of NMII activity. The biochemical properties of NMII, Mg^{2+}-ATPase activity and filament formation capacity, are regulated through phosphorylation and/or non-covalent binding of regulatory proteins. As previously mentioned, the Mg^{2+}-ATPase activity of NMII at steady state is low and is potentiated in the presence of actin. Upon phosphorylation of MLC2 at Ser19 the ATPase activity is even more enhanced and can still increase if MLC2 is additionally di-phosphorylated at Thr18. Contrary, the presence of caldesmon 1 (CALD1), an F-actin binding protein, inhibits the NMII ATPase activity by blocking the NMII/actin interaction. And finally, the inhibitory effect of CALD1 is reverted by CALM, a protein that is homologous to the N-terminal region of MLC2 [Solaro and Hasenfuss 2005], but contrary to MLC2, has kept its ability to bind calcium (Ca^{2+}). Due to its similarity in structure, CALM binds to the neck region of diverse myosin heavy chains, but not to the neck of NMII [Reynaert et al 2005]. However, CALM can indirectly impact on NMII [Marston and Smith 1985, Smith et al 1987, Wang et al

1997] by binding to actin, CALD and MLCK [Wang et al 1991]. The regulation of MLC2 phophorylation at Ser19/Thr18 is highly complex and several kinases are capable to carry out this phosphorylation. Amongst those kinases are MLCK [Ikebe and Hartshorne 1985], RHO-associated kinase 1 and 2 (ROCK1, ROCK2) [Suzuki et al 1999, Ueda et al 2002, Ren et al 2004a], citron kinase (CK) [Yamashiro et al 2003], myotonic dystrophy kinase-related CDC42-binding kinase (MRCK) [Tan et al 2008], death-associated protein kinase 3 (DAPK3) [Murata-Hori et al 2001], PAK1 [Tan et al 2008] and integrin-linked protein kinase (ILK) [Deng et al 2001, Huang et al 2006]. MLC2 phosphorylation is reverted by myosin phosphatase (MLCP), which can be inactivated by some of these MLC2 phophorylating kinases (Figure 17). Generally, the MLC2 Ser19/Thr18 phosphorylating kinases are activated via different routes. For instance, MLCK is activated by Ca^{2+}-CALM binding and so far MLCK appears to only phosphorylate MLC2 [reviewed by Vincente-Manzanares et al 2009]. The major pathway that increases NMII activity resulting in contraction, migration and cancer cell metastasis is via the RHOA-mediated activation of ROCK1. ROCK1 activity leads to an increase in MLC2 phosphorylation via two ways, first it phosphorylates and inactivates a regulatory subunit (MYPT1) of MLCP and thus blocks MLCP-mediated dephosphorylation of MLC2, and second it directly phosphorylates MLC2 [reviewed by Somlyo and Somlyo 2003, Rottner and Stradal 2011]. Notably, RHOA also activates CK to phosphorylate MLC2. In contrast, MRCKß is stimulated by CDC42 and activates NMII via MLCP-inactivating phosphorylation of MYPT1 and and by MLC2 phosphorylation [reviewed by Vicente-Manzanares et al 2005]. Activation of DAPK3, in turn, involves its activating phosphorylation by ROCK1 [Yamashiro et al 2003, Hagerty et al 2007] and thus seems

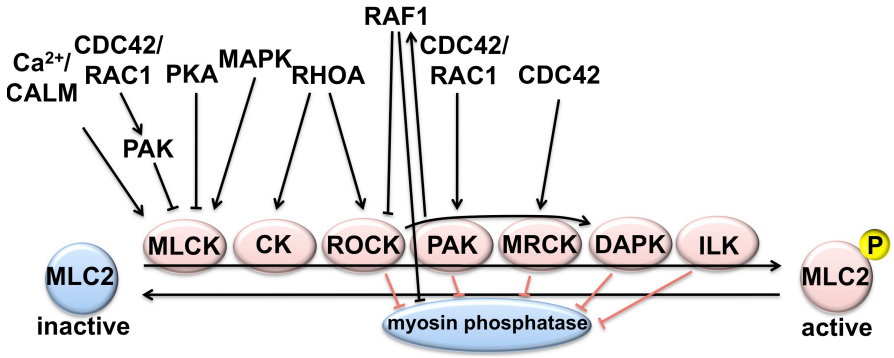

Figure 17: Complexity of MLC2 Ser19/Thr18 phosphorylation. Many MLC2 Ser19/Thr18 phosphorylating and activating kinases (red) also phosphorylate and inactivate (red lines) MLC2 de-phosphorylating and inhibiting myosin phosphatase (blue). For details see text. The figure is based on the idea of [Matsumura et al 2005].

to depend on RHOA. Activated DAPK3 phophorylates MYPT1 to inhibit MLCP and at the same time phosphorylates MLC2 to activate NMII. PAK1 is activated upon binding of the RHO-GTPases RAC1 and CDC42 and similar to DAPK3, PAK1 inactivates MLCP, activates MLC2, and, in addition, inhibits MLCK by phosphorylation [Sanders et al 1999]. Finally, ILK, which connects integrins to the actin cytoskeleton and regulates adaptor molecule recruitment and integrin signalling, is activated by integrin-mediated cell adhesion, which recruits FAK to subsequently activate PI3K and then ILK. Of note, increase in NMII activity does not necessarily require MLC2 phosphorylating kinase activities, but can solely be facilitated by MLCP. For instance, PKC, which phosphorylates and activates an inhibitory subunit (CPI17) of protein phosphatase 1 (PP1), leads to PP1 inhibition, which blocks its MLCP-activating dephosphorylation, resulting in increased MLC2 phosphorylation levels [reviewed by Somlyo and Somlyo et al 2000]. As mentioned above, also the assembly of NMII molecules into filaments is regulated by MLC2 phosphorylation [Scholey et al 1980, Ikebe et al 1988]. Although *in vivo* demonstration is lacking, *in vitro* sedimentation experiments showed that if MLC2 is phosphorylated, the head-tail interaction of the closed, circular, inactive NMII structure is disrupted and opens into a linear shape capable to form bipolar filaments with other NMII molecules (Figure 15, B). The opposite effect, the disassembly of NMII filaments, is caused by 2 events (Figure 18). Either the phosphorylation of NMHCII in the coiled-coil rod or the non-helical tail region by diverse kinases, or the binding of the metastasis-associated S100 calcium-binding protein A4 (S100A4) to the NMHCII tail induces NMII filament disassembly. Binding of S100A4 is inhibited by casein kinase 2 (CK2)-mediated phosphorylation of the NMHCII tail [reviewed by Vicente-Manzanares et al 2009]. Whilst filament disassembly by NMHCII phosphorylation is thought to regulate NMII contractility, dismantling of NMII fibers by S100A4 usually occurs at the leading edge of tumour cells and is therefore thought to enable tumour cell dissemination [reviewed by Clark et al 2007]. Importantly, CDC42 can activate RAC1 and high RAC1 activity can effectively inhibit NMII contractility by inducing NMHCII phosphorylation through RAC1 effector kinases like PAK1 [Even-Faitelson and Ravid 2006]. RAC1 signalling is counteracted by ROCK1 [reviewed by Rottner and Stradal 2011]. Thus, RHO-GTPases are essential regulators of NMII activity.

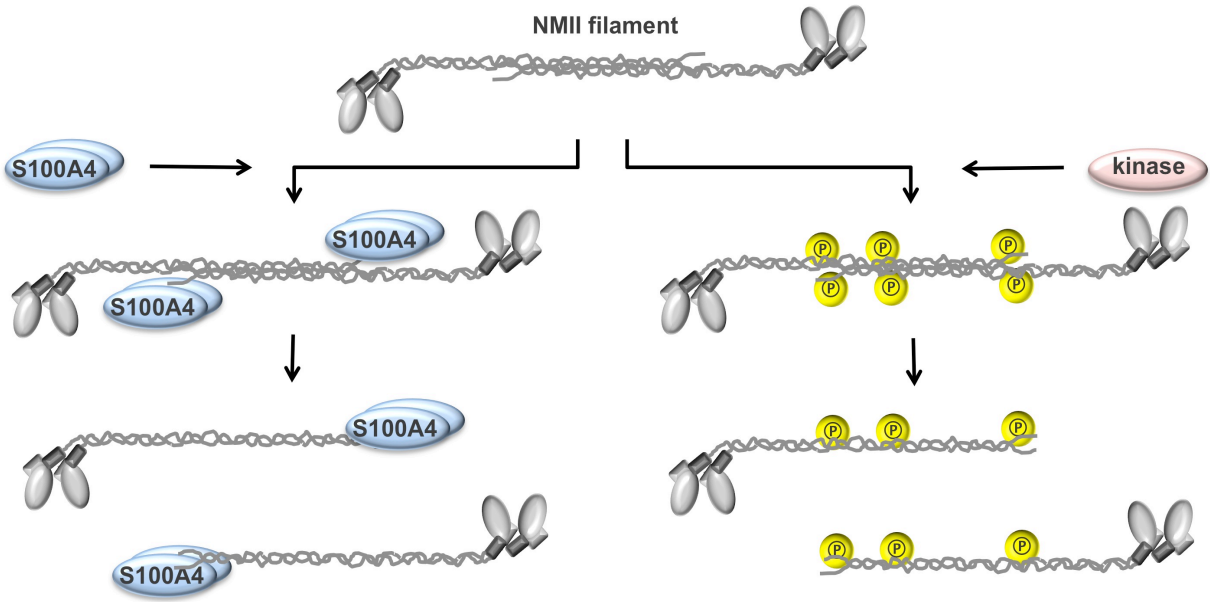

Figure 18: NMII filament disassembly is promoted by non-covalent binding of regulatory proteins or NMHCII phosphorylation. Proteins like S100A4 (blue) bind to the non-helical NMHCII tail, which is essential for NMII bipolar filament formation (left). Phosphorylation (yellow) of NMHCII by various kinases (for instance PAK1) (red) destabilises the electrostatic interactions between the coiled-coil NMHCII rods. The figure is based on the idea of [Clark et al 2007].

AIMS OF THE THESIS

The overall aim of the thesis was to contribute to our understanding of the molecular features that account for the tumour-selective apoptosis induction by TRAIL. By applying commonly used immunoprecipitation, Western blot and mass spectrometry methods, the DISC composition of TRAIL-resistant normal cells and TRAIL-sensitive transformed cells was defined. The individual subgoals included in this thesis were:

- To overexpress, affinity-purify and biologically validate the extracellular, soluble portion of untagged recombinant human TRAIL (amino acids 114-281).

- To immunoprecipitate and analyse the native DISC composition of normal and transformed cells using antibodies directed against single DISC components.

- To identify differentially represented factors in the DISC of TRAIL-insensitive and TRAIL-sensitive cells by mass spectrometry.

- To scrutinise identified factors regarding their impact on tumour-selective apoptosis using pharmacological inhibition and knockdown strategies.

MATERIALS & METHODS

Antibodies. For immunoprecipitation (IP) anti-CASP8 p20 (C-20) (Santa Cruz), anti-DR4 (R&D), anti-DR5 (Diaclone or R&D), anti-immuneglobulin G (IgG) (human IgG, in-house purification) and anti-TRAIL (R&D) were used. For Western blot analysis anti-ßACT (ACTBD11B7) (Santa Cruz), anti-phospho BAD (Ser112) (Cell Signaling), anti-Bid (Cell Signaling), anti-CALD (Sigma), anti-CALM (Upstate), anti-cleaved CASP3 (ASP175) (Cell Signaling), anti-cleaved CASP7 (Asp198) (Cell Signaling), anti-CASP8 (1C12) (Cell Signaling), anti-CASP9 (Cell Signaling), anti-CASP10 (MBL), anti-cFLIP, anti-DcR1 (Chemicon), anti-DcR2 (Chemicon), anti-DR4 (Chemicon), anti-DR5 (Sigma), anti-FADD (BD Laboratories), anti-MEK1/2 (Cell Signaling), anti-phospho MEK1/2 (Ser217/221) (Cell Signaling), anti-MLC2 (Cell Signaling), anti-phospho MLC2 (Thr18/Ser19) (Cell Signaling), anti-MLCK (Sigma), anti-NMHCIIa (Sigma), anti-NMHCIIb (Sigma), anti-PAK1 (Cell Signaling), anti-PARP (Cell Signaling), anti-RAF1 (BD Biosciences), anti-phospho RAF1 (Ser338) (Cell Signaling), anti-ROCK1 (BD Biosciences), anti-TIF1a (in-house generated mouse monoclonal AB), anti-TRADD (Santa Cruz), anti-TRAIL (R&D). Secondary antibodies produced in chicken (Santa Cruz) were used when revealing for proteins in inputs or IPs. Secondary antibodies used for Western blot analysis of whole cell lysates originated from Santa Cruz or Cell Signaling. For fluorescence-activated cell sorting (FACS) analyses phycoerythrin (PE)-labeled anti-Apo2.7 (Beckman Coulter), anti-DR5-PE (Diaclone) and anti-IgG1-PE (Beckman Coulter) were applied.

Apoptosis assays. The mitochondrial membrane protein 7A6 was used as apoptosis marker. The protein of unknown function is also called APO2.7 after the monoclonal antibody recognising the protein. If human cells undergo cell death by apoptosis the 7A6 antigen flips on the outside of the mitochondrial membrane and marks one of the earliest events in the apoptosis process (Figure 19) [Zhang et al 1996, Koester et 1997, Büssing et al 1999]. Unless otherwise indicated, all following volumes and cell numbers refer to 1 cm^2 growth surface of cell culture vessel. Cells treated in apoptosis assays were plated 1d prior to rhTRAIL treatment at a density of $10x10^4$ cells in case of BJAB cells, $10x10^3$ cells if BJ cells were assayed or $50x10^3$ cells if BJELR cells

were investigated. Cells were plated in 250µL medium. In knockdown experiments, which required prolonged cell culture prior to apoptosis assay, the cell culture medium was renewed 1d ahead of rhTRAIL addition. Treatment with rhTRAIL itself was performed in 175 µL conditioned medium. Pre-dilutions of rhTRAIL were generated at appropriate concentrations so that 2.5µL of the cytokine dilution could be added per well. After 16h incubation cell supernatants were collected in FACS tubes and cells were rinsed once with 250µL phosphate buffered saline (PBS) that also was collected in the FACS tube. Adherent cells were trypsinised with 125µL 0.5% trypsin-ethylenediaminetetraacetic acid (EDTA) (Gibco). To ensure the generation of single cell suspensions, cells were monitored under the microscope and if necessary cells were carefully triturated with pipettes. Detached cells were transferred to the FACS tubes and the cell culture well was washed with 500µL PBS. Thereafter viable and dead cells were pelleted at 240xg and 4°C for 5 min. The supernatants were removed and cells were

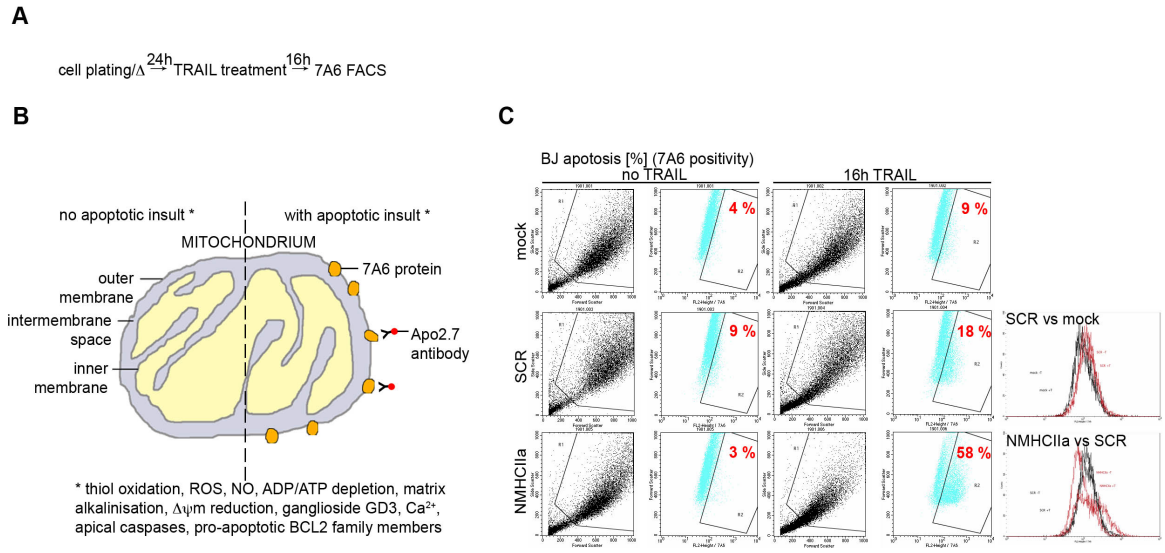

Figure 19: Experimental set-up and principle of 7A6 apoptosis assays. (A) Cells used in apoptosis assays were plated or the cell culture medium was renewed (Δ) 24h prior the start of rhTRAIL treatment. For 16h cells were incubated with rhTRAIL, collected, immunostained for the antigen 7A6 and analysed by FACS. (B) The outer mitochondrial membrane of viable cells is negative or weakly positive for the protein 7A6, which translocates to the outer mitochondrial membrane upon apoptotic insult. Permeabilisation of apoptotic cells allows cell entry of the 7A6-specific monoclonal antibody Apo2.7 that is directly labeled with a fluorescence dye. (C) Representative FACS plots of normal (BJ) cells that were transfected with lipofectamine (mock), scrambled control siRNA (SCR) or siRNA targeting non-muscle myosin heavy chain IIa (NMHCIIa). Cells were left untreated (no rhTRAIL) or were treated with 1µg mL^{-1} rhTRAIL for 16h (16h rhTRAIL). Plots depict total cell populations that were gated for analysis in black and cell populations plotted versus fluorescence in blue. Gated blue cell populations are positive for 7A6 (Apo2.7 fluorescence) and cell percentages are given in red. Plots to the very right show fluorescence intensities of 7A6 positive cells in an overlay, whereby mock, respectively SCR control cells are depicted in black and SCR, respectively NMHCIIa knockdown cells are shown in red.

permeabilised adding 100µL of an ice-cold solution of digitonin, dissolved at a final concentration of 0.1µg mL-1 in 0.25% fetal calf serum (FCS) and PBS. To ensure proper permeabilisation, cells were again carefully pipetted up and down to obtain single cells. After incubating the cells for 10min at 4°C, permeabilisation was checked with trypan blue stain under the microscope and was then stopped with 2mL ice-cold 2.5% FCS in PBS. Cells were centrifuged at 240xg and 4°C for 5 min, supernatants were removed and cells were stained with 5µL Apo2.7 antibody diluted in 25µL 2.5% FCS and PBS in the dark at room temperature (RT) for 25min. After staining, cells were resuspended in 250-500µL 2.5% FCS and PBS and immediately analysed by FACS.

Bacterial transformation. For bacterial transformations competent *Escherichia coli* strains were used: *BL21(DE3)* was transformed when aiming for protein production and *DH5α* served for the amplification of plasmid DNA. 1µg plasmid DNA was mixed with 100µL KCM buffer [100mM potassium chloride (KCl), 30mM calcium chloride ($CaCl_2$), 50mM magnesium chloride ($MgCl_2$)] and chilled on ice for 10 min to enable proper dissolution of the DNA molecules prior to transformation. The DNA mix was then added to 100µL competent bacteria that were thawed on ice. Keeping the DNA/bacteria mix on ice for 20min, DNA will stick to the bacterial membrane, which is then incorporated into the bacterium upon thermic shock performed for 10min at RT. Transformed bacteria were resuspended in 1mL LB medium, incubated for 1h at 37°C to allow recovery from the stress of transformation and finally 75µL of bacteria were spread on Luria Brothe (LB)-agar plates supplemented with the respective selection antibiotics encoded in the plasmid to enable clonal selection.

Bacterial expression of rhTRAIL. The basic protocol for the bacterial expression and purification of rhTRAIL originates from [Kim et al 2004] and shall briefly be described in the following. Prior to large-scale production of rhTRAIL, an induction test was performed to choose the bacterial clone with highest rhTRAIL productivity. Therefore, 3mL LB cultures supplemented with selection antibiotic were inoculated with different bacterial clones and grown ON at 37°C and 190rpm. The following day 10mL LB medium cultures containing selection antibiotics and 100µM zinc sulfate

($ZnSO_4$) to stabilise rhTRAIL's homotrimeric structure were inoculated with 10μL of the ON starter culture. Bacterial cultures were grown at 18 to 21°C and 190rpm to prevent aggregation and formation of insoluble inclusion bodies upon overexpression of the recombinant protein, which is counterproductive to purification of native proteins. Once the culture has reached an optical density (OD) of 0.3 to 0.6, the bacterial expression of the rhTRAIL gene was induced adding the lactose analog isopropyl β-D-1-thiogalactopyranoside (IPTG) to a final concentration of 0.5mM. The cultures were induced at RT and 190rpm until the OD has doubled (≈ 14h). Aliquots of un-induced and induced cultures were taken, whereby the aliquot volume was calculated according to the measured OD. Bacteria were pelleted, washed once with ice-cold PBS, lysed in identical volumes of lysis buffer and analysed on 12% sodium dodecyl sulfate (SDS)-polyacrylamide gel electrophoresis (PAGE) gels that were stained with Coomassie brilliant blue. The bacterial clone with the strongest rhTRAIL protein band was chosen for large-scale rhTRAIL production and purification. Therefore, 3x 1L LB medium cultures containing selection antibiotics and 100μM $ZnSO_4$ were inoculated with 1mL of culture used for the induction test and grown at 18-20°C and 190rpm. When the culture has reached an OD of 0.3-0.6 (which can take up to 23h since bacteria transformed with the untagged rhTRAIL grow slower than bacteria transformed with 6x histidine (His)-tagged rhTRAIL), rhTRAIL gene expression was induced with 1mM IPTG at 18-20°C and 190rpm until the OD has doubled (≈ 26h). Like in the induction test, also at large scale rhTRAIL expression aliquots of the un-induced and induced cultures were analysed for expression efficiency. Bacterial cultures were centrifuged at 6000rpm and 4°C for 30min and cell pellets were stored at -80°C until protein purification.

Bacterial lysis and batch-purification of rhTRAIL. Due to it's 6 histidine (His) residues, untagged soluble rhTRAIL comprising amino acids 114 to 281 can be purified via nickel (Ni^{2+}) affinity purification procedures [Ashkenazi et al 1999, Kim et al 2004, The Qiaexpressionist 06/2003]. Bacterial cell pellets were defrozen on ice and resuspended in one-fortieth volume of ice-cold lysis buffer [50mM monobasic sodium phosphate monohydrate (NaH_2PO_4*H2O), 300mM sodium chloride (NaCl), 5mM imidazole, 5mM dithiothreitol (DTT), pH 8.0] related to the initial bacterial culture. Once the complete pellet was resuspended upon repeated pipetting up and down, the

bacterial cell wall was weakened by adding lysozyme to a final concentration of 200µg to 1mg ml^{-1} and incubating the mixture for 30min on ice and subsequently for 5min at 37°C. Then, bacterial cell walls were ruptured sonicating the mixture at 30% intensity for 2 min on ice, whereby every 10s of sonication were followed by 10s breaks to prevent the solution from heating and hence rhTRAIL from denaturation. Upon addition of 1-fold the volume of lysis buffer -related to the initial lysis buffer volume- the 2min sonication procedure was repeated, keeping the 10s intervals. Fully homogenized lysates then were cleared from bacterial debris ultracentrifuging at 35,000rpm and 4°C for 40min. Resulting supernatants were recovered as crude extracts. At each step of bacterial lysis and rhTRAIL purification a constant aliquot volume was sampled for an SDS-PAGE analysis to control protein solubility and purity. As Ni^{2+} ions of commercially available HiTrap columns chelated when using lysis buffers containing 5mM DTT, native rhTRAIL was purified in batch purification procedure using Ni^{2+}-nitriloacetic acid (NTA) agarose beads (Qiagen, Hilden, Germany) in accordance to manufacturer's instructions. In brief, cooled Ni^{2+}-NTA slurry was equilibrated washing the beads 4x with ice-cold double-distilled water (ddH_2O) water and 5x with ice-cold lysis buffer. For each washing step at least 4x the bead volume was used and between the washing steps Ni^{2+}-NTA beads were pelleted centrifuging at 4°C and 1000xg for 10s. Equilibrated Ni^{2+}-NTA beads were mixed with crude extract in a 1:4 ratio and gently tilt over on a head-to-head shaker at 4°C ON. The following day Ni^{2+}-NTA beads, to which rhTRAIL has bound, were sedimented and resulting supernatant containing unbound rhTRAIL, herein referred to as flow through, was mixed a second time with equilibrated Ni^{2+}-NTA beads for 1h at 4°C on a head-to-head shaker. The pelleted Ni^{2+}-NTA beads of both rhTRAIL binding rounds were pooled and washed 7x with ice-cold lysis buffer using at least 4x the beads volume. To liberate rhTRAIL from it's binding to the Ni^{2+}-ions, the beads are washed with excess concentrations of imidazole, an organic compound that builds a side chain of His and therefore is especially abundant in this amino acid. Excess imidazole washings displaces His residues from nickel co-ordination, freeing the His-rich rhTRAIL. For rhTRAIL elution Ni^{2+}-NTA beads were incubated 5x with ice-cold elution buffer [50mM $Na_2PO_4*H_2O$, 300mM NaCl, 40mM imidazole, 5mM DTT, pH 8.0] whereby each time 4x the beads volume was used. Resulting eluates were not pooled but separately dialysed in a 3 KDa cut-off dialysis tube (Spectra/Por Spectrum Laboratories) versus ice-cold PBS containing 5mM DTT carefully stirring at 4°C ON. The dialysis buffer was renewed 12h

and 18h after dialysis start and it was observed that the degree of protein precipitation during dialysis decreased if the initial eluate protein concentration was low. Upon dialysis, concentrations of single rhTRAIL eluates were determined by using the Bradford assay and aliquots taken during all steps of the lysis and purification procedure were analysed for protein solubility and purity on SDS-PAGE gels stained with Coomassie brilliant blue. Once the purity of the rhTRAIL preparations was confirmed, the single eluates were tested for their biological activity in *in vitro* apoptosis assays and surface plasmon resonance assays.

Cell culture conditions. BJAB suspension cells were grown at densities between $4x10^5$ – $1.6x10^6$ cells ml^{-1} medium [Roswell Park Memorial Institute medium (RPMI) 1640 without Hepes, 10% heat-inactivated FCS #K3398, freshly supplemented 2mM glutamine]. Cells were diluted in fresh medium latest every second day removing half of the consumed medium and cells and replacing the volume with fresh medium. If cells were grown to densities above 1.2 $x10^6$ cells, the dilution was performed in consecutive steps allowing the cells to adapt to the lower cell density for at least 2h. Cell viability was routinely checked with trypan blue and only cells with a viability of >90% were used in experiments. Normal BJ fibroblasts and transformed BJELR cells were cultured in the same medium [Dulbecco's Modified Eagle medium (DMEM)/M199 (4:1), 10% heat-inactivated FCS #97] and split every 2d. BJ cells were plated at a density of $8x10^3$ cells and BJELR cells were plated at densities ranging from 1.15-$1.6x10^4$ cells per cm^2 growth surface, depending on their proliferation rate they exhibited in the applied FCS. Importantly, BJELR cells should never exceed 80% confluency, as this would impact on TRAIL sensitivity. We recommend to rather split BJELR cells on 2 consecutive days than letting them overgrow. For selection, medium of BJELR cells was freshly supplemented with 100µg mL^{-1} hygromicine, 400µg mL^{-1} G418 and 0.5µg mL^{-1} puromicin. Same cell culture rules than for BJELR cells applied for transformed HA1ER cells, except the basic cell culture medium differed [DMEM 1g L^{-1} glucose, 10% FCS #97]. All cells were grown at 37°C, 5% carbon dioxide (CO_2) and constant humidity.

Chemical NMII inhibition. For chemical inhibition of NMII function blebbistatin (Sigma) dissolved in dimethyl sulfoxide (DMSO) or ML7 (Sigma) resuspended in a 1:1 mixture of ethanol and water were used. Prior to challenging of cells with rhTRAIL, cells were incubated for 30min with the respective agent or solvent and then co-incubated with rhTRAIL.

DISC immunoprecipitation. The basic protocol for immunoprecipitating the DISC was described by Walczak and Haas (2008) and originated from the book Apoptosis and Cancer, but shall below be described in brief. Per immunoprecipitation $30x10^6$ BJAB cells [targeted total protein amount per IP: 0.5-1.5mg] were stimulated for 1h in fresh medium supplemented with 1µg mL^{-1} rhTRAIL. Lysing equal numbers of BJAB and stepwise system cells yielded 3-fold higher protein concentrations for stepwise cells. Therefore, for DISC-IP experiments $10x10^6$ stepwise system cells were utilised for equal volumes of beads and identical amounts of IP-ABs. Cells were scraped in warm medium and immediately transferred to pre-cooled tubes containing 5x the volume ice-cold phosphate-buffered-saline (PBS), to stop DISC formation and to preserve the DISC. Cells were spun down at 200xg and 4°C for 5 min and washed once with ice-cold PBS. Cell pellets were resuspended by careful pipetting up and down in 1.1 mL ice-cold lysis buffer [30 mM Tris-hydrochloride (HCl) pH7.4, 150mM NaCl, 5mM KCl, 10% glycerol, 2 mM EDTA] freshly supplemented with complete, EDTA-free protease inhibitor cocktail (Roche, Mannheim Germany, # 11873580001), phosphatase inhibitors (PhosStop, Roche) and 1% Triton-X100 (BioRad) for the lysis of membrane lipids. Samples were incubated on a head-to-head shaker at 4°C or on ice for 30 min. Obtained lysates were spun at 20800xg and 4°C for 15 min to clear away debris. Meanwhile protein G sepharose beads (GE Healthcare) were equilibrated by washing the beads 3x with lysis buffer supplemented with Triton-X100 and spinning the beads at 106xg and 4°C for 2 min. The lysate supernatants were pre-cleared with 50µL of equilibrated G-protein sepharose beads for at least 1h at 4° on a head-to-head shaker. A volume of 50µL G-protein Sepharose beads was coupled with 4µg DR5 IP-antibody (AB), 1.4µg DR4 IP-AB or 0.6µg CASP8 IP-AB for a minimum of 2h at 4°C on a head-to-head shaker. Pre-cleared lysates were centrifuged at 106xg for 2 min to pellet the sepharose beads. Thereafter 2mL of pre-cleared supernatants (corresponding to 2mg of total protein)

were mixed with 50µL of beads coupled to one of the IP-AB. A fraction of the pre-cleared supernatant was kept as 'input' controls. After over night (ON) incubation shaking head-to-head at 4°C, IP beads were pelleted at 4°C and 106x for 2 min and washed in 1mL ice-cold lysis buffer containing 1% Triton-X100, protease- and phosphatase inhibitors. Importantly, flicking the tube was avoided, instead the tubes were reversed 3-5 times, until all beads were removed from the tip of the tube. All tubes in one round of washing were removed an equal number of times. In total, the washing and centrifugation steps were repeated 5 times. To elute the DISC proteins from the beads 50µL of 2-fold concentrated Laemmli buffer [125mM Tris-HCl pH 6.8, 4% SDS, 10% 2-mercaptoethanol, 10% glycerol] was added, tubes were carefully flicked to bathe all beads and samples were incubated at 75°C for 10 min. In the following the samples were centrifuged at 4460xg for 2 min and the supernatants were recovered as 'IP'. Collected 'inputs' were supplemented with 10-fold concentrated Laemmli buffer [100mM Tris pH 8.0, 25% SDS, 50% 2-mercaptoethanol]. Both 'inputs' and 'IP' were either immediately analysed by Western blot or stored at -80°C. For analysis samples were defrozen on ice and then heated at 75°C for 10 min prior to loading equal volumes onto SDS-PAGE gels.

DR5 surface level determination. Per condition and treatment $1x10^5$ normal BJ or transformed BJELR cells were used and per condition and treatment cell autofluorescence (no staining), DR5 surface levels (DR5-PE stain) and IgG surface levels (IgG-PE stain) was assessed. After trypsinisation cells were collected in FACS-tubes containing 1.5mL ice-cold PBS supplemented with 2.5% FCS. Cell culture wells were washed with ice-cold PBS and 2.5% FCS. Then, cells were spun down at 240xg and 4°C for 5 min and incubated in ice-cold PBS containing 2.5% FCS 30min on ice. After an additional centrifugation step at 240xg and 4°C for 5 min, cells were stained in a total volume of 30µL PBS and 2.5% FCS complemented with 5µL DR5-PE antibody solution, respectively 5µL IgG-PE or were left unstained. Cells were incubated in the dark on ice for 1h. To each tube 250µL ice-cold PBS containing 2.5% FCS was added and cells were immediately analysed by FACS. Importantly, cells were kept to all times on ice and cautiously pipettet up and down prior to FACS analysis, to revert cell clumping. After the first analysis 0.25µg mL^{-1} propidium iodide was added to each sample and cells were again passed through the FACS, which enables discrimination of viable cells and thus ensures analysis of surface stain. Resulting mean (or median) fluorescence intensities

(MFI) of the second viable cell analysis were taken for analysis. Values were normalised to the rescpective autofluorescence.

DR5 internalisation analyses. Principally, DR5 internalisation experiments were performed as described under 'DR5 surface level determination', except that cells were treated with 1μg mL^{-1} rhTRAIL for 5 to 60min. Addition of rhTRAIL was started at the latest time-point and was continued to earliest time-point to enable simultaneous sample collection. Recorded MFI was normalised to autofluorescence and resulting MFI in absence of rhTRAIL was set to 100%. Each further MFI value obtained at the single rhTRAIL incubation time-points were subtracted from the initial 100% of DR5 surface level.

Generation of competent bacteria. Initial 3mL starter cultures were grown in LB-medium ON at 37°C. Bacteria were diluted 1:100 in fresh LB medium and grown at 37°C to an OD of 0.6. Bacterial cells then were pelleted for 5min at 3000xg and 4°C, resuspended in 1/20th volume of competent medium [LB medium supplemented with 10% polyethylene glycol (PEG) 3350, 5% DMSO, 10mM $MgCl_2$, 10mM magnesium sulfite ($MgSO_4$)] and incubated for 10min on ice. Competent cells were then supplemented with 10% glycerol, distributed in 100μL aliquots, frozen in liquid nitrogen and stored at -80°C.

Immunocytochemistry. Cell medium was removed and cells were fixed with ice-cold 4% paraformaldehyde (PFA) for 10min at RT. After fixation, cells were rinsed 3 times with ice-cold PBS for 5min each. Thereafter, cells were blocked and permeabilised in 1% (w/v) bovine serum albumin (BSA) and 0.05% (w/v) saponin in PBS for 1h at RT. Staining was performed with 6.25nM rhodamine-phalloidine (Cytoskeleton) and Hoechst, diluted in PBS containing 1% BSA and 0.05% saponin for 30min at 37°C. After 3 consecutive washes with ice-cold PBS, cells were mounted in ProLong Gold Antifade Reagent (Invitrogen). Mounting medium was hardened for 24h at RT before samples were analysed by fluorescence microscopy.

Mass spectrometry. On-membrane digestion of protein bands was performed according to described protocols [Luque-Garcia et al 2006] and in-solution digestion of IP-eluates according to IGBMC standards. Modifications of the original protocols shall be described herein. In case of on-membrane digestion experiments, the Ponceau S stained nitrocellulose membranes were destained in ddH_2O. To avoid sticking of trypsin to membrane pieces, non-specific protein binding sites on the membrane were blocked in 0.5mL 0.5% (w/v) polyvinylpyrrolidone (PVP-40) prepared in 100mM acetic acid at 37°C for 30min. Membrane pieces were washed 6-10 times with 1mL ddH_2O prior the digestion in 20µL trypsin solution [12.5ng μL^{-1} sequencing grade modified trypsin (Promega) dissolved in 25mM ammonium bicarbonate (NH_4HCO_3) pH 8-8.5] at 37°C for 16h. Digested samples were vacuum-dried, digested peptides were resuspended in 40µL H_2O, sonicated for 10min and 1µL of each sample was injected into the ion-trap mass spectrometer that allows protein identification according to its sequence. Results were aligned with two different search engines, Mascot and Sequest. Whilst Mascot integrates searches for peptide molecular mass data and amino acid sequence data, Sequest identifies proteins only by comparison of peptide mass generated from a protein digested with a specific enzyme. Importantly, we considered a protein to be identified if at least 2 peptides were identified per search engine and were judged significant if Mascot scores were ≥68 or XCorr scores were ≥2 [Perkins et al 1999, Washburn et al 2001].

Microscopic live-cell imaging. Normal BJ and transformed BJELR fibroblasts were grown under beforehand described regular cell culture conditions and imaged using a video-microscope (Leica DM IRE2). Recordings were processed with MetaMorph software.

Non-reducing (native) SDS-PAGE. For native gel analysis of rhTRAIL all devices were freed of SDS cleaning with a lot of water and some ethanol afterwards. The running buffer [60mM Tris-HCl, 40mM cyclohexylamino propanesulfonic acid (CAPS), pH 7.0] was cooled to 4°C and cooling of buffer, separating gel [12%/0.32% (v/v) acrylamide/Bis, 60mM Tris-HCl, 40mM CAPS, 0.1% (w/v) ammonium persulfate (APS),

0.1% (v/v) Temed] and stacking gel [4%/0.1% acrylamide/Bis, 60mM Tris-HCl, 40mM CAPS, 0.1% (w/v) APS, 0.1% (v/v) Temed] was ensured during the gel run placing the running chamber on ice. Gels were pre-run with reversed cathode and anode at 100V for 40min. Samples were mixes with loading buffer [25% glycerol, 60mM Tris-HCl, 40mM CAPS, 0.005% bromophenol blue solution] and 5µg protein and 5µL of isoelectric focusing (IEF) marker were loaded per slot. Protein separation was performed at 100V for 6.5h.

Pan-CASP inhibition. For the inhibition of CASP activation, we used the pan-CASP inhibitors zVAD (R&D). In pre-tests increasing concentrations (50, 100 and 200µM) of zVAD or equivalent concentrations of solvent (DMSO) were mixed into the medium of transformed BJELR cells for 30min prior to challenging the cells with 1µg mL^{-1} rhTRAIL for 1h. Cells were lysed, and whole cell lysates were analysed by Western blot for CASP8, CASP10 and CASP3 cleavage. For DR5-IP experiments under pan-caspase inhibition 100µM zVAD, respectively DMSO was added to the cells and the DISC was purified 1h after the start of 1µg mL^{-1} rhTRAIL treatment.

Plasmids. For the bacterial expression of rhTRAIL a pET9A vector was used encoding amino acid V114-G281 of human TRAIL [Pitti et al 1996].

Plasmid DNA purification. For the purification of plasmid DNA the NucleoBond Xtra Kit (Macherey-Nagel) was used in accordance to the manufacturers recommendation.

SDS-PAGE. To separate protein mixtures according their molecular weight, SDS-PAGE was performed. Therefore, running buffer [25mM Tris-base, 50mM glycine], separating gels [8-12%/0.21-0.32% (v/v) acrylamide/Bis, 25mM Tris-base, 50mM glycine, 0.05% (w/v) APS, 0.1% (v/v) Temed] and stacking gel [4%/0.1% (v/v)

acrylamide/Bis, 25mM Tris-base, 50mM glycine, 0.05% (w/v) APS, 0.1% (v/v) Temed] were utilised. Gels were run at 80-120V.

SDS-PAGE gel and nitrocellulose membrane stainings. Coomassie brilliant blue stainings of SDS-PAGE gels was performed boiling gels 2min in staining solution [2.5mg mL-1 coomassie blue R250, 50% ethanol, 10% acetic acid]. Excess staining solution was removed shaking gels in destaining solution [20% ethanol, 7% acetic acid]. Nitrocellulose membranes were stained for 10s in commercially available Ponceau S solution (Pierce). After removal of surplus stain with water, membranes were de-stained in salty buffer solution, usually TBST.

siRNA transfection. The siRNAs against NMHCIIa, NMHCIIb, GRB2 and the scrambled control were purchased from Qiagen. Target proteins were knocked down by reversed transfection. Therefore, per cm^2 cell culture surface 1.17μL lipofectamine (RNAiMax, Invitrogen) was mixed to a total volume of 26μL with Opti-MEM (Gibco). Likewise, per cm^2 growth surface the respective siRNA was diluted to a final concentration of 15nM in a total volume of 26μL Opti-MEM. Onto each cm^2 cell culture surface 47μL of the lipofectamine/siRNA mix was spread equally to cover the whole surface. Then, per cm^2 surface area $1.25x10^4$ normal BJ or $2.5x10^4$ transformed BJELR cells resuspended in 200μL cell culture medium were immediately plated onto the siRNAs covering the bottom of the cell culture vessel. Upon incubation of cells for 24h, the transfection reagents were removed from the cells and replaced by fresh culture medium. Usually, knockdown was allowed to proceed for 2d before cells were collected or used in experiments. If the knockdown was prolonged to 4d, cell culture medium again was renewed 3d after the start of transfection.

Surface plasmon resonance (Biacore) assays. Binding assays of rhTRAIL to its specific and unspecific receptors were performed as published elsewhere [Pavet et al 2010].

Western blot analysis. The transfer of proteins from SDS-PAGE gels to nitrocellulose membranes (Whatman) was performed in transfer buffer [25mM Tris-base, 50mM glycine, 20% (v/v) ethanol] at 300mA (and 150V) for 1.5h while cooling on ice. Nitrocellulose mambranes were routinely stained with Ponceau S to control equal protein transfer. After removal of Ponceau S coloration using Tris-buffered saline (TBS) [140mM NaCl, 2.7mM KCl, 25mM Tris-base, pH 7.4], unspecific protein binding sites the membrane was blocked in 5% milk powder (w/v) dissolved in TBS supplemented with 0.1% Tween 20 (TBST). To ensure proper dissolving, blocking solutions were heated to 80°C while stirring for at least 1h and then cooled down prior to use. Primary antibodies were applied in 5% milk and TBST or 5% BSA and TBST at 4°C ON moving on a head-to-head shaker. Membranes were then washed 3 times for 5 min each shaking in TBST and incubated with secondary antibody diluted in 5% milk and TBST at RT for 1h on a head-to-head shaker. Unbound secondary antibody was removed washing membranes 3 times for 5 min each shaking in TBST. Protein signals were detected incubating the membranes with enhanced chemiluminescence (ECL) reagent (GE Healthcare or Thermo Fisher Scientific) and exposing them to light-sensitive Hyperfilms (Hyperfilm MP, GE Healthcare).

RESULTS

We hypothesised that the differential sensitivity of normal and transformed cells towards TRAIL apoptosis arises at the DISC. Aiming to perform comparative DISC analyses in normal and transformed cells, several basic technologies needed to be inaugurated in the laboratory. Therefore the following first results section will provide protocols for the bacterial expression and purification of untagged recombinant human TRAIL. The purified ligand subsequently was characterised concerning its capacity to induce apoptosis, to bind to its specific and un-specific TNF family receptors and to activate the apoptotic cascade. Moreover, the protocol and pitfalls of the native DISC analysis as well as the specificity of the utilised IP-antibodies will be described.

In the second part of the results section the cells of the stepwise tumourigenesis model will be characterised regarding their cell culture characteristics, TRAIL sensitivity, DISC protein expression levels, DR5 surface expression, activation of the apoptotic cascade and DISC formation.

Since comparative DISC analyses did not reveal a complete explanation for the differential response of normal and transformed cells to TRAIL-apoptosis, we suspected the presence of unknown DISC-interacting proteins that regulate observed differential sensitivity. We therefore applied mass spectrometry-based analyses of DR5-immunoprecipitates and identified NMHCIIa, NMHCIIb, MLC2 and ßACT as novel DR5 and DR4 interactors that differentially co-purified with the DR of normal and transformed cells, as described in the third segment of the results section.

In contrast to actin contributing to FAS and TNFR1-mediated apoptosis, the co-purification of NMII with DR was entirely novel and by the time we identified NMII there was only one paper available linking NMII activity to TNFR1 cell surface transport. Therefore we focused our analyses on understanding the functional role of NMHCIIa and NMHCIIb in TRAIL-apoptosis, which will be presented in the fourth part of the results section. In brief, the fourth chapter will point out that chemical inhibition of NMII is associated with the loss of NMII/DR interaction and an increased response of normal cells to TRAIL apoptosis. Moreover, the deregulation of kinase expression levels in transformed cells controlling the NMII Mg^{2+}-ATPase activity will be shown. Finally, in the fourth section we will describe how NMHCIIa but not NMHCIIb siRNA-induced

protein loss removes the resistance block towards TRAIL-apoptosis in normal cells and how NMHCIIa loss alters the composition of the DISC.

According to literature, NMII function in cell adhesion and cell detachment is implicated in sensitivity to TRAIL-apoptosis. Above that, localisation and recruitment of signalling molecules (amongst others) to focal adhesions positively regulating fibroblast proliferation, depends on NMII Mg^{2+}-ATPase activity. Hence, we investigated whether anti-apoptotic TRAIL DISC-interacting proteins exist whose recruitment depends on NMII in normal cells. And so, the final results section will introduce the proliferation signalling adapter growth factor receptor-bound protein 2 (GRB2) and RAF1 proto-oncogene serine/threonine-protein kinase (RAF1) as constitutive DR5 interactors and uncover their NMII-independent binding to DR5.

Generation of tools to analyse the native TRAIL DISC

DISC immunoprecipitation experiments require considerable amounts (15-45µg) of sTRAIL, therefore the primary goal was to establish the cytokine production and purification in the laboratory. Undesirable cytotoxicity of certain TRAIL variants towards normal hepatocytes has been associated to the hyper-oligomerisation capacity of protein (FLAG)- or histidine (His)-tags [Lawrence et al 2001, Ganten et al 2006]. Therefore we decided to utilise a native, untagged, biologically active [Hymowitz et al 2000] rhTRAIL variant comprising amino acid 114 to 281, which has been proven as non-toxic to isolated [Lawrence et al 2001] or mouse-xenografted normal human hepatocytes [Hao et al 2004].

Establishment of protocols for the bacterial expression and purification of rhTRAIL. The rhTRAIL purification from bacterial cultures - conducted in accordance to described protocols [Kim et al 2004]- is accomplished via resin-immobilised Ni^{2+} metal ions that are able to bind electron-rich molecules, such as histidine. Importantly, also non-His-tagged rhTRAIL can be purified via Ni^{2+}-binding methods as the herein expressed native rhTRAIL sequence contains 6 histidines (Figure 20, A) that are sufficient for Ni^{2+} binding [Ashkenazi et al 1999, Kim et al 2004].

Although standard protocols [Kim et al 2004] immediately allowed the purification of native rhTRAIL purified from *Escherichia coli* strain *BL21DE3* (Figure 20, B-C), the ligand lacked pro-apoptotic activity when applied on transformed cells (not shown). Since this inactivation could be due to protein overexpression leading to protein aggregation and formation of inclusion bodies [Qiaexpressionist 2003], three major changes were incorporated in the purification protocol. Firstly, the growth temperature was decreased from 30°C to 18°C to reduce expression levels leading to a higher amount of soluble protein [Qiaexpressionist 2003]. Secondly, as the biologically active trimeric TRAIL structure [Bodmer et al 2000; Trabzuni et al 2000; Seol and Billiar 1999] is maintained by an unpaired cysteine residue (Cys^{230}) that coordinates one Zn^{2+}-ion per TRAIL trimer [Hymowitz et al 2000], the culture medium was supplemented with 100µM $ZnSO_4$. Thirdly, to enhance oligomerisation of native, untagged rhTRAIL and to decrease the yields of presumably biologically inactive monomers [Kim et al 2004],

the reducing agent contained in the purification buffer and the dialysis buffer was exchanged from 2-mercaptoethanol to 5mM DTT. Due to the new reducing agent rhTRAIL prufication was performed as batch purification using Ni^{2+}-NTA beads, because Ni^{2+} ions of commercially available HiTrap columns chelated at 5mM DTT. Finally, to increase yields of rhTRAIL through efficient breaking up of the bacterial cell wall, the sonication time was extended from 1 to 2min. In this way, the biological, pro-apoptotic activity of rhTRAIL could be conserved. The putative biologically active homotrimeric subunit structure of rhTRAIL can be seen in (Figure 20, D).

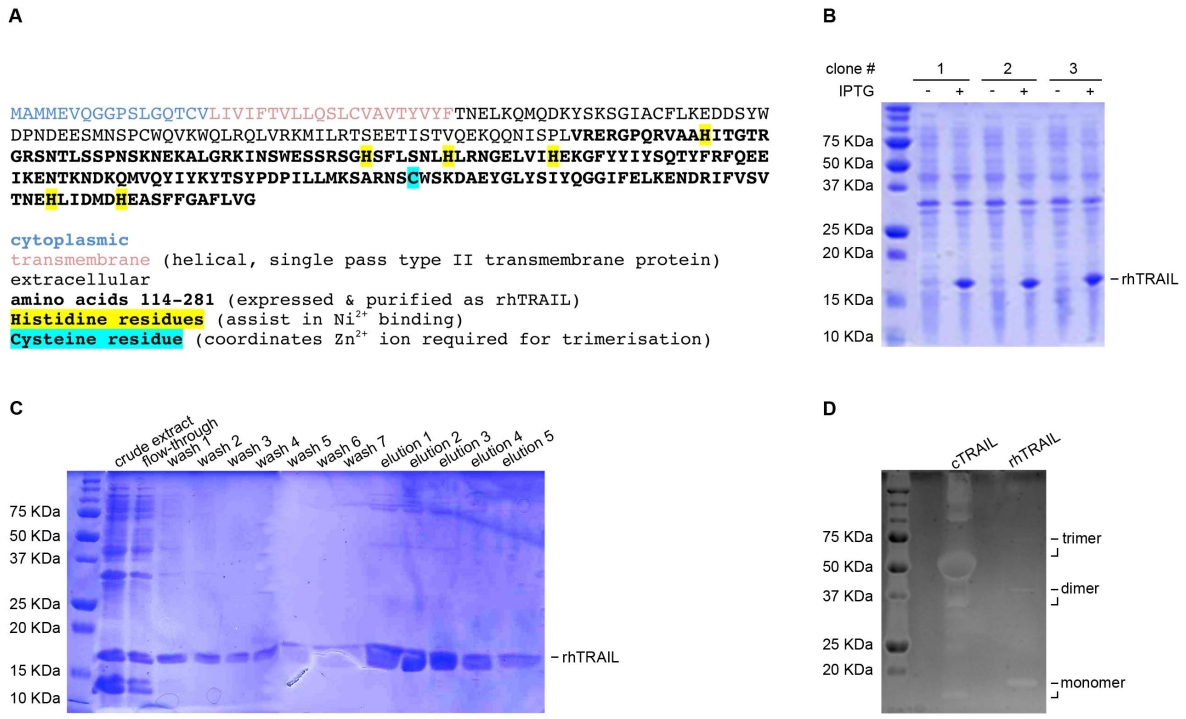

Figure 20: Expression, purification and subunit structure of recombinant human TRAIL (rhTRAIL). **(A)** Amino acid sequence of full-length human TRAIL. Indicated are the cytoplasmic (blue), transmembrane (red) and extracellular (black) domains as well as the extracellular portion that was expressed as untagged soluble recombinant human TRAIL (rhTRAIL, bold). **(B)** Coomassie stained 15% SDS-PAGE gel to control expression efficiencies of various *Escherichia coli* strain *BL21DE3* clones expressing the 18.59 KDa rhTRAIL upon 24 hours induction with 0.5mM isopropyl-beta-D-thiogalactopyranoside (IPTG). **(C)** SDS-PAGE gel containing equal volume loads of the single Ni^{2+} affinity chromatography-based rhTRAIL purification steps. **(D)** The rhTRAIL was purified by Ni^{2+} affinity chromatography, dialysed and then analysed by non-reducing (native) SDS-PAGE and silver staining. A commercially available, untagged TRAIL (cTRAIL) was included for comparison. The gel displays monomeric, dimeric and trimeric rhTRAIL, latter being considered as the biologically active (*here:* apoptosis-inducing) structure.

Characterisation of purified rhTRAIL regarding its potential for apoptosis induction, receptor binding and apoptotic cascade activation. Although TRAIL is expressed as a monomer, high-resolution X-ray structures have shown that it exists as a homotrimer [Hymowitz et al 2000]. Therefore one assumes that TRAIL spontaneously assembles into a homotrimeric structure in solution. Crystal structure studies have shown that the binding of TRAIL to DR5 takes place via the interface of TRAIL monomers, so that one homotrimeric sTRAIL molecule binds and clusters up to 3 extracellular DR5 domains [Hymowitz et al 1999]. Therefore an intact homotrimeric TRAIL structure is essential for TRAIL binding to its receptors and for its biological activity.

To examine if purified rhTRAIL properly binds to its receptors without cross-activating other TNF receptor family members, we performed surface plasmon resonance (SPR) experiments and determined rhTRAIL binding affinities towards each single receptor. In these SPR experiments sensor plates were used onto which the specific TRAIL receptors (DR5, DR4, DcR2 or DcR1) or unspecific TRAIL receptors of the TNF receptor family (FAS or receptor activator of NFKB (RANK)) were immobilised. The surfaces were objected to a constant flow of aqueous buffer into which varying rhTRAIL concentrations were injected. As rhTRAIL binds to the receptors the accumulation of rhTRAIL on the sensor plate results in an increase in the refractive index measured by an optical method. This change in refractive index is measured in real time, and the result plotted as response or resonance units (RU) versus time. As the continuous flow of running buffer over time washes rhTRAIL away, this again changes the measured refractive index. From these measurements the association (K_{on}) and dissociation constants (K_{off}) then can be calculated describing the binding affinity between rhTRAIL and its respective receptor (affinity = K_{on}/K_{off}).

SPR experiments revealed that purified rhTRAIL *in vitro* binds to the TRAIL receptors DR5, DR4, DcR1 and DcR2 (Figure 21, A). Association constants were determined for all four TRAIL receptors being 0.25nM for DR5, 1.9nM for DR4, 0.6nM for DcR1 and 0.44nM for DcR2, whereby all association constants were calculated from six different binding curves generated at varying rhTRAIL concentrations, except the one of DR4 which was calculated only from three different binding curves [Pavet et al 2010]. Accordingly with previously reported data for other soluble rhTRAIL preparations [Degli-Esposti et al 1997, Emery et al 1998, Truneh et al 2000, Hymowitz et al 2000, Lee

et al 2005], rhTRAIL displays a slightly stronger affinity for DR5, intermediate for the DcRs and lowest for DR4 (DR5>DcR2>DcR1>DR4). Importantly, in surface plasmon experiments purified rhTRAIL did not bind to the receptors of other TNF family members, such as FAS and RANK (Figure 21, A). The specificity of ligand-receptor recognition hence could be maintained for the purified rhTRAIL.

After the binding of rhTRAIL to its specific receptors was confirmed *in vitro*, we tested whether rhTRAIL can execute its apoptotic function and if so, whether rhTRAIL induces apoptosis specifically via its DRs and not via unwanted cytotoxic side effects. Therefore we used the TRAIL-sensitive malignant B-cells, the Burkitt's lymphoma cells (BJAB), which express DR5, DR4, DcR1 and DcR2 on their cell surface and whose major apoptosis mediator is DR5 [Thomas et al 2004]. BJAB cells are monoallelic for their major TRAIL-apoptosis signalling receptor *DR5* (BJAB$^{DR5-/+}$), allowing the depletion of the DR5 gene by chemical mutagenesis (BJAB$^{DR5-/-}$) [Thomas et al 2004]. To date, BJAB$^{DR5-/-}$ cells are currently the only patient-derived cancer cell system for which a constitutive *DR5* knockout (BJAB$^{DR5-/-}$) is available. BJAB$^{DR5-/+}$ and BJAB$^{DR5-/-}$ cells were treated with different concentrations of rhTRAIL for 16h and the percentage of apoptotic cells were quantified. For that, we detected cell populations positive for 7A6, a protein that translocates from the inner to the outer mitochondrial membrane if the cell undergoes apoptosis. Importantly, rhTRAIL induced dose-dependent apoptosis in BJAB$^{DR5-/+}$ cells, whilst no substantial (< 10%) cell death was evidenced in BJAB$^{DR5-/-}$ (Figure 21, B). Therefore, the purified ligand specifically induces apoptosis via its receptors and does not display unspecific cytotoxicity.

In the chronological sequence of apoptosis 7A6 positivity is posterior to the formation of the DISC with cleavage-mediated CASP8 activation as its key signature. The next goal was to evaluate whether rhTRAIL induced apoptosis in accordance to its apoptotic signalling model [Newsom-Davis et al 2009] and to define the time-point of maximal CASP8 cleavage that is required for optimal timing of DISC-IPs. For that purpose, BJAB$^{DR5-/+}$ and BJAB$^{DR5-/-}$ cells were stimulated with 1µg mL^{-1} rhTRAIL for different time spans, whole cell lysates (WCL) were collected and CASP8 activation was analysed by Western blot. Stimulation of BJAB$^{DR5-/+}$ with purified rhTRAIL induced a maximal cleavage of CASP8 after 1h of treatment. Contrary, neither the large subunit of CASP8 p43/p41 nor the p18 catalytic subunit were evidenced in untreated BJAB$^{DR5-/+}$

cells and treated BJAB$^{DR5-/-}$ cells (Figure 21, C). Thus in BJAB cells purified rhTRAIL initiates apoptosis via DR5-dependent CASP8 activation.

Since CASP8 activation represents only the first level of extrinsic DR-mediated apoptosis, we explored if rhTRAIL initiates the full apoptotic cascade in BJAB cells. For that, BJAB$^{DR5-/+}$ and BJAB$^{DR5-/-}$ cells were treated with 1µg mL^{-1} rhTRAIL for 1h and activation of initiator CASP8 and CASP9, full-length BID, and effector CASP3 and CASP7 was analysed by Western blot (Figure 21, D). Whereas no changes were detected in BJAB$^{DR5-/-}$ cells, in BJAB$^{DR5-/+}$ cells 1h of rhTRAIL treatment induced maximal processing of initiator CASP8 and was sufficient to elicit effector CASP3 and CASP7 cleavage. In line with previous reports [Menke et al 2011], we observed that the death signal in BJAB$^{DR5-/+}$ cells is enhanced via the intrinsic apoptotic pathway. Particularly, a decline of the full-length BID signal as well as processing of CASP9 was observed. Although BID is cleaved by CASP8, BJAB cells are type I signalling cells, since BID knockdown neither inhibited nor decreased rhTRAIL-induced apoptosis [Menke et al 2011].

Once the biological activity and the specificity of the purified rhTRAIL to its receptors were confirmed, the next goal was to assess the stability of the recombinant protein upon storage. Repeated freeze-thaw cycles usually degrade a protein [Deutscher 2009]. Therefore we applied different concentrations of single rhTRAIL eluates immediately after purification and dialysis (no freeze), as well as after the first (1st freeze) and second (2nd freeze) freezing at -20°C for 1 day each on BJAB$^{DR5-/+}$ cells and measured apoptosis 16 h after start of treatment. Even at very low rhTRAIL concentrations like 0.1 or 0.5ng mL^{-1} no significant decline in the pro-apoptotic activity could be observed for rhTRAIL eluates that were used either before or after freezing. Therefore purified rhTRAIL is stable in the selected buffer composition for at least 2 consecutive freeze-thaw cycles.

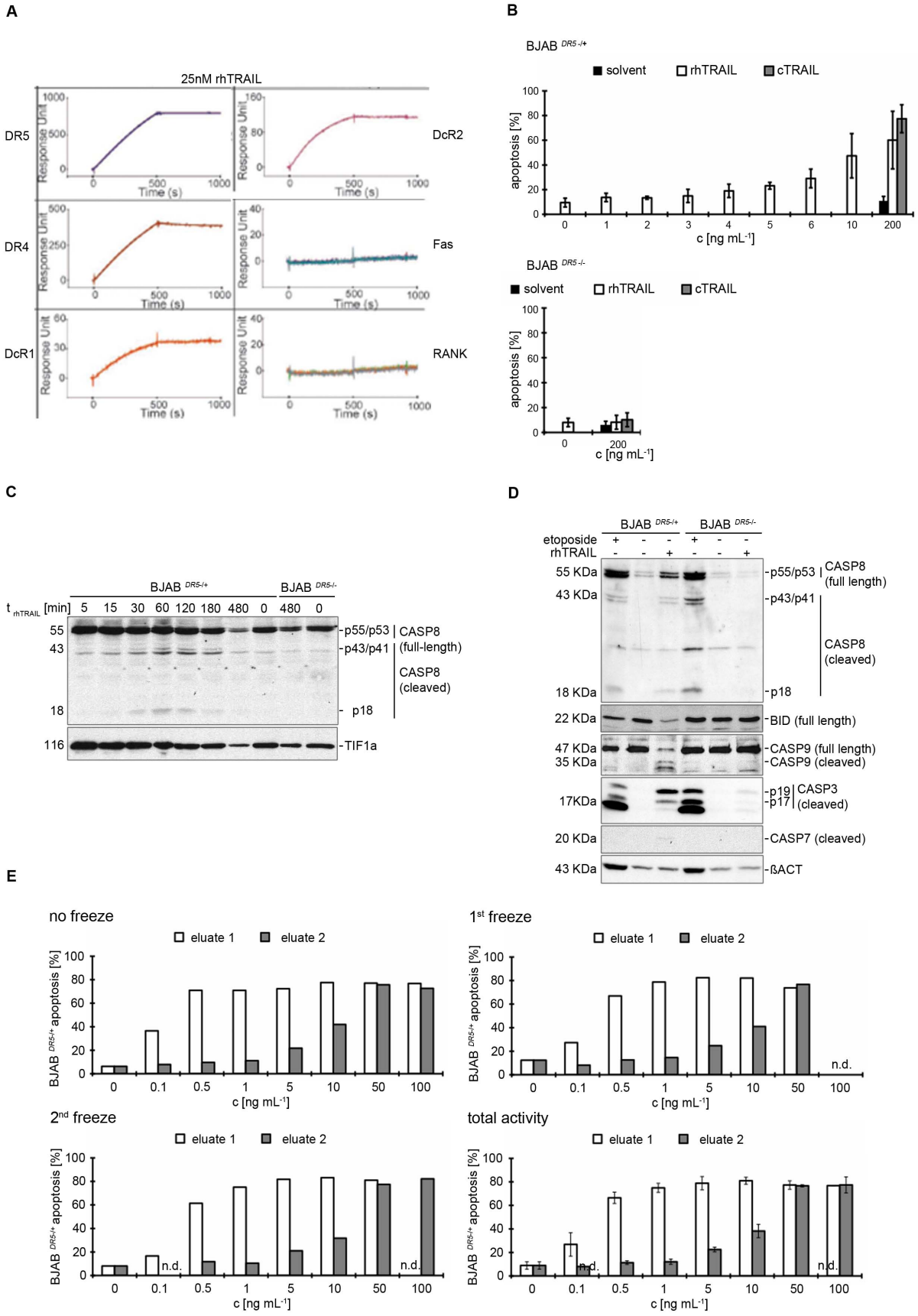

Figure 21: Biological activity of purified untagged recombinant human TRAIL (rhTRAIL). **(A)** Representative binding curves for rhTRAIL to its specific receptors (DR5, DR4, DcR1, DcR2) and to other TNF family receptors (FAS, RANK) determined by surface plasmon resonance experiments at 25nM rhTRAIL. Binding curves were recorded with varying rhTRAIL concentrations in 3 (DR4) to 6 (all other

Implementation of the native DISC analysis and cross-reactivity test of the DR5 immunoprecipitation antibody with DR4. A key step of this project was to setup optimal conditions to analyse the native DISC composition. Thus, neither TRAIL, the receptors nor other DISC components should be tagged and the complex should be immunopurified by using antibodies targeting the endogenous DISC-members [Walczak and Haas 2008].

Several problems are linked to native DISC-IP. Foremost, IP-ABs targeting single DISC components can cross-react non-specifically with other proteins. Especially if one aims to discriminate homologous proteins such as DR5 and DR4, epitope specificity of single ABs is imperative to inspect. In order to enable a controlled set-up of DISC-IP conditions and to monitor specificities of ABs used for IP, BJAB$^{DR5-/+}$ cells were chosen as a transient model. Utilising BJAB$^{DR5-/+}$ cells that express all TRAIL receptors (DR4, DR5, DcR1, DcR2) on the cell surface and BJAB$^{DR5-/-}$ cells that express all TRAIL receptors but DR5 [Thomas et al 2004] facilitates the assessment of cross-reactivity of the DR5 IP-AB towards DR4, which is displayed by the levels of DR4 detected in DR5-IPs of untreated BJAB$^{DR5-/-}$ cells. Similarly, a comparison of this cell system under untreated and rhTRAIL-treated conditions allows the validation of cross-reactivity of the DR4 IP-AB towards DR5, which is reflected by the levels of DR5 detected in DR4-IPs of untreated BJAB$^{DR5-/+}$ cells. Upon DR5-IP from untreated BJAB$^{DR5-/-}$ cells no DR4 signal could be detected (Figure 22, A) and upon DR4-IP from untreated BJAB$^{DR5-/+}$ cells no DR5 signal could be

Figure 21 continued: receptors) independent experiments. **(B)** Dosage-response curve for purified rhTRAIL in Burkitt's lymphoma (BJAB) cells monoallelic for DR5 (BJAB$^{DR5-/+}$) and in BJAB cells whose DR5 receptor was knocked out (BJAB$^{DR5-/-}$). Apoptosis was quantified as 7A6 positivity in FACS analysis after 16h of treatment. Commer-cially available TRAIL (cTRAIL) was included as positive control. Values derive from 3-4 independent experiments. **(C)** Representative Western blot for caspase-8 (CASP8) cleavage kinetics in BJAB$^{DR5-/+}$ and BJAB$^{DR5-/-}$ cells upon administration of 1μg mL^{-1} rhTRAIL for the indicated times. The antibody reveals the full-length CASP8 and its active p43/p41 and p18 fragments. The blot for transcription intermediary factor 1-alpha (TIF1a) served as loading control. Depicted is 1 of 2 independent experiments. **(D)** Western blots for the apoptotic cascade activation in BJAB$^{DR5-/+}$ and BJAB$^{DR5-/-}$ cells after 1h incubation with 1μg mL^{-1} purified rhTRAIL. The antibodies against the initiator caspases CASP8 and caspase-9 (CASP9) detect both the full-length and the cleaved fragments. The antibodies against effector caspase-3 (CASP3) and -7 (CASP7) specifically react with the active p19/p17 CASP3, respectively with the active p20 CASP7 cleavage products. The BID antibody exclusively reacts with the full-length protein. Whole cell lysates originating from cells treated for 1h with 25μM etoposide were included as positive control. Indicated are the blots for 1 of 2 independent experiments. **(E)** Dosage-response curves for different rhTRAIL eluates that were applied at indicated concentrations on BJAB$^{DR5-/+}$ cells either immediately after purification (no freeze) or after the first and second freezing. Apoptosis was assessed as in (B). Values of the upper 3 diagrams derive from one single experiment and are fused in the diagram at the bottom. The abbrevation 'N.d.' is used for 'not determined'.

detected (Figure 22, B). Thus the DR5-IP AB does not significantly cross-react with DR4 and the DR4-IP AB does not substantially cross-react with DR5.

A second DISC-IP challenge originates from the mode of IP-ABs immobilisation to the beads that allow DISC isolation by sedimentation. Usually, beads are covalently coupled to immunoglobulin-binding proteins to which the IP-AB binds. Unfortunately these immunoglobulin-binding proteins can hamper Western blot analyses of IPs as they cross-react with detection-ABs, leading to an unspecific signal at the molecular weight (MW) of the immunoglobulin-binding protein (*here*: protein G ≈ 30KDa, e.g. signal above FADD and in between CASP8 p43/p41 and p18 in DR5-IP, Figure 25, F). Depending on the host organism in which the secondary AB was generated and the type of immunoglobulin-binding protein employed in the experiment, this cross-reactivity is weaker or stronger [Frank 1997]. Therefore we tested different sets of detection antibodies with different types of immunoglobulin-binding proteins. While optimising the DISC-IP and Western blot analysis protocol, we found that the use of protein G-coupled sepharose beads in combination with chicken-derived secondary antibodies give lowest unspecific signals (not shown).

Thirdly, Western blot detection of the single members comprising the DISC can be hampered by a cross-reaction of detection-AB with IP-AB, which still can occur although crossing species [Lal et al 2005]. Due to this cross-reaction that gives rise to unspecific signals at the MWs of the IP-AB's heavy and light chain (50 and 25KDa), certain members that linger in the DISC cannot be doubtlessly identified. This is the case for cFLIP(L) and cFLIP(S) (MW=55KDa, 25 KDa respectively) when co-immunoprecipitated with DR5, DR4 or CASP8 (Supplementary, Figure 31). The degree of cross reaction and AB-leakage from the beads depends on the applied IP-AB. Due to the unspecific cross-reactions between detection ABs and immunoglobulin-binding proteins or IP-ABs, we think it is indispensable to load eluates of IP-AB-coupled beads next to the respective DISC immunoprecipitates. In this way a clear identification of specific signals is ensured.

Finally, the abundance of the single DISC members within the DISC varies drastically depending on the cellular response upon TRAIL and certain AB affinities are weak so that the detection becomes difficult as it is the case with FADD. In the course of DISC-IP protocol optimisation we found that loading of 15μL IP-eluate suffices for detection of all DISC members studied here.

Despite these basic technical considerations the intact DISC was successfully immunoprecipitated targeting DR5, DR4 or CASP8 (Figure 22). In accordance to the prevalent signalling model rhTRAIL stimulation of BJAB cells induced the formation of DR5/DR4 heterocomplexes, recruitment of FADD and activation of CASP8 at the receptors. TRAIL receptors contain a PLAD allowing ligand-independent homotypic and heteroypic receptor interactions [Clancy et al 2005]. Therefore we investigated whether preformed DR5/DR4 heterocomplexes exist prior to ligand addition. In the absence of rhTRAIL DR5-IP does not co-immunoprecipitate DR4 and DR4-IP does not co-immunoprecipitate DR5 (Figure 22, A-B). Thus, in the absence of ligand there are no pre-formed DR5/DR4 heterocomplexes present in BJAB cells. In line with the apoptotic signalling model [Gonzalvez and Ashkenazi 2010, Dickens et al 2012, Schleich et al 2012] rhTRAIL induces FADD recruitment to the DISC and CASP8 cleavage at the DISC (Figure 22, A-C). Whether DR5 and/or DR4 form homotrimeric complexes in absence of TRAIL cannot be investigated using this approach.

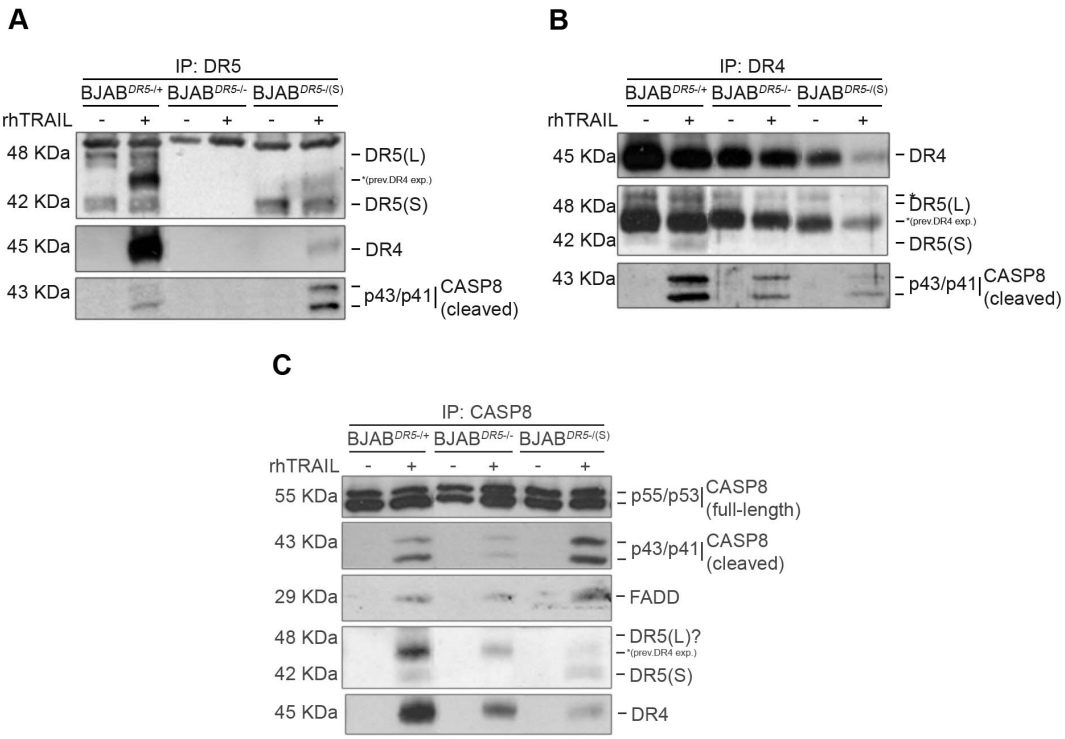

Figure 22: The TRAIL-DISC of BJAB cells. Immunoprecipitation (IP) of the DISC targeting **(A)** death receptor 5 (DR5), **(B)** death receptor 4 (DR4) or **(C)** caspase 8 (CASP8) from unstimulated (-) and rhTRAIL-stimulated (+)Burkitt's lymphoma cells (BJAB) cells. Wildtype BJAB cells monoallelic for DR5 ($BJAB^{DR5-/+}$), DR5 negative cells ($BJAB^{DR5-/-}$) or DR5(S) rescue cells ($BJAB^{DR5-/(S)}$) were incubated with 1µg mL^{-1} purified rhTRAIL for 1h. Lysates originating of each cell line and treatment were split into 3 fractions to immunoprecipitate either DR5, DR4 or CASP8. Immunoprecipitates were run on 12% SDS-PAGE gels and analysed by Western blotting. Depicted are representative blots from 1 out of 2 independent experiments.

Interim summary and conclusions I

The expression and purification of untagged rhTRAIL was successfully established and the alleged biologically active homotrimeric structure was detected on non-reducing SDS-PAGE gels. As shown by SPR experiments purified rhTRAIL binds with high affinity specifically to its receptors, but not non-specific receptors from the TNF family. FACS-assisted 7A6 immunogenicity and Western blot analyses demonstrated the biological (*here*: pro-apoptotic) activity of purified rhTRAIL in patient-derived BJAB lymphoma cells and that rhTRAIL activates the extrinsic and intrinsic apoptotic pathway in a DR5-dependent manner. Moreover, apoptosis assays with 7A6 confirmed that purified rhTRAIL maintains its pro-apoptotic activity for at least 2 freeze-thaw cycles without myjor activity loss.

DISC analyses revealed that purified rhTRAIL induces DISC formation in accordance to prevalent models in BJAB cells. Furthermore, no PLAD-mediated heterotypic receptor interactions were detected under our experimental conditions, indicating that either ligand-independent DR5/DR4 clustering does not occur in this cell model or that this interaction is lost under the given IP conditions. Importantly, the DR5-IP AB does not cross-react with DR4 and the DR4-IP AB does not cross-react with DR5.

In summary the basic tools required for the isolation and analysis of the native TRAIL DISC have been established and validated. The action of rhTRAIL on cells of the stepwise transformation model and TRAIL DISC formation in that cell system are investigated in the following chapter.

The stepwise tumourigenesis cells as model system to study the gain of TRAIL sensitivity through transformation

By the time tumour explants are taken, of which patient-derived cancer cell lines are generated, tumour cells usually have accumulated genetic alterations that exceed the mutations required for cancer cell initiation. Moreover, if the tumour has metastasised, no 2 tumour samples from the same patient are genetically identical [Gerlinger et al 2012]. And, as tumour cells tend to dedifferentiate, cancer cell lines not uncommonly originate from a mixture of different cell types. All these circumstances complicate the choice for normal reference cell populations from patients, if a comparison of normal versus tumour cells is envisaged. In this work we aimed to understand how a normal cell gains TRAIL sensitivity through the process of transformation. Due to beforehand mentioned disadvantages and limits of patient-derived cell lines, we chose to exploit the stepwise transformation system of Hahn and Weinberg [Hahn et al 1999] as a model, which provides transformed cells with defined genetic alterations as well as normal cells with isogenic background.

DISC analyses require considerable (10^7) cell numbers and normal BJ fibroblasts proliferated better than normal HEK or HMEC cells. Therefore, all of the following work was performed in normal foreskin fibroblasts (BJ) and their HTERT, SV40ER and HRASG12V-transformed counterparts (BJELR).

Normal and transformed cells of the stepwise transformation model differ in cell culture characteristics. When grown *in vitro* normal BJ cells have a flat morphology, form one or several cellular protrusions (Figure 23, left image) and appear as large cells that rapidly and firmly attach to the cell culture vessel. Upon transformation fibroblasts change their morphology drastically, they become elevated, spindle-shaped and their margins display dynamic membrane blebbing (Figure 23, right image), a common phenomenon in cells during apoptosis [Mills et al 1998], cytokinesis [Fishkind et al 1991, Burton and Taylor 1997] and cell movement [Trinkaus 1973, Friedl and Wolf 2003]. In addition, membrane blebbing was observed on diverse viable cancer cells [Cunningham 1995, Sahai and Marshall 2003, Charras et al 2005, Charras et al 2006]. Although BJERL appear much smaller than BJ cells (Figure 23), lysis of the same

cell numbers yielded equal amounts of total protein (not shown). We therefore employed equal cell numbers of BJ and BJELR cells in DISC-IP experiments. In addition, we assumed that BJELR cells appear much smaller than BJ cells either because of their slow and loose attachment to the growth surface or because of their high proliferation rate that might not leave enough time for a full de-novo synthesis of cytoplasm. In fact, whilst BJ cells duplicate once every 48h, BJELR divide on average every 24h.

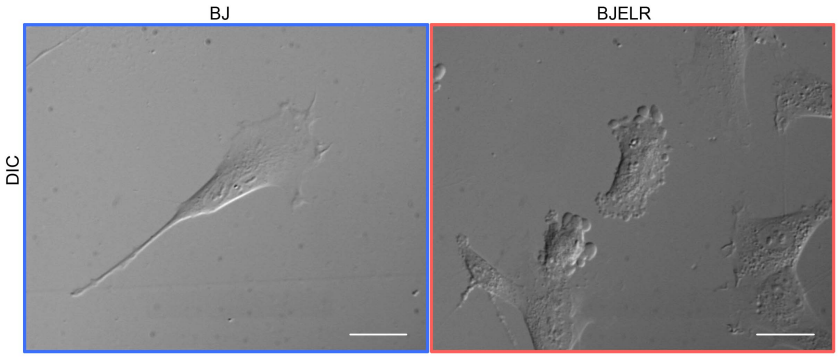

Figure 23: Morphology of normal (BJ) and HTERT, SV40ER and HRASG12V-transformed (BJELR) human foreskin fibroblasts. Images were taken from living cells by differential interference contrast microscopy (DIC). The size bar represents 30µm (left image) and 19µm, respectively (right image).

Transformed but not normal cells die upon rhTRAIL, even though DISC proteins are expressed at comparable levels and a DISC is formed in normal cells. After the apoptotic activity of purified rhTRAIL has been confirmed on BJAB lymphoma cells (Figure 21, B-D), we tested the ligand on normal BJ and transformed BJELR cells of the stepwise transformation model. Thereby we applied high dosages (1µg mL^{-1}) of purified rhTRAIL to ensure receptor saturation with ligand (Figure 24, A). Following 16h of treatment with 1µg mL^{-1} rhTRAIL, significantly more BJELR than BJ cells died (44% (± 10%) versus 11% (±4), p=0.002) (Figure 24, B). The analyses leads us to conclude that purified rhTRAIL acts in a tumor-specific manner inducing apoptosis in transformed but not normal cells, likewise it has been reported for other recombinant TRAIL preparations [Ashkenazi et al 1999, Walczak et al 1999].

The observation that purified rhTRAIL specifically induces apoptosis in cancer cells adds meaning for addressing the central question of this work: how does a cell which is initially TRAIL-resistant become sensitive to TRAIL-apoptosis via the process of transformation?

Earlier publications comparing HTERT and SV40ER-pre-transformed (BJEL, HA1E) cells with fully transformed (BJELR, HA1ER) cells [Nesterov et al 2004, Lund et al 2011] or overexpressing oncogenes in normal BJ [Wang et al 2004] and cancer cells [Drosopoulos et al 2005], respectively, related the gain of TRAIL-sensitivity upon oncogenic transformation to an increase in DR5 total protein and surface expression levels. Therefore we tested the possibility that rhTRAIL-resistance in normal BJ cells could arise from absent or aberrant protein expression of key DISC members. Analysing BJ and BJELR WCLs by Western blot, we found no obvious difference in total protein expression levels of DR5, DR4, FADD, CASP8, cFLIP, DcR1 and DcR2 (Figure 24, C). Experiments in which cell viability of rhTRAIL-stimulated BJ and BJERL cells was investigated subsequent to the depletion of either DR5 or DR4 by siRNA-mediated knockdown (KD), identified DR5 as the main TRAIL-apoptosis signalling receptor in the BJ stepwise transformation model (unpublished data). Hence, we assessed relative DR5 surface levels by direct immunofluorescence and FACS analysis of mean fluorescence intensities (MFI) and observed no difference in DR5 surface levels between BJ and BJELR cells (Figure 24, D). The diverging TRAIL sensitivity of normal and transformed cells therefore cannot be explained by a divergence in DISC protein expression levels or DR5 surface levels.

Having eliminated the possibility that altered DISC protein levels or DR5 surface levels account for the different TRAIL-response, we aimed to isolate the signalling level at which the TRAIL apoptotic signal does not propagate and/or is potentially blocked in normal cells. Therefore we stimulated normal and transformed cells with 1μg mL^{-1} rhTRAIL for 1h and compared total levels of cleaved CASP8, CASP3 and PARP, which were reduced in BJ and enhanced in BJELR cells (Figure 24, E). Thus, TRAIL-resistance in normal BJ cells is accompanied by an inefficient apoptotic cascade activation that originates from impaired CASP8 recruitment or CASP8 cleavage at the DISC.

The decreased apoptotic cascade activation observed in normal BJ cells after 1h of rhTRAIL treatment (Figure 24, E) prompted the question whether CASP8 and/or downstream signalling molecules could be activated at later timepoints in normal than in transformed cells. Therefore we performed time course experiments treating normal and transformed cells for diverse times with rhTRAIL. Subsequently, we investigated the WCLs for CASP8 and CASP3 cleavage. Even though on average only 11% of BJ cells are dying upon 16h of rhTRAIL exposure (Figure 24, B), cleavage of CASP8 and CASP3 into

the active p18, p19 and p17 fragments was detectable in BJ cells already 30 min after rhTRAIL addition. The onset of active CASP8 p18 fragment generation in WCL of normal cells occurred simultaneously with CASP3 cleavage into its active p19 fragment (Figure 24, F, left panel). With regard to the timing of rhTRAIL-induced CASP8 p18 and CASP3 p19 appearance, normal BJ cells do not differ from their transformed BJELR analogues (Figure 24, F, right panel). However, since total CASP8 p18 and CASP3 p19/p17 after 1h of rhTRAIL were clearly lower in normal than transformed cells (Figure 24, E), we concluded that at all times total CASP cleavage levels in the sum of analysed normal cells do not reach the ones in transformed cells.

Activation of CASP8 and/or CASP10 marks the initial step of TRAIL apoptotic signalling. Contrary, CASP3 cleavage can be carried out by initiator CASP8 and/or CASP10 (type I cells) or by effector CASP9 (type II cells), which is activated at the apoptosome. Apoptosome formation requires mitochondrial perturbation initiated by CASP8-facilitated cleavage of BID to tBID (Introduction, Figure 3). Regarding the fact that the onset of CASP8 or CASP3 processing in normal BJ versus transformed BJELR cells was detectable at equal moments in time course experiments (after 30min of rhTRAIL treatment) (Figure 24, F), we assumed that BJ and BJELR cells do not differ in their type of TRAIL signal propagation. Thus, events of the apoptosis cascade occurring after CASP8 and prior to CASP3 activation were analysed in BJELR cells only.

We detected rapid cleavage of CASP8, but not CASP10 upon rhTRAIL addition. Therefore CASP8 seems to be the initiator CASP of rhTRAIL signalling and CASP10 appears to play (if at all) only a minor role during apoptosis-induction in stepwise-system cells, a finding supported by others [Dickens et al 2012].

Moreover, for the investigated time-points no decline in full-length BID levels and no appearance of cleaved CASP9 p35 fragments was observed (Figure 24, F, right panel), which is in line with previous observations [Nesterov et al 2004]. Since BID knockdown prevents rhTRAIL-apoptosis in BJELR cells [Lund et al 2011] and 7A6 exposure on the mitochondrial membrane requires insertion of tBID into the mitochondrial membrane [Nagahara et al 2007], BID cleavage must occur after 4h of rhTRAIL treatment. Notably, BID phosphorylation inhibits cleavage by CASP8 [Desagher et al 2001, Degli-Esposti et al 2003] and CASP8 activation and BID cleavage are temporally uncoupled events in type II HeLa cells [Hellwig et al 2010]. Thus, CASP3 cleavage by CASP8 could precede BID

cleavage in the stepwise system cells and BID cleavage then could be mediated by CASP3 or other effector caspases [Li et al 1998, Slee et al 2000, Hayakawa et al 2008].

We detected cleavage of effector CASP7 into its active p20 fragment only 4h after rhTRAIL additon (Figure 24, F). Considering that CASP7 is a substrate of granzyme B, CASP10 and CASP3 [Gu et al 1996, Fernandes-Alnemri et al 1996, Fernandes-Alnemri et al 1995] and that no CASP10 processing but early CASP3 cleavage was observed (Figure 24, E), CASP7 presumably is processed by CASP3 in transformed BJELR cells.

Low total CASP8 cleavage levels in the whole entity of analysed normal cell populations and high CASP8 processing in populations of transformed cells substantiated the underlying hypothesis that TRAIL resistance in normal cells has its origin in the DISC formation and/or composition itself. Analyses of DISC compositions of cells of the stepwise tumorigenesis revealed that comparative levels of DR5 were immunoprecipitated from normal BJ and transformed BJELR cells. Moreover, similar signals of co-immunorecipitated rhTRAIL indicated that at the moment of rhTRAIL treatment, comparable levels of DR5 and DR4 molecules were exposed to the cell surface of BJ and BJELR cells (Figure 24, G), which confirmed results of DR5 surface level measurements (Figure 24, D). In the absence of the ligand no pre-formed DR5/DR4 heterocomplexes were detected, which is evidenced by the observation that in absence of rhTRAIL no association between DR4 and DR5 is observed in IP assays. In transformed BJELR cells rhTRAIL stimulation induced the formation of DR5/DR4 heterocomplexes, recruitment of FADD and cleavage of CASP8. Interestingly we found that normal cells are indeed capable of forming a DISC, as displayed by comparable rhTRAIL-induced DR4 recruitment to DR5. However, even if comparable amounts of DR5 can be immunoprecipitated from normal and transformed cells and rhTRAIL induced similar microaggregation with DR4, lower FADD recruitment and reduced CASP8 cleavage and/or recruitment occurs at the DISC of normal cells. Thus, rhTRAIL-resistance in normal cells is associated with poor CASP8 activation at the DISC. Importantly, reduced CASP8 cleavage at the DISC was not associated with a co-immunoprecipitation of DcR1 or DcR2 (Figure 24, G). Thus, recruitment of DcR2 into the TRAIL-DISC does not account for the inhibition of CASP8 activation [Merino et al 2006]. Similar DISC compositions as described for DR5-IP, were obtained when DR4 or CASP8 was immunoprecipitated in normal BJ and transformed BJELR cells (Supplementary, Figure 31). Contrary to reports demonstrating TRADD co-immunoprecipitation with

GST-tagged rhTRAIL from murine embryonic fibroblasts [Cao et al 2010] or with FADD upon HIS-TRAIL-stimulation of H460 lung carcinoma cells [Jin and El-Deiry 2006], we could not detect the co-purification of TRADD with CASP8 in normal or transformed cells (Supplementary, Figure 31). Although we cannot exclude that in stepwise system cells TRADD interacts with DISC components at a different timepoint than at 1h of rhTRAIL stimulation, the chosen analysis time laid in the middle of the reported TRADD recruitment time which was between 15min [Cao et al 2010] and 1.5 and 3h [Jin and El-Deiry 2006] of TRAIL stimulation. Although there is currently no indication for complex II formation in stepwise-system cells, analyses of the co-immunoprecipitation of other pro-survival proteins constituting complex II await completion.

Observed differences in the composition of the DISC in normal BJ and transformed BJELR cells and simultaneous absence of DcR2 and TRADD supported our initial hypothesis that there could be unknown DISC interactors in normal and transformed cells regulating DISC formation, composition and TRAIL signalling.

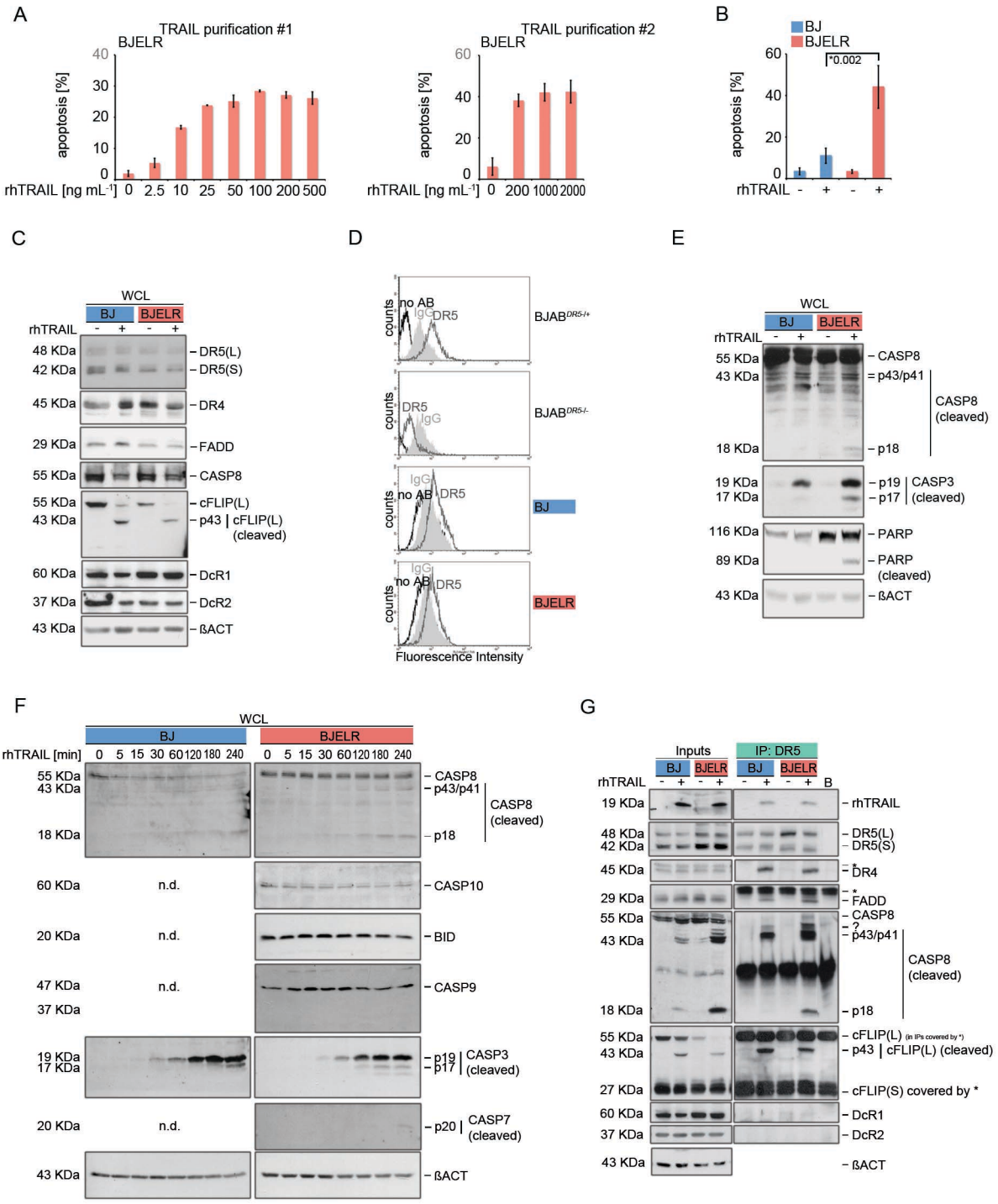

Figure 24: Characterisation of TRAIL-signalling features in normal BJ and transformed BJELR cells. **(A)** Receptor saturation of HTERT, SV40ER and HRASG12V-transformed (BJELR) cells for 2 different lots of recombinant human TRAIL (rhTRAIL) preparations. BJELR cells were stimulated with the indicated concentrations of rhTRAIL and the percentage of apoptotic cells was quantified as 7A6 positivity in FACS analysis after 16h of treatment. Mean values were generated from 2 independent experiments. **(B)** Apoptotic response of normal (BJ) and BJELR cells treated with 1µg mL^{-1} purified rhTRAIL. Apoptosis was quantified as described in (A). Values derive from 3 to 5 independent experiments. Significance was calculated using unpaired, 2-tailed Student's t-test. **(C)** Representative Western blots demonstrating average DISC protein expression levels in whole cell lysates (WCL) of BJ and BJELR cells.* **(D)** DR5 surface levels of BJAB cells monoallelic for DR5 (BJAB$^{DR5-/+}$), BJAB DR5 knockout (BJAB$^{DR5-/-}$), BJ and BJELR stepwise system cells. Cells were left unlabelled (no AB), or were immunolabelled with phycoerythrine-conjugated antibodies against DR5 or IgG. Overlays depict fluorescence intensities as assessed by FACS.*

Interim summary and conclusion II

As evidenced on cells of the BJ stepwise transformation system, purified rhTRAIL acts in a tumor-specific manner, killing transformed but not normal cells. WB analyses and FACS-assisted readouts of DR5 surface stainings revealed that the varying rhTRAIL response of normal BJ and transformed BJELR cells is not due to differential DISC protein expression or DR5 surface levels. Instead, WB analyses unveiled that rhTRAIL-resistance in BJ cells originates from poor initial CASP8 cleavage and/or recruitment, which is not compensated at prolonged rhTRAIL incubation. Apparently CASP8 is the apical caspase of rhTRAIL signalling in the stepwise-system cells, as rapid CASP8 but no CASP10 cleavage was observed in BJELR cells.

Interestingly, DISC analyses showed that normal BJ cells are capable of forming a partial DISC. Even though rhTRAIL-stimulated DR5/DR4 heterocomplex formation was similar in normal and transformed cells, FADD recruitment, CASP8 processing and/or recruitment was inefficient in normal cells. Reduced FADD recruitment, CASP8 cleavage and/or recruitment at the DISC was not due to translocation of anti-apoptotic DcR2 into the DISC. So far, no indications for complex II formation was observed, as there was no TRADD co-recruited.

In summary, rhTRAIL-resistance in normal cells is associated with poor CASP8 activation at the DISC that cannot be fully explained by previously described resistance mechanisms. The identification of novel DISC interactors that could regulate the divergent DISC formation is described in the next chapter.

Figure 24 continued: (E) Western blots presenting caspase 8 (CASP8), caspase 3 (CASP3) and Poly-[ADP-ribose]-polymerase (PARP) cleavage in BJ and BJELR cells treated with 1μg mL^{-1} rhTRAIL for 1h.* **(F)** Caspase cleavage in BJ and BJELR after addition of 1μg mL^{-1} rhTRAIL for the indicated times.** **(G)** DR5-DISC analysis of equal numbers of BJ and BJELR cells incubated with 1μg mL^{-1} rhTRAIL for 1h. Left 4 lanes served as loading control and contain equal volumes of pre-cleared WCL (inputs) that were used in the immunoprecipitation (IP) experiment. The 5 lanes on the right contain equal volumes of DR5-IP eluates originating either from the indicated cell line, or from the DR5/beads mixture (B) utilised in the experiment.*** Depicted are Western blots for 1 of *3, **2 or ***4 independent experiments.

Identification and validation of NMHCIIa, NMHCIIb, MLC2 and ßACT as novel DR5 and DR4 interactors

Precedent DISC analysis of normal BJ and transformed BJELR cells did not reveal the reason for a lower FADD recruitment, CASP8 recruitment and/or cleavage and thus TRAIL resistance in normal cells. We therefore hypothesised there would be yet unknown DISC interacting proteins that regulate DISC composition and associated response to TRAIL apoptosis.

NMHCIIa, NMHCIIb, MLC2 and ßACT interact differentially with the DRs of normal and transformed cells. Motivated to find factors that modulate DISC composition and/or activation and hence that potentially account for the diverging response of normal and transformed cells to rhTRAIL, we performed DR5-IPs followed by liquid chromatography-supported mass spectrometry (MS) (Figure 25, A-D). Poinceau S staining of Western blot membranes loaded with BJ and BJELR DR5-IPs clearly detected differential banding patterns at 230KDa and 43 KDa ranges (Figure 25, B, left image). Therefore we excised these bands (Figure 25, B, right image) and performed on-membrane digestion according to described protocols [Luque-Garcia et al 2006]. Analysis of protein digests by MS identified NMHCIIa and ßACT in the 230KDa, respectively 43KDa samples. Importantly, in digests originating from control lanes containing eluates of DR5-IP-beads (B), no NMHCIIa, respectively only few ßACT peptides were detected as compared to DR5-IP-eluates derived from BJ or BJELR cell lysates (Figure 25, B-C).

In the following, we intended to confirm the identified NMHCIIa/DR5 and ßACT/DR5 interaction. We therefore expanded regular Western blot-based DISC analysis on the detection of NMHCIIa and ßACT, which affirmed their interaction with DR5 and DR4. Both MS and Western blot analyses showed higher levels of NMHCIIa and ßACT interacting with DR5 in normal cells in the unstimulated state. Upon rhTRAIL stimulus, NMHCIIa and ßACT were disassembled from DR5 in transformed but not in normal cells (Figure 25, D; for the full DISC analysis please see Supplementary, Figure 31). Fibroblasts, like a variety of cultured cells express 2 (IIa, IIb) of 3 existing (IIa, IIb, IIc) NMHC isoforms [Lo et al 2004]. We therefore controled DR-IPs for the interaction

with NMHCIIb and found that also NMHCIIb was co-purified with DR5, following the same pattern than NMHCIIa (Figure 25, D). It is well established that 2 NMHC molecules homodimerise and bind 2 ELC and 2 MLC2 [Vicente-Manzanares et al 2009]. This hecameric complex forms one NMII molecule (Introduction, Figure 14, A). Due to the fact that MLC2 are critical for NMII conformation, activity and filament formation capacity (Introduction, Figure 15, B) [Vicente-Manzanares et al 2009], we analysed and confirmed the association of MLC2 with the DISC-IPs (Supplementary, Figure 31). Importantly, analysis of the DISC immunoprecipitating DR4 gave comparable interaction patterns of cytoskeleton proteins with DR4 than with DR5 (Figure 25, D and Supplementary, Figure 31).

Questioning the biological significance of the NMII/DR and ßACT/DR interaction in cells other than mesenchymal fibroblasts, we analysed HTERT, SV40ER and HRASG12V-transformed HA1ER cells and confirmed the interaction of NMHCIIa, NMHCIIb and ßACT with DR5 in those cells (Supplementary, Figure 32). Analysis of normal HEK cells as their normal counterparts so far was hampered by poor cell growth, not yielding sufficient sample material. Whilst the co-purification of NMHCIIa, NMHCIIb and ßACT was confirmed in transformed HA1ER cells, no association of NMHCIIa or NMHCIIb with the DR5 or DR4 of highly rhTRAIL-sensitive BJAB cell was found (data not shown). This suggests a difference in cells growing in adhesion or suspension.

In a secondary MS approach where whole DR5-IP eluates immediately were given for in-solution digestion and analysis (Supplementary, Figure 33, A), again NMHCIIa and ßACT and in addition NMHCIIb was identified (Supplementary, Figure 33, B). In sample conditions where DR5 was identified in DR5-IP, parallel control IgG-IP purified neither DR5, nor co-precipitated NMHCIIa (Supplementary, Figure 33, C).

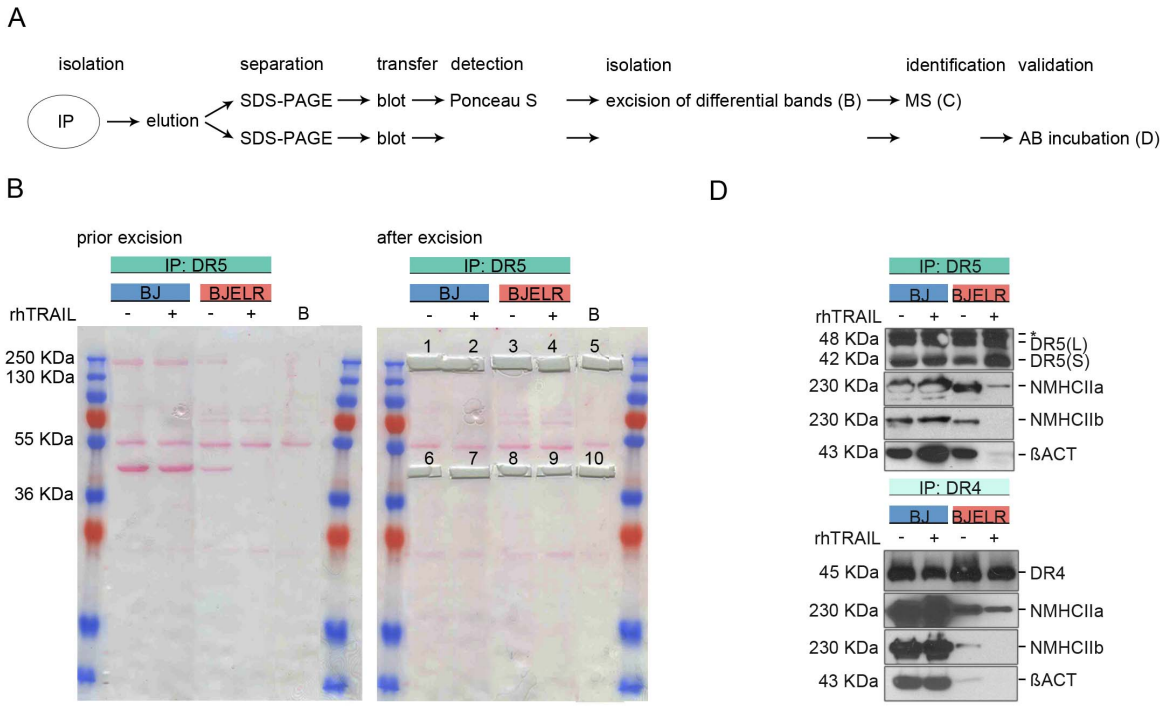

C

NMHCIIa [MYH9_HUMAN; Accession P35579; MW 226.4 kDa]

			Sequest			Mascot		
sample #	ΣCoverage	Σ# Peptides	Score A3	Coverage A3	# Peptides A3	Score A4	Coverage A4	# Peptides A4
1	5,61	24	55,92	5,26	13	223,70	4,34	11
2	4,08	12	21,55	1,68	3	80,04	4,08	9
3	1,48	4	13,53	0,71	1	64,93	1,48	3
4	0	0	0	0	0	0	0	0
5	0	0	0	0	0	0	0	0

ßACT [ACTB_HUMAN; Accession P60709; MW 41.7 kDa]

			Sequest			Mascot		
sample #	ΣCoverage	Σ# Peptides	Score A3	Coverage A3	# Peptides A3	Score A4	Coverage A4	# Peptides A4
6	26,67	58	111,53	26,67	32	652,51	23,20	26
7	21,07	44	90,83	21,07	23	535,70	16,27	21
8	22,40	29	58,58	22,40	16	348,23	14,13	13
9	19,47	30	50,62	19,47	14	223,09	16,00	16
10	5,60	4	5,74	5,60	2	47,59	5,60	2

Figure 25: Identification of novel TRAIL-DISC interactors immunoprecipitating DR5 in normal BJ and transformed BJELR fibroblasts followed by on-membrane digestion of differential bands and mass spectrometry. **(A)** DR5 was isolated from normal (BJ) and HTERT, SV40ER and HRASG12V-transformed (BJELR) cells that were left unstimulated (-) or that were stimulated for 1h with 1µg mL^{-1} rhTRAIL (+) by immunoprecipitation (IP). IP eluates were split into two fractions of which both were separated by SDS-PAGE and blotted onto nitrocellulose membranes. **(B)** One nitrocellulose membrane onto which one portion of the DR5-DISC IP was blotted was stained with Ponceau S and differential bands were cut out, digested and given for mass-spectrometrical peptide identification. **(C)** Mass spectrometry results obtained from the single cutouts generated in (B). **(D)** Another nitrocellulose membrane onto which the other portion of the DR5-DISC IP was blotted was subjected to regular Western blot analysis to validate the mass-spectrometric results obtained from (B, C) (upper panel). Western blot analysis of a DR4-IP (lower panel).

NMHCIIa, NMHCIIb and ßACT are expressed at similar protein levels in normal BJ and transformed BJELR cells whereas MLC2 is increased in transformed cells. Cellular transformation is often associated with the down-regulation of actin-associated proteins such as TM, CALD, MLC2, calponin, transgelin, ABP280, alpha-actinin, MARCKS, schwannomin, thymosin ß4, gelsolin [Button et al 1995, Pawlak and Helfman 2001, Iida et al 2009]. Given the reduced interaction of NMHCIIa, NMHCIIb, MLC2 and ßACT with the DR of BJERL cells (Figure 25, D, Supplementary, Figure 31), we carried out Western blot analysis of BJ and BJELR whole cell lysates and found that whilst NMHCIIa, NMHCIIb and ßACT were expressed at comparable levels, MLC2 protein levels are increased in transformed cells (Figure 26). Importantly, the applied anti-MLC2 antibody detects all three existent MLC2 isoforms, namely smMLC2, nmMLC2 and nmlMLC2. Due to their sequence homology no antibody can be generated capable to distinguish between these MLC2 isoforms. An oncogenic HRAS-transformation associated decrease of only the smMLC2 isoform mRNA and protein levels has been reported, whilst same studies describe no transformation-associated alterations of nmMLC2 and nmlMLC2 protein levels [Kumar et al 1991, Kumar et al 1992, Gerrits et al 2012]. This apparent discrepancy to our results might be due to the fact that oncogenic HRAS-transformation was investigated in fibroblasts [Kumar et al 1991, Kumar et al 1992] and immortalised mouse embryonic fibroblasts [Gerrits et al 2012], but not in SV40ER-pretransformed cells, and therefore could depend on the genetic background. Indeed, Gerrits et al demonstrate Western blots with constantly higher nmMLC2 (and seemingly also smMLC2 and nmlMLC2) protein levels in tumourigenic human cancer cells in comparison to nontumourigenic cells, but unfortunately do not discuss this result.

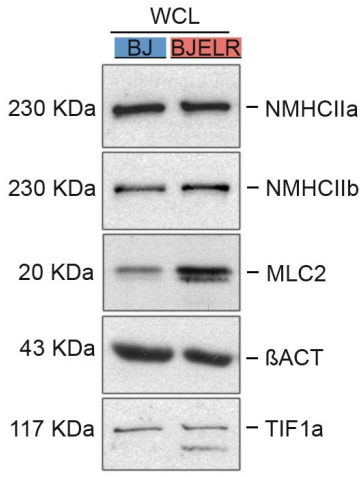

Figure 26: Cytoskeletal protein expression levels in normal BJ and transformed BJELR cells. The expression levels of non-muscle myosin heavy chain IIa and IIb (NMHCIIa, NMHCIIb), myosin regulatory light chain 2 (MLC2) and beta-actin (ßACT) was assessed in whole cell lysates (WCL) of normal (BJ) and HTERT, SV40ER and HRASG12V-transformed (BJELR) cells. Transcription intermediary factor 1-alpha (TIF1a) served as loading control. Depicted are representative Western blots of 3 independent experiments.

Interim summary and conclusion III

Mass spectrometry probing of either on-membrane digested differential bands or whole DR5-IP eluates of unstimulated and rhTRAIL-treated normal BJ and transformed BJELR cells identified NMHCIIa, NMHCIIb and ßACT as novel DR5-interactors. Subsequent Western blot analysis confirmed the interaction and revealed that MLC2 was additionally co-purifed. Intriguingly, whilst MS and Western blot detection yielded more peptides and strong detection signals for the DR5-IP of unstimulated and rhTRAIL-treated normal BJ cells, DR5-IP of transformed BJELR cells brought about less peptides and weak Western blot signals that declined even more upon rhTRAIL addition. Importantly, exact same interaction patterns were found for DR4-IP of BJ and BJELR cells and for DR5-IP of transformed HA1ER cells. Unfortunate poor growth of normal HEK cells complicated an analysis of the DR5 interaction hitherto. However, detecting the NMII/DR and ßACT/DR interaction in transformed cells of two different transformation models (BJELR and HA1ER) underscores the biological significance of interaction.

Even though a weaker interaction of NMHCIIa, NMHCIIb, MLC2 and ßACT with DR5 and DR4 of transformed BJELR than normal BJ cells was found, Western blots indicated similar protein expression levels for all proteins except MLC2 that was increased in transformed cells.

In summary, rhTRAIL-resistance in normal cells is associated with robust and sustained NMHCII/DR interaction, which is weaker and lost in TRAIL-sensitive transformed cells. Explorations of whether the newly identified interaction is of functional meaning for TRAIL apoptosis are communicated in the subsequent chapter.

IV - Functional characterisation of the NMHCII/DR interaction with respect to TRAIL apoptotic response

Arrangement of the actomyosin cytoskeleton differs in normal and cancer cells, being disrupted in the latter [Weber et al 1974, Bar-Sagi et al 1986]. As actin cytoskeleton constituent, NMII are implicated to function in central processes such as cell adhesion and migration [reviewed by Vicente-Manzanares et al 2009], cell spreading [Hirata et al 2009], Golgi vesicle budding and transport [Stow et al 1998, Lin et al 2012], exocytosis [Ludowyke et al 2006], ligand-induced receptor capping [Lorimer and De Lanerolle 1996, Komatsu et al 2000], redistribution of membrane proteins [Kuo et al 2011] and receptor endocytosis [Rey et al 2007]. Interestingly, not only some of these processes have been implicated in TRAIL signalling and/or sensitisation (adhesion/spreading [Goldberg et al 2001, Algeciras-Schimnich et al 2002, Kurenova et al 2004, Laguinge et al 2008, Phipps et al 2011], transport [reviewed by Weinlich et al 2010], redistribution [Song et al 2007, Rossin et al 2009], endocytosis [Jin et al 2004, Cheng et al 2006, Zhang et al 2008]) but also kinases known to modulate TRAIL sensitivity and/or signalling in tumour cells (CK2 [Ravi and Bedi 2002, Izeradjene et al 2004, Izeradjene et al 2005, Shin et al 2005, Wang et al 2006, Llobet et al 2008, Pallares et al 2008], TRPM7 [Liu et al 2012], PKCβ [Kaunisto et al 2009, Meng et al 2010], ROCK [Hoogwater et al 2010, Ehrenschwender et al 2010], PAK1 [Wei et al 2010]) are key NMHCIIa and IIb regulators (see 'Introduction' and [Vicente-Manzanares et al 2009]). Therefore we investigated whether the prominent NMHCII/DR interaction in normal cells is of functional relevance for TRAIL resistance and / or apoptosis.

Chemical inhibition of NMII Mg2+-ATPase activity decreased NMHCIIa, NMHCIIb and MLC2 association with DR5 and DR4 and increased rhTRAIL-induced apoptosis in normal BJ cells. The non-competitive inhibitor blebbistatin specifically acts on skeletal muscle and non-muscle myosin II isoforms [Limouze et al 2004] blocking the actin-activated Mg^{2+}-ATPase activity housed in the head domain. Blebbistatin preferentially binds to the myosin II head when ADP and phosphate are still bound at the active site of the Mg^{2+}-ATPase domain, whereby it blocks the phosphate release process that is required for the binding of NMII to actin (Figure 27, A) [Kovacs et

al 2004, Allingham et al 2005, Sandquist and Means 2008]. Treatment of normal BJ cells with 25μM blebbistatin for 30 min sufficed to diminish NMHCIIa, NMHCIIb and MLC2 co-immunoprecipitation with DR5 and DR4. Of note, ßACT binding to DR5 and DR4 was unaffected by blebbistatin treatment (Figure 27, B), suggesting that ßACT binds to DR5 and DR4 independently of NMIIa and NMIIb. Normal cells pre-incubated for 30 min with increasing blebbistatin concentrations and successively treated with blebbistatin and 1μg mL^{-1} rhTRAIL for 16h, demonstrated an elevated dose-dependent response to rhTRAIL-apoptosis as compared to vehicle and TRAIL treated cells. Cells pre-treated with 25μM blebbistatin yielded 52% ±3 apoptotic cells, which was significantly more than obtained in cells pre-incubated with equal concentrations of solvent (DMSO) or without pre-treatment (19% ±5, p=0.02 and 13% ±4, respectively) (Figure 27, C). Given that blebbistatin blocks NMII in an actin-detached state (Figure 27, A) [Kovacs et al 2004] and blebbistatin removes NMII but not ßACT from DR, we assume that ßACT binding to DR does not require NMII Mg^{2+}-ATPase activity. Contrary, the magnitude of NMIIa and NMIIb co-purification depends on NMII Mg^{2+}-ATPase activity.

Preceding blebbistatin experiments revealed that inhibiting NMII Mg^{2+}-ATPase activity lead to a weakening of NMII/DR interaction and an increase in rhTRAIL-apoptosis in normal cells. Aiming to reinforce these data we anticipated another chemical approach to interfere with NMII Mg^{2+}-ATPase activity. Reportedly NMIIs are highly regulated by phosphorylation events amongst which MLC2 phosphorylation at serine 19 (Ser19) and threonine 18 (Thr18) is of utmost importance for NMIIs to display active conformation and to enable NMII/protein interaction (Figure 27, D). Importantly, MLC2 phosphorylation at Ser19 and Thr18 increases the actin-activated Mg^{2+}-ATPase function of NMII [Vicente-Manzanares et al 2009]. Even though MLCK is not the only kinase capable to phosphorylate MLC2 at these residues (Introduction, Figure 17) [please see Vicente-Manzanares et al 2009 for detailed information], MLCK has the advantage of having a limited substrate reservoir. In fact, MLC2 so far is the only accepted MLCK substrate for that *in vivo* data exist [phosphosite.org]. Aiming to minimize effects arising from impaired phosphorylation of secondary proteins, we therefore decided to interfere with NMII Mg^{2+}-ATPase activity by blocking MLCK-mediated MLC2 phosphorylation. For that we used ML7, an MLCK-specific inhibitor [Saitoh et al 1987, Bain et al 2003] that competes with ATP binding to MLCK. Of note, 30 min after ML7 addition at concentrations ≤50μM normal cells began to display

retraction of cell protrusions and cell rounding, which was then followed by a recovery phase. At 2.5h after addition of ≤50μM ML7, cells fully recovered normal morphology. Normal BJ cells that were incubated for 30 min with 50μM ML7 showed a reduction in NMHCIIa and MLC2 binding to DR5. In contrast to the results achieved with blebbistatin, ML7 treatment additionally decreased ßACT-co-purification with DR5 (Figure 27, E), indicating a requirement of MLC2 phosphorylation for the association of MLC2 and ßACT to NMHCII or DR5. Pre-incubation for 30 min with varying ML7 concentrations followed by subsequent additon of 1μg mL^{-1} rhTRAIL for 16h increased the percentages of apoptotic cells in dosage-dependent manner. Co-treatment of BJ cells with 50μM ML7 and 1μg mL^{-1} rhTRAIL resulted in 29% ±0.3 apoptotic cells, which was significantly more than what was acquired for cells co-incubated with equal concentrations of vehicle (ethanol/water mix at a ratio 1:1) (7% (±3), p=0.0002) (Figure 27, F). Notably, increasing ML7 concentrations to 100μM or 200μM resulted in detachment of BJ cells from the surface and apoptosis induction in absence of rhTRAIL (43% (±0.3), respectively 81 (±4)) (Supplementary, Figure 34).

As the observed overall sensitising effect of normal BJ cells to TRAIL-apoptosis was stronger with blebbistatin than with ML7 (52% ±3 versus 29% ±0.3), both agents reduced the NMII/DR interaction, blebbistatin did not affect the ßACT/DR interaction whilst ML7 abolished ßACT from DR, we concluded that TRAIL-DISC mediated apoptosis may require the interaction with ßACT.

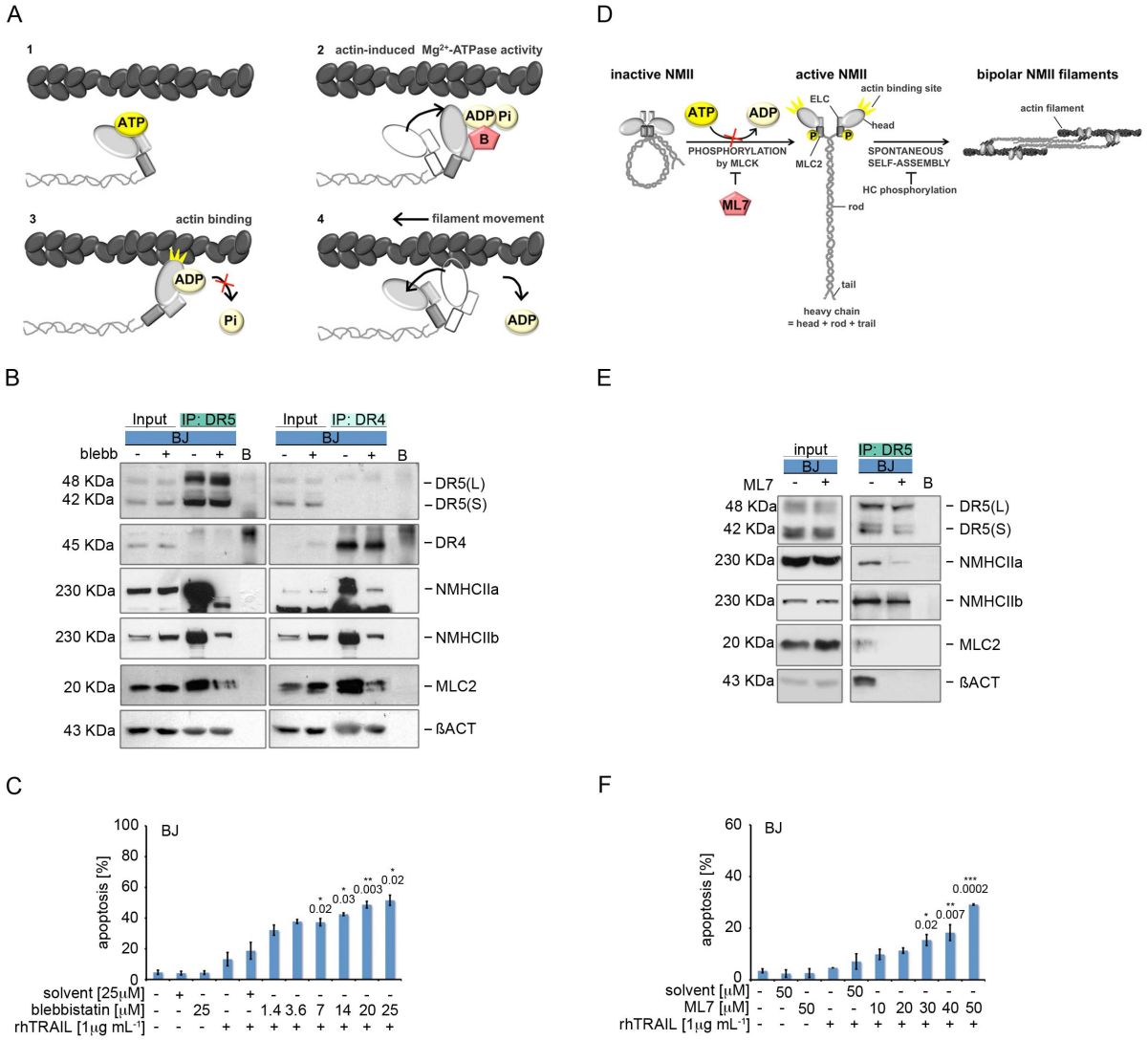

Figure 27: Effects of NMII inhibition on NMHCIIa, NMHCIIb interaction with DR5 and DR4 and TRAIL-sensitivity in normal BJ cells. **(A)** During the NMII crossbridge cycle blebbistatin preferentially binds to the NMII head with ADP and phosphate bound at the active site of the Mg^{2+}-ATPase domain. Since it slows down phosphate release, NMII does not bind to actin. **(B)** NMHCII/DR5 and NMHCII/DR4 interaction upon inhibition of NMII ATPase activity. Normal (BJ) cells were incubated for 30 minutes with vehicle DMSO (-) or 25µM NMII ATPase inhbitor blebbistatin (+) and then collected the cells to immunoprecipitate (IP) death receptor 5 and 4 (DR5, DR4). The IP-eluates were analysed for the interaction with non-muscle myosin heavy chains IIa and IIb (NMHCIIa, NMHCIIb), the myosin regulatory light chain (MLC2) and beta-actin (ßACT).* **(C)** rhTRAIL-induced apoptosis under the inhibition of NMII ATPase activity. BJ cells were pre-treated for 30 minutes with the indicated concentrations of solvent or blebbistatin and then co-treated with 1µg mL^{-1} rhTRAIL (+). Apoptosis was assessed as 7A6 positivity 16 hours after the addition of rhTRAIL.** **(D)** ML7 binds at the ATP-binding site of MLCK inhibiting its catalytic activity. In the absence of MLC2 phosphorylation the NMII molecule has a circular, inactive and assembly-incompetent conformation (left), cannot open (middle) or spontaneously assemble into myosin filaments (right). The figure is based on the idea of [Vicente-Manzanares et al 2009, Book: Alberts et al Molecular Biology of the Cell (Garland Science)]. **(E)** NMHCII/DR5 interaction upon inhibition of NMII activity. Normal BJ cells were incubated for 30 minutes with vehicle ethanol:water (1:1) (-) or 50µM MLC2-phosphorylating kinase (MLCK) inhibitor ML7 (+) and then collected to IP DR5. The IP-eluates were analysed as described in (A).*** **(F)** rhTRAIL-induced apoptosis under the inhibition of the MLC2-phosphorylating kinase (MLCK). BJ cells were pre-treated for 30 minutes with the indicated concentrations of solvent or ML7 and then co-treated with 1µg mL^{-1} rhTRAIL (+). Apoptosis was assessed as in (B).**** Depicted are Western blots for 1 of *3, respectively ***2 independent experiments. Values derive from **3 to 4, respectively ****2 to 5 independent experiments. Significances were calculated using unpaired, 2-tailed Student's t-test.

Deregulated signalling pathways decreasing NMII Mg2+ ATPase activity in transformed cells. Prior results revealed that chemical inhibition of NMII activity results in weakened NMII/DR interaction and reinforced TRAIL apoptosis in normal BJ fibroblasts. In contrast, NMII/DR interaction intensities in transformed BJELR cells generally are low and TRAIL response is high. We reasoned that if inhibition of NMII activity in normal cells leads to a similar phenotype than in transformed cells, general NMII activity should differ in normal and transformed cells. Thus, it should be possible to identify signalling mechanisms that inhibit NMII activity in transformed cells in a similar mode than blebbistatin or ML7 do in normal cells.

As MLC2 phosphorylation is necessary for NMIIs to increase basal, actin-activated Mg^{2+}-NMII ATPase activity and to acquire active conformation (Figure 27, A&D) [Ikebe et al 1986, reviewed by Friedl and Wolf 2003, Somlyo and Somlyo 2003, Vicente-Manzanares et al 2009], we compared levels of phosphorylated MLC2 in WCL of normal BJ and transformed BJELR cells by Western blot. We found higher MLC2 phosphorylation in BJ cells, although total MLC2 expression levels were upregulated in BJELR cells (Figure 28, A), indicating hindered MLC2 regulation by phosphorylation and altered NMII function in transformed cells. Exploring upstream kinases that could account for reduced MLC2 phosphorylation levels in transformed cells (Introduction, Figure 17), we observed that MLCK but not ROCK1 was downregulated and the MLCK inhibiting kinase PAK1 was upregulated in BJELR cells (Figure 28, B). Furthermore, we monitored an induction of MLCK expression in BJ and BJELR cells within 15min of TRAIL treatment and this induction of MLCK expression was weaker in BJELR than in BJ cells (Figure 28, B). Findings of reduced MLC2 phosphorylation levels and downregulated MLCK expression in BJELR cells were supported by apoptosis assays upon high ML7 dosages, which revealed that BJELR cells did not survive ML7 levels as high as BJ cells (Supplementary, Figure 34). These data suggest that NMII activity in transformed BJELR cells is hindered (at least) by deregulation of MLCK and PAK1.

Work on further inherent mechanisms blocking NMII ATPase activity were not concluded at the time this manuscript was generated, and therefore can be read in the section ‘Work in Progress’.

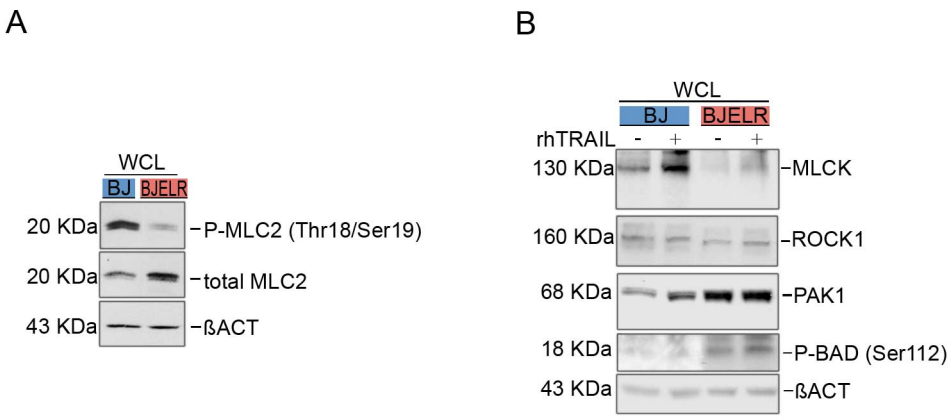

Figure 28: Differences in MLC2 phosporylation and kinase expression levels in normal BJ and transformed BJELR cells. **(A)** Normal (BJ) and HTERT, SV40ER and HRASG12V-transformed transformed (BJELR) cells were lysed and whole cell lysates (WCL) were subjected to Western blot analysis to explore the relative expression levels of the myosin regulatory light chain (MLC2). **(B)** BJ and BJELR cells were left untreated (-) or were treated for 15min with 1µg mL^{-1} rhTRAIL (+) and analysed for protein expression levels of the MLC2 phosphorylating kinases myosin light chain kinase (MLCK), Rho-associated kinase 1 (ROCK1) and the MLCK phosphorylating and inactivating p21-activated protein kinase 1 (PAK1). PAK1 activity was assessed immuno-blotting for phosphorylated BAD. Representative Western blots for 1 of 2 independent experiments.

NMHCIIa but not NMHCIIb protein depletion enhances rhTRAIL apoptosis in normal BJ cells by altering the DISC composition. Low NMHCIIa/DR and NMHCIIb/DR interaction prior to rhTRAIL stimulation correlated with high apoptosis outcome in transformed cells and in normal cells where the NMII/DR interaction has been disrupted (Figure 24, B, Figure 25, D, Figure 27). NMIIa and NMIIb differ in their actin-activated Mg^{2+}-ATPase activity (highest in NMIIa), the time that myosin is bound to actin in a force-generating state (highest in NMIIb) and their C-terminal tails that determine their intracellular localization [Vicente-Manzanares et al 2009]. We therefore questioned if a functional variation between both NMII isoforms exists with regard to TRAIL apoptosis signalling. Aiming to specifically interfere with either or isoform function, we performed NMHCII siRNA knockdown (KD) experiments in normal BJ cells. Although NMHCIIa and NMHCIIb are highly homologous [Bresnick et al 1999], siRNA-mediated knockdown is specific (Figure 29, A). Depletion of NMHCIIb but not NMHCIIa impaired cell proliferation in normal cells as compared to scramble (SCR) control cells (NMHCIIb=$2.18x10^5$±$4.4x10^4$ cells, p=0.03; NMHCIIa=$4.3x10^5$±$1.3x10^5$ cells; SCR=$3.6x10^5$±$5.3x10^4$ cells) (Figure 29, B). We noted a differential influence of NMHCIIa or NMHCIIb protein loss on the adhesive properties of normal BJ cells, since KD of

NMHCIIa but not NMHCIIb decreased attachment of BJ cells to the cell culture plate, which is in line with reported loss of focal adhesions in NMHCIIa KD cells [Li et al 2008]. NMHCIIa-KD cells detached much faster during trypsinisation than SCR-transfected control, mock-transfected control or NMHCIIb-KD BJ cells. Significantly ($p=6.9x10^{-6}$) more NMHCIIa-KD cells underwent rhTRAIL-induced apoptosis (63% ±7) than NMHCIIb-KD (21% ±10) or SRC-control BJ cells (14% ±5) (Figure 29, C). Questioning whether the increased rhTRAIL apoptosis was mediated at the level of the DISC, we performed Western blot analysis of KD cells treated with TRAIL and revealed blots for CASP8 cleavage. We found stronger CASP8 cleavage product signals in NMHCIIa- (Figure 29, D) but not in NMHCIIb-KD cells (not shown) corresponding to the fact that upon NMHCIIa-KD more normal cells respond to rhTRAIL-induced apoptosis. Given that CASP8 ativation was increased upon NMHCIIa-KD, we performed DISC analyses in NMHCIIa-KD BJ cells immunoprecipitating DR5. Importantly, NMHCIIa-KD did not alter total expression levels of DISC protein members (Figure 29, E). We found that upon NMHCIIa-KD and rhTRAIL-induction DR4 recruitment to DR5 was lowered, whereas CASP8 cleavage an/or recruitment was increased and in turn cFLIP(L) processing and/or recruitment was reduced (Figure 29, E). Thus, NMHCII depletion sensitises normal BJ cells to rhTRAIL-induced apoptosis reducing anti-apoptotic cFLIP(L) levels and increasing active CASP8 levels at the DISC. Likewise we have observed in blebbistatin experiments (Figure 27, B), NMHCIIa-depletion did not abrogate the interaction of ßACT with DR5, supporting the hypothesis that ßACT binding to DR5 occurs independent of NMIIa.

Attempts to measure DR5 and DR4 surface levels upon NMHCIIa-KD in normal BJ cells were not finished at the time this manuscript was generated, and hence were incorporated into the section ‘Work in Progress’.

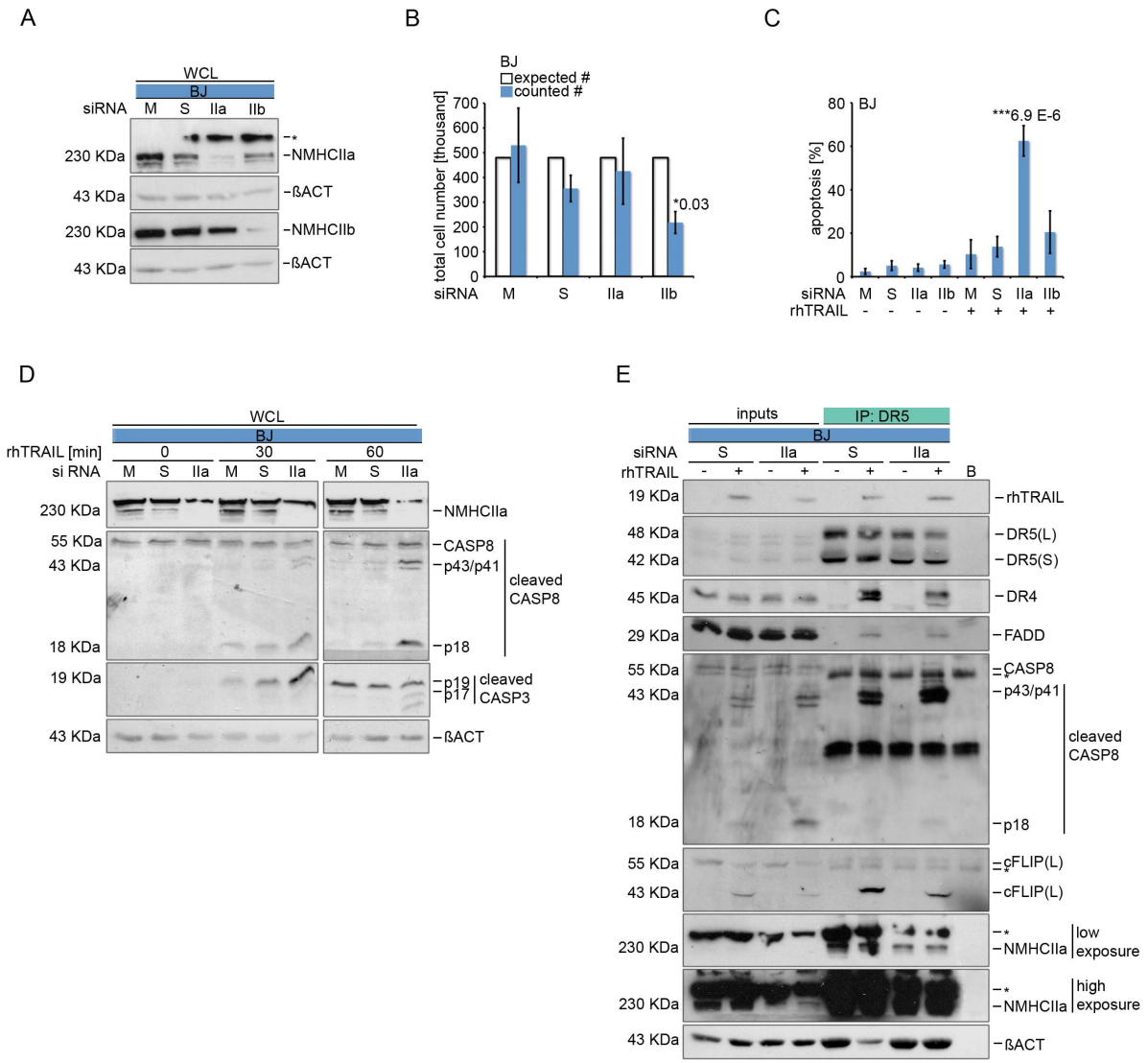

Figure 29: Effects of NMHCIIa- and NMHCIIa siRNA knockdown on cell proliferation, rhTRAIL apoptosis, caspase cleavage and DISC formation in normal BJ cells. Normal (BJ) cells were transfected with 15nM siRNA against non-muscle myosin heavy chain IIa or IIb (IIa, IIb), scramble control siRNA (S) or were mock-transfected with lipofectamine (M) for 4d. Cell culture medium was renewed 1d and 3d after start of transfection. **(A)** Whole cell lysates (WCL) of BJ cells were analysed for NMHCIIa and NMHCIIb expression levels upon 4d knockdown (KD) by Western blot.* **(B)** Total BJ cell numbers were counted at 4d of KD. Values are means of 3 independent experiments. **(C)** TRAIL-induced apoptosis upon NMHCIIa and NMHCIIb siRNA KD. Four days after start of KD BJ cells were left untreated (-) or were treated with 1µg mL^{-1} rhTRAIL (+). Apoptosis was assessed as 7A6 positivity 16 hours after the addition of rhTRAIL. Values represent mean values of 4 independent experiments. **(D)** BJ cells were treated with 1µg mL^{-1} rhTRAIL for the indicated time 4 days after start of KD. Whole cell lysates were analysed for NMHCIIa knockdown efficiency and caspase-8 and -3 (CASP8, CASP3) cleavage by Western blot.** **(E)** TRAIL-induced DISC formation upon NMHCIIa siRNA KD. BJ cells were left untreated (-) or were treated with 1µg mL^{-1} rhTRAIL (+) for 1h 4 days after start of KD. Death receptor 5 (DR5) was immunoprecipitated and analysed for co-purified proteins by Western blot. Pre-cleared cell lysates (inputs) served as loading controls and as indicators for KD-mediated alterations in protein expression.** Depicted are Western blots for 1 out of *3 and **2 independent experiments. Significances were calculated using unpaired, 2-tailed Student's t-test.

Interim summary and conclusion IV

Blocking NMII ATPase activity using chemical inhibitors that keep NMII in actin-detached state (blebbistatin), or that lock NMII in a closed conformation (ML7) released NMHCIIa, NMHCIIb and MLC2 from DR5 and DR4 of normal BJ cells and sensitised them to rhTRAIL apoptosis in a dose-dependent manner. This supported the hypothesis that the basal level of NMII/DR interaction regulates cell response to TRAIL and the level of apoptosis. Since actin binding to DR was unaffected when treating BJ cells with blebbistatin or when depleting NMHCIIa protein, ßACT appears to bind to DR independently of NMII. Contrary, it cannot be excluded that NMII binding to DR is mediated by ßACT.

Transformed BJELR cells displayed lower NMII activity, as evidenced by reduced MLC2 phosphorylation levels and Western blot. Decreased NMII activity and NMII/DR interaction in transformed BJELR cells was accompanied by low MLCK and high PAK1 protein expression levels in BJELR as compared to BJ cells. In addition, short-term rhTRAIL induction increased MLCK expression levels in BJ and BJELR cells. The observed increase in MLCK expression upon rhTRAIL treatment however, was less pronounced in BJELR than BJ cells. Importantly, lower MLCK expression in BJELR cells was supported by the finding that BJELR cells do not survive ML7 concentrations in the height than normal BJ cells do as demonstrated in FACS-assisted apoptosis assays. Therefore, deregulation of MLCK and PAK1 and a consequently reduced MLC2 phosphorylation level in BJELR cells suggests one cause for the decrease NMII/DR interaction in BJELR cells.

Isoform-specific intervention with NMHCIIa and NMHCIIb function by siRNA-facilitated knockdown revealed that loss of NMHCIIa but not NMHCIIb decreased normal BJ cell attachment. Contrary, decline in NMHCIIb but not NMHCIIa protein levels impaired normal BJ cell proliferation, as demonstrated by total cell counts. According to literature cell sensitivity to TRAIL-apoptosis can be modulated either by reducing cell attachment or by alterations in concentrations of cellular factors that are secreted into the medium. Therefore both observations are of importance. FACS-assisted apoptosis assays showed that reductions in NMHCIIa but not NMHCIIb protein levels removed the TRAIL resistance block in normal BJ cells and significantly increased the percentage of apoptotic cells. Given that NMHCIIb KD hindered normal cell proliferation, changes in

percentages of TRAIL-apoptosis might have arisen from lowered concentrations of secreted factors required for TRAIL-apoptosis to occur. The sensitisation effect of NMHCIIa-loss was reinforced by increased CASP8 and CASP3 cleavage signals of NMHCIIa-KD cells compared to scramble-transfected control BJ cells. Finally, although total DR4, CASP8 and cFLIP(L) expression levels were unaltered in KD cells, DISC analyses immunprecipitating DR5 showed that less DR4 is recruited, more CASP8 active fragment is generated and /or CASP8 is recruited and less cFLIP(L)p43 is produced and/or less cFLIP(L) is recruited if NMHCIIa protein levels at the DR5/DISC are reduced. Thus, NMHCIIa is a novel DR interactor that regulates the response of normal cells to TRAIL.

Identification of TRAIL DISC binding proteins that putatively are influenced by or that influence the NMHCIIa/DR5 interaction

Interfering with cell adhesion and spreading is a way to sensitise to TRAIL-apoptosis and adherent cells were reported as more sensitive to TRAIL if they were treated in suspension [Goldberg et al 2001, Algeciras-Schimnich et al 2002, Kurenova et al 2004, Laguinge et al 2008, Phipps et al 2011]. Recently, a study analysing the proteome of focal adhesions in presence and absence of blebbistatin reported the recruitment of signalling proteins regulating adhesion, spreading, migration, proliferation and survival to focal adhesions was either promoted or prevented by NMII contractility [Kuo et al 2011]. We observed a strong NMII/DR interaction and resistance to rhTRAIL-apoptosis in normal cells and a weak NMII/DR interaction and sensitivity to rhTRAIL-apoptosis in transformed BJELR cells. Hence, we hypothesised that NMII could bring pro-survival proteins into the DISC of normal cells.

Pro-survival adapter protein GRB2 and serine/threonine kinase RAF1 constitutively bind to DR5 and their binding is not dependent on NMHCIIa. Interestingly, the proliferation signalling adapter and SH3 protein GRB2 was indicated to interact with NMHCIIa [Blagoev et al 2003] and proven to directly bind to TNFR1 via a PLAP motif in the receptor sequence [Hildt and Oess 1999]. Generally, SH3 proteins recognise PXXP and RXXK motifs [Cohen et al 1995, Berry et al 2002] that are found in both DR5 long and short isoforms (Figure 30, A). Therefore we investigated DR5- and DR4-immunoprecipitates for the co-purification of GRB2. Like it is the case for TNFR1 [Hildt and Oess 1999], GRB2 interacts constitutively with DR5 (Figure 30, B). Even though the cytoplamic sequence of DR4 does not contain a PXXP or RXXK motif (Figure 30, A), GRB2 co-immunoprecipitated when DR4 was targeted (not shown). This could on one hand be due to the diversity of SH3 domain-binding motifs of which there are new ones constantly identified [Kaneko et al 2008]. On the other hand the GRB2/DR4 interaction could be mediated via GRB2's SH2 domain, just as it is the case for tyrosine kinase receptors such as EGFR [Batzer et al 1994, Okutani et al 1994, Chook et al 1996, Jones et al 2006]. Of note, no co-purification of TNFR1 or EGFR occurred in DR5-IPs (not shown), indicating that co-purification of GRB2 with DR5-IPs is due to GRB2 binding to

DR5, not to an interaction of DR5 with TNFR1 or EGFR that consequently would bring GRB2. To test the hypothesis that NMII could bring GRB2 to the receptor, we analysed DR5-IP eluates originating from previous NMHCIIa KD experiments in normal BJ cells for differential GRB2 recruitment and found no alterations (Figure 30, C). Thus, GRB2 binding to DR5 in normal BJ cells does not depend on NMHCIIa.

Binding of GRB2 to TNFR1 is essential for TNFα-induced activation of RAF1 [Hildt and Oess 1999]. In TNFα- and FAS-signalling RAF1 is recruited into and activated at the DISC by cleaved cFLIP(L)p43 [Kataoka et al 2000, Park et al 2001]. RAF1 phosphorylates and activates MEK1 [Zheng et al 1996], it regulates apoptosis targeting FAS, apoptosis signal-regulating kinase 1 (ASK1), mammalian STE20-like protein kinase 2 (MST2), and ROCK2 [Piazzolla et al 2005, Matallanas et al 2011] and it inhibits MYPT1 by phosphorylation [Broustas et al 2002]. Of note, RAF1 gene knockout in mice lead to apoptosis and embryonic lethality, a phenotype that could be rescued using RAF1 mutants without kinase activity towards MEK [Mikula et al 2001, Hüser et al 2001, Matallanas et al 2011]. Previous experiments demonstrated that siRNA-mediated NMHCIIa depletion amongst others resulted in reduced cFLIP(L) recruitment and/or processing at the DR5-DISC (Figure 29, E). We reasoned that if cFLIP(L)p43 would recruit RAF1 into the DISC and if lower cFLIP(L)p43 levels are observable in NMHCIIa KD cells, one would be able to detect less RAF1 recruitment. Therefore we investigated DR5-IP eluates originating from previous NMHCIIa KD experiments for the presence of RAF1. Surprisingly, RAF1 constitutively co-purified with DR5 to comparable levels in scrambled transfected and NMHCIIa KD normal BJ cells (Figure 30, C). Thus, like with GRB2, RAF1 interaction with the DR5 DISC appears to be independent of the NMHCIIa/DR5 interaction.

Depletion of GRB2 does not enhance the DISC-mediated rhTRAIL apoptosis in normal BJ cells. In contrast to NMHCIIa KD, GRB2 ablation in normal BJ cells increased cell adhesion and critically decreased cell proliferation as assessed by total cell counts 4d after start of siRNA-mediated KD (GRB2=$1.54x10^5$±$2.4x10^4$cells, p=0.03; SCR=$4.3x10^5$±$1.4x10^4$ cells) (Figure 30, D). Loss of GRB2 protein was accompanied by a decline in phosphorylated RAF1, phosphorylated MEK1/2 and total MEK1/2 levels as evidenced by Western blot analyses of normal BJ cell WCL 4d after transfection (Figure

30, E). To explore effects of GRB2 deficiency on TRAIL sensitivity, we left lipofectamine-transfected (mock), scramble siRNA-transfected (SCR), and GRB2 siRNA-transfected cells 4d after start of transfection untreated or treated them with 1µg mL^{-1} rhTRAIL for 16h and assessed the percentage of apoptotic cells. Results yielded a mild but significant difference in rhTRAIL-induced apoptosis between GRB2 depleted and SCR control cells (GRB2=27% ±1.3, p=0.03; SCR=20% ±1). However, solely the reduction of GRB2 protein levels without rhTRAIL stimulation was sufficient to decrease cell viability of normal BJ cells (GRB2=7% ±2, p=0.06; SCR=3% ±1.6) (Figure 30, F). Thus, GRB2 deficiency in normal BJ cells did not drastically enhance the apoptosis response to TRAIL. Instead, it reduced cell proliferation and basal cell viability. Investigating the effects on TRAIL sensitivity therefore was difficult to assess, as cell densities and secreted factors at the moment of rhTRAIL addition are critical for the cell response to TRAIL.

Aiming to compensate cell density differences at the start of rhTRAIL treatment, we reduced the KD duration of GRB2 from 4 to 2 days and assessed the rhTRAIL apoptosis response by analysing CASP8 and CASP3 cleavage in normal BJ cells in Western blots. We found that 2d KD was sufficient to reduce GRB2 protein levels. However, after 30min or after 17h of 1µg mL^{-1} rhTRAIL we did not observe enhanced signals for CASP8 or CASP3 cleavage, indicating that loss of GRB2 has no impact on the DISC-mediated rhTRAIL apoptotic response in normal BJ cells (Figure 30, G).

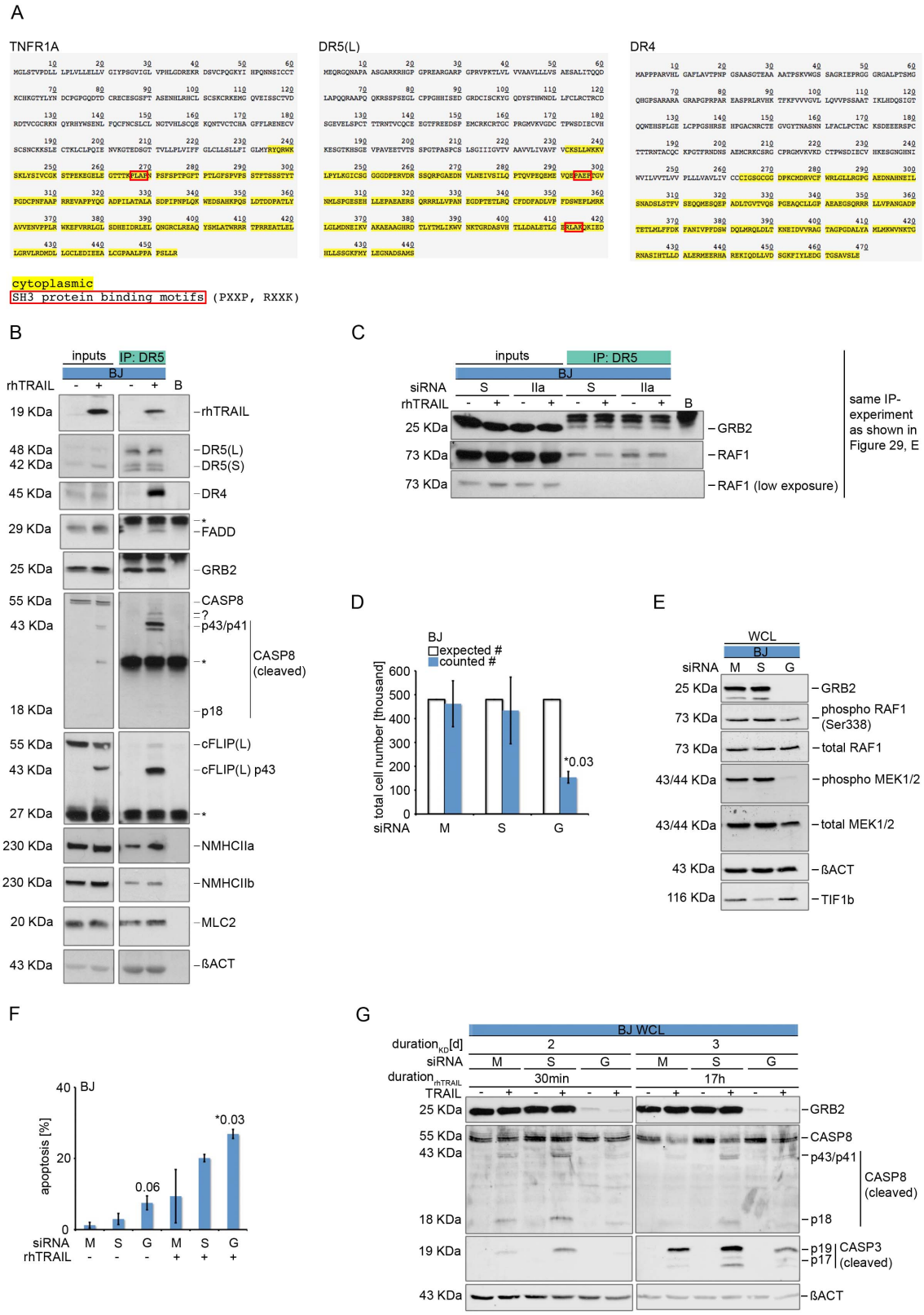

Figure 30: GRB2 and RAF1 binding to DR5 and effects of GRB2 siRNA knockdown on cell proliferation, TRAIL apoptosis and TRAIL-induced caspase cleavage in normal BJ cells. **(A)** Amino acid sequences of tumor necrosis factor receptor 1 (TNFR1) and death receptor 5 and 4 (DR5, DR4). Highlighted in yellow are the cytoplasmic domains and boxed in red are SH3 protein binding motifs. **(B)** Normal (BJ) fibroblasts were left untreated (-) or were treated with 1µg mL^{-1} rhTRAIL and the DISC isolated by immunoprecipitation (IP) targeting DR5. Equal volumes of pre-cleared lysates (inputs) or DR5-IP eluates

Interim summary and conclusion V

GRB2 and RAF1 constitutively bind to DR5 and in case of GRB2 also to DR4. Their binding to DR5 is not dependent on NMIIa activity, since NMHCIIa siRNA-mediated protein depletion diminished NMHCIIa/DR5 interaction, but had no influence on the levels of co-immunoprecipitated GRB2 and RAF1 upon immunoprecipitation of DR5.
The finding that RAF1 constitutively co-purifies with DR5 implies that RAF1 recruitment into the TRAIL DISC cannot be mediated by cFLIP(L)p43, denoting an apparent difference to TNFα and FAS signalling.

Reduction of GRB2 protein levels using siRNA KD in normal BJ cells decreased cell proliferation as assessed by total cell counts. This was associated with an observed decline in levels of phosphorylated RAF1, phosphorylated MEK1/2 and total MEK1/2 protein in Western blot. Thus the RAF1/MEK1/2 pathway that is known to activate the growth-stimulating extracellular signal-regulated kinase 1/2 (ERK1/2) is impaired upon GRB2 loss in BJ cells. Diminished GRB2 protein levels lead to a decline in basal BJ cell viability and moderate enhancement of rhTRAIL-induced apoptosis. However, even at shorter GRB2 KD duration we did not find evidence that GRB2 sensitises normal BJ cells to TRAIL via a DISC-mediated mechanism, since 2days of GRB2 KD did not reveal enforced CASP8 cleavage signals in Western blot analyses of whole cell lysates. Depletion of pro-survival molecule GRB2 from DR5 hence does not tune rhTRAIL signalling to apoptosis in normal cells.

Figure 30 continued: were loaded onto SDS-PAGE gels and analysed by regular Western blot for the presence of DISC components and growth factor receptor-bound protein 2 (GRB2).* **(C)** Inputs and DR5-IP eluates originating from experiments described in Figure 29 and analysed in Figure 29, E were explored for co-purification of GRB2 and RAF proto-oncogene serine/threonine-protein kinase (RAF1).* **(D)** BJ cells were transfected with 15nM siRNA against GRB2 (G), scramble control siRNA (S) or mock-transfected with lipofectamine (M) for 4d. Cell culture medium was renewed 1d and 3d after start of transfection. Total cell numbers were counted 4d after start of transfection. Values are means of 3 independent experiments. **(E)** Whole cell lysates (WCL) of BJ cells transfected as described in (D) were analysed for expression, respectively phosphorylation levels of GRB2, RAF1 and MEK1/2 4d after start of knockdown (KD).* **(F)** TRAIL-induced apoptosis upon GRB2 siRNA KD in BJ cells. Four days after start of KD BJ cells were left untreated (-) or were treated with 1μg mL^{-1} rhTRAIL (+). Apoptosis was assessed as 7A6 positivity 16 hours after the addition of rhTRAIL. Values represent mean outcome of 3 independent experiments. **(G)** TRAIL-induced caspase cleavage after 2d of GRB2 KD in BJ cells. BJ cells were transfected as described in (D) and cell culture medium was renewed 1d after start of transfection. At day 2 of transfection cells were left untreated (-) or were treated with 1μg mL^{-1} rhTRAIL for 30 min or for 17h. After that whole cell lysates (WCL) were analysed for GRB2 expression and caspase 8 and 3 (CASP8, CASP3) cleavage. Depicted are Western blots for 1 out of *2 independent experiments. Significances were calculated using unpaired, 2-tailed Student's t-test.

SUPPLEMENTARY

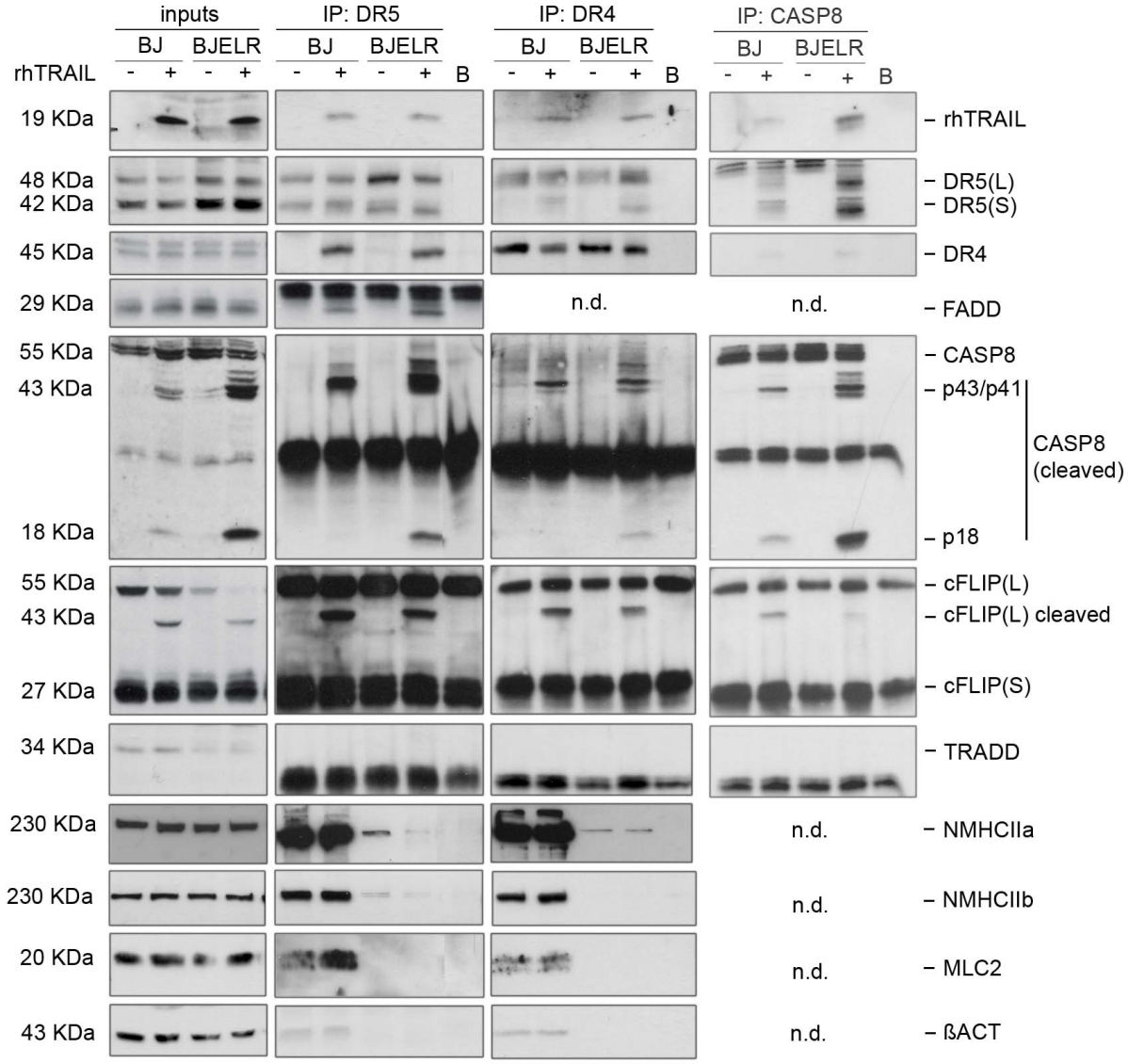

Figure 31: DR5-, DR4- and CASP8-DISC formation of normal BJ and transformed BJELR cells and the interaction with NMHCIIa and NMHCIIb. Equal numbers of normal (BJ) and HTERT, SV40ER and HRASG12V-transformed (BJELR) cells were left unstimulated (-) or were incubated with 1μg mL^{-1} rhTRAIL for 1h. Cell lysates were pre-cleared (inputs) and subsequently split into 3 fractions of which death receptor 5 or 4 (DR5, DR4) or caspase-8 (CASP8) were immunoprecipitated. Identical volumes of inputs, and immunoprecipitation (IP) eluates were separated by SDS-PAGE gel-electrophoresis and surveyed for DISC and cytoskeletal proteins by Western blot. The control lane (B) contains the eluate of IP-antibody coupled beads that were utilised in this experiment. Shown are Western blots of 1 full experiment out of 2 independent attempts.

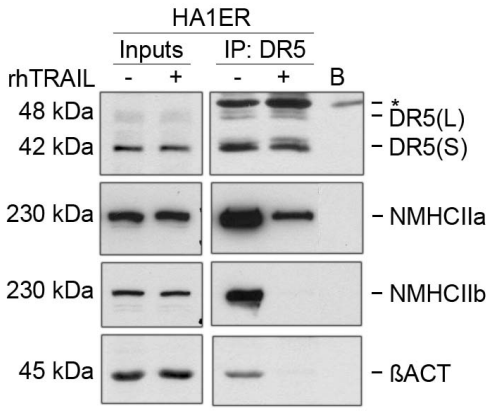

Figure 32: Interaction of NMHCIIa and NMHCIIb with DR5 of transformed HA1ER cells. Equal numbers of HTERT, SV40ER and HRASG12V-transformed human embryonic kidney (HA1ER) cells were left unstimulated (-) or treated with 1µg mL^{-1} rhTRAIL (+) for 1h. Cell lysates were pre-cleared (inputs) and then DR5 was immunoprecipitated. Equal volumes of inputs and immunoprecipitates (IP) were analysed by Western blot for the presence of non-muscle myosin heavy chain IIa, IIb (NMHCIIa, NMHCIIb) and beta-actin (ßACT). The eluate of DR5-coupled beads (B) utilised for IP were loaded to control unspecific background signals. Depicted are the Western blots of 1 out of 2 independent experiments.

A

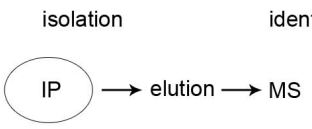

B

NMHCIIa [MYH9_HUMAN; Accession P35579; MW 226.4 kDa]

			Sequest			Mascot		
sample ID	ΣCoverage	Σ# Peptides	Score A3	Coverage A3	# Peptides A3	Score A4	Coverage A4	# Peptides A4
BJATCC -T	22,04	36	209,46	22,04	36	961,21	17,60	27
BJATCC +T	26,84	47	234,69	26,84	47	815,60	16,53	29
BJELR -T	18,21	25	128,06	18,21	25	607,17	12,30	16
BJELR +T	2,96	4	19,62	2,96	4	33,03	0	
B	0	0	0	0	0	0	0	0

NMHCIIb [MYH10_HUMAN; Accession P35580; MW 228.9 kDa]

			Sequest			Mascot		
sample ID	ΣCoverage	Σ# Peptides	Score A3	Coverage A3	# Peptides A3	Score A4	Coverage A4	# Peptides A4
BJATCC -T	6,17	11	33,04	6,17	11	113,09	3,04	4
BJATCC +T	9,01	14	64,59	9,01	14	109,01	2,13	4
BJELR -T	0	0	0	0	0	0	0	0
BJELR +T	0	0	0	0	0	0	0	0
B	0	0	0	0	0	0	0	0

ßACT [ACTB_HUMAN; Accession P60709; MW 41.7 kDa]

			Sequest			Mascot		
sample ID	ΣCoverage	Σ# Peptides	Score A3	Coverage A3	# Peptides A3	Score A4	Coverage A4	# Peptides A4
BJATCC -T	49,60	11	70,57	49,60	11	369,83	30,93	8
BJATCC +T	43,73	13	72,13	43,73	13	272,14	32,00	8
BJELR -T	16,53	5	28,02	16,53	5	171,33	16,53	5
BJELR +T	17,33	4	14	17,33	4	30	5,87	1
B	0	0	0	0	0	0	0	0

C

						Sequest			Mascot		
sample ID	total # proteins	protein ID	rank (# peptides)	ΣCoverage	Σ# Peptides	Score A3	Coverage A3	# Peptides A3	Score A4	Coverage A4	# Peptides A4
DR5-IP	11	NMHCIIa	1	18,21	25	128,06	18,21	25	607,17	12,30	16
		DR5	7	10,00	3	10,58	10,00	3	70,16	6,36	2
IgG-IP	15	NMHCIIa	0	0	0	0	0	0	0	0	0
		DR5	0	0	0	0	0	0	0	0	0

Figure 33: Identification of novel TRAIL DR5-DISC interactors by in-solution digestion of whole DR5-DISC-IP eluates of normal BJ and transformed BJELR cells followed by mass spectrometry. **(A)** The TRAIL-induced DISC was isolated immunoprecipitating (IP) DR5 from normal (BJ) and transformed (BJELR) cells that were left unstimulated (-T) or that were stimulated for 1h with 1µg mL^{-1} rhTRAIL (+T). DR5 and co-purified proteins were eluted from beads, digested in-solution and given for mass-spectrometric analysis. Parallel control-IPs using a non-specific immunoglobulin G (IgG)-antibody (AB) were performed and processed as DR5-IPs. Eluates of utilised IP-AB-coupled beads were analysed to determine levels of contamination. **(B)** Mass spectrometry results for non-muscle myosin heavy chain IIa and IIb (NMHCIIa, NMHCIIb) and beta-actin (ßACT) obtained from DR5-IP indicated cells and condition and of control DR5-IP-AB-coupled beads (B). **(C)** Showcase mass spectrometry results acquired from parallel DR5- and IgG-IP of unstimulated BJELR cells. Indicated are total numbers of identified proteins per IP (total # proteins) and the position of NMHCIIa and DR5 in each IP that were ranked according to the number of identified peptides (rank (# peptides)). A protein was considered 'identified' if at least 2 peptides were specified.

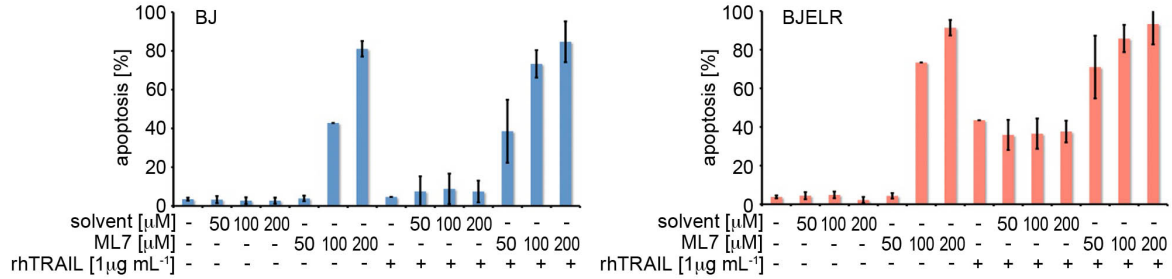

Figure 34: Apoptosis induction at high levels of myosin light chain kinase (MLCK) inhibitor ML7 in normal BJ and transformed BJELR cells. Apoptotic response of normal (BJ) and HTERT, SV40ER and HRASG12V-transformed (BJELR) cells were assessed in paralleled experiments. Cells were pre-incubated with indicated concentrations of ML7 or solvent (ethanol/water mix at a 1:1 ratio) for 30 min and then co-treated with 1μg mL^{-1} purified rhTRAIL. Apoptosis was quantified as 7A6 positivity in FACS analysis after 16h of treatment. Values derive from 2 independent experiments.

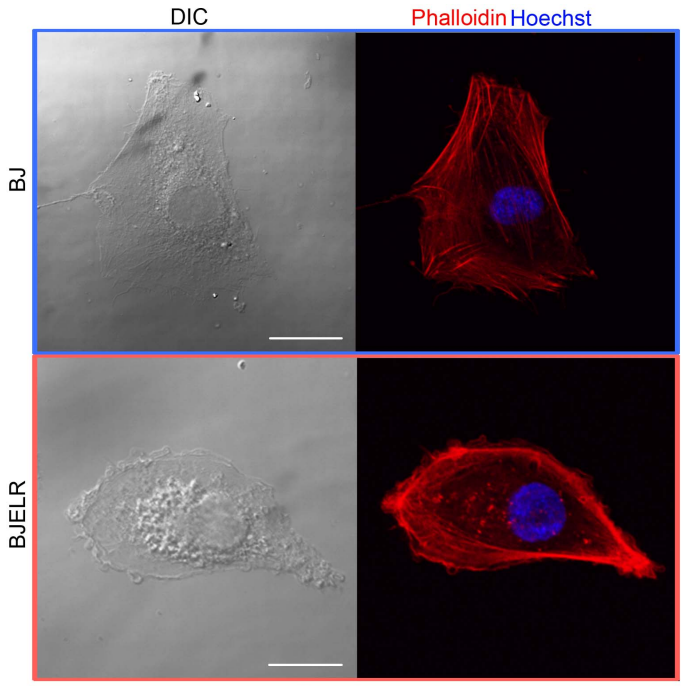

Figure 35: Actin stress fiber formation in normal BJ and transformed BJELR cells. Normal (BJ) and HTERT, SV40ER and HRASG12V-transformed (BJELR) human foreskin fibroblasts were fixed and stained with rhodamine-phalloidin and Hoechst. Images were taken by differential interference contrast microscopy (DIC) and fluorescence microscopy. Size bar in the upper image represents 30μm and in the lower image 19μm.

WORK IN PROGRESS

By the time this thesis manuscript was prepared, certain aspects regarding (I) the DISC definition in normal and transformed cells, (II) the mechanism of the NMII/DR interaction, (III) the molecular basis for the reduced NMII activity in transformed cells, (IV) the implication of NMII in DR transport and (V) the NMII/DR interaction in BJEL cells were not fully resolved. Since they are, in parts, essential to the previously shown results, these aspects shall be introduced herein.

I - Optimisation of DISC analyses to enable the distinction between divergence in protein recruitment or processing

As described in the 'Results' section, DISC analyses of normal BJ and transformed BJELR cells revealed lower rhTRAIL-induced levels of the CASP8 p18 cleavage product at the DR of normal cells (Results, Figure 24, G, Supplementary, Figure 31). Since processing of full-length CASP8 within the DISC appears to be accomplished rapidly, we currently cannot specify whether the reduction in CASP8 p18 fragments in normal BJ cells is due to reduced CASP8 processivity or due to reduced recruitment of CASP8 to the DR. DISC-analyses of normal and transformed cells that will be incubated with a pan-CASP inhibitor (zVAD) prior to challenge with rhTRAIL will allow us to answer whether the reduced sensitivity of normal cells to rhTRAIL-apoptosis solely is due to reduced CASP8 processing or additionally involves diminished recruitment of the full-length CASP8 protein.

Likewise described for CASP8, comparative DISC analyses of normal BJ and transformed BJELR cells and of scrambled- and NMHCIIa-siRNA transfected normal BJ cells, respectively, revealed alterations in the signal levels of the cFLIP(L) p43 cleavage product. As the full-length cFLIP(L) signal always is covered by unspecific signals originating from cross-reaction of the primary cFLIP(L) antibody with the heavy chain of the IP-antibody (Results, Figure 24, E & Figure 29, E, Supplementary, Figure 31), we cannot conclude that observed changes in cFLIP(L) p43 levels originate from lowered cFLIP(L) processing in the DISC or a reduced recruitment of cFLIP(L) to the DISC.

Therefore, finding a primary anti-cFLIP antibody that does not cross-react with the IP will help to clarify this issue. Tests for suitable anti-cFLIP antibodies are ongoing.

II - Analyses of the NMII/DR interaction nature

We attempted to understand the molecular basis of the NMII/DR interaction. On one hand we observed differential interaction intensities comparing unstimulated normal and transformed cells, which might be related to a differential NMII activity in those cells. On the other hand we found that in transformed cells rhTRAIL induced the loss of NMII from DR. Since rhTRAIL was indicated to induce caspase-dependent (apoptosis) and caspase-independent (survival or necrosis) signalling pathways (see 'Introduction'), we decided to explore the rhTRAIL-induced NMII/DR loss in more detail.

MLC2 phosphorylation potentially regulates the NMII/DR interaction. Aforementioned results demonstrated a stronger NMII/DR interaction and higher MLC2 phosphorylation levels in unstimulated normal BJ than in transformed BJELR cells (Results, Figure 28, A). Moreover, the NMII/DR interaction in normal cells was abrogated if MLC2 phosphorylation was inhibited with the MLCK inhibitor ML7. Therefore, we hypothesised that the NMII/DR interaction is regulated by MLC2 phosphorylation. Above that, NMHCIIa, NMHCIIb, MLC2 and ßACT were lost from DR upon rhTRAIL addition in transformed BJELR and HA1ER cells but not in normal BJ cells (Results, Figure 25, D, Supplementary, Figure 31 & 32). Alterations in MLC2 phosphorylation levels subsequent to TNFα-stimulation have been described in TNFR1-signalling [reports describing a decrease: Yokoyama et al 1999, Petrache et al 2001; reports describing an increase: Jin et al 2001, Hunter et al 2003 (associated with ROCK1-dependent inactivating phosphorylation of MLCP), Wang et al 2005b (associated with an increase in MLCK expression), McKenzie and Ridley 2007]. We therefore aimed to investigate if the strong NMII/DR interaction in normal BJ cells was evoked by phosphorylated MLC2 and if the rhTRAIL-induced release of NMII from DR in transformed BJELR cells resulted from reductions in MLC2 phosphorylation levels.

Unfortunately, attempts to detect phosphorylated MLC2 at the DR-IP of normal cells or to assess MLC2 phosphorylation levels upon rhTRAIL stimulus in transformed cells failed as yet due to signal instability and missing reproducibility, respectively. To the current state we thus cannot finally prove that a direct causal relation between the observed divergence of NMII/DR interaction intensities and differences in MLC2 phosphorylation levels between normal and transformed cells exists. Therefore, exogenous expression of tagged MLC2 mutants mimicking the di-phosphorylated and the unphosphorylated form, respectively, will help to identify which form interacts with DR. The generation of the MLC2 constructs [Uchimura et al 2002], which were validated *in vitro* [Watanabe et al 2007], are ongoing.

Proteolytic caspase activity is required for the rhTRAIL-induced loss of NMHCIIa-, NMHCIIb- and MLC2/DR interaction in transformed BJELR cells. NMHCIIa, NMHCIIb, MLC2 and ßACT were lost from DR after rhTRAIL stimulation in transformed BJELR and HA1ER cells but not in normal BJ cells (Results, Figure 25, D, Supplementary, Figure 31 & 32). Contrary to normal cells, transformed cells underwent apoptosis and showed full CASP8 activation at the DISC upon rhTRAIL exposure (Results Figure 24, B&G). Caspase-facilitated cleavage of cytoskeleton proteins during apoptosis progression is well documented (actin filaments [Chen et al 1996, Van Damme et al 2005], intermediate filaments [Oshima et al 2002], microtubules [Gerner et al 2000], microtubule motors [Lane et al 2001, Dix et al 2008]). More specifically, during FAS-induced apoptosis cleavage of NMHCIIa, IIb, MLC2 and ßACT by CASP8, 3 and 7, respectively was reported [Fischer et al 2003, Van Damme et al 2005]. Since proteolytic cleavage can modulate protein interactions, we asked whether cleavage of DR-interacting actin cytoskeleton proteins can be observed during TRAIL-apoptosis. As expected, in transformed BJELR cells that were treated with 1µg mL^{-1} rhTRAIL for 16h we observed a decline of full-length NMHCIIa and NMHCIIb protein signals as well as the appearance of small-molecular weight fragments below the full-length signals of NMHCIIa, NMHCIIb and ßACT (Figure 36, A). Parallel experiments in normal BJ cells gave no cleavage of cytoskeleton proteins (not shown). Thus, NMHCIIa, NMHCIIb and ßACT are broken up during TRAIL-apoptosis. We then asked if the NMII dissociation from DR5 and DR4 observed at 1h of rhTRAIL (Results, Figure 24, D, Supplementary,

Figure 31 & 32) could be due to CASP-mediated proteolysis. For that, BJELR cells were pre-incubated with 100µM pan-CASP inhibitor (zVAD) or vehicle (DMSO) for 30 min, challenged with 1µg mL^{-1} rhTRAIL for 1h and the DISC was immunoprecipitated targeting DR5. In paralleled experiments the percentage of apoptotic cells was quantified as 7A6 positivity 16h after start of TRAIL treatment to control apoptosis progression and inhibitor efficacy, respectively. Of note, both apoptosis and rhTRAIL-induced dissociation of NMIIs from the DISC were inhibited in the presence of the pan-CASP inhibitor (Figure 36, B). The rhTRAIL-stimulated loss of NMIIs from the DISC in BJELR cells is thus CASP-dependent and occurs posterior to CASP activation. Interestingly, the initial rhTRAIL-stimulated microaggregation of DR5 and DR4 was unaffected by CASP inhibition (Figure 36, B), demonstrating that DR microaggregation in transformed cells does not require CASP activity. Unfortunately, we cannot state whether initiator or effector CASP account for the loss of the NMII/DR interaction, since the conditions for sufficient and specific CASP inhibition using initiator or effector CASP inhibitors (zIETD, zDEVD) were not fully set-up at the time this manuscript was prepared.

Both direct caspase-mediated cleavage of NMHCIIa, NMHCIIb, MLC2 and/or ßACT decline in MLC2 phosphorylation could induce the rhTRAIL-stimulated DR interaction loss in transformed cells. Even though prior results have shown that the rhTRAIL-stimulated loss of NMIIs from the DR in BJELR cells depended on CASP activity (Figure 36, B), it remained unclear if the abrogation of interaction is fulfilled by direct destructive CASP-mediated proteolysis of NMHCIIa, IIb, MLC2 and/or ßACT, or via indirect CASP-facilitated activating cleavage of NMII Mg^{2+}-ATPase-regulatory kinases and thus altered MLC2 phosphorylation. Importantly, CASP can positively contribute to MLC2 phosphorylation, NMII Mg^{2+}-ATPase activity and coupling of NMII-filaments to the plasma membrane by activating cleavage of MLCK [Petrache et al 2003] and ROCK1 [Coleman et al 2001, Sebbagh et al 2001, Ueda et al 2001, Chang et al 2006, Gabet et a 2011]. At the same time, CASP also negatively influence MLC2 phosphorylation and NMII Mg^{2+}-ATPase activity through cleavage of PAK2 [Lee et al 1997, Fischer et al 2006], but not PAK1 [Lee et al 1997]. Whilst active full-length PAK2 is signalling towards survival phosphorylating and inhibiting BAD, PAK2 cleavage resulted in a pro-apoptotic,

constitutively active kinase [Fischer et al 2006], which induced cell detachment and apoptosis in epithelial HeLa and CHO cells [Lee et al 1997]. How the pro-apoptotic version of PAK2 mediates apoptosis is unknown, but has been suggested to involve the production of reactive oxygen species [Lee et al 1997] or mechanical stress due to cytoskeleton rearrangements [Vilas et al 2006]. Like PAK1, PAK2 phosphorylates and inactivates MLCK [Goeckeler et al 2000] and in this way could inhibit NMII Mg^{2+}-ATPase activity leading to the disassembly of NMII from DR. At present, nothing can be stated of whether rhTRAIL-stimulated PAK2 cleavage in transformed cells occurs, but will be investigated in future experiments. At least, evidence for the occurrence of an increase in MLC2 phosphorylation levels upon rhTRAIL in transformed cells is low since the observed an rhTRAIL-mediated induction of MLCK expression was weak in transformed BJELR and robust in normal BJ cells. Moreover, the ROCK1 full-length protein signals remained unaltered upon rhTRAIL stimulation in BJELR cells (Results, Figure 28, B). This suggests that a CASP-mediated activating cleavage of MLCK or ROCK1 do not play a role in the early TRAIL apoptosis signalling steps of BJELR cells.

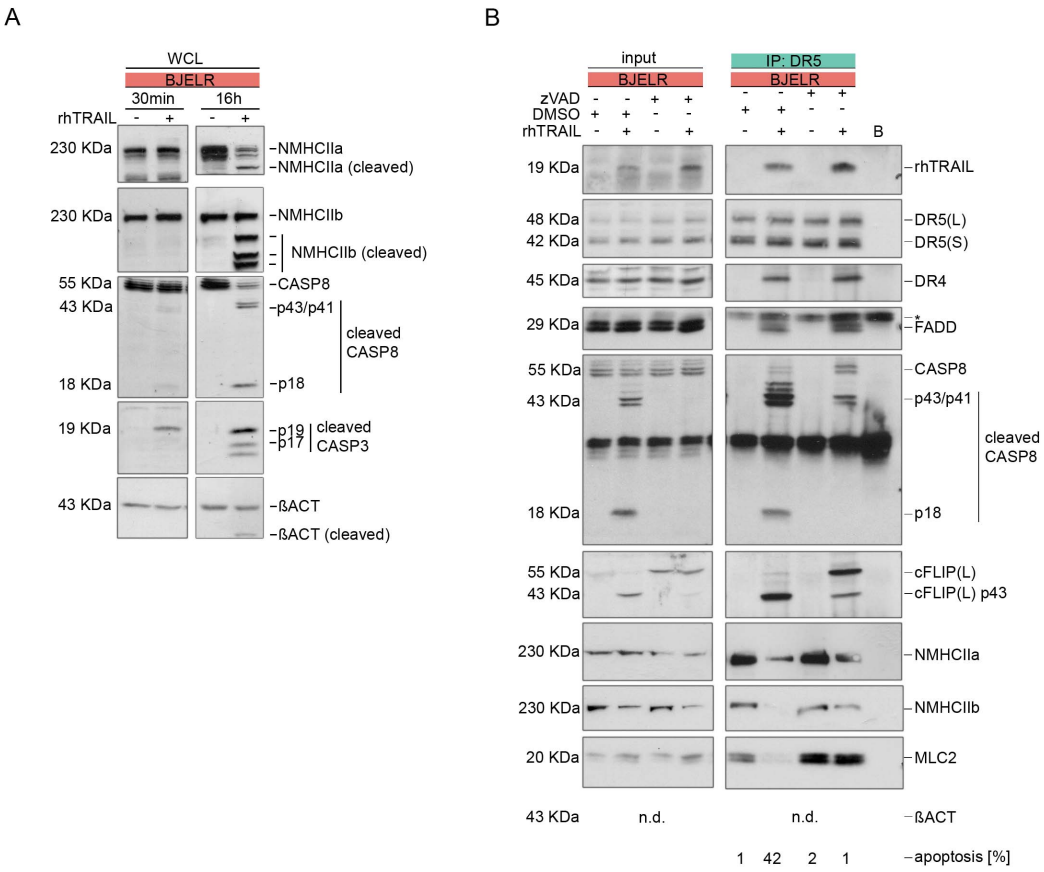

Figure 36: Fragmentation of NMHCIIa, NMHCIIb and ßACT during rhTRAIL apoptosis and NMII/DR5 interaction in transformed BJELR cells with pan-caspase inhibition. **(A)** Transformed (BJELR) cells were

III - Innate signalling mechanisms that putatively inhibit NMII Mg^{2+}-ATPase activity in transformed cells

Inhibition of NMII Mg^{2+}-ATPase activity using blebbistatin resulted in the weakening of the NMII/DR interaction and an increase in rhTRAIL apoptosis in normal BJ cells. The NMII/DR interaction in transformed cells per se is reduced and rhTRAIL response is high. Therefore we tried to identify innate signalling mechanisms other than phosphorylation events that may lead to the inhibition of NMII Mg^{2+}-ATPase activity in transformed BJELR cells. Inhibition of myosin II Mg^{2+}-ATPase function can be caused by binding of CALD1 to actin or directly to myosin II, blocking the interaction of actin with myosin [Ikebe and Reardon 1988, Helfman et al 1999, Wang 2008, Mayanagi and Sobue 2011]. Expecting to find a stronger CALD/DR interaction in transformed than in normal cells, we purified DR5 and DR4 and analysed Western blots generated from IP-eluates for CALD1. Surprisingly, pilot-experiments demonstrated that CALD1 co-purified with DR5 and DR4 of normal but not transformed cells (Figure 37, A). Since CALD downregulation in transformation [Owada et al 1984, Wang 2008, Mayanagi and Sobue 2011] and a reduction in the myosin II Mg^{2+}-ATPase inhibitory ability upon CALD phosphorylation by kinases such as PAK2, ERK1 and ERK2 are reported [Mayanagi and Sobue 2011], we searched for explanations for the unexpected high levels of co-immunoprecipitated CALD1 levels in normal BJ cells. Hence, we compared the interaction-levels of DR with CALM, another reported direct binding partner of the FAS DD [Ahn et al 2004, Wu et al 2005, Chen et al 2008]. Interestingly, CALM activates MLCK [reviewed by Vicente-Manzanares et al 2009] and CALM antagonists induced apoptosis [Wu et al 2005]. Analysis of DR5-IP-eluates of normal BJ

Figure 36 continued: left untreated (-) or were stimulated with 1μg mL^{-1} rhTRAIL (+) for 30min or 16h. Whole cell lysates (WCL) were analysed for caspase-8 and -3 (CASP8, CASP3) cleavage and for fragmentation of cytoskeleton proteins non-muscle heavy chain IIa, IIb (NMHCIIa, NMHCIIb) and beta-actin (ßACT).* **(B)** BJELR cells were pre-treated with vehicle (DMSO) or with 100μM pan-caspase inhibitor (zVAD) for 30 minutes and then either no (-), or 1μg mL^{-1} rhTRAIL (+) was added for 1h. After cells lysis, death receptor 5 (DR5) was immunoprecipitated (IP) and IP-eluates were subjected to Western blot analysis to determine the levels of co-immunoprecipitated NMHCIIa, NMHCIIb, myosin regulatory light chain (MLC2) and to perform a full DISC analysis. Levels of interacting ßACT were not determined (n.d.). The efficacy of pan-caspase inhibition was monitored by the parallelled assessment of apoptosis (7A6 positivity) after 16 hours of rhTRAIL and the percentages of apoptosis for the respective treatments are given underneath the blots.** Shown are Western blots for 1 full trial out of *3, respectively **2 independent experiments.

and transformed BJELR cells showed more intense CALM co-immunopurification with DR5 of BJ than with DR5 of BJELR (Figure 37, B). Thus, a putatively inhibitory effect of CALD1 on NMIIa Mg^{2+}-ATPase activity occurring at DR could be counterbalanced by CALM. However, establishment of the biological significance of CALD1 and CALM interaction with the DR and their role in the regulation of NMII Mg^{2+}-ATPase activity and/or NMII/DR interaction appears complex and requires further investigation.

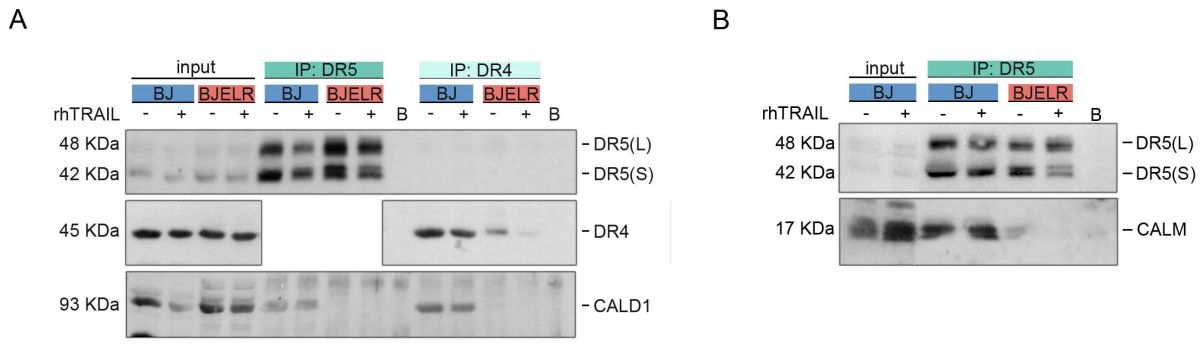

Figure 37: Caldesmon 1 and calmodulin co-purify with DR5 in normal BJ and transformed BJELR fibroblasts. **(A)** Normal (BJ) and hTERT, SV40ER and HRASG12V-transformed (BJELR) cells that were left unstimulated (-) or that were stimulated with 1µg mL^{-1} rhTRAIL (+) for 1h by immunoprecipitation (IP). IP eluates were split into two fractions of which the death receptors 5 or 4 (DR5, DR4) were immunopurified. DR5- and DR4-IP-eluates were separated by SDS-PAGE, blotted onto nitrocellulose membranes and investigated for caldesmon 1 (CALD1) signals.* **(B)** DR5 was purified and analysed as in (A), except that cells were stimulated for 45min with rhTRAIL and that blots were explored for calmodulin (CALM).** Indicated are Western blots for 1 of *1, respectively of **2 independent experiments.

IV - Implication of NMII in DR transport to the cell surface and/or internalisation

We found the initial NMII/DR5 interaction and NMII activity to be more pronounced in normal BJ than in transformed BJELR cells. NMII activity has been implicated in TNFR1 transport to the cell surface [Jin et al 2001]. Immunolabelling of DR5 surface receptors and FACS analysis of mean fluorescence intensities (MFI) revealed equal DR5 surface levels in BJ and BJELR cells (Results, Figure 24, D), meaning that there is no correlation between the intensity of NMII/DR5 interaction observed in IP-experiments and the relative DR5 surface levels.

Recently, the loss of TNFR1-internalisation upon NMHCIIb but not NMHCIIa knockdown was reported [Flynn et al 2010], which is a process required for TNFR1 apoptosis to occur. In TRAIL signalling TRAIL DISC internalisation in breast cancer cells accounted for TRAIL-resistance [Zhang and Zhang 2008] whilst this process was required for TRAIL induced apoptosis in malignant hepatocytes [Akazawa et al 2009]. Based on their difference in NMII/DR interaction, we questioned whether normal BJ and transformed BJELR cells display a differential TRAIL-induced DR5 internalisation pattern. For that we stimulated BJ and BJELR cells with 1µg mL^{-1} rhTRAIL for different minutes and subsequently assessed DR5 surface levels by direct immuno-staining and analysis of alterations (Δ) in mean or median fluorescence intensities (MFI) by FACS. We found that rhTRAIL-induced DR5 internalisation was less pronounced in normal BJ than in transformed BJELR cells (Figure 38, A). This suggested that NMII activity and NMII/DR5 interaction prevents rather than promotes internalisation of DR5. On the other hand, if NMII activity and NMII/DR5 interaction were involved in the DR5 transport to the cell surface, lower TRAIL-induced DR5 internalisation in normal BJ cells could result from enhanced transport processes in normal cells.

Probing whether inhibition of NMII activity and NMII/DR5 interaction would increase the level of DR internalisation observed in normal BJ cells, we treated cells with 25µM blebbistatin for 30min before assessing rhTRAIL-induced DR5 internalisation. We found that FACS-assisted immunostaining of DR5 is inappropriate to assess rhTRAIL-induced DR5 internalisation under the influence of blebbistatin, because single blebbistatin treatment lead to a decline in DR5 surface levels over time. Whilst DR5 surface levels were equal to vehicle treated cells after 30 min of treatment with agent, 90 and 210 min after agent addition DR5 surface levels were decreased (Figure 38, B). This result implies a functional role of NMII activity in the cell surface transport of DR5 transport in normal BJ cells, which contrasts previously mentioned absence of correlation between NMII/DR5 interaction intensity and NMII activity and general DR5 surface levels in normal BJ and transformed BJELR cells.

Attempts to measure DR5 surface levels upon inhibition of NMII activity by siRNA-mediated KD of NMHCIIa protein revealed that the assessment of DR5 surface levels by immunostaining and FACS analysis appears to be inappropriate, since the normalisation of mean fluorescence intensities (MFI) to autofluorescence causes a bias. We observed that 4d NMHCIIa KD significantly increased normal BJ cell

autofluorescence as compared to scramble control cells (NMHCIIa=15.6 (±0.4) (p=0.03), SCR=13.3 (±0.7)) (Figure 38, C, central plot). Whilst absolute measured MFI of DR5 revealed no difference in NMHCIIa KD and control cells (Figure 38, C, upper left plot), after normalisation to autofluorescence values it appears as if NMHCIIa KD would be associated with decreased DR5 surface levels (Figure 38, C, upper right plot). This result would confirm data obtained in blebbistatin experiments. However, to the current state we refrain from drafting a final conclusion about the function of NMII regarding DR5 surface transport and rather work on direct immunofluorescence analyses to verify beforehand mentioned data.

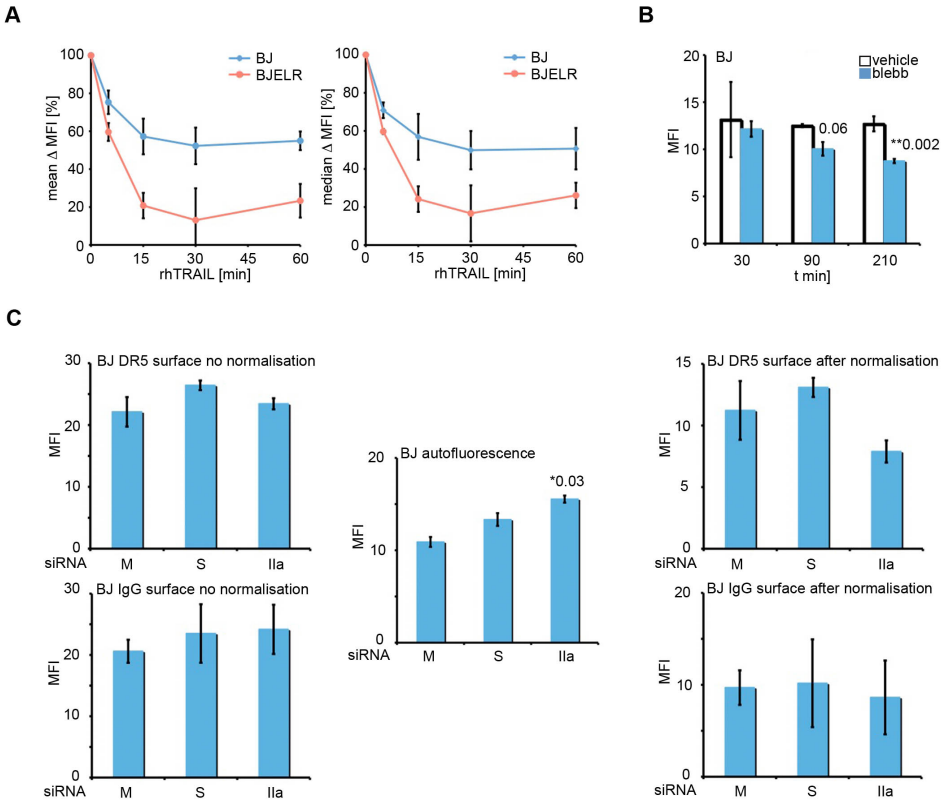

Figure 38: DR5 internalisation and DR5 surface levels upon blebbistatin treatment and NMHCIIa siRNA knockdown in normal BJ cells. **(A)** TRAIL-mediated DR5 internalisation in normal (BJ) and transformed (BJELR) cells. Graphs depict the decline of the mean DR5 fluorescence intensity (MFI) in dependence of the time of rhTRAIL incubation [minutes]. MFIs were normalised to the mean autofluorescence intensity of each cell line and treatment, respectively. To enable a comparison between cell lines and treatments, normalised MFIs at 0 min of rhTRAIL were set to 100% and all normalised MFIs measured during rhTRAIL incubation were referred to this value. Left plot depicts mean fluorescence values [%], right plot shows median fluorescence intensities [%]. **(B)** DR5 surface levels upon blebbistatin-mediated inhibition of NMII activity in BJ cells. Graph depicts the decline of the mean DR5 MFI in dependence of the time of 25µM blebbistatin or vehicle (DMSO) incubation (in minutes). **(C)** DR5 surface levels upon NMHCIIa siRNA KD in BJ cells. Plots depict the decline of the mean DR5 MFI after 4d of transfection with lipofectamin (M), scambled siRNA (S) or NMHCIIa (IIa). Prior to DR5 surface level assessment cell culture medium was changed 1d and 3d after start of transfection. Values of each of the presented plots derive from 3 independent experiments.

V - Analysis of the NMII/DR interaction pre-transformed BJEL cells

We observed that in comparison to TRAIL-resistant normal BJ cells, TRAIL-sensitive HTERT, SV40ER and HRASG12V-transformed BJELR cells have strongly reduced NMII/DR5 interaction levels. Moreover, it appeared that the NMII/DR interaction requires NMII activity, which is positively stimulated via RHOA/ROCK1/MLCK and negatively regulated via CDC42/RAC1/PAK1 [Even-Faitelson and Ravid 2006]. Since ST expression was associated with reduced RHOA expression levels and loss of RHOA-dependent stress fibers as well as increased CDC42 and RAC1 expression levels [Nunbhakdi-Craig et al 2003], we questioned whether the NMII/DR interaction was as low in HTERT and SV40ER pre-transformed BJEL cells as it was in BJELR cells. A pilot experiment, in which we immunoprecipitated DR5 from unstimulated BJEL and BJELR cells to investigate the IP-eluates for NMHCIIa and NMHCIIb in Western blots, indicated that the NMII/DR5 interaction is lower in BJELR than in BJEL cells (Figure 39). Thus, transfection of an SV40ER background with HRASG12V appears to reduce NMII activity. Further experiments will be required to confirm these preliminary data and will necessitate the comparison of NMII regulators to identify (the) essential signalling factor(s) modified by HRASG12V-expression in an SV40ER-background. We hypothesise that the introduction of HRASG12V into pretransformed BJEL cells leads to a surplus activation of PAK2 and/or PAK1 via RAC1/CDC42, which might break synergistic MYC/RHOA interactions [Bustelo 2010] and the MYC-mediated repression of PAK2 [Guo et al 2000] in pretransformed BJEL cells.

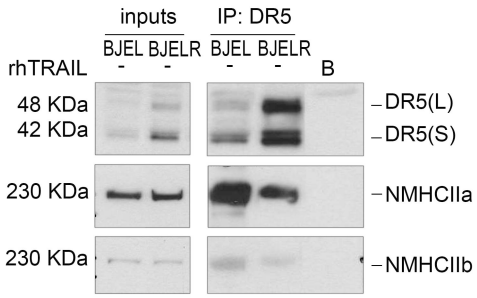

Figure 39: NMII/DR5 interaction in pre-transformed BJEL and transformed BJELR cells. Unstimulated (-) HTERT and SV40ER pre-transformed cells (BJEL) and hTERT, SV40ER and HRASG12V-transformed (BJELR) cells were subjected to immunoprecipitation (IP) targeting death receptor 5 (DR5). IP eluates were separated by SDS-PAGE, blotted onto nitrocellulose membranes and investigated for non-muscle myosin heavy chain IIa and IIb (NMHCIIa, NMHCIIb) signals. Shown are the Western blot results of a single experiment.

DISCUSSION & PERSPECTIVES

TRAIL DISC formation as the key-initiating event of the extrinsic pathway enables activation of the CASP cascade resulting in apoptotic cell death in transformed but not in normal cells. Whilst extensive research is performed in transformed cells studying DISC composition, resistance and sensitising mechanisms, to the best of our knowledge no studies on TRAIL DISC assembly in normal cells are available. Consequently, our understanding of how normal cells are refractory to TRAIL-apoptosis and gain sensitivity through the process of transformation is virtually non-existent. Using immunoprecipitation, mass spectrometry and classical biochemical approaches, we have characterised the DISC of normal BJ and transformed BJELR cells and identified an interaction of NMHCIIa with DR acting as a potent resistance block to TRAIL-apoptosis in normal cells.

NMIIa function in TRAIL DISC composition and/or formation. Whilst total expression levels of DISC protein components remained unaltered, NMHCIIa protein depletion in normal BJ cells resulted in reduced DR4 recruitment, elevated levels of CASP8 cleavage products and reduced reading of cFLIP(L) cleavage product at the DISC immunoprecipitated via DR5 (Results, Figure 29, E). Since rhTRAIL-stimulated DR4 recruitment into the DISC was reduced in NMHCIIa KD BJ cells and NMII have been implicated in the transport of TNFR1 to the cell surface [Jin et al 2001], NMIIa could function in DR4-specific transport processes. Indeed, evidence exists that the intracellular localisation of DR5 and DR4 are differentially regulated [Ren et al 2004b]. However, how DR4 or DR5 find their way to the plasma membrane is unknown. Assessment of DR4 cell surface levels in NMHCIIa KD cells will clarify, whether NMIIa at all is involved in DR4-selective transport processes or not.

Our analysis of WCL and the DISC in NMHCIIa KD normal BJ cells showed an increased CASP8 activation (Results, Figure 29, D&E). Whether this increase in CASP8 activation is due to higher numbers of CASP8 molecules being activated per cell or to same quantities of CASP8 molecules are activated in a higher number of cells is currently unclear. In line with our findings, an enhancement of CASP8 recruitment to the FLAG-TRAIL immunoprecipitated DISC was reported if the NMII regulatory kinase CK2,

whose activity prevents S100A4/NMHCII binding and NMII filament disassembly, was inhibited [Izeradjene et al 2004], an effect that was not caused by altered DR5 surface levels. Generally, CK2 activity is high in TRAIL resistant and low in TRAIL sensitive cancer cells [Shin et al 2005] and CK2 inhibition augments and elicits, respectively, sensitivity to TRAIL-apoptosis in rhabdomyosarcoma [Izeradjene et al 2004], colon carcinoma [Izeradjene et al 2005] and prostatic cancer cell lines [Wang et al 2006] and in primary endometrial cacinoma cells [Llobet et al 2008]. These data suggest that active NMII filaments might inhibit TRAIL apoptosis and limit DR-mediated CASP8 activation also in malignant cells, mechanically inhibiting CASP8 recruitment by compartmentalisation. Like the actin cytoskeleton protein spectrin [reviewed by Sheetz et al 2006], NMIIa-tethered fibers could form a barrier to membrane protein lateral diffusion. Consistent with the refined DISC model (Introduction, Figure 6) [Schleich et al 2012, Dickens et al 2012], NMIIa activity may even determine CASP8 chain lengths by compartmentalisation. Verification of this aspect will require the DISC characterisation in NMHCIIa KD cells under inhibition of CASP activation (please see also 'Work in Progress', p131), as it will demonstrate whether increased levels of CASP8 cleavage products are caused by enhanced CASP8 recruitment or CASP8 cleavage.

Finally, we observed reduced cFLIP(L)p43 levels in the DISC of NMHCIIa KD normal BJ cells as compared to SCR control cells, whilst cFLIP(L) protein levels were unaltered (Results, Figure 29, E) and normal cell adhesion was reduced. As NMII function in integrin-mediated cell adhesion (Introduction, Figure 16) [reviewed by Vicente-Manzanares et al 2009], these data provide an important link to studies on FAS signalling, which demonstrated that the cytosolic solubility and availability of cFLIP(L) for binding to FADD in the DISC and for inhibiting CASP8 activation decreased upon disruption of β1 integrin-mediated adhesion to fibronectin [Shain et al 2002]. Notably, a transcriptional or translational regulation of cFLIP(L) by integrin-mediated adhesion was excluded and the adhesion-induced increase of cytosolic cFLIP(L) originated from pre-existing cFLIP(L) that was associated to the membrane fraction. Thus, during adhesion NMIIa activity may control intracellular cFLIP(L) localisation, positively regulating the availability of cFLIP(L) to bind to the DISC.

NMIIa-facilitated TRAIL resistance in suspension cells. Given the prominent role of NMII in cell adhesion, it remains to be investigated if an NMII/DR interaction in TRAIL-resistant suspension cells at all occurs and, if so, whether NMIIa likewise confers TRAIL-resistance. Investigating a potential NMII/DR interaction and function in suspension cells is particularly interesting since aplidin-induced apoptosis in Jurkat cells depended on the clustering of FAS in lipid rafts, an event that required an intact actin cytoskeleton and that was accompanied by the co-recruitment of RHOA and RHO-GDI into lipid rafts (see 'Introduction', p36) [Gajate and Mollinedo et al 2005]. Since RHO-GDI sequesters inactive (GDP-bound) RHOA, preventing RHOA- and ultimately ROCK/NMII activation, NMII activity is most probably not involved in the formation of those FAS caps. Contrary, since RHO-GDI recruitment can be strongly inhibited by NMII Mg^{2+}ATPase activity [Kuo et al 2011], it seems more likely that the disruption of NMII activity leads to a 'misorganisation' of plasma membrane proteins. Notably, whilst in most cases we could detect at least some residual NMII signals at the DR of BJELR cells, no signal at all was discovered at the DR of BJAB cells. If this is due to the higher TRAIL sensitivity of BJAB cells, or due to their growth in suspension, remains to be elucidated. If and how NMII could compartmentalise suspension cells is difficult to predict. Even if suspension cells are capable to form fibers upon surface attachment [Rosengart et al 2002, Nakamura et al 2005], there is nothing known about the existence of actomyosin fibers in cells while being in suspension.

Isoform specificity of observed effects on TRAIL sensitivity. We found that only NMHCIIa KD, but not NMHCIIb KD lead to a decrease in cell adhesion and a robust release of the TRAIL resistance block in normal BJ cells. Contrary, loss of NMHCIIb strongly reduced normal BJ cell proliferation, whilst cell adhesion and TRAIL-sensitivity were left unaltered (Results, Figure 29, C). This finding to a certain degree reflects the importance of the NMHCIIa and IIb isoforms for *in vivo* functions. Whilst gene depletion of NMHCIIa results in a complete failure of organogenesis in mice, NMHCIIb diminuition primarily affects the morphogenesis of heart and brain. Thus, NMHCIIa appears to have a more generalised role in the cell adhesion processes and differentiation than NMHCIIb. Since NMHCIIa *in vivo* can at least partially replace NMHCIIb gene function, we cannot rule out that observed consistent TRAIL-resistance upon NMHCIIb KD is due to

compensation by NMHCIIa. Unfortunately, no *in vivo* data exist where NMHCIIb was substituted for NMHCIIa. Thus, it is unknown if NMHCIIb can functionally replace NMHCIIa to a similar degree. Finally, since the biochemical properties of NMHCIIc and NMHCIIb more closely resemble than NMHCIIc and NMHCIIa (see 'Introduction', p64), NMHCIIc could compensate NMHCIIb but not NMHCIIa, which could be the underlying reason for the differential effects of isoform KD on TRAIL-sensitivity [Golomb et al 2004]. The NMHCIIc isoform has not at all been considered in this study, as it was never detected in mass-spectrometrical analyses. Nevertheless, we cannot exclude that it might impact on TRAIL signalling.

Mode of NMII/DR interaction. To the current state we can only speculate about how NMII may interact with DR5 and DR4. Like it has been reported for other membrane receptors [Rey et al 2002, Timmermann et al 2004, Rey et al 2007], in a direct binding situation NMII theoretically could bind to DR via the NMHCII tail, via the NMHCII head domain, via the region N-terminal of the head (SH3-like fold), or via MLC2 (Introduction, Figure 14, A) [Amparan et al 2005, Bajaj et al 2009]. Interestingly, MLC2 binding to N-methyl-D-aspartate receptor subunits occurred via the recognition of an incomplete IQ2-motif (GXXXR) [Bajaj et al 2009], a sequence pattern which can be found in the intracellular region, just upstream the DD of DR5(L), DR5(S) and DR4 and in the intracellular region of DcR2, but not in the DcR1 sequence. If SH3-like folds, such as the one located N-terminal of the NMII head, indeed behave like SH3 domains [D'Aquino and Ringe 2003], then SH3-like folds preferentially bind to PXXP (and RXXK) motifs [Cohen et al 1995, Berry et al 2002]. All TRAIL receptors except DR4 contain a PXXP sequence in their protein sequence. Thus, at least 2 different direct binding options are possible.

In an indirect binding setting one or several proteins could act as bridge. Whilst we found that ßACT binds to the DR independently of NMII (Results, Figure 27, B) and NMIIa and NMIIb bind independently of each other (Results, Figure 27, E), we cannot exclude that ßACT mediates the interaction between NMIIa and DR since we have not created a situation in which NMIIa remained at the DR and ßACT was lost. To verify this, we will deplete ezrin and moesin in normal BJ cells, immunoprecipitate DR5 and control the co-purification of ßACT and NMIIa. Apart from ßACT, NMII could bind to DR5 and DR4 via a yet unidentified linker protein.

From the receptor side the minimally required DR domain to interact with NMII is unknown. Since the interaction may not be direct or the interaction could require proper protein folding, we will generate N-terminally tagged DR5 mutants, deleting section-wise from its C-terminal end, and express these constructs in normal BJ cells to control the NMII interaction upon immunoprecipitation. Thereby, special focus will be put on the depletion of the beforehand mentioned IQ2-binding motif.

NMII activity in normal and transformed cells. Comparing MLC2 phosphorylation levels and MLC2 regulatory kinase expression levels in normal BJ and transformed BJELR cells (Results, Figure 28, B&C) we concluded that general NMII Mg^{2+}-ATPase activity in transformed cells must be low. Indeed, comparison with pre-existing transcriptomic data of the stepwise tumourigenesis system cells revealed that in transformed BJELR and HA1ER cells transcript levels of ROCK or MLCK are decreased. Contrary, PAK1 transcripts were unaltered, indicating a post-translational regulation of PAK1, which is often overexpressed in multiple cancer types [reviewed by Molli et al 2009, Dummler et al 2009, Eswaran et al 2009]. Interestingly, PAK1 protein accumulation upon TNFα-or IL2-stimulation in human dermal fibroblasts and keratinocytes was also concluded to be regulated at post-translational level, based on the evidence that suppression of protein synthesis did not inhibit PAK1 accumulation under TNFα [Zhou et al 2009]. The mechanism for how PAK1 protein is stabilised is unknown, but seems to be independent of the kinase catalytic activity and RAS-GTPase binding capacities [Zhou et al 2009].

No comparative study between normal and transformed cells exists, which directly demonstrates an altered NMII Mg^{2+}-ATPase activity. So far, relative studies only compared phospho-MLC2 levels. Interestingly, contrary to our findings of reduced MLC2 phosphorylation levels, transformation with HRAS or HRASG12V [Zhong et al 1997] or with the RHO-guanine nucleotide exchange factor (RHO-GEF) DBS [Liu et al 2006] was linked to an increase of phospho-MLC2 levels associated with RHOA hyperactivation [Zhong et al 1997] and enhanced actin stress-fiber formation [Liu et al 2006], respectively. The reason for this discrepancy is most probably due to the fact that normal mammary epithelial cells [Zhong et al 1997] or normal murine fibroblasts [Liu et al 2006] have been transformed, whereas in our case HRAS transformation was carried

out in an SV40ER-pretransformed background in which RHOA expression might be already lost. Loss of RHOA activity in HRASG12V-expressing cells has been reported earlier [Izawa et al 1998]. In support of this assumption, BJELR cells poorly attach (see 'Results', p99) and do not exhibit actin stress fibers (Supplementary, Figure 35). Future Western blot analyses will assess total RHOA levels in cells of the stepwise system, as well as CDC42 and RAC1 levels, which counteract RHOA routes.

In transformed BJELR cells we observed increased total MLC2 expression levels, evidenced by an antibody, which recognises all 3 MLC2 isoforms, smMLC2, nmMLC2 and nmlMLC2. This result somewhat contradicts findings that transformation is often associated with the downregulation of cytoskeletal proteins [Iida et al 2009] and that HRAS-transformation induced the decrease of smMLC2, but not nmMLC2 and nmlMLC2, mRNA and protein levels [Kumar et al 1991, Kumar et al 1992, Gerrits et al 2012]. Interestingly, interference with DR signalling in myoblasts by different means (pan-CASP or CASP8 inhibition, expression of dominant-negative FADD or DR5 constructs), decreased mRNA and protein levels of the transcription factor myoblast determination protein 1 (MYOD) [Freer-Prokop et al 2009]. Binding sites for MYOD can be found in the gene promoter of smMLC2, but not nmMLC2 or nmlMLC2. Moreover, MYOD levels are downregulated by calpains [Stuelsatz et al 2010], which in turn are activated by ERK at focal adhesions [Glading et al 2000, Glading et al 2004]. In transformed BJELR cells the whole RHOA signalling pathway required for focal adhesion formation might have collapsed due to their SV40ER background. As a result, BJELR cells most likely have few and/or disorganised focal adhesions, so that they adhere poorly to growth surfaces and so that ERK and calpains do not co-localise. This way, ERK cannot activate calpains, MYOD is not downregulated, which would finally explain why total MLC2 expression levels in BJELR cells are higher than in normal BJ cells. Intriguingly, also the expression of cFLIP was shown to be dependent on calpains [Benayoun et al 2008] and it was indicated that cFLIP is expressed in myofibers [Nagaraju et al 2000, Benayoun et al 2008]. Thus, active NMII fibers and mature focal adhesions seem to be of central importance for TRAIL resistance.

TRAIL-DISC composition in normal and transformed cells. Even though an ERK-driven stabilisation of MYC and a subsequent MYC-driven upregulation of DR5 and DR4 were reported to account for TRAIL-sensitivity of transformed stepwise system cells [Nesterov et al 2004, Wang et al 2005], we detected equal protein expression levels and equal DR5 surface levels in normal BJ and transformed BJELR cells (Results, Figure 24, C&D). Moreover, rhTRAIL-induced recruitment of DR4 to DR5 (and vice versa) occured similarly in both cell lines (Results, Figure 24, G, Supplementary, Figure 31). Of note, papers by Nesterov and Wang do not show an immediate comparison of ERK phosphorylation levels or endogenous MYC expression levels in normal and transformed cells. Instead, Nesterov et al compared ERK phosphorylation levels of HTERT and SV40ER-immortalised HA1E cells with those of HA1ER cells. The comparison of normal and transformed cells would be essential, as ERK phosphorylation is stimulated by growth factors or by cell adhesion. Growth factors stimulate GRB2 recruitment to cell surface receptors and thus ERK activation via the SOS/RAS/RAF1/MEK1 pathway. Contrary, cell adhesion stimulates focal adhesion kinases (FAK, SRC) to either mediate GRB2 recruitment and SOS/RAS/RAF1/MEK1 activation, or to recruit RA1C and activate ERK via the PAK/RAF1/MEK1 pathway [del Pozo et al 2000, Eblen et al 2002, reviewed by Parsons et al 2003, Mitra et al 2005]. Importantly, the FAK/SRC-mediated RAC/RAF1/MEK1/ERK activation is RAS independent. Thus, normal cells, which commonly adhere much stronger than transformed cells might reach equal ERK phosphorylation levels than transformed cells expressing constitutively active RAS. In conclusion, the magnitude of changes must exceed ERK hyperactivation to explain ERK-driven TRAIL-sensitisation in transformed BJELR cells, as reported by Nesterov et al. Data from our laboratory revealed that MYC expression is absent in normal stepwise system cells, increases in HTERT and SV40ER pre-transformed cells and reach the maximum in HTERT, SV40ER and HRAS-transformed cells (unpublished observations). Thus, high DR5 expression in normal BJ cells may result from the action of other transcription factors regulating DR5 expression, such as CCAAT/enhancer-binding protein–homologous protein (CHOP), p53 or NFKB [Yamaguchi and Wang 2004, Yoshida et al 2005, Takimoto and El-Deiry 2000, Shetty et al 2005].

One of the biggest limitations performing DISC immunoprecipitations is that obtained DISC analyses represent the signalling response of a heterogeneous cell

population. Therefore, to increase chances for de-novo discovery of new DISC interactors, we chose to analyse the DISC of the 2 extremes in TRAIL sensitivity normal and transformed cells. Since, DISC immunoprecipitations do not allow us to discriminate between single DISCs but represent the net outcome of plenty of DISCs formed, we do not know, whether CASP8 and cFLIP(L) bind simultaneously to the same FADD/DR complex, or whether they bind to very distal ones. Moreover, in normal cells, which survive rhTRAIL treatment minimally to 90%, DISC analyses do not reveal whether rhTRAIL-induced CASP8 cleavage is low in every single cells, or whether only in a few cells (maximally 10%) CASP8 cleavage is occuring, whilst in the remaining 90% only cFLIP(L) is bound to the DR. Only FACS analyses, staining for the active CASP8 p18 cleavage fragment, will help us to answer these issues in the future.

Interestingly, in the DISC of normal BJ cells we observed almost no CASP8 cleavage, whilst we did obtain profound cFLIP(L)p43 cleavage fragments (Results, Figure 24, G), raising the question of what mediates cFLIP(L) processing if not CASP8? With respect to the refined DISC model (Introduction, Figure 6) it could be that the initiator CASP and cFLIP 'chains' binding to one FADD molecule in normal BJ cells primarily consist of cFLIP(L) molecules. In this case, few activated CASP8 molecules would process many cFLIP(L) proteins.

Proposed model of NMII function in TRAIL signalling of normal and transformed cells. TRAIL is known to induce NFKB-dependent cell differentiation into osteoclasts [Yen et al 2008] and another study demonstrated that lumen-formation of non-transformed breast epithelial cells was dependent on cFLIP(L) levels [Yerbes et al 2011]. Since NMII activity controls organogenesis and differentiation [Conti et al 2004, Swailes et al 2006, reviewed by Vicente-Manzanares et al 2009], and we observe a reduction in rhTRAIL-induced cFLIP(L)p43 generation upon NMHCIIa protein depletion in normal cells, we suggest that NMIIa at the DR in normal cells not only confers resistance to TRAIL-induced apoptosis, but might as well regulate TRAIL-induced morphogenesis events in normal cells (Figure 40). Since NMIIa was indicated to inhibit cell migration [Even-Ram et al 2007] we assume that NMIIb rather than NMIIa could be involved in the regulation of TRAIL-induced migration events in normal cells.

During the process of transformation NMIIa activity might be reduced to enable detachment/reattachment cycles during enhanced proliferation and to facilitate migration. Therefore, NMIIa fibers are dissolved leading to the repeal of cell compartmentalisation, the loss of NMIIa from the DR of transformed cells, decreased cFLIP(L) availability and hence increased CASP8 cleavage and TRAIL sensitivity. Due to high basal NMII activity in normal cells, cFLIP(L) availability is elevated and thus TRAIL-stimulated CASP8 activation is low. Thus, MLC2-phosphorylating kinases, which are activated by CASP8 cleavage, strengthen the NMII/DR interaction and in this way might even limit effector CASP activation through CASP8. Contrary, in transformed cells initial NMII activity and hence cFLIP(L) levels are low, leading to strong CASP8 activation which cannot be compensated by CASP8-activated kinases positively influencing NMII fiber formation.

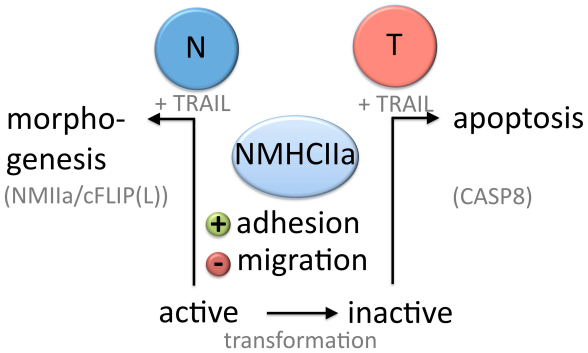

Figure 40: Proposed model of the NMIIa/DR interaction regulating the cFLIP(L)-mediated switch between morphogenic and apoptotic TRAIL signalling in normal (N) and transformed (T) cells. In normal cells NMHCIIa positively regulates cell adhesion and cytoplasmic cFLIP(L) levels whilst it blocks cell migration. During the process of transformation NMIIa activity is reduced to enable detachment/reattachment cycles during enhanced proliferation and to facilitate migration putatively mediated by NMIIb. Therefore NMIIa is lost from the DR of transformed cells which leads to decreased cFLIP(L) availablility and hence increased CASP8 cleavage. In normal cells that have high NMIIa activity and a strong NMIIa/DR interaction, TRAIL stimulation induces robust cFLIP(L) cleavage. Thus, the NMIIa/cFLIP(L) axis in normal cells promotes TRAIL-induced morphogenesis.

Potential functions of GRB2 and RAF1 at the TRAIL DISC of normal cells. Likewise it has been reported for TNFR1 [Hildt and Oess 1999], we found GRB2 to constitutively co-immunoprecipitate with DR5 (Results, Figure 30, B&C) and DR4 (not shown) in normal BJ cells. GRB2 is a communicator that links membrane receptors and membrane-bound proteins to intracellular cytoskeletal regulators, increasing their local concentrations at the membrane and facilitating enzymatic reactions and activation and

couples to mitogenesis and cytoskeletal reorganisation [reviewed by Giubellino et al 2008]. Depletion of GRB2 from normal BJ cells decreased overall levels of active RAF1 and MEK1/2, which is in line with findings that the TNFR1/GRB2 interaction was essential for TNFα-dependent activation of RAF1 kinase [Hildt and Oess 1999]. Contrary to the FAS-DISC, at which RAF1 recruitment was induced upon ligand stimulation and RAF1 was suggested to directly interact with and to be activated by cFLIP(L)p43 [Kataoka et al 2000, Park et al 2001], we found RAF1 to constitutively interact with DR5 (Results, Figure 30, C). This suggests that at the DR of normal cells RAF1 might be activated via GRB2/SOS1/RAS in a ligand-independent fashion. Upon TRAIL-stimulation, RAF1 could additionally be induced by cFLIP(L)p43. Whilst RAF1 plays an essential role in maintaining the organization of the cytoskeleton and thus in cell polarity and migration [Ehrenreiter et al, 2005], GRB2 signalling leads to the activation of MAPK pathways (JNK, p38, ERK1/2). The impact of a putative TRAIL-induced complex II in the activation of these signalling routes therefore might be lower than initially assumed. As previously mentioned, DISC analyses do not allow us to conclude whether FADD, CASP8 and/or cFLIP binding occurs at the same DR than GRB2 and RAF1 binding.

Constitutive GRB2 and RAF1 interactions with DR5 and DR4 in normal BJ cells strongly point to a pro-survival signalling function of the DR. Indeed, observed equal DR expression levels and similar rhTRAIL-induced DR clustering in normal BJ and transformed BJELR cells, but absent apoptosis induction in normal cells implied the question about the function of TRAIL signalling in normal cells. Why should normal cells express DR at high levels if they were of no function? The notion that DR via RAF1 may signal towards survival in normal cells is supported by the fact that all attempts to generate constitutive DR5 or DR4 knockout cells failed as yet either because of cell death or poor cell growth.

Contribution of this study to the understanding of TRAIL resistance mechanisms in transformed cells and possible therapeutic implications. This study provides direct evidence that TRAIL apoptosis signalling requires a disrupted (NMIIa-) cytoskeleton. Unlike normal cells, cancer cells do not undergo apoptosis upon cytoskeletal changes. This is most probably due to activated survival pathways (XYZ) counterbalancing the cytoskeleton-mediated apoptosis signal allowing the cancer cell to

survive (or to an inactivated cytoskeleton/apoptosis pathway). If TRAIL is added to transformed cells, this balance is challenged/abolished and moved towards apoptosis. Contrary, in normal cells we find regular cytoskeleton architecture, therefore TRAIL does not induce apoptosis. Inherently TRAIL-resistant cancer cells might escape from TRAIL-apoptosis either because they have maintained their NMIIa/DR interaction, or in these cells the XYZ-pathway(s) signal(s) stronger than in TRAIL-sensitive cancer cells and thus counterbalance TRAIL-apoptotic challenge. Future studies investigating the NMIIa/DR interaction in TRAIL-insensitive (solid) cancer cells will have to elucidate this assumption. For TRAIL-based cancer therapies one can only hope that the second situation is the case since a safe cancer cell-specific rupture of the NMIIa/DR interaction is unlikely to be achieved by the combined use of cytoskeleton inhibitors and rhTRAIL preparations. If TRAIL-resistance in cancer cells is based on hyperactive XYZ-survival pathway(s) at least those could be blocked in targeted therapies and a combo-therapy of those cancers with XYZ-inhibitors and TRAIL were imaginable.

Findings presented in this study might help to calculate the risk for an enhanced migratory cancer phenotype in TRAIL-therapy. At least in cancer cells with inactivated NMII activity, through for instance down-regulated RHOA and/or increased RAC1 or CDC42 activity, TRAIL will most probably not enhance migration, but will signal to apoptosis.

Concluding remarks. Plenty remains to be learnt about the initial steps of TRAIL signalling. Certainly, the DISCome is not yet fully defined and the complete understanding of its single compounds stays a challenge. In future DISC studies extra care should be taken on the cell context, the model cells' genetic background as well as on the stimulus applied. The development of technologies enabling quantitative analyses of single DISC formation events would help to advance our understanding of TRAIL apoptotic signalling.

EXTENDED SUMMARY

In this PhD thesis we conducted a study on the transformation-associated mechanisms that lead to the gain of TNF-α-related apoptosis inducing ligand (TRAIL) sensitivity. In that context the cytoskeletal protein nonmuscle myosin heavy chain IIa (NMHCIIa) was identified as entirely novel TRAIL death receptor interactor that proved critical for TRAIL resistance of normal cells. This study was performed at the Institut de Genetique et de Biologie Moleculaire et Cellulaire (IGBMC), Illkirch, France.

TRAIL is a cytokine of the TNF-superfamily that binds 4 specific membrane-bound receptors inducing their oligomerisation [Wiley et al 1995, Pitti et al 1996, Chaudhary et al 1997, Degli-Esposti et al 1997, Pan et al 1997a, 1997b, Sheridan et al 1997, Schneider et al 1997, Walczak et al 1997]. The death receptors 5 and 4 (DR5, DR4) contain a death domain (DD) that serves for the assembly of signaling complexes [MacFarlane et al 1997, Pan et al 1997a, Pan et al 1997b, Schneider et al 1997, Walczak et al 1997]. The other 2 TRAIL receptors, the decoy receptors (DcR1, DcR2), possess no or a truncated DD and do not transduce apoptotic signals [MacFarlane et al 1997, Pan et al 1997b, Schneider et al 1997, Degli-Esposti et al 1997]. Oligomerisation of DR upon TRAIL binding induces interaction with adaptor molecules such as Fas-associated death domain (FADD) that in turn recruits initiator caspase-8 (CASP8) and/or 10 (CASP10) [Chaudhary et al 1997, MacFarlane et al 1997, Bodmer et al 2000, Kischkel et al 2000, Sprick et al 2000; Kischkel et al 2001, Wang et al 2001, Sprick et al 2002]. Similarly, anti-apoptotic cellular FLICE-like inhibitory protein (cFLIP) is recruited to the DR competing with CASP8 for FADD binding and triggering survival pathways [Thome et al 1997, Burns and El-Deiry 2001, Krueger et al 2001, Chang et al 2002, Jin et al 2004]. The complex comprising TRAIL-receptors, FADD and initiator caspases constitutes the death-inducing signaling complex (DISC) (Figure 1) [Bodmer et al 2000]. Whilst DISC formation in transformed cells is extensively studied, almost no information is available about native DISC composition in normal cells.

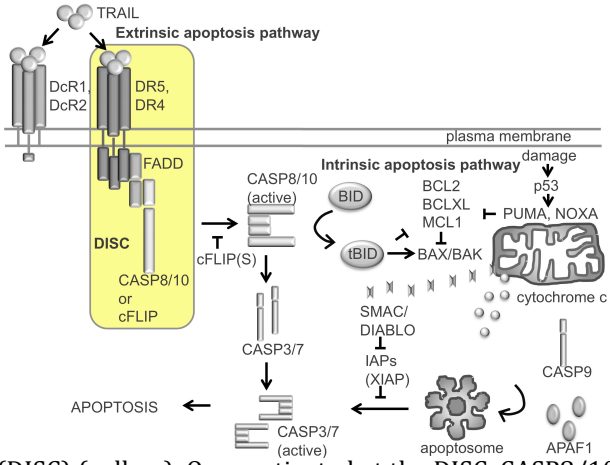

Figure 1: TRAIL DISC formation and apoptotic signalling. TNFalpha-related-apoptosis inducing ligand (TRAIL) binding induces the formation of death receptor 5 and 4 (DR5, DR4) microaggregates. Receptor aggregation leads to the recruitment of the adaptor molecule Fas-associated death domain (FADD) that co-recruits initiator pro-caspase 8, 10 (CASP8, CASP10) or the anti-apoptotic cellular Flice-like inhibitory protein (cFLIP), which lacks protease activity. Resulting close proximity of CASP molecules and/or cFLIP at the DR results in their mutual cleavage and activation. The complex minimally comprising DR, FADD, CAP8/10 and/or cFLIP is called the death inducing signalling complex (DISC) (yellow). Once activated at the DISC, CASP8/10 can directly cleave and activate effector caspases 3 and 7 (CASP3, CASP7) and hence fulfil the so-called extrinsic apoptosis pathway. In certain cells the apoptotic signal is propagated and enhanced via the intrinsic apoptotic cascade. Therefore DISC-activated CASP8/10 proteolytically convert BH3-interacting domain death agonist (BID) to the active, truncated form (tBID) that induces BCL2-antogonist/killer (BAK) and BCL2-associated X protein (BAX) at the mitochondria and in turn results in permeabilisation of the outer mitochondrial membrane and release of proteins such as cytochrome c, second mitochondria-derived activator of caspases (SMAC)/direct inhibitor of apoptosis protein (IAP)-binding protein with low pI (DIABLO). Cytochrome c binds to adaptor molecule apoptotic protease-activating factor 1 (APAF1) that binds to initiator procaspase 9 (CASP9) to form the apoptosome. At the apoptosome, CASP9 is activated leading to processing of CASP3/7 and eventually cell death. The figure is based on the idea of [White-Gilbertson et al 2008, Newsom-Davis et al 2009].

TRAIL is the only human cytokine known to induce death of diverse tumour cells while sparing healthy normal ones [Pitti et al 1996, Walczak et al 1999], therefore representing an attractive therapeutic option for cancer therapy [Russo et al 2010, Gerspach et al 2011, Pavet et al 2011, Yerbes et al 2011, Martinez-Lostao et al 2012]. Although TRAIL promotes cell death in a plethora of cancer cells, some tumour cells are either insensitive or acquire resistance upon TRAIL exposure [Gerspach et al 2011, Yerbes et al 2011]. Albeit multiple modulators of TRAIL signalling are known [Newsom-Davis et al 2009, Gonzalvez and Ashkenazi 2010, Gerspach et al 2011, Shirley et al 2011, Martinez-Lostao et al 2012], the molecular mechanisms underlying the lack of TRAIL sensitivity in normal cells remain obscure. Understanding the mechanistic basis of normal cells being refractory to TRAIL stimulation will be important to decipher how normal cells loose their TRAIL resistance upon transformation. The present thesis work therefore focused on the central question how normal cells that are originally TRAIL-resistant gain TRAIL-sensitivity by the process of tumourigenic transformation.

Since DISC formation is at the origin of TRAIL signalling (Figure 1), we hypothesised that as yet unknown DISC interactors may be critically involved in DISC function and that tumourigenic transformation would alter their recruitment, modification and/or expression and thus result in differential TRAIL-sensitivity. Therefore, we set out to identify novel DISC-interacting proteins that are differentially recruited in normal and tumour cells. We used stepwise human cell-based transformation models [Hahn et al 1999] that enabled a direct comparison of cancer cells with the normal isogenic progenitors (Figure 2). Notably, such a comparative analysis is not possible with established cancer and so-called 'normal' cell lines. While transformed cells derived from stepwise models display tumourigenic features [Hahn et al 1999] and TRAIL sensitivity, the normal human cells were resistant to TRAIL [Nesterov et al 2004, Wang et al 2005].

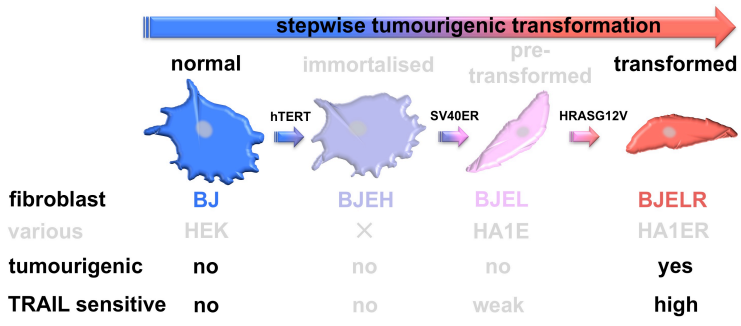

Figure 2: Scheme of Hahn and Weinberg's stepwise transformation model. Normal cells (*here:* human foreskin fibroblasts (BJ) or human embryonic kidney (HEK)) were gradually transformed by introducing the human telomerase catalytic subunit (HTERT), simian virus 40 early region (SV40ER) and a constitutively active HRAS mutant (HRASG12V). Whilst hTERT maintains telomere length and confers replicative immortality to BJ cells, HEK cells require additional SV40ER-encoded elements to reach immortality. Obtained transformed cells (*here:* BJELR or HA1ER) display cancer cell features like unlimited proliferation, anchorage-independent growth and tumour formation in vivo and are sensitive to TRAIL-induced apoptosis.

The 'results' section includes the protocols for the production and purification of recombinant human TRAIL and for native DISC immunoprecipitation. These protocols required establishment in the laboratory to facilitate analysis of the initial steps of TRAIL signalling in stepwise system cells as well as the identification of novel DISC interactors. In the following DISC analyses are presented showing that both normal and tumour cells formed DR5/DR4 DISC upon TRAIL stimulus. However, a reduced amount of cleaved CASP8 was seen in normal cells indicating poor pro-apoptotic signal intensity. Moreover, FADD recruitment was diminished and cFLIP(L) cleavage was higher in normal cells, suggesting that the resistance to TRAIL arises at the DISC (Figure 3).

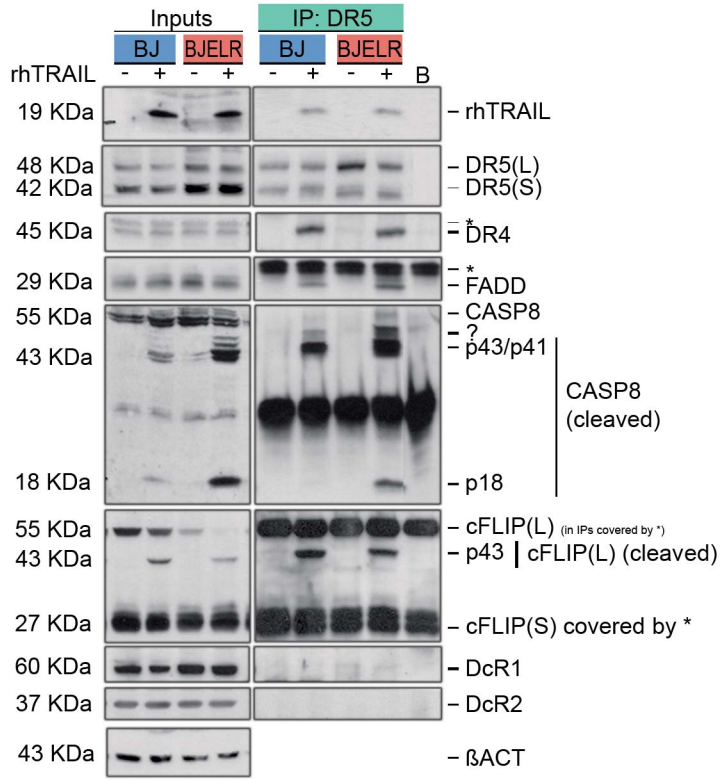

Figure 3: TRAIL-DISC formation of normal BJ and transformed BJELR cells. Equal numbers of BJ and BJELR cells were incubated with 1µg mL^{-1} recombinant human TRAIL (rhTRAIL) for 1h and lysed. The death receptor 5 (DR5) was immunoprecipitated (IP) using an antibody against the endogenous protein. IP-eluates were analysed for co-purified proteins. Left 4 lanes served as loading control and contain equal volumes of pre-cleared whole cell lysates (inputs) that were used in the IP-experiment. The 5 lanes on the right contain equal volumes of DR5-IP eluates originating either from the indicated cell line, or from the DR5/beads mixture (B) utilised in the experiment. Depicted are Western blots for 1 of 4 independent experiments.

Indeed, using mass spectrometry of differential protein bands co-purifying with DR-immunoprecipitations in normal and transformed cells and DR-immunoprecipitations followed by Western blot analyses, the cytoskeleton proteins nonmuscle myosin heavy chain IIa and IIb (NMHCIIa, NMHCIIb), myosin regulatory light chain 2 (MLC2) (not shown) and beta-actin (ßACT) were identified as novel DR-interactors in DISC immunoprecipitates (Figure 4, A&B). Importantly, normal cells displayed higher levels of NMHCIIa and IIb co-immunoprecipitating with DR5 and DR4 than transformed cells. Upon TRAIL stimulus, NMHCIIa and IIb interaction with DR was sustained in normal cells, whilst they were largely lost from the DISC formed in transformed cells (Figure 4, B).

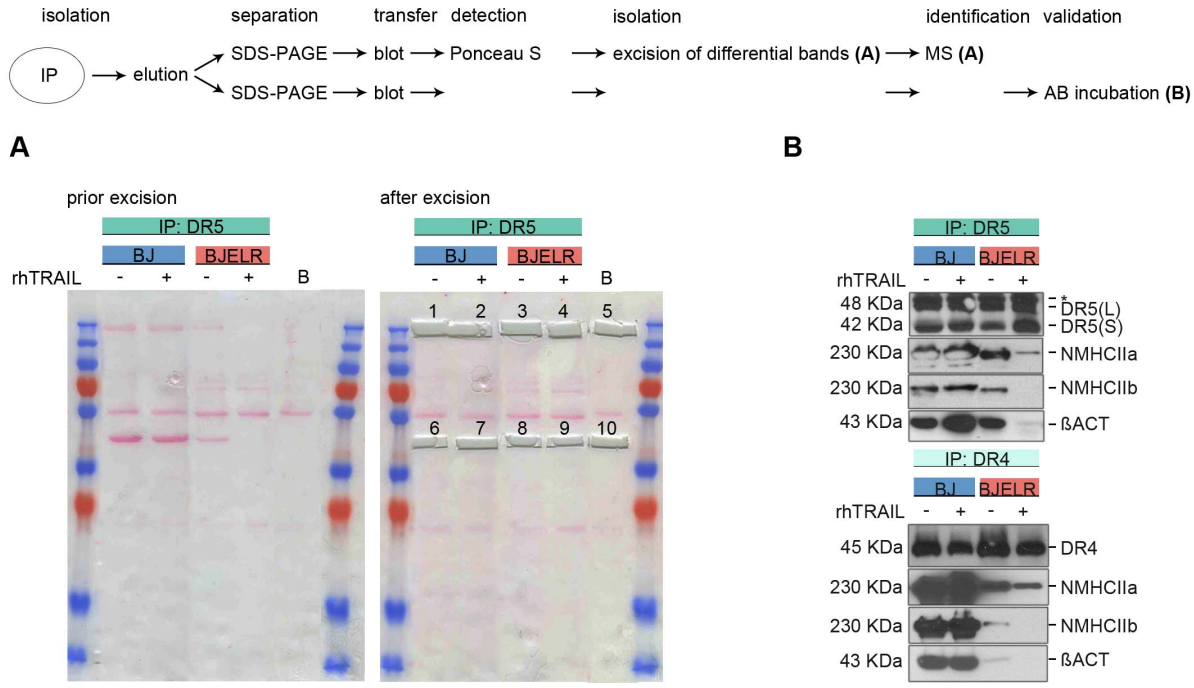

Figure 4: Identification of novel TRAIL-DISC interactors in normal BJ and transformed BJELR fibroblasts. The scheme indicates the experimental set-up. After immunoprecipitation (IP), proteins were eluted and eluates were split into 2 fractions. One aliquot was separated on SDS-PAGE gels and transferred onto nitrocellulose membranes that were stained with Ponceau S. Observed differential bands were excised from the membranes, proteins were digested and analysed by mass spectrometry (MS). The other aliquot was separated on SDS-PAGE gels, blotted onto nitrocellulose membranes and analysed for protein interactions using specific antibodies (AB). In this way **(A)** death receptor 5 (DR5) was purified from lysates of BJ and BJELR cells that were left unstimulated (-) or that were stimulated for 1h with 1µg mL^{-1} recombinant human TRAIL (rhTRAIL) (+). Differential bands visualised with Ponceau S were cut out, digested and given for mass-spectrometrical peptide identification. **(B)** Western blot analysis of DR5-IP eluates to validate the mass-spectrometric results obtained in (A) (upper panel). Death receptor 4 (DR4) was purified under similar experimental conditions and analysed by Western blot (lower panel). Depicted are representative blots from 1 out of 2 independent experiments.

Abrogation of the NMHCII/DR interaction using the nonmuscle myosin II (NMII) inhibitor blebbistatin or the myosin light chain kinase (MLCK) inhibitor ML7 increased the response of normal cells to TRAIL-induced apoptosis (Figure 5).

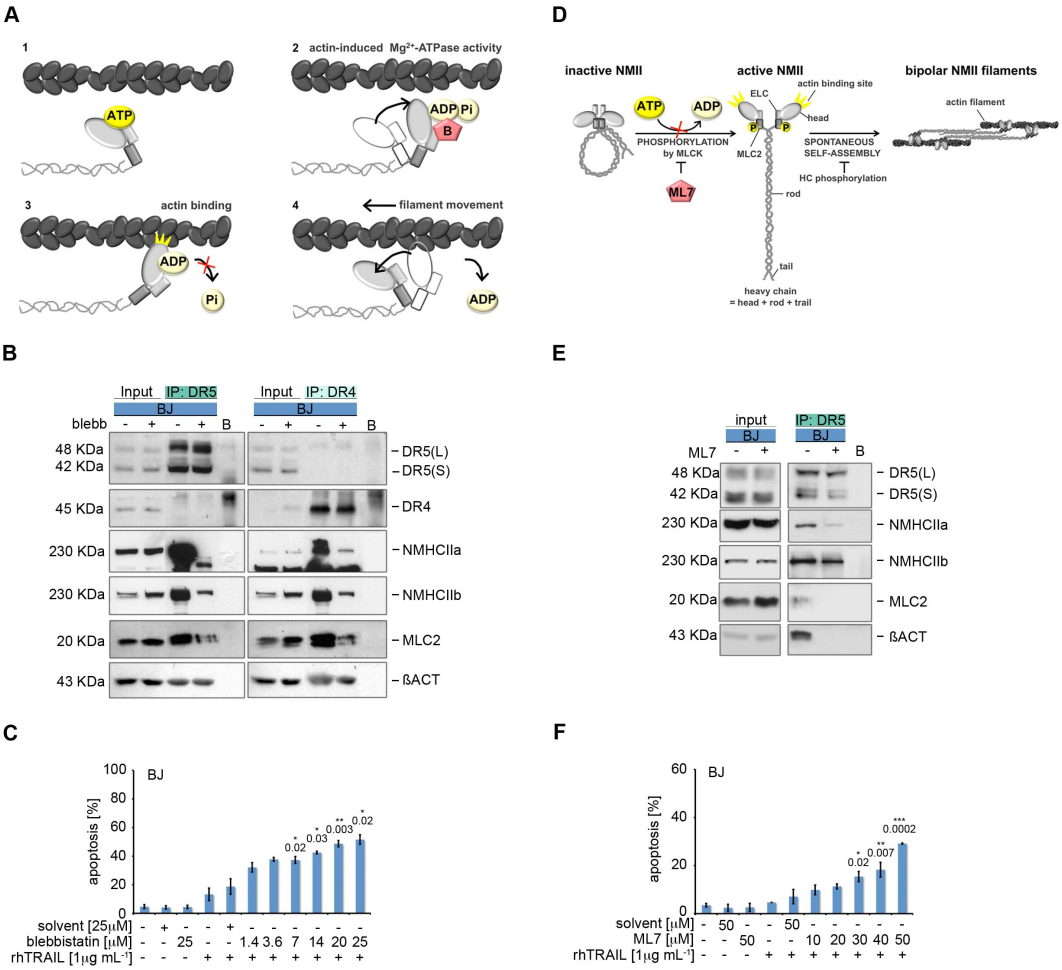

Figure 5: Effects of NMHCII Mg^{2+}-ATPase inhibition on the NMHCII/DR interaction in normal BJ cells. **(A)** The crossbridge cycle regulated by the Mg^{2+}-ATPase activity housed in the non-muscle myosin heavy chain II (NMHCII) head domain and mechanism of blebbistatin inhibitor action. 1. ATP binding to the NMHCII head leads to a conformation which cannot bind actin. 2. ATP-hydrolysis lets the head swing into a cocked position, whereby ADP and Pi remain bound. 3. When Pi leaves NMHCII, the head binds actin and a power stroke is released. 4. ADP is liberated to continue the cycle. At this stage NMHCII is tightly bound to actin. Blebbistatin preferentially binds to the NMHCII head with ADP and phosphate bound at the active site of the Mg^{2+}-ATPase domain. Since it slows down phosphate release, NMHCII does not bind to actin. **(B)** NMHCII/DR interaction upon blebbistatin treatment. Normal (BJ) cells were incubated for 30 minutes with vehicle DMSO (-) or 25µM blebbistatin (+) and then collected to immunoprecipitate (IP) death receptor 5 and 4 (DR5, DR4). The IP-eluates were analysed for the interaction with NMHCIIa, NMHCIIb, myosin regulatory light chain (MLC2) and beta-actin (ßACT).* **(C)** TRAIL-induced apoptosis upon blebbistatin treatment. BJ cells were pre-treated for 30 minutes with indicated concentrations of solvent or blebbistatin and then co-treated with 1µg mL^{-1} rhTRAIL (+). Apoptosis was assessed as 7A6 positivity 16 hours after the addition of rhTRAIL.** **(D)** Enhancement of Mg^{2+}-ATPase activity by MLC2 phosphorylation and mechanism of ML7 inhibitor action. In the absence of MLC2 phosphorylation NMHCII has a circular, inactive and assembly-incompetent conformation (left). Upon MLC2 phosphorylation by the myosin light chain kinase (MLCK) NMHCIIs unfold into an open, active conformation (middle) and spontaneously assemble into myosin filaments (right). ML7 binds at the ATP-binding site of MLCK inhibiting its catalytic activity. The figure idea is based on [Vicente-Manzanares et al 2009, Book: Alberts et al Molecular Biology of the Cell (Garland Science)]. **(E)** NMHCII/DR5 interaction upon ML7 treatment. Normal BJ cells were incubated for 30 minutes with vehicle ethanol:water (1:1) (-) or 50µM MLC2-phosphorylating kinase (MLCK) inhibitor ML7 (+) and then collected to IP DR5. The IP-eluates were analysed as described in (B).*** **(F)** TRAIL-induced apoptosis upon ML7 treatment. BJ cells were pre-treated for 30 minutes with the indicated concentrations of solvent or ML7 and then co-treated with 1µg mL^{-1} rhTRAIL (+). Apoptosis was assessed as mentioned in (C).**** Depicted are Western blots for 1 of *3, respectively ***2 independent experiments. Mean values derive from **3 to 4, respectively ****2 to 5 independent experiments. Significances were calculated using unpaired, 2-tailed Student's t-test.

Intriguingly, siRNA-mediated knockdown of NMHCIIa but not NMHCIIb robustly released the TRAIL resistance block in normal cells and was characterised by reduced DR4 recruitment, decreased processing of cFLIP(L) and elevated CASP8 cleavage at the DR5-DISC (Figure 6).

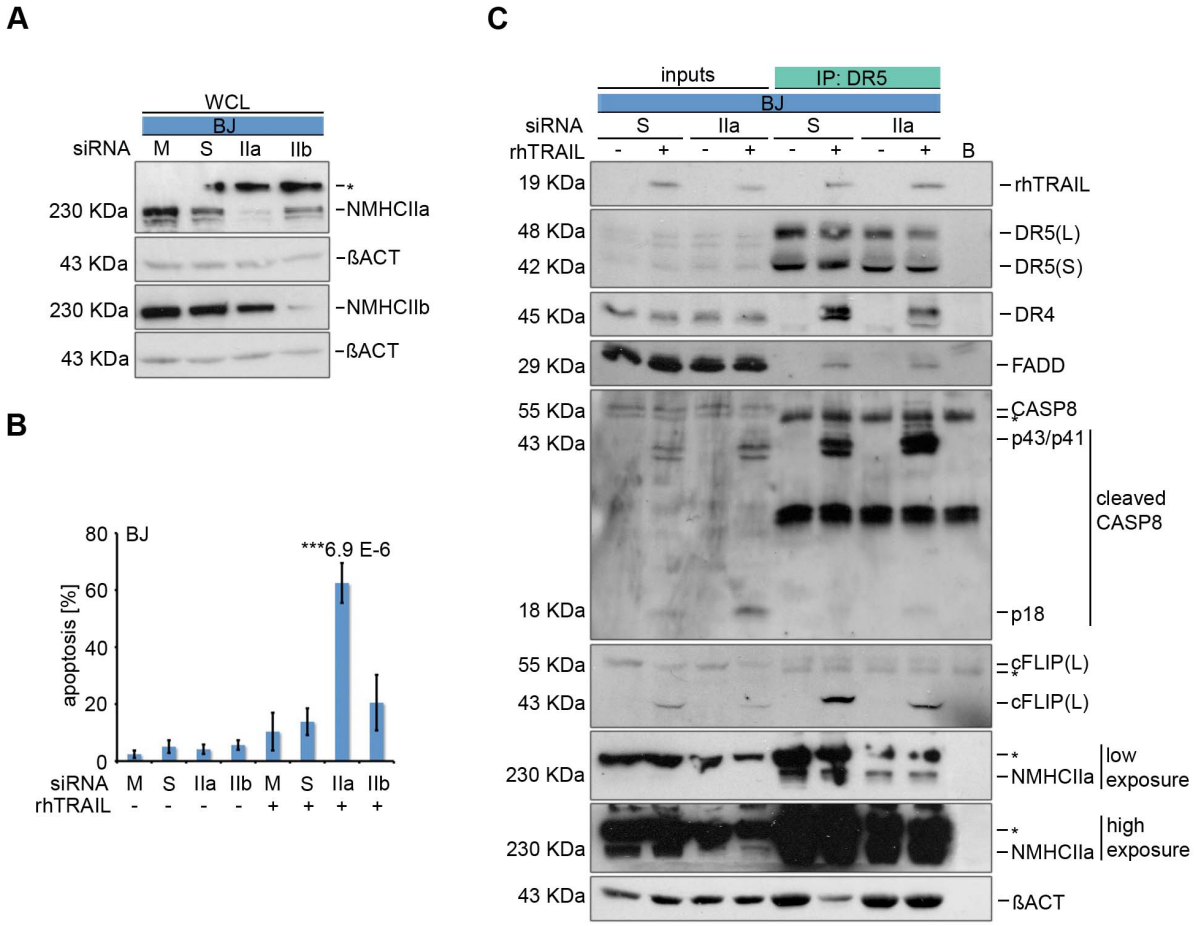

Figure 6: Effects of NMHCIIa- and NMHCIIa siRNA knockdown on TRAIL apoptosis and DISC formation in normal BJ cells. BJ cells were transfected with 15nM siRNA against non-muscle myosin heavy chain IIa or IIb (IIa, IIb), scramble control siRNA (S) or were mock-transfected with lipofectamine (M) for 4d. Cell culture medium was renewed 1d and 3d after start of transfection. **(A)** Whole cell lysates (WCL) of BJ cells were analysed for NMHCIIa and NMHCIIb expression levels upon 4d knockdown (KD) by Western blot analysis.* **(B)** TRAIL-induced apoptosis upon NMHCIIa and NMHCIIb siRNA KD. Four days after start of KD BJ cells were left untreated (-) or were treated with 1µg mL^{-1} rhTRAIL (+). Apoptosis was assessed as 7A6 positivity 16 hours after the addition of rhTRAIL. Values represent mean values of 4 independent experiments. **(C)** TRAIL-induced DISC formation upon NMHCIIa siRNA KD. BJ cells were left untreated (-) or were treated with 1µg mL^{-1} rhTRAIL (+) for 1h 4 days after start of KD. Death receptor 5 (DR5) was immunoprecipitated and analysed for co-purified proteins by Western blot. Pre-cleared cell lysates (inputs) served as loading controls and as indicators for KD-mediated alterations in protein expression. Depicted are Western blots for 1 out of *3, independent experiments. Significances were calculated using unpaired, 2-tailed Student's t-test.

Exploration of the signalling cascade dictating differential regulation of the NMHC/DR interaction in normal and transformed cells showed higher NMHC activity in normal cells as indicated by increased MLC2 phosphorylation levels. In transformed cells MLC2-phosphorylating kinase (MLCK) activity is impaired, as supported by the observation that MLCK protein levels were downregulated, MLCK inhibitory kinase (PAK1) protein levels were increased and the circumstance that normal cells survived higher doses of MLCK inhibitor (ML7) levels than transformed cells (Figure 7).

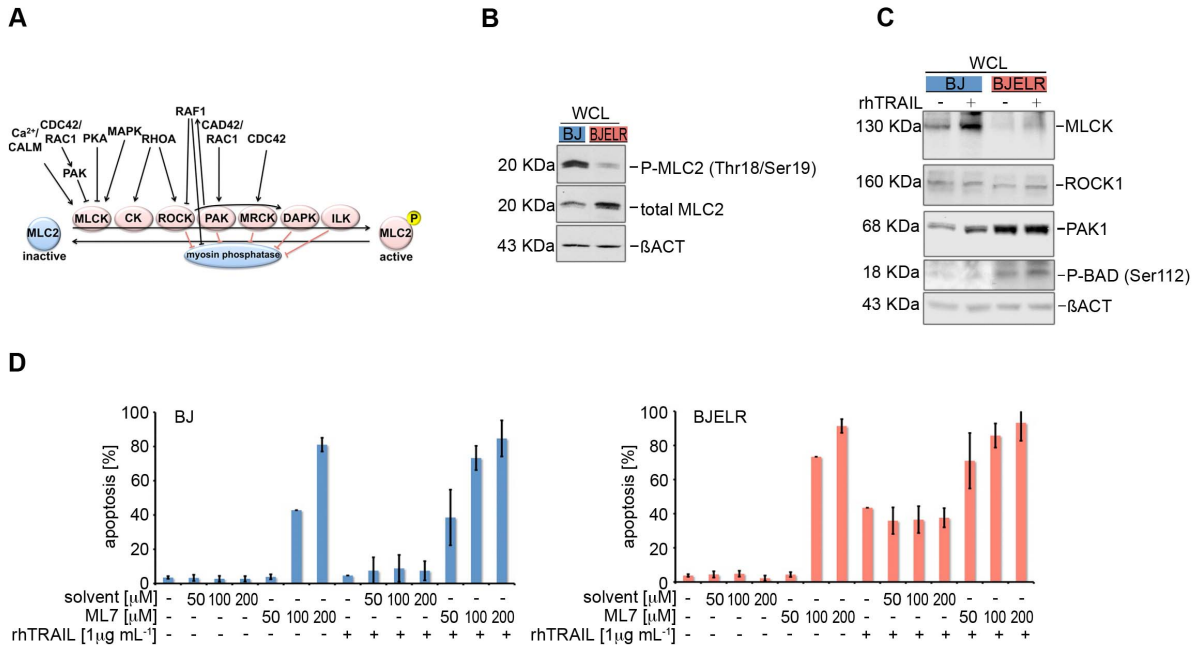

Figure 7: Myosin regulatory light chain (MLC2) Ser18/Thr19 phosphorylation and kinase expression in normal BJ and hTERT, SV40ER and H-Ras transformed BJELR cells. **(A)** Complexity of MLC2 Thr18/Ser19 phosphorylation. Myosin regulatory light chain (MLC2) is activated by phosphorylation of Thr18/Ser19. Major phosphorylation site is Ser19 that allows non-muscle myosin II (NMII) to form NMII filaments, to interact with actin, to assemble actomyosin complexes and to initiate contraction. Di-phosphorylation at both Ser19 and Thr18 further promotes filament assembly. Many kinases known to phosphorylate and activate MLC2 Thr18/Ser19 (red) also phosphorylate and inhibit (red lines) MLC2 inactivating myosin phosphatase (blue). The figure is based on [Matsumura 2005] **(B)** Difference in MLC2 phosporylation levels. Whole cell lysates (WCL) of BJ and BJELR cells were analysed by Western blot for the relative phosphorylation and expression levels of MLC2. **(C)** BJ and BJELR cells were left untreated (-) or were treated with 1µg mL^{-1} rhTRAIL for 15min (+) and analysed for protein expression levels of MLCK, ROCK and PAK1. PAK1 activity was assessed immuno-blotting for phosphorylated BAD. Imaged were representative Western blots for 1 of 2 independent experiments. **(D)** Apoptosis induction at high levels of MLCK inhibitor ML7. Apoptotic response of BJ and BJELR cells were assessed in paralleled experiments. Cells were pre-incubated with indicated concentrations of ML7 or solvent (ethanol/water mix at a 1:1 ratio) for 30 min and then co-treated with 1µg mL^{-1} purified TRAIL. Apoptosis was quantified as 7A6 positivity in FACS analysis after 16h of treatment. Values derive from 2 independent experiments.

Together these data support a model in which the newly identified NMHCIIa interaction with DR maintains TRAIL resistance in normal cells. Moreover, they suggest a functional role of NMHCIIa in the acquisition of TRAIL responsiveness through the process of transformation. Finally, since NMHCIIa has a central role in cell adhesion, our model provides a direct link between the correlation of cell detachment and TRAIL sensitivity described in literature.

Future work will focus on the identification of the domain minimally required for NMHCIIa to interact with DR aiming at understanding the (structural) basis of interaction. The biological significance of this interaction will be confirmed in other existing cell models of neoplastic transformation. Cytoskeletal changes will be investigated in immortalised and pre-transformed cells of the stepwise transformation system to define whether observed differences in transformed cells are mediated by Ras. Unravelling differences in the DISC composition of normal and transformed cells will decipher the molecular basis of TRAIL sensitivity/resistance and provide a solid platform for the exploitation of TRAIL-based anti-cancer therapies.

RÉSUMÉ

Dans ce projet de thèse, nous avons mené une étude sur les mécanismes associés à la transformation cellulaire qui aboutissent à une sensibilité accrue au TNF-α-related apoptosis inducing ligand (TRAIL). Dans ce contexte, la protéine du cytosquelette non-muscle myosin heavy chain IIa (NMHCIIa) a été identifiée comme un tout nouveau partenaire du récepteur de mort de TRAIL. Il est essentiel pour la résistance à TRAIL des cellules normales. Cette étude a été menée à l'Institut de Génétique et de Biologie Moléculaire et Cellulaire (IGBMC), Illkirch, France dans l'équipe du Dr. Hinrich GRONEMEYER.

TRAIL est une cytokine de la superfamille du TNF qui se lie à 4 récepteurs membranaires spécifiques, induisant leur oligomérisation [Wiley et al 1995, Pitti et al 1996, Chaudhary et al 1997, Degli-Esposti et al 1997, Pan et al 1997a, 1997b, Sheridan et al 1997, Schneider et al 1997, Walczak et al 1997]. Les récepteurs de mort 5 et 4 (DR5, DR4) contiennent un domaine de mort (DD) qui sert à l'assemblage de complexes de signalisation [MacFarlane et al 1997, Pan et al 1997a, Pan et al 1997b, Schneider et al 1997, Walczak et al 1997]. Les 2 autres récepteurs de TRAIL sont des récepteurs leurres (DcR1, DcR2) qui possèdent un DD tronqué et ne transmettent pas de signaux [MacFarlane et al 1997, Pan et al 1997b, Schneider et al 1997, Degli-Esposti et al 1997]. L'oligomérisation des DR après liaison de TRAIL induit une interaction avec des molécules adaptatrices comme Fas-associated death domain (FADD) qui à leur tour recrutent les caspases initiatrices 8 (CASP8) et / ou 10 (CASP10) [Chaudhary et al 1997, MacFarlane et al 1997, Bodmer et al 2000, Kischkel et al 2000, Sprick et al 2000; Kischkel et al 2001, Wang et al 2001, Sprick et al 2002]. De la même manière, la protéine anti-apoptotique cellular FLICE-like inhibitory protein (cFLIP) est recrutée au niveau des DR. Elle rentre en compétition avec la caspase 8 pour la liaison de FADD et déclenche alors des voies de signalisation pour la survie [Thome et al 1997, Burns and El-Deiry 2001, Krueger et al 2001, Chang et al 2002, Jin et al 2004]. Les récepteurs de TRAIL, FADD et les caspases initiatrices constituent le complexe de signalisation de mort (DISC) (Figure 1) [Bodmer et al 2000]. Alors que la formation du DISC dans les cellules transformées est bien étudiée, on ne dispose d'aucune information sur la composition du DISC natif dans les cellules normales.

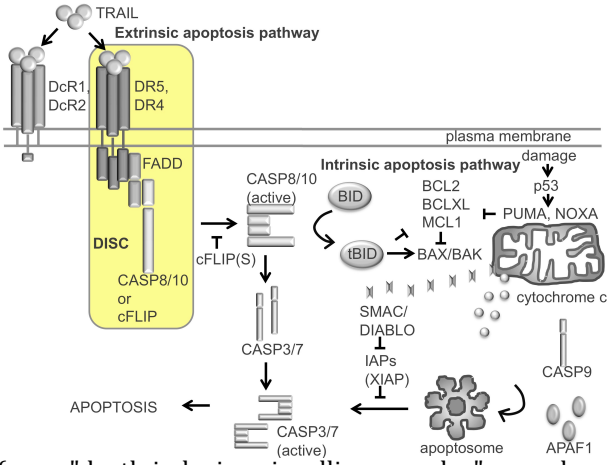

Figure 1: Formation de TRAIL-DISC et voie de signalisation apoptotique. La liaison de TRAIL (TNFalpha-related-apoptosis inducing ligand) induit la micro-agrégation des "récepteurs de mort" (DR ou "Death Receptors") DR4 et DR5. L'agrégation de ces récepteurs conduit au recrutement de la molécule adaptatrice FADD (Fas-associated death domain) qui co-recrute les pro-caspases initiatrices 8 et 10 (CASP8, CASP10), ou le facteur anti-apoptitique cFLIP (cellular Flice-like inhibitory protein), qui ne possède pas d'activité protéolytique. La promiscuité au niveau des DR des CASP et/ou de cFLIP permet leur activation par clivage. Le complexe minimal DR, FADD, CASP8/10 et/ou cFLIP est nommé DISC (pour "death inducing signalling complex", complexe de signalisation induisant la mort, en jaune dans la figure). Une fois activée dans DISC, les CASP8/10 peuvent directement cliver et activer les caspases effectrices 3 et 7 (CASP3, CASP7) et ainsi s'acquitter de la voie dite d'apoptose extrinsèque. Dans certaines cellules, le signal d'apoptose est propagé et amplifié via la voie dite d'apoptose intrinsèque. Ainsi, les CASP8/10 activées au sein de DISC protéolysent la protéine BID (BH3-interacting domain death agonist) en sa forme tronquée et active, tBID. A son tour, tBID active BAK et BAX (respectivement "BCL2-antogonist/killer" et "BCL2-associated X protein") à la mitochondrie, ce qui résulte en une perméabilisation de la membrane externe mitochondriale, et à la libération de facteurs tels le cytochrome C et SMAC/DIABLO [second mitochondria-derived activator of caspases (SMAC)/direct inhibitor of apoptosis protein (IAP)-binding protein with low pI (DIABLO)]. Le cytochrome C se lie à la molécule adaptatrice APAF1 (apoptotic protease-activating factor 1) qui se lie à la pro-caspase initiatrice 9 (CASP9) pour former l'apoptosome. A l'apoptosome, CASP9 est activée, ce qui entraîne le clivage de CASP3/7 et la mort cellulaire. La figure est basée sur les propositions de [White-Gilbertson et al 2008, Newsom-Davis et al 2009].

TRAIL est la seule cytokine humaine connue pour induire la mort des cellules tumorales tout en épargnant les cellules normales [Pitti et al 1996, Walczak et al 1999]. C'est pourquoi elle représente une option thérapeutique prometteuse pour le traitement du cancer [Russo et al 2010, Gerspach et al 2011, Pavet et al 2011, Yerbes et al 2011, Martinez-Lostao et al 2012]. Bien que TRAIL induise la mort cellulaire dans une pléthore de cellules cancéreuses, il existe certaines cellules tumorales qui y sont soit insensibles soit qui acquièrent une résistance à la suite d'une exposition à TRAIL [Gerspach et al 2011, Yerbes et al 2011]. Même si de nombreux modulateurs de la signalisation de TRAIL sont connus [Newsom-Davis et al 2009, Gonzalvez and Ashkenazi 2010, Gerspach et al 2011, Shirley et al 2011, Martinez-Lostao et al 2012], les mécanismes moléculaires qui sont à la base de l'absence de sensibilité à TRAIL dans les cellules normales restent obscurs. Comprendre quel est le mécanisme à la base de la résistance de cellules normales à la mort induite par TRAIL est important car il permettrait de découvrir la façon dont les cellules normales perdent leur résistance à TRAIL au cours de la transformation. Ce travail de thèse porte donc sur cette question centrale : comment une

cellule normale qui est à l'origine résistante à TRAIL acquiert la sensibilité à TRAIL au cours du processus de transformation oncogénique.

Etant donné que la formation du DISC est à l'origine de la signalisation de TRAIL (Figure 1), nous avons émis l'hypothèse qu'il devait exister des partenaires encore inconnus dans le fonctionnement du DISC. Ces facteurs seraient recrutés, modifiés ou exprimés différemment au cours de la transformation oncogénique et entraineraient une différence dans la sensibilité à TRAIL. Par conséquent, nous avons entrepris l'identification de nouveaux facteurs du DISC qui sont recrutés de manière différente dans les cellules normales et tumorales.

Nous avons utilisé un modèle cellulaire de transformation par étapes [Hahn et al 1999] qui permet une comparaison directe des cellules cancéreuses avec leurs cellules progénitrices normales isogéniques (Figure 2). Une telle analyse comparative n'est pas possible entre des lignées de cellules cancéreuses et des lignées cellulaires soi-disant 'normales'. Alors que les cellules transformées issues de ce modèle par étapes présentent des caractéristiques tumorigéniques [Hahn et al 1999] et de sensibilité à TRAIL, les cellules humaines normales parentales y sont résistantes [Nesterov et al 2004, Wang et al 2005].

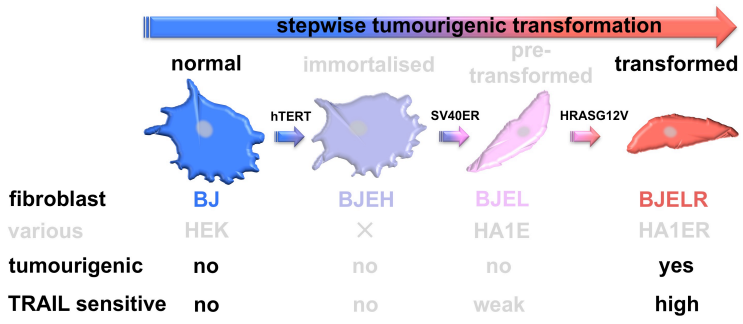

Figure 2: Schéma de Hahn et Weinberg expliquant le modèle de transformation progressive. Des cellules normales [ici fibroblastes de prépuce humain (BJ) ou cellules embryonnaires de rein humain (HEK)] sont progressivement transformées en introduisant la sous-unité catalytique télomérique HTERT, la séquence virale SV40ER (simian virus 40 early region) et HRASG12V, un mutant constitutivement actif de la protéine HRAS. Alors que hTERT permet de maintenir la longueur des télomères et de conférer l'immortalité réplicative aux cellules BJ, les cellules HEK requièrent des éléments additionnels encodés par SV40ER pour atteindre l'immortalité. Les cellules transformées ainsi obtenues (ici: BJELR ou HA1ER) présentent des propriétés de cellules cancéreuses: une prolifération illimitée, une croissance indépendante de leur adhésion, leur capacité de former des tumeurs in vivo, et leur sensibilité à l'apoptose après stimulation par TRAIL.

La section 'résultats' comprend les protocoles pour la production et la purification de TRAIL recombinant humain et pour l'immunoprécipitation du DISC natif. La mise au point de ces protocoles a été nécessaire dans le laboratoire, d'une part pour faciliter l'analyse des étapes d'initiation de la signalisation de TRAIL dans les cellules du système de transformation par étapes et d'autre part pour identifier de nouveaux

partenaires du DISC. Lors des analyses du DISC, nous avons montré l'implication de DR5 et DR4 dans la formation du DISC lors de la stimulation par TRAIL aussi bien dans les cellules normales que tumorales. Cependant, une quantité réduite de CASP8 clivée a été détectée dans les cellules normales indiquant dans ce cas un signal pro-apoptotique de faible intensité. Par ailleurs, le recrutement de FADD est diminué alors que le clivage de cFLIP (L) est plus élevé dans les cellules normales, ce qui nous permet de suggérer que la résistance à TRAIL s'établit au niveau du DISC (Figure 3).

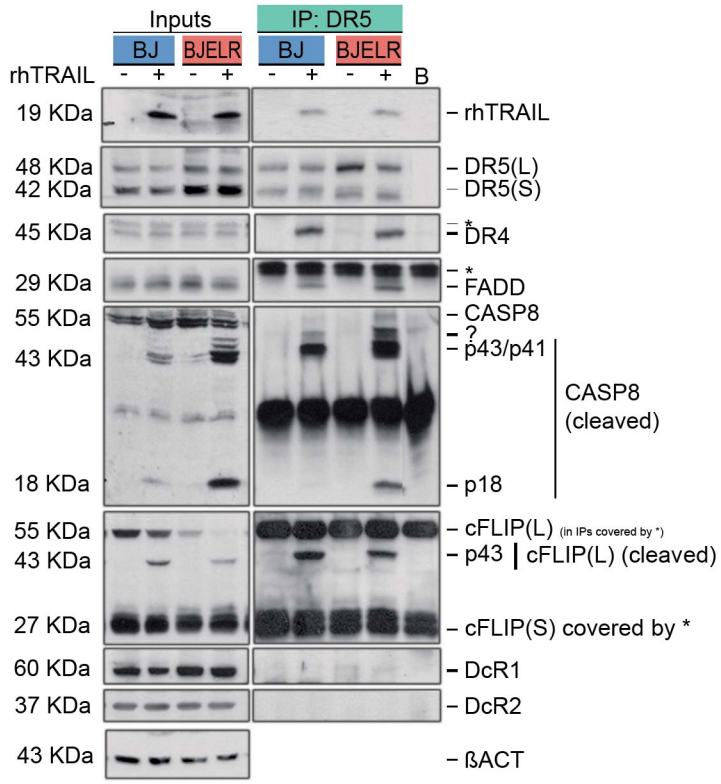

Figure 3: Formation de TRAIL-DISC de cellules normales BJ et de cellules transformées BJELR. Un nombre équivalent de cellules BJ et BJELR sont incubées avec 1µg/ml de TRAIL humain recombinant (rhTRAIL) pendant 1h, puis lysées. Le récepteur de mort DR5 est immuno-précipité (IP) au moyen d'un anticorps dirigé contre la protéine endogène. Les protéines co-purifiées dans les éluats de l'IP sont analysées. Les 4 pistes de gauche, chargées par des volumes identiques d'extraits cellulaires (BJ ou BJELR) totaux pré-clarifiés (inputs) utilisés dans l'expérience d'IP, servent de contrôle. Les 5 pistes de droite sont chargées par des volumes identiques d'éluats d'IP de DR5 (IP:DR5), provenant soit de la lignée cellulaire indiquée (BJ ou BJELR), soit du mélange DR5/résine (B) utilisé dans l'expérience. Le résultat montré est une analyse par immuno-buvardage (western-blot).

En effet, grâce à des analyses par western-blot et spectrométrie de masse des protéines co-purifiées par l'IP des DR dans les cellules normales et transformées, nous avons identifié que les protéines du cytosquelette ; nonmuscular myosin heavy chain IIa and IIb (NMHCIIa, NMHCIIb), myosin regulatory light chain 2 (MLC2) et la beta-actine (ßACT) interagissent avec les récepteurs de mort dans le DISC immuno-précipité (Figure 4, A&B). Il est important de noter que les cellules normales affichent des taux plus élevés de NMHCIIa et IIb lors de l'immunoprécipitation de DR5 et DR4 que les cellules transformées. Lorsqu'on stimule les cellules par TRAIL, l'interaction de NMHCIIa et IIb avec les DR est soutenue dans les cellules normales, alors qu'elle est largement affaiblie dans le DISC formé dans les cellules transformées (Figure 4, B).

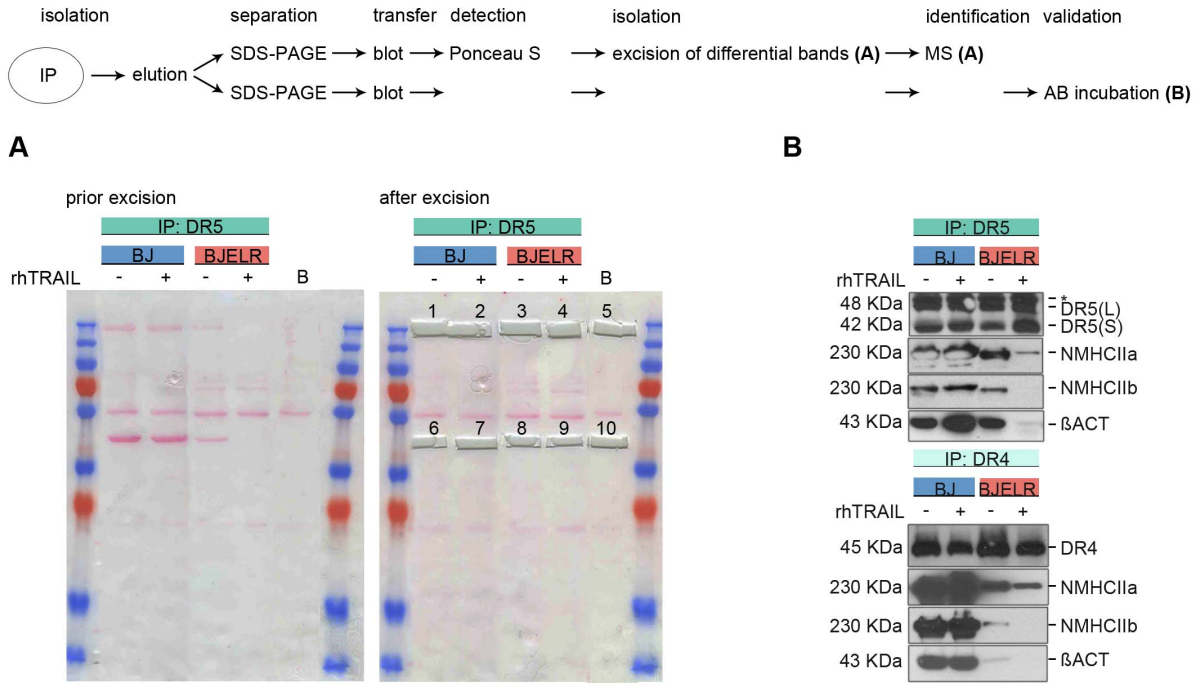

Figure 4: Identification de nouveaux partenaires de TRAIL-DISC dans des fibroblastes normaux (BJ) ou transformés (BJELR) stimulés ou non (+/-) par TRAIL. Le schéma (en haut) montre les étapes de l'expérience. Après immuno-précipitation (IP), les protéines sont éluées et les éluats séparés en 2 fractions. Un aliquot est séparé par électrophorèse en conditions dénaturantes (SDS-PAGE) et transféré sur membrane de nitrocellulose, qui est alors colorée au rouge Ponceau. Les bandes observées différant d'une condition à l'autre ont été excisées de la membrane, et leur contenu protéique digéré et analysé par spectrométrie de masse (MS). Ultérieurement, l'autre aliquot est ultérieurement séparé par SDS-PAGE, transféré sur membrane de nitrocellulose, et analysé par western-blot en utilisant des anticorps spécifiques (AB) des partenaires de la protéine immuno-précipitée nouvellement identifiés par MS, afin de confirmer leur identité. (A) Ainsi, DR5 est immuno-purifié à partir de lysats de cellules BJ ou BJELR, stimulées (+) ou non-stimulées (-) au préalable pendant 1h avec 1µg/ml de TRAIL humain recombinant (rhTRAIL). Les bandes différentielles visualisées par le rouge Ponceau sont coupées et analysées par MS afin d'identifier par leur signature peptidique les partenaires protéiques potentiels de DR5 présents dans ces bandes. (B) L'analyse par Western-Blot des DR5-IP (panneau du haut) permet de valider les partenaires identifiés en (A) par MS. Le récepteur de mort DR4 est analysé selon le même procédé expérimental, le panneau du bas montre l'analyse finale par western blot. Chaque western-blot présenté est représentatif de deux expériences menées indépendamment.

L'abrogation de l'interaction NMHCII / DR en utilisant la blebbistatine, un inhibiteur de la myosine non musculaire (NMII) ou ML7, un inhibiteur de la kinase de la chaîne légère de myosine (MLCK) augmente l'apoptose induite par TRAIL dans les cellules normales (Figure 5).

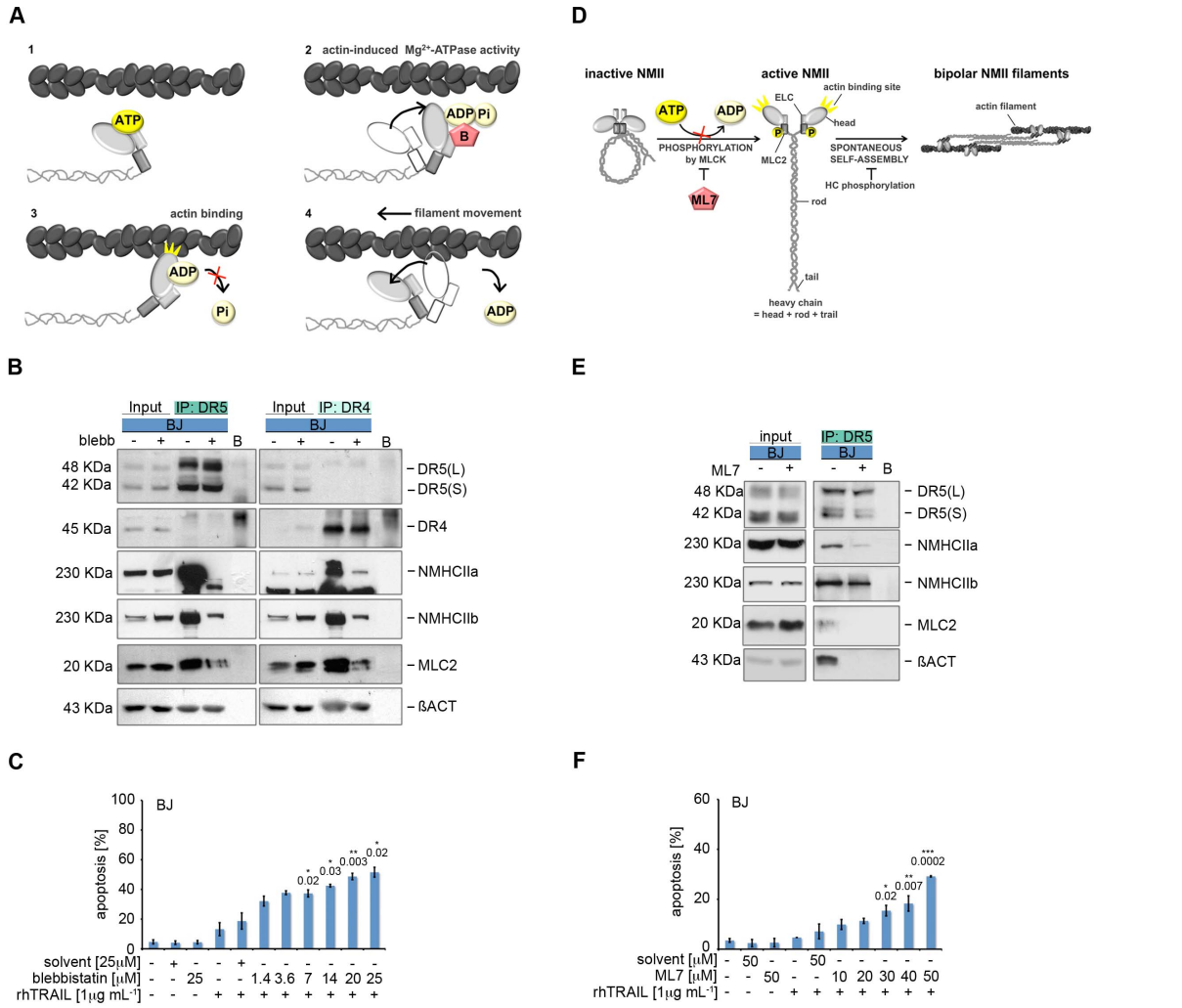

Figure 5: Effets de l'inhibition de l'activité Mg2+-ATPase de NMHCII sur l'interaction NMHCII/DR dans les cellules normales. (A) Schéma représentant le cycle dit "crossbridge" régulé par l'activité Mg2+-ATPase associée au domaine "Head" de la chaîne lourde II non-musculaire de myosine (NMHCII), ainsi que le mécanisme d'action de l'inhibiteur blebbistatine. 1. la liaison de l'ATP à NMHCII-Head induit une conformation ne pouvant pas lier l'actine. 2. L'hydrolyse de l'ATP entraîne l'adoption par le domaine Head d'une conformation dite "chargée", dans laquelle ADP et Pi restent liés. Lorsque le Pi quitte NMHCII, le domaine Head se lie à l'actine, ce qui conduit à une libération subite d'énergie mécanique. 4. L'ADP est libéré et le cycle peut reprendre. A ce stade NMHCII est fortement lié à l'actine. La blebbistatine se fixe préférentiellement à NMHCII-Head dont le site actif Mg2+-ATPase est occupé par l'ADP et le Pi. La libération d'ADP est alors fortement ralentie et la liaison à l'actine est empêchée. (B) Interaction NMHCII/DR lors d'un traitement à la blebbistatine. Des cellules BJ normales sont incubées 30 minutes avec le solvant DMSO (-) ou la blebbistatine à 25µM dans du DMSO (+), puis collectées pour immuno-précipiter DR4 ou DR5. Les éluats d'IP sont analysés quant à l'interaction de NMHCIIa, NMHCIIb, de la chaîne légère de myosine regulatrice (MLC2) et de la beta-actine (ßACT) *. (C) Apoptose induite par TRAIL pendant traitement à la blebbistatine. Des cellules BJ sont pré-traitées pendant 30 minutes avec les concentrations indiquées de solvant ou de blebbistatine, puis co-traitées avec rhTRAIL (1µg/ml). ** (D) Schéma expliquant l'accroissement de l'activité Mg2+-ATPase par la phosphorylation de MLC2 et le mécanisme d'action de l'inhibiteur ML7. En absence de phosphorylation, NMHCII a une conformation circulaire, inactive et non-compétente pour assemblage (gauche). Après phosphorylation par MLC2 par la kinase de chaînes légères de myosine (MLCK), NMHCIIs adopte une conformation plus ouverte et active (centre) et s'assemble spontanément sous forme de filaments de myosine (droite). ML7 se lie au site de liaison à l'ATP de MLCK et inhibe son activité catalytique. La figure est inspirée de [Vicente-Manzanares et al 2009, Book: Alberts et al Molecular Biology of the Cell (Garland Science)]. (E) Interaction NMHCII/DR5b pendant traitement au ML7. Des cellules BJ normales sont incubées pendant 30 minutes avec le solvant éthanol:eau (1:1) (-) ou avec l'inhibiteur ML7 (MLC2-phosphorylating kinase (MLCK) inhibitor) à 50µM dans un solvant éthanol:eau (1:1) (+), puis collectées pour IP DR5. les éluats d'IP sont anaylysés comme décrit en (B). *** (F) Apoptose induite par TRAIL pendant traitement au ML7. Des cellules BJ sont pré-traitées pendant 30 minutes avec les concentrations indiquées de solvant ou de ML7, puis co-traitées avec rhTRAIL (1µg/ml). L'apoptose est estimée comme expliqué en (C). **** Les western-blots montrés sont représentatifs de respectivement 3 (*) et 2 (***) expériences indépendantes. Les valeurs moyennes sont calculées respectivement de 3 à 4 (**) et 2 à 5 (****) expériences indépendantes. Les significances statistiques sont calculées par test "unpaired, 2-tailed Student".

Curieusement, le knockdown par siRNA de NMHCIIa mais pas de NMHCIIb abolit la résistance des cellules normales à TRAIL. Cette abrogation est caractérisée par une réduction du recrutement de DR4 et du clivage de cFLIP (L) et d'une augmentation du clivage de la CASP8 au niveau du DR5-DISC (Figure 6).

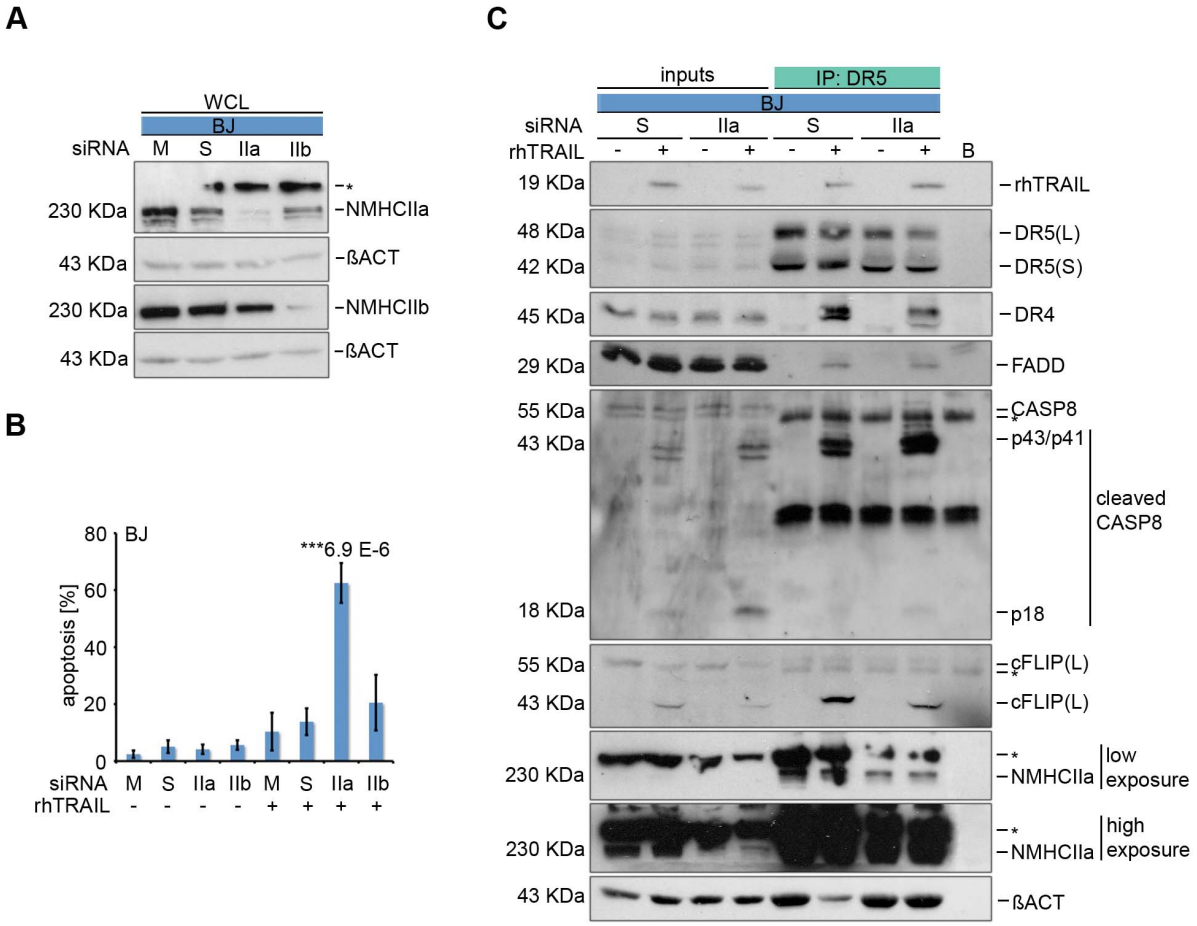

Figure 6: Effets du "Knock-down" par siRNA de NMHCIIa et NMHCIIb sur l'apoptose liée à TRAIL et la formation de DISC dans des cellules normales BJ. Des cellules BJ sont transfectées en présence de lipofectamine par 15nM de siRNA dirigé contre NMHCIIa ou NMHCIIb (IIa, IIb), 15nM de siRNA contrôles "scramble" (S = non spécifiques), ou à vide (M = "mock") et cultivées pendant 4 jours. Le milieu de culture est changé 1 jour, puis 3 jours après transfection. (A) Les lysats totaux cellulaires (WCL) de cellules BJ ont été analysés quant au niveau d'expression de NMHCIIa et NMHCIIb après 4 jours de knockdown (KD) par western blot. * (B) Apoptose liée à TRAIL après Knock-Down de NMHCIIa et NMHCIIb par siRNA. Quatre jours après le début du KD, les cellules BJ sont non-traitées (-) ou traitées (+) avec rhTRAIL à 1µg/ml. L'apoptose est estimée 16h après addition de TRAIL par positivité à 7A6. Les valeurs indiquées représentent la moyenne de 4 expériences indépendantes. (C) Formation de DISC induite par TRAIL après siRNA-KD de NMHCIIa. Quatre jours après début du KD, des cellules BJ sont non-traitées (-) ou traitées (+) par rhTRAIL à 1µg/ml pendant 1h. DR5 est alors immuno-précipité et les protéines co-purifiées sont analysées par western blot. Des lysats cellulaires pré-clarifiés (inputs) servent de contrôles de chargement et sont indicateurs des altérations d'expression protéique liées au KD. Les western-blots montrés sont représentatifs de 3 expériences indépendantes (*). Les significances statistiques sont calculées par test "unpaired, 2-tailed Student".

L'exploration de la cascade de signalisation régissant la régulation des interactions entre NMHC et DR dans les cellules normales et transformées a montré une activité plus élevée de NMHC dans les cellules normales mise en évidence par l'augmentation des niveaux de phosphorylation de MLC2. Dans les cellules transformées, l'activité de la kinase phosphorylant MLC2 (MLCK) est compromise, ce qui est confirmée par la diminution du taux de MLCK, l'augmentation du taux de la kinase inhibitrice de MLCK (PAK1) et le fait que les cellules normales soit moins sensibles que les cellules transformées à ML7, l'inhibiteur de MLCK (Figure 7).

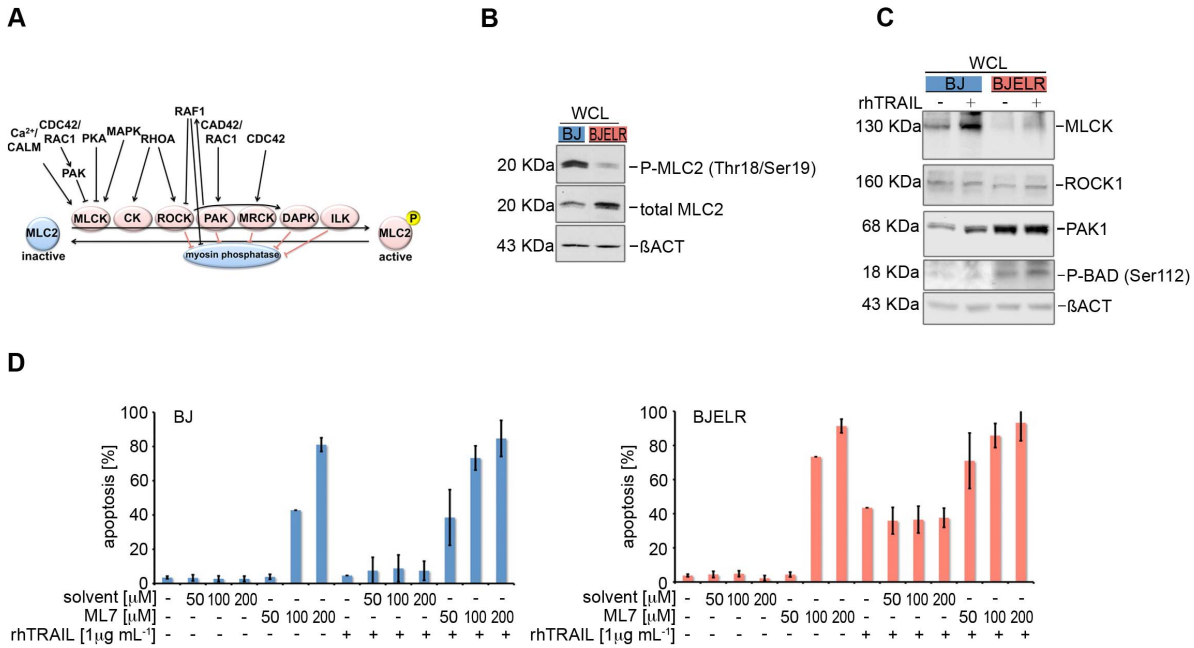

Figure 7: Phosphorylation de la chaîne légère régulatrice de myosine (MLC2) aux résidus Thr18/Ser19 et expression de kinase, dans des cellules normales BJ et dans des cellules BJELR transformées par hTERT, SV40ER et H-Ras. (A) Le patron de phosphorylation de MLC2 aux résidus Thr18/Ser19 est complexe. La chaîne légère régulatrice de myosine MLC2 est activée par phosphorylation de Thr18/Ser19. Le site majeur de phosphorylation est Ser19, qui permet à la myosine non-musculaire II (NMII) de former des filaments NMII, d'interagir avec l'actine, d'assembler des complexes d'actomyosin et d'initier la contraction. La double phosphorylation aux résidus Thr18/Ser19 stimule davantage l'assemblage en filaments. De nombreuses kinases connues pour phosphoryler et activer MLC2 Thr18/Ser19 (rouges) phosphorylent aussi et inhibent ainsi (lignes rouges) la phosphatase qui inactive MLC2 (bleue). La figure s'inspire de [Matsumara 2005]. (B) Différences de niveaux de phosphorylation de MLC2. Des extraits cellulaires totaux (WCL) de cellules BJ et BJELR sont analysés par western blot quant à la phosphorylation relative et aux niveaux d'expression de MLC2. (C) Des cellules BJ et BJELR sont soit non-traitées (-), soit traitées (+) par rhTRAIL à 1µg/ml pendant 15 minutes, et les niveaux d'expression des protéines MLCK, ROCK and PAK1 sont analysés. L'activité de PAK1 est estimée par western-blot au moyen d'un anticorps dirigé contre une forme phosphorylée de BAD. La figure montre un western blot représentatif de deux expériences indépendantes. (D) Forte induction d'apoptose pour des niveaux élevés de ML7, l'inhibiteur de MLCK. La réponse apoptotique de cellules normales BJ et tumorales BJELR est estimée dans des expériences menées en parallèle. Les cellules sont pré-incubées pendant 30 minutes avec les concentrations indiquées de ML7 ou de solvant (éthanol:eau au ratio 1:1), puis co-traitées avec TRAIL purifié à 1µg/ml. L'apoptose est quantifiée par la positivité à 7A6 par tri cellulaire (FACS) après 16h de traitement. Les valeurs données découlent de deux expériences indépendantes.

L'ensemble de ces données confirme un modèle dans lequel l'interaction que nous avons identifiée entre les récepteurs de mort et NMHCIIa maintient la résistance à TRAIL dans les cellules normales. En outre, elles suggèrent un rôle fonctionnel de NMHCIIa dans l'acquisition de la réponse à TRAIL dans le processus de transformation cellulaire. Enfin, comme NMHCIIa a un rôle central dans l'adhésion cellulaire, notre modèle fournit une corrélation entre le détachement cellulaire et la sensibilité à TRAIL décrit dans la littérature.

Les travaux futurs porteront sur l'identification du domaine minimal d'interaction entre NMHCIIa et les DR dans le but de comprendre la base structurelle de cette interaction. De plus, la signification biologique de cette interaction sera confirmée dans d'autres modèles cellulaires de transformation néoplasique. Les changements au niveau du cytosquelette seront étudiés dans les cellules immortalisées et pré-transformées de notre système de transformation par étapes afin de définir si les différences observées dans les cellules transformées sont dépendantes de Ras. La révélation des différences de composition du DISC entre les cellules normales et transformées nous a permis de déchiffrer les bases moléculaires de la sensibilité / résistance à TRAIL et nous procure une base solide pour l'exploitation de la signalisation de TRAIL pour des thérapies anti-cancer.

ACKNOWLEDGEMENT

The presented study was performed at the Department of Functional Genomics and Cancer at the Institut de Génétique et de Biologie Moléculaire et Cellulaire (IGBMC), Strasbourg University. Financial support was received from the EU-funded consortia EPITRON and APO-SYS and from the French public donation organisation Fondation Recherche Médicale (FRM). I would like to thank everybody who has facilitated and contributed to this thesis. Particulary, I would like to express my sincere gratitude to:

Prof. Peter Vandenabeele, Dr. Miguel Vicente-Manzanares and Dr. Michel Labouesse, my jury board, for having accepted to read and judge my thesis work.

Dr. Hinrich Gronemeyer, my supervisor and Doktorvater, for having entrusted me with this interesting project. Thank you for allowing independent academic development and for being ready to support and discuss whenever needed. Thank you for encouraging and enabling travels to trainings and meetings and for proofreading this manuscript.

Dr. Olivier Micheau for being my co-supervisor and jury member.

Dr. Valeria Pavet for enabling SPR experiments and assistance in imaging. Thank you very much for your valuable advice in fellowship application and scientific writing, as well as for proofreading this manuscript. I am very grateful for our constant discussions, your constructive criticism and your guidance in scientific and non-scientific issues. I have learnt a lot from you.

Dr. Maximiliano Portal for patiently and competently answering any technical or scientific question.

Dr. Shankara Narayanan Pattabhiraman, aka Shandoka, le tigre d'Illkirch, for generous and immediate helpfulness in minor and major emergency situations.

Dr. Megan Astle and Dr. Marco Antonio Mendoza Parra for brisk exchange during labmeetings.

Dr. Irene Yujnovsky for proofreading, shortening and translating fellowship applications, research projects and summaries. For spreading information and organising events.

Cathie Erb for guiding me during my first days at the IGBMC and giving assistance in initial TRAIL purifications. Thank you for designing cloning strategies and for proofreading the French summary. Let me know when you will have established your farm with mohair rabbits, I will assist you combing.

Michèle Lieb for teaching FACS, proofreading the French summary and the lectures about life. She is the only human in the world who has encountered dinosaurs. Happy 29th birthday forever.

Dr. Claudine Gaudon for precious input on IP-setup. Carole Peluso Iltis for kind advice on HPLC, native gel electrophoresis and gel filtration.

Dr. Adeline Page and Frank Ruffenach of the IGBMC Proteomics platform for assistance in mass spectrometry experiments.

Jean-Marie Garnier of the IGBMC Molecular Biology service for generating the construct for rhTRAIL expression and Pascal Eberling of the IGBMC Peptide Synthesis service for generating peptides.

Dr. Fabrice Klein for translating the abstract and figure legends. Marie-Therese Peney for ordering article for article for article...

Judith Vallet and Wouter van Gool for the good spirit in the lab.

Dr. Mannu Walia, Dr. Harshal Khanwalkar and Jelena Vjetrovic for sharing this experience with me. Mannu, your funny and unconventional entertainment program is severely missed. Harshal, that facial expression at the poster presentation will be unforgotten. Jelena, your 'PhD in microbiology with Prof. Gronemeyer in Salzburg' will soon come to its end. Best of luck to all of you.

Meinem Mann Thomas für die Weitsicht.

REFERENCES

Aggarwal, B.B., Gupta, S.C. & Kim, J.H. (2012) Historical perspectives on tumor necrosis factor and its superfamily: 25 years later, a golden journey. *Blood,* 119**,** 651-65.

Ahmadian, M.R., Wittinghofer, A. & Schmidt, G. (2002) The actin filament architecture: tightly regulated by the cells, manipulated by pathogens. International Titisee Conference on the actin cytoskeleton: from signalling to bacterial pathogenesis. *EMBO Rep,* 3**,** 214-8.

Ahn, E.Y., Lim, S.T., Cook, W.J., et al. (2004) Calmodulin binding to the Fas death domain. Regulation by Fas activation. *J Biol Chem,* 279**,** 5661-6.

Akazawa, Y., Mott, J.L., Bronk, S.F., et al. (2009) Death receptor 5 internalization is required for lysosomal permeabilization by TRAIL in malignant liver cell lines. *Gastroenterology,* 136**,** 2365-2376 e1-7.

Algeciras-Schimnich, A. & Peter, M.E. (2003) Actin dependent CD95 internalization is specific for Type I cells. *FEBS Lett,* 546**,** 185-8.

Algeciras-Schimnich, A., Shen, L., Barnhart, B.C., et al. (2002) Molecular ordering of the initial signaling events of CD95. *Mol Cell Biol,* 22**,** 207-20.

Allingham, J.S., Smith, R. & Rayment, I. (2005) The structural basis of blebbistatin inhibition and specificity for myosin II. *Nat Struct Mol Biol,* 12**,** 378-9.

Altschul, S.F., Gish, W., Miller, W., et al. (1990) Basic local alignment search tool. *J Mol Biol,* 215**,** 403-10.

Amanullah, A., Liebermann, D.A. & Hoffman, B. (2002) Deregulated c-Myc prematurely recruits both Type I and II CD95/Fas apoptotic pathways associated with terminal myeloid differentiation. *Oncogene,* 21**,** 1600-10.

Amparan, D., Avram, D., Thomas, C.G., et al. (2005) Direct interaction of myosin regulatory light chain with the NMDA receptor. *J Neurochem,* 92**,** 349-61.

Arii, J., Goto, H., Suenaga, T., et al. (2010) Non-muscle myosin IIA is a functional entry receptor for herpes simplex virus-1. *Nature,* 467**,** 859-62.

Arroyo, J.D. & Hahn, W.C. (2005) Involvement of PP2A in viral and cellular transformation. *Oncogene,* 24**,** 7746-55.

Ashkenazi, A. (2008) Directing cancer cells to self-destruct with pro-apoptotic receptor agonists. *Nat Rev Drug Discov,* 7**,** 1001-12.

Ashkenazi, A. & Herbst, R.S. (2008) To kill a tumor cell: the potential of proapoptotic receptor agonists. *J Clin Invest,* 118**,** 1979-90.

Ashkenazi, A., Holland, P. & Eckhardt, S.G. (2008) Ligand-based targeting of apoptosis in cancer: the potential of recombinant human apoptosis ligand 2/Tumor necrosis factor-related apoptosis-inducing ligand (rhApo2L/TRAIL). *J Clin Oncol,* 26**,** 3621-30.

Ashkenazi, A., Holland, P. & Eckhardt, S.G. (2008) Ligand-based targeting of apoptosis in cancer: the potential of recombinant human apoptosis ligand 2/Tumor necrosis factor-related apoptosis-inducing ligand (rhApo2L/TRAIL). *J Clin Oncol,* 26**,** 3621-30.

Ashkenazi, A., Pai, R.C., Fong, S., et al. (1999) Safety and antitumor activity of recombinant soluble Apo2 ligand. *J Clin Invest,* 104**,** 155-62.

Askew, D.S., Ashmun, R.A., Simmons, B.C., et al. (1991) Constitutive c-myc expression in an IL-3-dependent myeloid cell line suppresses cell cycle arrest and accelerates apoptosis. *Oncogene,* 6**,** 1915-22.

Audo, R., Calmon-Hamaty, F., Baeten, D., et al. (2011) Mechanisms and clinical relevance of TRAIL-triggered responses in the synovial fibroblasts of patients with rheumatoid arthritis. *Arthritis Rheum,* 63**,** 904-13.

Austin, C.D., Lawrence, D.A., Peden, A.A., et al. (2006) Death-receptor activation halts clathrin-dependent endocytosis. *Proc Natl Acad Sci U S A,* 103**,** 10283-8.

Azab, N.A., Rady, H.M. & Marzouk, S.A. (2012) Elevated serum TRAIL levels in scleroderma patients and its possible association with pulmonary involvement. *Clin Rheumatol*.

Bachireddy, P., Bendapudi, P.K. & Felsher, D.W. (2005) Getting at MYC through RAS. *Clin Cancer Res,* 11**,** 4278-81.

Bain, J., McLauchlan, H., Elliott, M., et al. (2003) The specificities of protein kinase inhibitors: an update. *Biochem J,* 371**,** 199-204.

Bajaj, G., Zhang, Y., Schimerlik, M.I., et al. (2009) N-methyl-D-aspartate receptor subunits are non-myosin targets of myosin regulatory light chain. *J Biol Chem,* 284**,** 1252-66.

Bao, J., Jana, S.S. & Adelstein, R.S. (2005) Vertebrate nonmuscle myosin II isoforms rescue small interfering RNA-induced defects in COS-7 cell cytokinesis. *J Biol Chem,* 280**,** 19594-9.

Bao, J., Ma, X., Liu, C., et al. (2007) Replacement of nonmuscle myosin II-B with II-A rescues brain but not cardiac defects in mice. *J Biol Chem,* 282**,** 22102-11.

Bar-Sagi, D. & Feramisco, J.R. (1986) Induction of membrane ruffling and fluid-phase pinocytosis in quiescent fibroblasts by ras proteins. *Science,* 233**,** 1061-8.

Basu, S. (2011) PP2A in the regulation of cell motility and invasion. *Curr Protein Pept Sci,* 12**,** 3-11.

Batzer, A.G., Rotin, D., Urena, J.M., et al. (1994) Hierarchy of binding sites for Grb2 and Shc on the epidermal growth factor receptor. *Mol Cell Biol,* 14**,** 5192-201.

Bellail, A.C. & Hao, C. (2012) The roadmap of TRAIL apoptotic pathway-targeted cancer therapies: what is next? *Expert Rev Anticancer Ther,* 12**,** 547-9.

Benaud, C.M. & Dickson, R.B. (2001) Regulation of the expression of c-Myc by beta1 integrins in epithelial cells. *Oncogene,* 20**,** 759-68.

Benayoun, B., Baghdiguian, S., Lajmanovich, A., et al. (2008) NF-kappaB-dependent expression of the antiapoptotic factor c-FLIP is regulated by calpain 3, the protein involved in limb-girdle muscular dystrophy type 2A. *FASEB J,* 22**,** 1521-9.

Benest, A.V. & Augustin, H.G. (2009) Tension in the vasculature. *Nat Med,* 15**,** 608-10.

Berent-Maoz, B., Salemi, S., Mankuta, D., et al. (2010) Human mast cells express intracellular TRAIL. *Cell Immunol,* 262**,** 80-3.

Bernardi, S., Milani, D., Fabris, B., et al. (2012) TRAIL as Biomarker and Potential Therapeutic Tool for Cardiovascular Diseases. *Curr Drug Targets,* 13**,** 1215-21.

Bernstein, B.W. & Bamburg, J.R. (1982) Tropomyosin binding to F-actin protects the F-actin from disassembly by brain actin-depolymerizing factor (ADF). *Cell Motil,* 2**,** 1-8.

Beroukhim, R., Mermel, C.H., Porter, D., et al. (2010) The landscape of somatic copy-number alteration across human cancers. *Nature,* 463**,** 899-905.

Berry, D.M., Nash, P., Liu, S.K., et al. (2002) A high-affinity Arg-X-X-Lys SH3 binding motif confers specificity for the interaction between Gads and SLP-76 in T cell signaling. *Curr Biol,* 12**,** 1336-41.

Bertram, H., Nerlich, A., Omlor, G., et al. (2009) Expression of TRAIL and the death receptors DR4 and DR5 correlates with progression of degeneration in human intervertebral disks. *Mod Pathol,* 22**,** 895-905.

Bharadwaj, S., Thanawala, R., Bon, G., et al. (2005) Resensitization of breast cancer cells to anoikis by tropomyosin-1: role of Rho kinase-dependent cytoskeleton and adhesion. *Oncogene,* 24**,** 8291-303.

Blagoev, B., Kratchmarova, I., Ong, S.E., et al. (2003) A proteomics strategy to elucidate functional protein-protein interactions applied to EGF signaling. *Nat Biotechnol,* 21**,** 315-8.

Boatright, K.M., Renatus, M., Scott, F.L., et al. (2003) A unified model for apical caspase activation. *Mol Cell,* 11**,** 529-41.

Bode, A.M. & Dong, Z. (2009) Cancer prevention research - then and now. *Nat Rev Cancer,* 9**,** 508-16.

Bodmer, J.L., Meier, P., Tschopp, J., et al. (2000) Cysteine 230 is essential for the structure and activity of the cytotoxic ligand TRAIL. *J Biol Chem,* 275**,** 20632-7.

Bray, D. & White, J.G. (1988) Cortical flow in animal cells. *Science,* 239**,** 883-8.

Bresnick, A.R. (1999) Molecular mechanisms of nonmuscle myosin-II regulation. *Curr Opin Cell Biol,* 11**,** 26-33.

Bretscher, A., Edwards, K. & Fehon, R.G. (2002) ERM proteins and merlin: integrators at the cell cortex. *Nat Rev Mol Cell Biol,* 3**,** 586-99.

Brosh, R. & Rotter, V. (2009) When mutants gain new powers: news from the mutant p53 field. *Nat Rev Cancer,* 9**,** 701-13.

Brosh, R., Shalgi, R., Liran, A., et al. (2008) p53-Repressed miRNAs are involved with E2F in a feed-forward loop promoting proliferation. *Mol Syst Biol,* 4**,** 229.

Broustas, C.G., Grammatikakis, N., Eto, M., et al. (2002) Phosphorylation of the myosin-binding subunit of myosin phosphatase by Raf-1 and inhibition of phosphatase activity. *J Biol Chem,* 277**,** 3053-9.

Bryce, N.S., Schevzov, G., Ferguson, V., et al. (2003) Specification of actin filament function and molecular composition by tropomyosin isoforms. *Mol Biol Cell,* 14**,** 1002-16.

Burton, K. & Taylor, D.L. (1997) Traction forces of cytokinesis measured with optically modified elastic substrata. *Nature,* 385**,** 450-4.

Bussing, A., Vervecken, W., Wagner, M., et al. (1999) Expression of mitochondrial Apo2.7 molecules and caspase-3 activation in human lymphocytes treated with the ribosome-inhibiting mistletoe lectins and the cell membrane permeabilizing viscotoxins. *Cytometry,* 37**,** 133-9.

Bustelo, X.R. (2010) A transcriptional cross-talk between RhoA and c-Myc inhibits the RhoA/Rock-dependent cytoskeleton. *Small GTPases,* 1**,** 69-74.

Button, E., Shapland, C. & Lawson, D. (1995) Actin, its associated proteins and metastasis. *Cell Motil Cytoskeleton,* 30**,** 247-51.

Camidge, D.R., Herbst, R.S., Gordon, M.S., et al. (2010) A phase I safety and pharmacokinetic study of the death receptor 5 agonistic antibody PRO95780 in patients with advanced malignancies. *Clin Cancer Res,* 16**,** 1256-63.

Campioni, D., Secchiero, P., Corallini, F., et al. (2005) Evidence for a role of TNF-related apoptosis-inducing ligand (TRAIL) in the anemia of myelodysplastic syndromes. *Am J Pathol,* 166**,** 557-63.

Cantarella, G., Uberti, D., Carsana, T., et al. (2003) Neutralization of TRAIL death pathway protects human neuronal cell line from beta-amyloid toxicity. *Cell Death Differ,* 10**,** 134-41.

Cao, X., Pobezinskaya, Y.L., Morgan, M.J., et al. (2010) The role of TRADD in TRAIL-induced apoptosis and signaling. *FASEB J,* 25**,** 1353-8.

Carrington, P.E., Sandu, C., Wei, Y., et al. (2006) The structure of FADD and its mode of interaction with procaspase-8. *Mol Cell,* 22**,** 599-610.

Carroll, J.S., Swarbrick, A., Musgrove, E.A., et al. (2002) Mechanisms of growth arrest by c-myc antisense oligonucleotides in MCF-7 breast cancer cells: implications for the antiproliferative effects of antiestrogens. *Cancer Res,* 62**,** 3126-31.

Cavallo, F., De Giovanni, C., Nanni, P., et al. (2011) 2011: the immune hallmarks of cancer. *Cancer Immunol Immunother,* 60**,** 319-26.

Chaigne-Delalande, B., Mahfouf, W., Daburon, S., et al. (2009) CD95 engagement mediates actin-independent and -dependent apoptotic signals. *Cell Death Differ,* 16**,** 1654-64.

Chamorro, A., Busse, O., Obach, V., et al. (2005) The rapid anticoagulation prevents ischemic damage study in acute stroke--final results from the writing committee. *Cerebrovasc Dis,* 19**,** 402-4.

Chan, F.K., Chun, H.J., Zheng, L., et al. (2000) A domain in TNF receptors that mediates ligand-independent receptor assembly and signaling. *Science,* 288**,** 2351-4.

Chang, D.W., Xing, Z., Capacio, V.L., et al. (2003) Interdimer processing mechanism of procaspase-8 activation. *EMBO J,* 22**,** 4132-42.

Chang, D.W., Xing, Z., Pan, Y., et al. (2002) c-FLIP(L) is a dual function regulator for caspase-8 activation and CD95-mediated apoptosis. *EMBO J,* 21**,** 3704-14.

Charras, G.T., Hu, C.K., Coughlin, M., et al. (2006) Reassembly of contractile actin cortex in cell blebs. *J Cell Biol,* 175**,** 477-90.

Charras, G.T., Yarrow, J.C., Horton, M.A., et al. (2005) Non-equilibration of hydrostatic pressure in blebbing cells. *Nature,* 435**,** 365-9.

Chen, S., Liu, X., Yue, P., et al. (2007) CCAAT/enhancer binding protein homologous protein-dependent death receptor 5 induction and ubiquitin/proteasome-mediated cellular FLICE-inhibitory protein down-regulation contribute to enhancement of tumor necrosis factor-related apoptosis-inducing ligand-induced apoptosis by dimethyl-celecoxib in human non small-cell lung cancer cells. *Mol Pharmacol,* 72**,** 1269-79.

Chen, W., Possemato, R., Campbell, K.T., et al. (2004) Identification of specific PP2A complexes involved in human cell transformation. *Cancer Cell,* 5**,** 127-36.

Chen, Y., Pawar, P., Pan, G., et al. (2008) Calmodulin binding to the Fas-mediated death-inducing signaling complex in cholangiocarcinoma cells. *J Cell Biochem,* 103**,** 788-99.

Chen, Z., Naito, M., Mashima, T., et al. (1996) Activation of actin-cleavable interleukin 1beta-converting enzyme (ICE) family protease CPP-32 during chemotherapeutic agent-induced apoptosis in ovarian carcinoma cells. *Cancer Res,* 56**,** 5224-9.

Cheng, J., DeCaprio, J.A., Fluck, M.M., et al. (2009) Cellular transformation by Simian Virus 40 and Murine Polyoma Virus T antigens. *Semin Cancer Biol,* 19**,** 218-28.

Cheng, J., Hylander, B.L., Baer, M.R., et al. (2006) Multiple mechanisms underlie resistance of leukemia cells to Apo2 Ligand/TRAIL. *Mol Cancer Ther,* 5**,** 1844-53.

Cheresh, D.A., Leng, J. & Klemke, R.L. (1999) Regulation of cell contraction and membrane ruffling by distinct signals in migratory cells. *J Cell Biol,* 146**,** 1107-16.

Chhabra, D., Nosworthy, N.J. & dos Remedios, C.G. (2005) The N-terminal fragment of gelsolin inhibits the interaction of DNase I with isolated actin, but not with the cofilin-actin complex. *Proteomics,* 5**,** 3131-6.

Cho, Y.S., Challa, S., Moquin, D., et al. (2009) Phosphorylation-driven assembly of the RIP1-RIP3 complex regulates programmed necrosis and virus-induced inflammation. *Cell,* 137**,** 1112-23.

Choi, C.K., Vicente-Manzanares, M., Zareno, J., et al. (2008) Actin and alpha-actinin orchestrate the assembly and maturation of nascent adhesions in a myosin II motor-independent manner. *Nat Cell Biol,* 10**,** 1039-50.

Chook, Y.M., Gish, G.D., Kay, C.M., et al. (1996) The Grb2-mSos1 complex binds phosphopeptides with higher affinity than Grb2. *J Biol Chem,* 271**,** 30472-8.

Chrzanowska-Wodnicka, M. & Burridge, K. (1996) Rho-stimulated contractility drives the formation of stress fibers and focal adhesions. *J Cell Biol,* 133**,** 1403-15.

Chua, B.T., Volbracht, C., Tan, K.O., et al. (2003) Mitochondrial translocation of cofilin is an early step in apoptosis induction. *Nat Cell Biol,* 5**,** 1083-9.

Clancy, L., Mruk, K., Archer, K., et al. (2005) Preligand assembly domain-mediated ligand-independent association between TRAIL receptor 4 (TR4) and TR2 regulates TRAIL-induced apoptosis. *Proc Natl Acad Sci U S A,* 102**,** 18099-104.

Clark, K., Langeslag, M., Figdor, C.G., et al. (2007) Myosin II and mechanotransduction: a balancing act. *Trends Cell Biol,* 17**,** 178-86.

Clarke, N., Jimenez-Lara, A.M., Voltz, E., et al. (2004) Tumor suppressor IRF-1 mediates retinoid and interferon anticancer signaling to death ligand TRAIL. *EMBO J,* 23**,** 3051-60.

Cohen, G.B., Ren, R. & Baltimore, D. (1995) Modular binding domains in signal transduction proteins. *Cell,* 80**,** 237-48.

Coleman, M.L., Sahai, E.A., Yeo, M., et al. (2001) Membrane blebbing during apoptosis results from caspase-mediated activation of ROCK I. *Nat Cell Biol,* 3**,** 339-45.

Coller, H.A., Grandori, C., Tamayo, P., et al. (2000) Expression analysis with oligonucleotide microarrays reveals that MYC regulates genes involved in growth, cell cycle, signaling, and adhesion. *Proc Natl Acad Sci U S A,* 97**,** 3260-5.

Collison, A., Foster, P.S. & Mattes, J. (2009) Emerging role of tumour necrosis factor-related apoptosis-inducing ligand (TRAIL) as a key regulator of inflammatory responses. *Clin Exp Pharmacol Physiol,* 36**,** 1049-53.

Conti, M.A. & Adelstein, R.S. (2008) Nonmuscle myosin II moves in new directions. *J Cell Sci,* 121**,** 11-8.

Conti, M.A., Even-Ram, S., Liu, C., et al. (2004) Defects in cell adhesion and the visceral endoderm following ablation of nonmuscle myosin heavy chain II-A in mice. *J Biol Chem,* 279**,** 41263-6.

Cotter, T.G. (2009) Apoptosis and cancer: the genesis of a research field. *Nat Rev Cancer,* 9**,** 501-7.

Cretney, E., McQualter, J.L., Kayagaki, N., et al. (2005) TNF-related apoptosis-inducing ligand (TRAIL)/Apo2L suppresses experimental autoimmune encephalomyelitis in mice. *Immunol Cell Biol,* 83**,** 511-9.

Cretney, E., Shanker, A., Yagita, H., et al. (2006) TNF-related apoptosis-inducing ligand as a therapeutic agent in autoimmunity and cancer. *Immunol Cell Biol,* 84**,** 87-98.

Cretney, E., Takeda, K., Yagita, H., et al. (2002) Increased susceptibility to tumor initiation and metastasis in TNF-related apoptosis-inducing ligand-deficient mice. *J Immunol,* 168**,** 1356-61.

Cummins, N. & Badley, A. (2009) The TRAIL to viral pathogenesis: the good, the bad and the ugly. *Curr Mol Med,* 9**,** 495-505.

Cunningham, C.C. (1995) Actin polymerization and intracellular solvent flow in cell surface blebbing. *J Cell Biol,* 129**,** 1589-99.

Cursi, S., Rufini, A., Stagni, V., et al. (2006) Src kinase phosphorylates Caspase-8 on Tyr380: a novel mechanism of apoptosis suppression. *EMBO J,* 25**,** 1895-905.

D'Aquino, J.A. & Ringe, D. (2003) Determinants of the SRC homology domain 3-like fold. *J Bacteriol,* 185**,** 4081-6.

de The, H. & Chen, Z. (2010) Acute promyelocytic leukaemia: novel insights into the mechanisms of cure. *Nat Rev Cancer,* 10**,** 775-83.

De Toni, E.N., Kuntzen, C., Gerbes, A.L. (2007) P60-c-src suppresses apoptosis through inhibition of caspase 8 activation in hepatoma cells, but not in primary hepatocytes. *Journal of Hepatology,* 46**,** 682-691.

Degli Esposti, M., Ferry, G., Masdehors, P., et al. (2003) Post-translational modification of Bid has differential effects on its susceptibility to cleavage by caspase 8 or caspase 3. *J Biol Chem,* 278**,** 15749-57.

Degli-Esposti, M.A., Dougall, W.C., Smolak, P.J., et al. (1997b) The novel receptor TRAIL-R4 induces NF-kappaB and protects against TRAIL-mediated apoptosis, yet retains an incomplete death domain. *Immunity,* 7**,** 813-20.

Degli-Esposti, M.A., Smolak, P.J., Walczak, H., et al. (1997a) Cloning and characterization of TRAIL-R3, a novel member of the emerging TRAIL receptor family. *J Exp Med,* 186**,** 1165-70.

del Pozo, M.A., Price, L.S., Alderson, N.B., et al. (2000) Adhesion to the extracellular matrix regulates the coupling of the small GTPase Rac to its effector PAK. *EMBO J,* 19**,** 2008-14.

Deng, J.T., Van Lierop, J.E., Sutherland, C., et al. (2001) Ca2+-independent smooth muscle contraction. a novel function for integrin-linked kinase. *J Biol Chem,* 276**,** 16365-73.

Desagher, S., Osen-Sand, A., Montessuit, S., et al. (2001) Phosphorylation of bid by casein kinases I and II regulates its cleavage by caspase 8. *Mol Cell,* 8**,** 601-11.

Desouza, M., Gunning, P.W. & Stehn, J.R. (2012) The actin cytoskeleton as a sensor and mediator of apoptosis. *Bioarchitecture,* 2**,** 75-87.

Dickens, L.S., Boyd, R.S., Jukes-Jones, R., et al. (2012) A Death Effector Domain Chain DISC Model Reveals a Crucial Role for Caspase-8 Chain Assembly in Mediating Apoptotic Cell Death. *Mol Cell,* 47**,** 291-305.

Diehl, G.E., Yue, H.H., Hsieh, K., et al. (2004) TRAIL-R as a negative regulator of innate immune cell responses. *Immunity,* 21**,** 877-89.

Dix, M.M., Simon, G.M. & Cravatt, B.F. (2008) Global mapping of the topography and magnitude of proteolytic events in apoptosis. *Cell,* 134**,** 679-91.

Dohrman, A., Russell, J.Q., Cuenin, S., et al. (2005) Cellular FLIP long form augments caspase activity and death of T cells through heterodimerization with and activation of caspase-8. *J Immunol,* 175**,** 311-8.

Donepudi, M., Mac Sweeney, A., Briand, C., et al. (2003) Insights into the regulatory mechanism for caspase-8 activation. *Mol Cell,* 11**,** 543-9.

Drosopoulos, K.G., Roberts, M.L., Cermak, L., et al. (2005) Transformation by oncogenic RAS sensitizes human colon cells to TRAIL-induced apoptosis by up-regulating death receptor 4 and death receptor 5 through a MEK-dependent pathway. *J Biol Chem,* 280**,** 22856-67.

Du, C., Fang, M., Li, Y., et al. (2000) Smac, a mitochondrial protein that promotes cytochrome c-dependent caspase activation by eliminating IAP inhibition. *Cell,* 102**,** 33-42.

Dummler, B., Ohshiro, K., Kumar, R., et al. (2009) Pak protein kinases and their role in cancer. *Cancer Metastasis Rev,* 28**,** 51-63.

Eblen, S.T., Slack, J.K., Weber, M.J., et al. (2002) Rac-PAK signaling stimulates extracellular signal-regulated kinase (ERK) activation by regulating formation of MEK1-ERK complexes. *Mol Cell Biol,* 22**,** 6023-33.

Eddinger, T.J. & Meer, D.P. (2007) Myosin II isoforms in smooth muscle: heterogeneity and function. *Am J Physiol Cell Physiol,* 293**,** C493-508.

Ehrenreiter, K., Piazzolla, D., Velamoor, V., et al. (2005) Raf-1 regulates Rho signaling and cell migration. *J Cell Biol,* 168**,** 955-64.

Ehrenschwender, M., Siegmund, D., Wicovsky, A., et al. (2010) Mutant PIK3CA licenses TRAIL and CD95L to induce non-apoptotic caspase-8-mediated ROCK activation. *Cell Death Differ,* 17**,** 1435-47.

Ehrhardt, H., Fulda, S., Schmid, I., et al. (2003) TRAIL induced survival and proliferation in cancer cells resistant towards TRAIL-induced apoptosis mediated by NF-kappaB. *Oncogene,* 22**,** 3842-52.

Ehrlich, S., Infante-Duarte, C., Seeger, B., et al. (2003) Regulation of soluble and surface-bound TRAIL in human T cells, B cells, and monocytes. *Cytokine,* 24**,** 244-53.

Ekmekcioglu, S., Mumm, J.B., Udtha, M., et al. (2008) Killing of human melanoma cells induced by activation of class I interferon-regulated signaling pathways via MDA-7/IL-24. *Cytokine,* 43**,** 34-44.

Ellis, L.M. & Reardon, D.A. (2009) Cancer: The nuances of therapy. *Nature,* 458**,** 290-2.

Emery, J.G., McDonnell, P., Burke, M.B., et al. (1998) Osteoprotegerin is a receptor for the cytotoxic ligand TRAIL. *J Biol Chem,* 273**,** 14363-7.

Eswaran, J., Soundararajan, M. & Knapp, S. (2009) Targeting group II PAKs in cancer and metastasis. *Cancer Metastasis Rev,* 28**,** 209-17.

Etienne-Manneville, S. & Hall, A. (2002) Rho GTPases in cell biology. *Nature,* 420**,** 629-35.

Evan, G.I., Wyllie, A.H., Gilbert, C.S., et al. (1992) Induction of apoptosis in fibroblasts by c-myc protein. *Cell,* 69**,** 119-28.

Even-Faitelson, L. & Ravid, S. (2006) PAK1 and aPKCzeta regulate myosin II-B phosphorylation: a novel signaling pathway regulating filament assembly. *Mol Biol Cell,* 17**,** 2869-81.

Even-Ram, S., Doyle, A.D., Conti, M.A., et al. (2007) Myosin IIA regulates cell motility and actomyosin-microtubule crosstalk. *Nat Cell Biol,* 9**,** 299-309.

Evers, E.E., Zondag, G.C., Malliri, A., et al. (2000) Rho family proteins in cell adhesion and cell migration. *Eur J Cancer,* 36**,** 1269-74.

Fernandes-Alnemri, T., Armstrong, R.C., Krebs, J., et al. (1996) In vitro activation of CPP32 and Mch3 by Mch4, a novel human apoptotic cysteine protease containing two FADD-like domains. *Proc Natl Acad Sci U S A,* 93**,** 7464-9.

Fernandes-Alnemri, T., Takahashi, A., Armstrong, R., et al. (1995) Mch3, a novel human apoptotic cysteine protease highly related to CPP32. *Cancer Res,* 55**,** 6045-52.

Fernandez, P.C., Frank, S.R., Wang, L., et al. (2003) Genomic targets of the human c-Myc protein. *Genes Dev,* 17**,** 1115-29.

Fincham, V.J., James, M., Frame, M.C., et al. (2000) Active ERK/MAP kinase is targeted to newly forming cell-matrix adhesions by integrin engagement and v-Src. *EMBO J,* 19**,** 2911-23.

Fischer, U., Janicke, R.U. & Schulze-Osthoff, K. (2003) Many cuts to ruin: a comprehensive update of caspase substrates. *Cell Death Differ,* 10**,** 76-100.

Fischer, U., Stroh, C. & Schulze-Osthoff, K. (2006) Unique and overlapping substrate specificities of caspase-8 and caspase-10. *Oncogene,* 25**,** 152-9.

Fishkind, D.J., Cao, L.G. & Wang, Y.L. (1991) Microinjection of the catalytic fragment of myosin light chain kinase into dividing cells: effects on mitosis and cytokinesis. *J Cell Biol,* 114**,** 967-75.

Fluckey, W.M., Sanchez, M.X., McKee, S.R., et al. (2003) Establishment of a microbiological profile for an air-chilling poultry operation in the United States. *J Food Prot,* 66**,** 272-9.

Flynn, P.G. & Helfman, D.M. (2010) Non-muscle myosin IIB helps mediate TNF cell death signaling independent of actomyosin contractility (AMC). *J Cell Biochem,* 110**,** 1365-75.

Frank, M.B. (2001) Antibody Binding to Protein A and Protein G Beads. IN FRANK, M. B. (Ed.) *Molecular Biology Protocols.* Oklahoma City.

Frank, S., Kohler, U., Schackert, G., et al. (1999) Expression of TRAIL and its receptors in human brain tumors. *Biochem Biophys Res Commun,* 257**,** 454-9.

Franklin-Tong, V.E. & Gourlay, C.W. (2008) A role for actin in regulating apoptosis/programmed cell death: evidence spanning yeast, plants and animals. *Biochem J,* 413**,** 389-404.

Freer-Prokop, M., O'Flaherty, J., Ross, J.A., et al. (2009) Non-canonical role for the TRAIL receptor DR5/FADD/caspase pathway in the regulation of MyoD expression and skeletal myoblast differentiation. *Differentiation,* 78**,** 205-12.

Friedl, P. & Wolf, K. (2003) Tumour-cell invasion and migration: diversity and escape mechanisms. *Nat Rev Cancer,* 3**,** 362-74.

Gabet, A.S., Coulon, S., Fricot, A., et al. (2011) Caspase-activated ROCK-1 allows erythroblast terminal maturation independently of cytokine-induced Rho signaling. *Cell Death Differ,* 18**,** 678-89.

Gajate, C. & Mollinedo, F. (2005) Cytoskeleton-mediated death receptor and ligand concentration in lipid rafts forms apoptosis-promoting clusters in cancer chemotherapy. *J Biol Chem,* 280**,** 11641-7.

Galligan, L., Longley, D.B., McEwan, M., et al. (2005) Chemotherapy and TRAIL-mediated colon cancer cell death: the roles of p53, TRAIL receptors, and c-FLIP. *Mol Cancer Ther,* 4**,** 2026-36.

Galluzzi, L., Vitale, I., Abrams, J.M., et al. (2012) Molecular definitions of cell death subroutines: recommendations of the Nomenclature Committee on Cell Death 2012. *Cell Death Differ,* 19**,** 107-20.

Ganten, T.M., Koschny, R., Sykora, J., et al. (2006) Preclinical differentiation between apparently safe and potentially hepatotoxic applications of TRAIL either alone or in combination with chemotherapeutic drugs. *Clin Cancer Res,* 12**,** 2640-6.

Gasparian, M.E., Ostapchenko, V.G., Yagolovich, A.V., et al. (2007) Overexpression and refolding of thioredoxin/TRAIL fusion from inclusion bodies and further purification of TRAIL after cleavage by enteropeptidase. *Biotechnol Lett,* 29**,** 1567-73.

Gerl, R. & Vaux, D.L. (2005) Apoptosis in the development and treatment of cancer. *Carcinogenesis,* 26**,** 263-70.

Gerlinger, M., Rowan, A.J., Horswell, S., et al. (2012) Intratumor heterogeneity and branched evolution revealed by multiregion sequencing. *N Engl J Med,* 366**,** 883-92.

Gerner, C., Frohwein, U., Gotzmann, J., et al. (2000) The Fas-induced apoptosis analyzed by high throughput proteome analysis. *J Biol Chem,* 275**,** 39018-26.

Gerrits, L., Overheul, G.J., Derks, R.C., et al. (2012) Gene duplication and conversion events shaped three homologous, differentially expressed myosin regulatory light chain (MLC2) genes. *Eur J Cell Biol,* 91**,** 629-39.

Gerritsen, W.R. & Sharma, P. (2012) Current and emerging treatment options for castration-resistant prostate cancer: a focus on immunotherapy. *J Clin Immunol,* 32**,** 25-35.

Giubellino, A., Burke, T.R., Jr. & Bottaro, D.P. (2008) Grb2 signaling in cell motility and cancer. *Expert Opin Ther Targets,* 12**,** 1021-33.

Glading, A., Bodnar, R.J., Reynolds, I.J., et al. (2004) Epidermal growth factor activates m-calpain (calpain II), at least in part, by extracellular signal-regulated kinase-mediated phosphorylation. *Mol Cell Biol,* 24**,** 2499-512.

Glading, A., Chang, P., Lauffenburger, D.A., et al. (2000) Epidermal growth factor receptor activation of calpain is required for fibroblast motility and occurs via an ERK/MAP kinase signaling pathway. *J Biol Chem,* 275**,** 2390-8.

Gluck, U., Kwiatkowski, D.J. & Ben-Ze'ev, A. (1993) Suppression of tumorigenicity in simian virus 40-transformed 3T3 cells transfected with alpha-actinin cDNA. *Proc Natl Acad Sci U S A,* 90**,** 383-7.

Goeckeler, Z.M., Masaracchia, R.A., Zeng, Q., et al. (2000) Phosphorylation of myosin light chain kinase by p21-activated kinase PAK2. *J Biol Chem,* 275**,** 18366-74.

Goldberg, G.S., Jin, Z., Ichikawa, H., et al. (2001) Global effects of anchorage on gene expression during mammary carcinoma cell growth reveal role of tumor necrosis factor-related apoptosis-inducing ligand in anoikis. *Cancer Res,* 61**,** 1334-7.

Goldschneider, D. & Mehlen, P. (2010) Dependence receptors: a new paradigm in cell signaling and cancer therapy. *Oncogene,* 29**,** 1865-82.

Golks, A., Brenner, D., Fritsch, C., et al. (2005) c-FLIPR, a new regulator of death receptor-induced apoptosis. *J Biol Chem,* 280**,** 14507-13.

Golks, A., Brenner, D., Krammer, P.H., et al. (2006) The c-FLIP-NH2 terminus (p22-FLIP) induces NF-kappaB activation. *J Exp Med,* 203**,** 1295-305.

Golomb, E., Ma, X., Jana, S.S., et al. (2004) Identification and characterization of nonmuscle myosin II-C, a new member of the myosin II family. *J Biol Chem,* 279**,** 2800-8.

Gong, B. & Almasan, A. (2000) Genomic organization and transcriptional regulation of human Apo2/TRAIL gene. *Biochem Biophys Res Commun,* 278**,** 747-52.

Gonzalez-Santiago, L., Suarez, Y., Zarich, N., et al. (2006) Aplidin induces JNK-dependent apoptosis in human breast cancer cells via alteration of glutathione homeostasis, Rac1 GTPase activation, and MKP-1 phosphatase downregulation. *Cell Death Differ,* 13**,** 1968-81.

Gonzalvez, F. & Ashkenazi, A. (2010) New insights into apoptosis signaling by Apo2L/TRAIL. *Oncogene,* 29**,** 4752-65.

Gormley, G.J., Steele, W.K., Stevenson, M., et al. (2003) A randomised study of two training programmes for general practitioners in the techniques of shoulder injection. *Ann Rheum Dis,* 62**,** 1006-9.

Graessmann, A., Graessmann, M., Tjian, R., et al. (1980) Simian virus 40 small-t protein is required for loss of actin cable networks in rat cells. *J Virol,* 33**,** 1182-91.

Griffith, T.S., Wiley, S.R., Kubin, M.Z., et al. (1999) Monocyte-mediated tumoricidal activity via the tumor necrosis factor-related cytokine, TRAIL. *J Exp Med,* 189**,** 1343-54.

Grosse-Wilde, A. & Kemp, C.J. (2008) Metastasis suppressor function of tumor necrosis factor-related apoptosis-inducing ligand-R in mice: implications for TRAIL-based therapy in humans? *Cancer Res,* 68**,** 6035-7.

Gu, Y., Sarnecki, C., Fleming, M.A., et al. (1996) Processing and activation of CMH-1 by granzyme B. *J Biol Chem,* 271**,** 10816-20.

Guo, Q.M., Malek, R.L., Kim, S., et al. (2000) Identification of c-myc responsive genes using rat cDNA microarray. *Cancer Res,* 60**,** 5922-8.

Gustafsson, L., Leijonhufvud, I., Aronsson, A., et al. (2004) Treatment of skin papillomas with topical alpha-lactalbumin-oleic acid. *N Engl J Med,* 350**,** 2663-72.

Hagerty, L., Weitzel, D.H., Chambers, J., et al. (2007) ROCK1 phosphorylates and activates zipper-interacting protein kinase. *J Biol Chem,* 282**,** 4884-93.

Hahn, W.C., Counter, C.M., Lundberg, A.S., et al. (1999) Creation of human tumour cells with defined genetic elements. *Nature,* 400**,** 464-8.

Hahn, W.C., Dessain, S.K., Brooks, M.W., et al. (2002) Enumeration of the simian virus 40 early region elements necessary for human cell transformation. *Mol Cell Biol,* 22**,** 2111-23.

Hahn, W.C. & Weinberg, R.A. (2002) Rules for making human tumor cells. *N Engl J Med,* 347**,** 1593-603.

Halaas, O., Vik, R., Ashkenazi, A., et al. (2000) Lipopolysaccharide induces expression of APO2 ligand/TRAIL in human monocytes and macrophages. *Scand J Immunol,* 51**,** 244-50.

Hall, A. (1998) Rho GTPases and the actin cytoskeleton. *Science,* 279**,** 509-14.

Hall, A.K. (1995) Thymosin beta-10 accelerates apoptosis. *Cell Mol Biol Res,* 41**,** 167-80.

Hanahan, D. & Weinberg, R.A. (2000) The hallmarks of cancer. *Cell,* 100**,** 57-70.

Hanahan, D. & Weinberg, R.A. (2011) Hallmarks of cancer: the next generation. *Cell,* 144**,** 646-74.

Hao, C., Song, J.H., Hsi, B., et al. (2004) TRAIL inhibits tumor growth but is nontoxic to human hepatocytes in chimeric mice. *Cancer Res,* 64**,** 8502-6.

Harms, C., Bosel, J., Lautenschlager, M., et al. (2004) Neuronal gelsolin prevents apoptosis by enhancing actin depolymerization. *Mol Cell Neurosci,* 25**,** 69-82.

Harper, N., Farrow, S.N., Kaptein, A., et al. (2001) Modulation of tumor necrosis factor apoptosis-inducing ligand- induced NF-kappa B activation by inhibition of apical caspases. *J Biol Chem,* 276**,** 34743-52.

Hayakawa, A., Kawamoto, Y., Nakajima, H., et al. (2008) Bid truncation mediated by caspases-3 and -9 in vinorelbine-induced apoptosis. *Apoptosis,* 13**,** 523-30.

Hayakawa, K., Takemura, G., Koda, M., et al. (2002) Sensitivity to apoptosis signal, clearance rate, and ultrastructure of fas ligand-induced apoptosis in in vivo adult cardiac cells. *Circulation,* 105**,** 3039-45.

He, S., Wang, L., Miao, L., et al. (2009) Receptor interacting protein kinase-3 determines cellular necrotic response to TNF-alpha. *Cell,* 137**,** 1100-11.

Hebert, M., Potin, S., Sebbagh, M., et al. (2008) Rho-ROCK-dependent ezrin-radixin-moesin phosphorylation regulates Fas-mediated apoptosis in Jurkat cells. *J Immunol,* 181**,** 5963-73.

Helfman, D.M., Levy, E.T., Berthier, C., et al. (1999) Caldesmon inhibits nonmuscle cell contractility and interferes with the formation of focal adhesions. *Mol Biol Cell,* 10**,** 3097-112.

Hellwig, C.T., Ludwig-Galezowska, A.H., Concannon, C.G., et al. (2010) Activity of protein kinase CK2 uncouples Bid cleavage from caspase-8 activation. *J Cell Sci,* 123**,** 1401-6.

Hendricks, M. & Weintraub, H. (1981) Tropomyosin is decreased in transformed cells. *Proc Natl Acad Sci U S A,* 78**,** 5633-7.

Herbeuval, J.P., Boasso, A., Grivel, J.C., et al. (2005) TNF-related apoptosis-inducing ligand (TRAIL) in HIV-1-infected patients and its in vitro production by antigen-presenting cells. *Blood,* 105**,** 2458-64.

Herbst, R.S., Eckhardt, S.G., Kurzrock, R., et al. (2010) Phase I dose-escalation study of recombinant human Apo2L/TRAIL, a dual proapoptotic receptor agonist, in patients with advanced cancer. *J Clin Oncol,* 28**,** 2839-46.

Hermeking, H. (2003) The MYC oncogene as a cancer drug target. *Curr Cancer Drug Targets,* 3**,** 163-75.

Hernandez-Alcoceba, R., del Peso, L. & Lacal, J.C. (2000) The Ras family of GTPases in cancer cell invasion. *Cell Mol Life Sci,* 57**,** 65-76.

Higuchi, H., Yoon, J.H., Grambihler, A., et al. (2003) Bile acids stimulate cFLIP phosphorylation enhancing TRAIL-mediated apoptosis. *J Biol Chem,* 278**,** 454-61.

Hildt, E. & Oess, S. (1999) Identification of Grb2 as a novel binding partner of tumor necrosis factor (TNF) receptor I. *J Exp Med,* 189**,** 1707-14.

Hilliard, B., Wilmen, A., Seidel, C., et al. (2001) Roles of TNF-related apoptosis-inducing ligand in experimental autoimmune encephalomyelitis. *J Immunol,* 166**,** 1314-9.

Hirata, N., Takahashi, M. & Yazawa, M. (2009) Diphosphorylation of regulatory light chain of myosin IIA is responsible for proper cell spreading. *Biochem Biophys Res Commun,* 381**,** 682-7.

Holler, N., Zaru, R., Micheau, O., et al. (2000) Fas triggers an alternative, caspase-8-independent cell death pathway using the kinase RIP as effector molecule. *Nat Immunol,* 1**,** 489-95.

Hoogwater, F.J., Nijkamp, M.W., Smakman, N., et al. (2010) Oncogenic K-Ras turns death receptors into metastasis-promoting receptors in human and mouse colorectal cancer cells. *Gastroenterology,* 138**,** 2357-67.

Hu, W.H., Johnson, H. & Shu, H.B. (2000) Activation of NF-kappaB by FADD, Casper, and caspase-8. *J Biol Chem,* 275**,** 10838-44.

Huang, J., Mahavadi, S., Sriwai, W., et al. (2006) Gi-coupled receptors mediate phosphorylation of CPI-17 and MLC20 via preferential activation of the PI3K/ILK pathway. *Biochem J,* 396**,** 193-200.

Hueber, A.O., Zornig, M., Lyon, D., et al. (1997) Requirement for the CD95 receptor-ligand pathway in c-Myc-induced apoptosis. *Science,* 278**,** 1305-9.

Hughes, M.A., Harper, N., Butterworth, M., et al. (2009) Reconstitution of the death-inducing signaling complex reveals a substrate switch that determines CD95-mediated death or survival. *Mol Cell,* 35**,** 265-79.

Hunter, I., Cobban, H.J., Vandenabeele, P., et al. (2003) Tumor necrosis factor-alpha-induced activation of RhoA in airway smooth muscle cells: role in the Ca2+ sensitization of myosin light chain20 phosphorylation. *Mol Pharmacol,* 63**,** 714-21.

Huser, M., Luckett, J., Chiloeches, A., et al. (2001) MEK kinase activity is not necessary for Raf-1 function. *EMBO J,* 20**,** 1940-51.

Hymowitz, S.G., Christinger, H.W., Fuh, G., et al. (1999) Triggering cell death: the crystal structure of Apo2L/TRAIL in a complex with death receptor 5. *Mol Cell,* 4**,** 563-71.

Hymowitz, S.G., O'Connell, M.P., Ultsch, M.H., et al. (2000) A unique zinc-binding site revealed by a high-resolution X-ray structure of homotrimeric Apo2L/TRAIL. *Biochemistry,* 39**,** 633-40.

Hynes, N.E. & Lane, H.A. (2005) ERBB receptors and cancer: the complexity of targeted inhibitors. *Nat Rev Cancer,* 5**,** 341-54.

Ichikawa, K., Liu, W., Fleck, M., et al. (2003) TRAIL-R2 (DR5) mediates apoptosis of synovial fibroblasts in rheumatoid arthritis. *J Immunol,* 171**,** 1061-9.

Iida, M., Sasaki, T. & Komatani, H. (2009) Overexpression of Plk3 causes morphological change and cell growth suppression in Ras pathway-activated cells. *J Biochem,* 146**,** 501-7.

Ikebe, M. & Hartshorne, D.J. (1985) Phosphorylation of smooth muscle myosin at two distinct sites by myosin light chain kinase. *J Biol Chem,* 260**,** 10027-31.

Ikebe, M., Hartshorne, D.J. & Elzinga, M. (1986) Identification, phosphorylation, and dephosphorylation of a second site for myosin light chain kinase on the 20,000-dalton light chain of smooth muscle myosin. *J Biol Chem,* 261**,** 36-9.

Ikebe, M., Koretz, J. & Hartshorne, D.J. (1988) Effects of phosphorylation of light chain residues threonine 18 and serine 19 on the properties and conformation of smooth muscle myosin. *J Biol Chem,* 263**,** 6432-7.

Ikebe, M. & Reardon, S. (1988) Binding of caldesmon to smooth muscle myosin. *J Biol Chem,* 263**,** 3055-8.

Innan, H. (2009) Population genetic models of duplicated genes. *Genetica,* 137**,** 19-37.

Inoue, H., Shiraki, K., Yamanaka, T., et al. (2002) Functional expression of tumor necrosis factor-related apoptosis-inducing ligand in human colonic adenocarcinoma cells. *Lab Invest,* 82**,** 1111-9.

Irmler, M., Thome, M., Hahne, M., et al. (1997) Inhibition of death receptor signals by cellular FLIP. *Nature,* 388**,** 190-5.

Ishimura, N., Isomoto, H., Bronk, S.F., et al. (2006) Trail induces cell migration and invasion in apoptosis-resistant cholangiocarcinoma cells. *Am J Physiol Gastrointest Liver Physiol,* 290**,** G129-36.

Izawa, I., Amano, M., Chihara, K., et al. (1998) Possible involvement of the inactivation of the Rho-Rho-kinase pathway in oncogenic Ras-induced transformation. *Oncogene,* 17**,** 2863-71.

Izeradjene, K., Douglas, L., Delaney, A., et al. (2004) Influence of casein kinase II in tumor necrosis factor-related apoptosis-inducing ligand-induced apoptosis in human rhabdomyosarcoma cells. *Clin Cancer Res,* 10**,** 6650-60.

Izeradjene, K., Douglas, L., Delaney, A., et al. (2005) Casein kinase II (CK2) enhances death-inducing signaling complex (DISC) activity in TRAIL-induced apoptosis in human colon carcinoma cell lines. *Oncogene,* 24**,** 2050-8.

Jaalouk, D.E. & Lammerding, J. (2009) Mechanotransduction gone awry. *Nat Rev Mol Cell Biol,* 10**,** 63-73.

Janssen, R.A., Veenstra, K.G., Jonasch, P., et al. (1998) Ras- and Raf-induced down-modulation of non-muscle tropomyosin are MEK-independent. *J Biol Chem,* 273**,** 32182-6.

Jimenez-Baranda, S., Gomez-Mouton, C., Rojas, A., et al. (2007) Filamin-A regulates actin-dependent clustering of HIV receptors. *Nat Cell Biol,* 9**,** 838-46.

Jin, Y., Atkinson, S.J., Marrs, J.A., et al. (2001) Myosin ii light chain phosphorylation regulates membrane localization and apoptotic signaling of tumor necrosis factor receptor-1. *J Biol Chem,* 276**,** 30342-9.

Jin, Z. & El-Deiry, W.S. (2006) Distinct signaling pathways in TRAIL- versus tumor necrosis factor-induced apoptosis. *Mol Cell Biol,* 26**,** 8136-48.

Jin, Z., Li, Y., Pitti, R., et al. (2009) Cullin3-based polyubiquitination and p62-dependent aggregation of caspase-8 mediate extrinsic apoptosis signaling. *Cell,* 137**,** 721-35.

Jin, Z., McDonald, E.R., 3rd, Dicker, D.T., et al. (2004) Deficient tumor necrosis factor-related apoptosis-inducing ligand (TRAIL) death receptor transport to the cell surface in human colon cancer cells selected for resistance to TRAIL-induced apoptosis. *J Biol Chem,* 279**,** 35829-39.

Jo, M., Kim, T.H., Seol, D.W., et al. (2000) Apoptosis induced in normal human hepatocytes by tumor necrosis factor-related apoptosis-inducing ligand. *Nat Med,* 6**,** 564-7.

Johnsen, A.C., Haux, J., Steinkjer, B., et al. (1999) Regulation of APO-2 ligand/trail expression in NK cells-involvement in NK cell-mediated cytotoxicity. *Cytokine,* 11**,** 664-72.

Johnson, T.R., Stone, K., Nikrad, M., et al. (2003) The proteasome inhibitor PS-341 overcomes TRAIL resistance in Bax and caspase 9-negative or Bcl-xL overexpressing cells. *Oncogene,* 22**,** 4953-63.

Johnstone, R.W., Frew, A.J. & Smyth, M.J. (2008) The TRAIL apoptotic pathway in cancer onset, progression and therapy. *Nat Rev Cancer,* 8**,** 782-98.

Jones, R.B., Gordus, A., Krall, J.A., et al. (2006) A quantitative protein interaction network for the ErbB receptors using protein microarrays. *Nature,* 439**,** 168-74.

Jordan, K.M., Arden, N.K., Doherty, M., et al. (2003) EULAR Recommendations 2003: an evidence based approach to the management of knee osteoarthritis: Report of a Task Force of the Standing Committee for International Clinical Studies Including Therapeutic Trials (ESCISIT). *Ann Rheum Dis,* 62**,** 1145-55.

Jost, P.J., Grabow, S., Gray, D., et al. (2009) XIAP discriminates between type I and type II FAS-induced apoptosis. *Nature,* 460**,** 1035-9.

Kamijo, K., Ohara, N., Abe, M., et al. (2006) Dissecting the role of Rho-mediated signaling in contractile ring formation. *Mol Biol Cell,* 17**,** 43-55.

Kandasamy, K., Srinivasula, S.M., Alnemri, E.S., et al. (2003) Involvement of proapoptotic molecules Bax and Bak in tumor necrosis factor-related apoptosis-inducing ligand (TRAIL)-induced mitochondrial disruption and apoptosis: differential regulation of cytochrome c and Smac/DIABLO release. *Cancer Res,* 63**,** 1712-21.

Kaneko, T., Li, L. & Li, S.S. (2008) The SH3 domain--a family of versatile peptide- and protein-recognition module. *Front Biosci,* 13**,** 4938-52.

Kashii, Y., Giorda, R., Herberman, R.B., et al. (1999) Constitutive expression and role of the TNF family ligands in apoptotic killing of tumor cells by human NK cells. *J Immunol,* 163**,** 5358-66.

Kataoka, T., Budd, R.C., Holler, N., et al. (2000) The caspase-8 inhibitor FLIP promotes activation of NF-kappaB and Erk signaling pathways. *Curr Biol,* 10**,** 640-8.

Kataoka, T. & Tschopp, J. (2004) N-terminal fragment of c-FLIP(L) processed by caspase 8 specifically interacts with TRAF2 and induces activation of the NF-kappaB signaling pathway. *Mol Cell Biol,* 24**,** 2627-36.

Kaunisto, A., Kochin, V., Asaoka, T., et al. (2009) PKC-mediated phosphorylation regulates c-FLIP ubiquitylation and stability. *Cell Death Differ,* 16**,** 1215-26.

Kavuri, S.M., Geserick, P., Berg, D., et al. (2011) Cellular FLICE-inhibitory protein (cFLIP) isoforms block CD95- and TRAIL death receptor-induced gene induction irrespective of processing of caspase-8 or cFLIP in the death-inducing signaling complex. *J Biol Chem,* 286**,** 16631-46.

Kayagaki, N., Yamaguchi, N., Nakayama, M., et al. (1999) Type I interferons (IFNs) regulate tumor necrosis factor-related apoptosis-inducing ligand (TRAIL) expression on human T cells: A novel mechanism for the antitumor effects of type I IFNs. *J Exp Med,* 189**,** 1451-60.

Kedinger, V., Muller, S. & Gronemeyer, H. (2011) Targeted expression of tumor necrosis factor-related apoptosis-inducing ligand TRAIL in skin protects mice against chemical carcinogenesis. *Mol Cancer,* 10**,** 34.

Kelley, R.F., Totpal, K., Lindstrom, S.H., et al. (2005) Receptor-selective mutants of apoptosis-inducing ligand 2/tumor necrosis factor-related apoptosis-inducing ligand reveal a greater contribution of death receptor (DR) 5 than DR4 to apoptosis signaling. *J Biol Chem,* 280**,** 2205-12.

Kelley, S.K., Harris, L.A., Xie, D., et al. (2001) Preclinical studies to predict the disposition of Apo2L/tumor necrosis factor-related apoptosis-inducing ligand in humans: characterization of in vivo efficacy, pharmacokinetics, and safety. *J Pharmacol Exp Ther,* 299**,** 31-8.

Kelly, P.N. & Strasser, A. (2011) The role of Bcl-2 and its pro-survival relatives in tumourigenesis and cancer therapy. *Cell Death Differ,* 18**,** 1414-24.

Kemp, T.J., Elzey, B.D. & Griffith, T.S. (2003) Plasmacytoid dendritic cell-derived IFN-alpha induces TNF-related apoptosis-inducing ligand/Apo-2L-mediated antitumor activity by human monocytes following CpG oligodeoxynucleotide stimulation. *J Immunol,* 171**,** 212-8.

Kerr, J.F., Wyllie, A.H. & Currie, A.R. (1972) Apoptosis: a basic biological phenomenon with wide-ranging implications in tissue kinetics. *Br J Cancer,* 26**,** 239-57.

Khaider, N.G., Lane, D., Matte, I., et al. (2012) Targeted ovarian cancer treatment: the TRAILs of resistance. *Am J Cancer Res,* 2**,** 75-92.

Kim, S.H., Kim, K., Kwagh, J.G., et al. (2004) Death induction by recombinant native TRAIL and its prevention by a caspase 9 inhibitor in primary human esophageal epithelial cells. *J Biol Chem,* 279**,** 40044-52.

Kim, S.J., Hwang, S.G., Kim, I.C., et al. (2003) Actin cytoskeletal architecture regulates nitric oxide-induced apoptosis, dedifferentiation, and cyclooxygenase-2 expression in articular chondrocytes via mitogen-activated protein kinase and protein kinase C pathways. *J Biol Chem,* 278**,** 42448-56.

Kim, Y., Suh, N., Sporn, M., et al. (2002) An inducible pathway for degradation of FLIP protein sensitizes tumor cells to TRAIL-induced apoptosis. *J Biol Chem,* 277**,** 22320-9.

Kinzler, K.W. & Vogelstein, B. (1996) Lessons from hereditary colorectal cancer. *Cell,* 87**,** 159-70.

Kischkel, F.C., Hellbardt, S., Behrmann, I., et al. (1995) Cytotoxicity-dependent APO-1 (Fas/CD95)-associated proteins form a death-inducing signaling complex (DISC) with the receptor. *EMBO J,* 14**,** 5579-88.

Kischkel, F.C., Lawrence, D.A., Chuntharapai, A., et al. (2000) Apo2L/TRAIL-dependent recruitment of endogenous FADD and caspase-8 to death receptors 4 and 5. *Immunity,* 12**,** 611-20.

Kischkel, F.C., Lawrence, D.A., Tinel, A., et al. (2001) Death receptor recruitment of endogenous caspase-10 and apoptosis initiation in the absence of caspase-8. *J Biol Chem,* 276**,** 46639-46.

Klampfer, L., Huang, J., Sasazuki, T., et al. (2004) Oncogenic Ras promotes butyrate-induced apoptosis through inhibition of gelsolin expression. *J Biol Chem,* 279**,** 36680-8.

Klefstrom, J., Arighi, E., Littlewood, T., et al. (1997) Induction of TNF-sensitive cellular phenotype by c-Myc involves p53 and impaired NF-kappaB activation. *EMBO J,* 16**,** 7382-92.

Klemke, M., Weschenfelder, T., Konstandin, M.H., et al. (2007) High affinity interaction of integrin alpha4beta1 (VLA-4) and vascular cell adhesion molecule 1 (VCAM-1) enhances migration of human melanoma cells across activated endothelial cell layers. *J Cell Physiol,* 212**,** 368-74.

Koester, S.K., Roth, P., Mikulka, W.R., et al. (1997) Monitoring early cellular responses in apoptosis is aided by the mitochondrial membrane protein-specific monoclonal antibody APO2.7. *Cytometry,* 29**,** 306-12.

Kohlhaas, S.L., Craxton, A., Sun, X.M., et al. (2007) Receptor-mediated endocytosis is not required for tumor necrosis factor-related apoptosis-inducing ligand (TRAIL)-induced apoptosis. *J Biol Chem,* 282**,** 12831-41.

Kolega, J. (1998) Cytoplasmic dynamics of myosin IIA and IIB: spatial 'sorting' of isoforms in locomoting cells. *J Cell Sci,* 111 (Pt 15)**,** 2085-95.

Kolega, J. (2003) Asymmetric distribution of myosin IIB in migrating endothelial cells is regulated by a rho-dependent kinase and contributes to tail retraction. *Mol Biol Cell,* 14**,** 4745-57.

Kolotkin, R.L., Crosby, R.D., Pendleton, R., et al. (2003) Health-related quality of life in patients seeking gastric bypass surgery vs non-treatment-seeking controls. *Obes Surg,* 13**,** 371-7.

Komatsu, S., Yano, T., Shibata, M., et al. (2000) Effects of the regulatory light chain phosphorylation of myosin II on mitosis and cytokinesis of mammalian cells. *J Biol Chem,* 275**,** 34512-20.

Koschny, R., Holland, H., Sykora, J., et al. (2007) Bortezomib sensitizes primary human astrocytoma cells of WHO grades I to IV for tumor necrosis factor-related apoptosis-inducing ligand-induced apoptosis. *Clin Cancer Res,* 13**,** 3403-12.

Kothakota, S., Azuma, T., Reinhard, C., et al. (1997) Caspase-3-generated fragment of gelsolin: effector of morphological change in apoptosis. *Science,* 278**,** 294-8.

Kovacs, M., Toth, J., Hetenyi, C., et al. (2004) Mechanism of blebbistatin inhibition of myosin II. *J Biol Chem,* 279**,** 35557-63.

Koya, R.C., Fujita, H., Shimizu, S., et al. (2000) Gelsolin inhibits apoptosis by blocking mitochondrial membrane potential loss and cytochrome c release. *J Biol Chem,* 275**,** 15343-9.

Koyama, S., Koike, N. & Adachi, S. (2002) Expression of TNF-related apoptosis-inducing ligand (TRAIL) and its receptors in gastric carcinoma and tumor-infiltrating lymphocytes: a possible mechanism of immune evasion of the tumor. *J Cancer Res Clin Oncol,* 128**,** 73-9.

Kozma, R., Ahmed, S., Best, A., et al. (1995) The Ras-related protein Cdc42Hs and bradykinin promote formation of peripheral actin microspikes and filopodia in Swiss 3T3 fibroblasts. *Mol Cell Biol,* 15**,** 1942-52.

Kroemer, G., El-Deiry, W.S., Golstein, P., et al. (2005) Classification of cell death: recommendations of the Nomenclature Committee on Cell Death. *Cell Death Differ,* 12 Suppl 2**,** 1463-7.

Kumar, C.C., Chang, C., Rhim, J. (1991) Cytoskeletal changes in human transformed cells: studies on HOS cells. IN JOHNG S. RHIM, A. D. (Ed.) *Neoplastic Transformation in Human Cell Culture: Mechanisms of Carcinogenesis.* Totowa, New Jersey, The Humana Press Incorporated.

Kumar, C.C., Bushel, P., Mohan-Peterson, S., et al. (1992) Regulation of smooth muscle alpha-actin promoter in ras-transformed cells: usefulness for setting up reporter gene-based assay system for drug screening. *Cancer Res,* 52**,** 6877-84.

Kuo, J.C., Han, X., Hsiao, C.T., et al. (2011) Analysis of the myosin-II-responsive focal adhesion proteome reveals a role for beta-Pix in negative regulation of focal adhesion maturation. *Nat Cell Biol,* 13**,** 383-93.

Kuo, W.C., Yang, K.T., Hsieh, S.L., et al. (2010) Ezrin is a negative regulator of death receptor-induced apoptosis. *Oncogene,* 29**,** 1374-83.

Kurada, B.R., Li, L.C., Mulherkar, N., et al. (2009) MADD, a splice variant of IG20, is indispensable for MAPK activation and protection against apoptosis upon tumor necrosis factor-alpha treatment. *J Biol Chem,* 284**,** 13533-41.

Kurenova, E., Xu, L.H., Yang, X., et al. (2004) Focal adhesion kinase suppresses apoptosis by binding to the death domain of receptor-interacting protein. *Mol Cell Biol,* 24**,** 4361-71.

Kusano, H., Shimizu, S., Koya, R.C., et al. (2000) Human gelsolin prevents apoptosis by inhibiting apoptotic mitochondrial changes via closing VDAC. *Oncogene,* 19**,** 4807-14.

Laguinge, L.M., Samara, R.N., Wang, W., et al. (2008) DR5 receptor mediates anoikis in human colorectal carcinoma cell lines. *Cancer Res,* 68**,** 909-17.

Lal, A., Haynes, S.R. & Gorospe, M. (2005) Clean Western blot signals from immunoprecipitated samples. *Mol Cell Probes,* 19**,** 385-8.

Lalaoui, N., Morle, A., Merino, D., et al. (2011) TRAIL-R4 promotes tumor growth and resistance to apoptosis in cervical carcinoma HeLa cells through AKT. *PLoS One,* 6**,** e19679.

Lamhamedi-Cherradi, S.E., Zheng, S., Tisch, R.M., et al. (2003a) Critical roles of tumor necrosis factor-related apoptosis-inducing ligand in type 1 diabetes. *Diabetes,* 52**,** 2274-8.

Lamhamedi-Cherradi, S.E., Zheng, S.J., Maguschak, K.A., et al. (2003b) Defective thymocyte apoptosis and accelerated autoimmune diseases in TRAIL-/- mice. *Nat Immunol,* 4**,** 255-60.

Lane, D., Cartier, A., L'Esperance, S., et al. (2004) Differential induction of apoptosis by tumor necrosis factor-related apoptosis-inducing ligand in human ovarian carcinoma cells. *Gynecol Oncol,* 93**,** 594-604.

Lane, J.D., Vergnolle, M.A., Woodman, P.G., et al. (2001) Apoptotic cleavage of cytoplasmic dynein intermediate chain and p150(Glued) stops dynein-dependent membrane motility. *J Cell Biol,* 153**,** 1415-26.

Lavrik, I., Krueger, A., Schmitz, I., et al. (2003) The active caspase-8 heterotetramer is formed at the CD95 DISC. *Cell Death Differ,* 10**,** 144-5.

Lavrik, I.N. & Krammer, P.H. (2012) Regulation of CD95/Fas signaling at the DISC. *Cell Death Differ,* 19**,** 36-41.

Lawrence, D., Shahrokh, Z., Marsters, S., et al. (2001) Differential hepatocyte toxicity of recombinant Apo2L/TRAIL versions. *Nat Med,* 7**,** 383-5.

Leadsham, J.E., Kotiadis, V.N., Tarrant, D.J., et al. (2010) Apoptosis and the yeast actin cytoskeleton. *Cell Death Differ,* 17**,** 754-62.

Lee, H.W., Lee, S.H., Ryu, Y.W., et al. (2005) Homomeric and heteromeric interactions of the extracellular domains of death receptors and death decoy receptors. *Biochem Biophys Res Commun,* 330**,** 1205-12.

Lee, J.H., Katakai, T., Hara, T., et al. (2004) Roles of p-ERM and Rho-ROCK signaling in lymphocyte polarity and uropod formation. *J Cell Biol,* 167**,** 327-37.

Lee, K.H., Feig, C., Tchikov, V., et al. (2006) The role of receptor internalization in CD95 signaling. *EMBO J,* 25**,** 1009-23.

Lee, N., MacDonald, H., Reinhard, C., et al. (1997) Activation of hPAK65 by caspase cleavage induces some of the morphological and biochemical changes of apoptosis. *Proc Natl Acad Sci U S A,* 94**,** 13642-7.

Lee, S., Kang, J., Cho, M., et al. (2009) Profiling of transcripts and proteins modulated by K-ras oncogene in the lung tissues of K-ras transgenic mice by omics approaches. *Int J Oncol,* 34**,** 161-72.

Lee, S.H., Zhang, W., Choi, J.J., et al. (2001) Overexpression of the thymosin beta-10 gene in human ovarian cancer cells disrupts F-actin stress fiber and leads to apoptosis. *Oncogene,* 20**,** 6700-6.

Leist, M., Gantner, F., Kunstle, G., et al. (1996) The 55-kD tumor necrosis factor receptor and CD95 independently signal murine hepatocyte apoptosis and subsequent liver failure. *Mol Med,* 2**,** 109-24.

Leverkus, M., Neumann, M., Mengling, T., et al. (2000) Regulation of tumor necrosis factor-related apoptosis-inducing ligand sensitivity in primary and transformed human keratinocytes. *Cancer Res,* 60**,** 553-9.

Li, H. & Lin, X. (2008) Positive and negative signaling components involved in TNFalpha-induced NF-kappaB activation. *Cytokine,* 41**,** 1-8.

Li, H., Zhu, H., Xu, C.J., et al. (1998) Cleavage of BID by caspase 8 mediates the mitochondrial damage in the Fas pathway of apoptosis. *Cell,* 94**,** 491-501.

Li, P., Jayarama, S., Ganesh, L., et al. (2010) Akt-phosphorylated mitogen-activated kinase-activating death domain protein (MADD) inhibits TRAIL-induced apoptosis by blocking Fas-associated death domain (FADD) association with death receptor 4. *J Biol Chem,* 285**,** 22713-22.

Limouze, J., Straight, A.F., Mitchison, T., et al. (2004) Specificity of blebbistatin, an inhibitor of myosin II. *J Muscle Res Cell Motil,* 25**,** 337-41.

Lin, P., Zhu, H., Cai, C., et al. (2012) Nonmuscle myosin IIA facilitates vesicle trafficking for MG53-mediated cell membrane repair. *FASEB J,* 26**,** 1875-83.

Lin, Y., Devin, A., Cook, A., et al. (2000) The death domain kinase RIP is essential for TRAIL (Apo2L)-induced activation of IkappaB kinase and c-Jun N-terminal kinase. *Mol Cell Biol,* 20**,** 6638-45.

Liu, H., Li, J., Huang, Y., et al. (2012) Inhibition of transient receptor potential melastain 7 channel increases HSCs apoptosis induced by TRAIL. *Life Sci,* 90**,** 612-8.

Liu, S., Yu, Y., Zhang, M., et al. (2001) The involvement of TNF-alpha-related apoptosis-inducing ligand in the enhanced cytotoxicity of IFN-beta-stimulated human dendritic cells to tumor cells. *J Immunol,* 166**,** 5407-15.

Liu, Z., Kostenko, E.V., Mahon, G.M., et al. (2006) Transformation by the Rho-specific guanine nucleotide exchange factor Dbs requires ROCK I-mediated phosphorylation of myosin light chain. *J Biol Chem,* 281**,** 16043-51.

Llobet, D., Eritja, N., Encinas, M., et al. (2008) CK2 controls TRAIL and Fas sensitivity by regulating FLIP levels in endometrial carcinoma cells. *Oncogene,* 27**,** 2513-24.

Lo, C.M., Buxton, D.B., Chua, G.C., et al. (2004) Nonmuscle myosin IIb is involved in the guidance of fibroblast migration. *Mol Biol Cell,* 15**,** 982-9.

Lockshin, R.A., Zakeri, Z. (1994) Programmed cell death: early changes in metamorphosing cells. *Biochem Cell Biol. ,* 72**,** 589-596.

Lohmann-Matthes, M.L., Steinmuller, C. & Franke-Ullmann, G. (1994) Pulmonary macrophages. *Eur Respir J,* 7**,** 1678-89.

Lorimer, D.D., de Lanerolle, P. (2006) Myosin II – Physiological properties. IN BITTAR, E. E., BITTAR, N. (Ed.) *Cell chemistry and physiology.* Elsevier.

Lozupone, F., Lugini, L., Matarrese, P., et al. (2004) Identification and relevance of the CD95-binding domain in the N-terminal region of ezrin. *J Biol Chem,* 279**,** 9199-207.

Lub-de Hooge, M.N., de Vries, E.G., de Jong, S., et al. (2005) Soluble TRAIL concentrations are raised in patients with systemic lupus erythematosus. *Ann Rheum Dis,* 64**,** 854-8.

Luciani, F., Matarrese, P., Giammarioli, A.M., et al. (2004) CD95/phosphorylated ezrin association underlies HIV-1 GP120/IL-2-induced susceptibility to CD95(APO-1/Fas)-mediated apoptosis of human resting CD4(+)T lymphocytes. *Cell Death Differ,* 11**,** 574-82.

Ludowyke, R.I., Elgundi, Z., Kranenburg, T., et al. (2006) Phosphorylation of nonmuscle myosin heavy chain IIA on Ser1917 is mediated by protein kinase C beta II and coincides with the onset of stimulated degranulation of RBL-2H3 mast cells. *J Immunol,* 177**,** 1492-9.

Lund, P., Kotova, I., Kedinger, V., et al. (2011) Transformation-dependent silencing of tumor-selective apoptosis-inducing TRAIL by DNA hypermethylation is antagonized by decitabine. *Mol Cancer Ther,* 10**,** 1611-23.

Luo, X., Budihardjo, I., Zou, H., et al. (1998) Bid, a Bcl2 interacting protein, mediates cytochrome c release from mitochondria in response to activation of cell surface death receptors. *Cell,* 94**,** 481-90.

Luque-Garcia, J.L., Zhou, G., Sun, T.T., et al. (2006) Use of nitrocellulose membranes for protein characterization by matrix-assisted laser desorption/ionization mass spectrometry. *Anal Chem,* 78**,** 5102-8.

Ma, X., Bao, J. & Adelstein, R.S. (2007) Loss of cell adhesion causes hydrocephalus in nonmuscle myosin II-B-ablated and mutated mice. *Mol Biol Cell,* 18**,** 2305-12.

MacFarlane, M., Harper, N., Snowden, R.T., et al. (2002) Mechanisms of resistance to TRAIL-induced apoptosis in primary B cell chronic lymphocytic leukaemia. *Oncogene,* 21**,** 6809-18.

Machesky, L.M. & Hall, A. (1997) Role of actin polymerization and adhesion to extracellular matrix in Rac- and Rho-induced cytoskeletal reorganization. *J Cell Biol,* 138**,** 913-26.

Mahalingam, D., Szegezdi, E., Keane, M., et al. (2009) TRAIL receptor signalling and modulation: Are we on the right TRAIL? *Cancer Treat Rev,* 35**,** 280-8.

Mantovani, A. (2009) Cancer: Inflaming metastasis. *Nature,* 457**,** 36-7.

Maravillas-Montero, J.L. & Santos-Argumedo, L. (2012) The myosin family: unconventional roles of actin-dependent molecular motors in immune cells. *J Leukoc Biol,* 91**,** 35-46.

Mariani, S.M. & Krammer, P.H. (1998) Differential regulation of TRAIL and CD95 ligand in transformed cells of the T and B lymphocyte lineage. *Eur J Immunol,* 28**,** 973-82.

Marigo, V., Nigro, A., Pecci, A., et al. (2004) Correlation between the clinical phenotype of MYH9-related disease and tissue distribution of class II nonmuscle myosin heavy chains. *Genomics,* 83**,** 1125-33.

Marston, S.B. & Smith, C.W. (1985) The thin filaments of smooth muscles. *J Muscle Res Cell Motil,* 6**,** 669-708.

Mashima, T., Naito, M. & Tsuruo, T. (1999) Caspase-mediated cleavage of cytoskeletal actin plays a positive role in the process of morphological apoptosis. *Oncogene,* 18**,** 2423-30.

Matallanas, D., Birtwistle, M., Romano, D., et al. (2011) Raf family kinases: old dogs have learned new tricks. *Genes Cancer,* 2**,** 232-60.

Matsumura, F. (2005) Regulation of myosin II during cytokinesis in higher eukaryotes. *Trends Cell Biol,* 15**,** 371-7.

Matsumura, F., Yamashiro-Matsumura, S. & Lin, J.J. (1983) Isolation and characterization of tropomyosin-containing microfilaments from cultured cells. *J Biol Chem,* 258**,** 6636-44.

Mayanagi, T. & Sobue, K. (2011) Diversification of caldesmon-linked actin cytoskeleton in cell motility. *Cell Adh Migr,* 5**,** 150-9.

McDonald, E.R., 3rd & El-Deiry, W.S. (2004) Suppression of caspase-8- and -10-associated RING proteins results in sensitization to death ligands and inhibition of tumor cell growth. *Proc Natl Acad Sci U S A,* 101**,** 6170-5.

McKenzie, J.A. & Ridley, A.J. (2007) Roles of Rho/ROCK and MLCK in TNF-alpha-induced changes in endothelial morphology and permeability. *J Cell Physiol,* 213**,** 221-8.

Mehlen, P. & Puisieux, A. (2006) Metastasis: a question of life or death. *Nat Rev Cancer,* 6**,** 449-58.

Mellier, G., Huang, S., Shenoy, K., et al. (2010) TRAILing death in cancer. *Mol Aspects Med,* 31**,** 93-112.

Meng, X.W., Heldebrant, M.P., Flatten, K.S., et al. (2010) Protein kinase Cbeta modulates ligand-induced cell surface death receptor accumulation: a mechanistic basis for enzastaurin-death ligand synergy. *J Biol Chem,* 285**,** 888-902.

Menke, C., Bin, L., Thorburn, J., et al. (2011) Distinct TRAIL resistance mechanisms can be overcome by proteasome inhibition but not generally by synergizing agents. *Cancer Res,* 71**,** 1883-92.

Merino, D., Lalaoui, N., Morizot, A., et al. (2006) Differential inhibition of TRAIL-mediated DR5-DISC formation by decoy receptors 1 and 2. *Mol Cell Biol,* 26**,** 7046-55.

Meurette, O., Huc, L., Rebillard, A., et al. (2005) TRAIL (TNF-related apoptosis-inducing ligand) induces necrosis-like cell death in tumor cells at acidic extracellular pH. *Ann N Y Acad Sci,* 1056**,** 379-87.

Mi, Q.S., Ly, D., Lamhamedi-Cherradi, S.E., et al. (2003) Blockade of tumor necrosis factor-related apoptosis-inducing ligand exacerbates type 1 diabetes in NOD mice. *Diabetes,* 52**,** 1967-75.

Micheau, O., Thome, M., Schneider, P., et al. (2002) The long form of FLIP is an activator of caspase-8 at the Fas death-inducing signaling complex. *J Biol Chem,* 277**,** 45162-71.

Mikula, M., Schreiber, M., Husak, Z., et al. (2001) Embryonic lethality and fetal liver apoptosis in mice lacking the c-raf-1 gene. *EMBO J,* 20**,** 1952-62.

Milhas, D., Cuvillier, O., Therville, N., et al. (2005) Caspase-10 triggers Bid cleavage and caspase cascade activation in FasL-induced apoptosis. *J Biol Chem,* 280**,** 19836-42.

Mills, J.C., Stone, N.L., Erhardt, J., et al. (1998) Apoptotic membrane blebbing is regulated by myosin light chain phosphorylation. *J Cell Biol,* 140**,** 627-36.

Mitra, S.K., Hanson, D.A. & Schlaepfer, D.D. (2005) Focal adhesion kinase: in command and control of cell motility. *Nat Rev Mol Cell Biol,* 6**,** 56-68.

Miura, Y., Misawa, N., Maeda, N., et al. (2001) Critical contribution of tumor necrosis factor-related apoptosis-inducing ligand (TRAIL) to apoptosis of human CD4+ T cells in HIV-1-infected hu-PBL-NOD-SCID mice. *J Exp Med,* 193**,** 651-60.

Molli, P.R., Li, D.Q., Murray, B.W., et al. (2009) PAK signaling in oncogenesis. *Oncogene,* 28**,** 2545-55.

Mori, G., Brunetti, G., Colucci, S., et al. (2009) Osteoblast apoptosis in periodontal disease: role of TNF-related apoptosis-inducing ligand. *Int J Immunopathol Pharmacol,* 22**,** 95-103.

Morris, J.W., Vasuki, N.C., Baker, J.A., et al. (2003) Findings from long-term monitoring studies at MSW landfill facilities with leachate recirculation. *Waste Manag,* 23**,** 653-66.

Moss, M.L., Jin, S.L., Milla, M.E., et al. (1997) Cloning of a disintegrin metalloproteinase that processes precursor tumour-necrosis factor-alpha. *Nature,* 385**,** 733-6.

Mossberg, A.K., Wullt, B., Gustafsson, L., et al. (2007) Bladder cancers respond to intravesical instillation of HAMLET (human alpha-lactalbumin made lethal to tumor cells). *Int J Cancer,* 121**,** 1352-9.

Muhlenbeck, F., Schneider, P., Bodmer, J.L., et al. (2000) The tumor necrosis factor-related apoptosis-inducing ligand receptors TRAIL-R1 and TRAIL-R2 have distinct cross-linking requirements for initiation of apoptosis and are non-redundant in JNK activation. *J Biol Chem,* 275**,** 32208-13.

Mundt, B., Kuhnel, F., Zender, L., et al. (2003) Involvement of TRAIL and its receptors in viral hepatitis. *FASEB J,* 17**,** 94-6.

Mungre, S., Enderle, K., Turk, B., et al. (1994) Mutations which affect the inhibition of protein phosphatase 2A by simian virus 40 small-t antigen in vitro decrease viral transformation. *J Virol,* 68**,** 1675-81.

Nagaraju, K., Casciola-Rosen, L., Rosen, A., et al. (2000) The inhibition of apoptosis in myositis and in normal muscle cells. *J Immunol,* 164**,** 5459-65.

Nakajima, H., Yanase, N., Oshima, K., et al. (2003) Enhanced expression of the apoptosis inducing ligand TRAIL in mononuclear cells after myocardial infarction. *Jpn Heart J,* 44**,** 833-44.

Nakamura, H., Nagaoka, N., Hirata, A., et al. (2005) Distribution of actin filaments, non-muscle myosin, M-Ras, and extracellular signal-regulated kinase (ERK) in osteoclasts after calcitonin administration. *Arch Histol Cytol,* 68**,** 143-50.

Nam, G.H. & Choi, K.Y. (2002) Association of human tumor necrosis factor-related apoptosis inducing ligand with membrane upon acidification. *Eur J Biochem,* 269**,** 5280-7.

Naumanen, P., Lappalainen, P. & Hotulainen, P. (2008) Mechanisms of actin stress fibre assembly. *J Microsc,* 231**,** 446-54.

Nesterov, A., Ivashchenko, Y. & Kraft, A.S. (2002) Tumor necrosis factor-related apoptosis-inducing ligand (TRAIL) triggers apoptosis in normal prostate epithelial cells. *Oncogene,* 21**,** 1135-40.

Nesterov, A., Nikrad, M., Johnson, T., et al. (2004) Oncogenic Ras sensitizes normal human cells to tumor necrosis factor-alpha-related apoptosis-inducing ligand-induced apoptosis. *Cancer Res,* 64**,** 3922-7.

Newsom-Davis, T., Prieske, S. & Walczak, H. (2009) Is TRAIL the holy grail of cancer therapy? *Apoptosis,* 14**,** 607-23.

Nguyen, T., Zhang, X.D. & Hersey, P. (2001) Relative resistance of fresh isolates of melanoma to tumor necrosis factor-related apoptosis-inducing ligand (TRAIL)-induced apoptosis. *Clin Cancer Res,* 7**,** 966s-973s.

Ni, R., Tomita, Y., Matsuda, K., et al. (1994) Fas-mediated apoptosis in primary cultured mouse hepatocytes. *Exp Cell Res,* 215**,** 332-7.

Nitsch, R., Bechmann, I., Deisz, R.A., et al. (2000) Human brain-cell death induced by tumour-necrosis-factor-related apoptosis-inducing ligand (TRAIL). *Lancet,* 356**,** 827-8.

Nobes, C.D. & Hall, A. (1995) Rho, rac, and cdc42 GTPases regulate the assembly of multimolecular focal complexes associated with actin stress fibers, lamellipodia, and filopodia. *Cell,* 81**,** 53-62.

Nobes, C.D. & Hall, A. (1999) Rho GTPases control polarity, protrusion, and adhesion during cell movement. *J Cell Biol,* 144**,** 1235-44.

Noteborn, M.H. (2009) Proteins selectively killing tumor cells. *Eur J Pharmacol,* 625**,** 165-73.

Nummela, P., Yin, M., Kielosto, M., et al. (2006) Thymosin beta4 is a determinant of the transformed phenotype and invasiveness of S-adenosylmethionine decarboxylase-transfected fibroblasts. *Cancer Res,* 66**,** 701-12.

Nunbhakdi-Craig, V., Craig, L., Machleidt, T., et al. (2003) Simian virus 40 small tumor antigen induces deregulation of the actin cytoskeleton and tight junctions in kidney epithelial cells. *J Virol,* 77**,** 2807-18.

O'Reilly, L.A., Lin, T. Lee, L. (2009) Membrane-bound Fas ligand only is essential for Fas-induced apoptosis. *Nature,* 461**,** 659-663.

Oberst, A., Dillon, C.P., Weinlich, R., et al. (2011) Catalytic activity of the caspase-8-FLIP(L) complex inhibits RIPK3-dependent necrosis. *Nature,* 471**,** 363-7.

Ogasawara, J., Watanabe-Fukunaga, R., Adachi, M., et al. (1993) Lethal effect of the anti-Fas antibody in mice. *Nature,* 364**,** 806-9.

Ohtsu, M., Sakai, N., Fujita, H., et al. (1997) Inhibition of apoptosis by the actin-regulatory protein gelsolin. *EMBO J,* 16**,** 4650-6.

Okazaki, T., Pendleton, C.D., Lemonnier, F., et al. (2003) Epitope-enhanced conserved HIV-1 peptide protects HLA-A2-transgenic mice against virus expressing HIV-1 antigen. *J Immunol,* 171**,** 2548-55.

Okutani, T., Okabayashi, Y., Kido, Y., et al. (1994) Grb2/Ash binds directly to tyrosines 1068 and 1086 and indirectly to tyrosine 1148 of activated human epidermal growth factor receptors in intact cells. *J Biol Chem,* 269**,** 31310-4.

Oleinik, N.V., Krupenko, N.I. & Krupenko, S.A. (2010) ALDH1L1 inhibits cell motility via dephosphorylation of cofilin by PP1 and PP2A. *Oncogene,* 29**,** 6233-44.

Oshima, R.G. (2002) Apoptosis and keratin intermediate filaments. *Cell Death Differ,* 9**,** 486-92.

Ostap, E.M. (2008) Tropomyosins as discriminators of myosin function. *Adv Exp Med Biol,* 644**,** 273-82.

Owada, M.K., Hakura, A., Iida, K., et al. (1984) Occurrence of caldesmon (a calmodulin-binding protein) in cultured cells: comparison of normal and transformed cells. *Proc Natl Acad Sci U S A,* 81**,** 3133-7.

Ozoren, N. & El-Deiry, W.S. (2002) Defining characteristics of Types I and II apoptotic cells in response to TRAIL. *Neoplasia,* 4**,** 551-7.

Pallares, J., Llobet, D., Santacana, M., et al. (2009) CK2beta is expressed in endometrial carcinoma and has a role in apoptosis resistance and cell proliferation. *Am J Pathol,* 174**,** 287-96.

Paranjape, A.N., Mandal, T., Mukherjee, G., et al. (2012) Introduction of SV40ER and hTERT into mammospheres generates breast cancer cells with stem cell properties. *Oncogene,* 31**,** 1896-909.

Park, H.H., Lo, Y.C., Lin, S.C., et al. (2007) The death domain superfamily in intracellular signaling of apoptosis and inflammation. *Annu Rev Immunol,* 25**,** 561-86.

Park, I., Han, C., Jin, S., et al. (2011) Myosin regulatory light chains are required to maintain the stability of myosin II and cellular integrity. *Biochem J,* 434**,** 171-80.

Park, S.J., Kim, Y.Y., Lim, J.Y., et al. (2001) Opposite role of Ras in tumor necrosis factor-alpha-induced cell cycle regulation: competition for Raf kinase. *Biochem Biophys Res Commun,* 287**,** 1140-7.

Parlato, S., Giammarioli, A.M., Logozzi, M., et al. (2000) CD95 (APO-1/Fas) linkage to the actin cytoskeleton through ezrin in human T lymphocytes: a novel regulatory mechanism of the CD95 apoptotic pathway. *EMBO J,* 19**,** 5123-34.

Parsons, J.T. (2003) Focal adhesion kinase: the first ten years. *J Cell Sci,* 116**,** 1409-16.

Parsons, J.T., Horwitz, A.R. & Schwartz, M.A. (2010) Cell adhesion: integrating cytoskeletal dynamics and cellular tension. *Nat Rev Mol Cell Biol,* 11**,** 633-43.

Paul, C., Lacroix, M., Iankova, I., et al. (2006) The LIM-only protein FHL2 is a negative regulator of E4F1. *Oncogene,* 25**,** 5475-84.

Pavet, V., Beyrath, J., Pardin, C., et al. (2010) Multivalent DR5 peptides activate the TRAIL death pathway and exert tumoricidal activity. *Cancer Res,* 70**,** 1101-10.

Pavet, V., Portal, M.M., Moulin, J.C., et al. (2011) Towards novel paradigms for cancer therapy. *Oncogene,* 30**,** 1-20.

Pawlak, G. & Helfman, D.M. (2002) Post-transcriptional down-regulation of ROCKI/Rho-kinase through an MEK-dependent pathway leads to cytoskeleton disruption in Ras-transformed fibroblasts. *Mol Biol Cell,* 13**,** 336-47.

Payton, A., Holland, F., Diggle, P., et al. (2003) Cathepsin D exon 2 polymorphism associated with general intelligence in a healthy older population. *Mol Psychiatry,* 8**,** 14-8.

Peckham, M., Knight, P.J. (2009) When a predicted coiled coil is really a single a-helix, in myosins and other proteins. *Soft Matter,* 5**,** 2493–2503.

Peeper, D.S., Dannenberg, J.H., Douma, S., et al. (2001) Escape from premature senescence is not sufficient for oncogenic transformation by Ras. *Nat Cell Biol,* 3**,** 198-203.

Pelengaris, S., Khan, M. & Evan, G. (2002) c-MYC: more than just a matter of life and death. *Nat Rev Cancer,* 2**,** 764-76.

Pendleton, A. (2003) AAA releases results of first anatomy salary/faculty survey. *Anat Rec B New Anat,* 275**,** 181.

Pendleton, A., Pope, B., Weeds, A., et al. (2003) Latrunculin B or ATP depletion induces cofilin-dependent translocation of actin into nuclei of mast cells. *J Biol Chem,* 278**,** 14394-400.

Pendleton, P. & Wu, S.H. (2003) Kinetics of dodecanoic acid adsorption from caustic solution by activated carbon. *J Colloid Interface Sci,* 266**,** 245-50.

Pendleton, V., Karduck, J., Reitz, T., et al. (2003) Videoconferencing technology capabilities. Distance education support for geographically isolated EMS providers. *JEMS,* 28**,** 56-65.

Peng, D.J., Sun, J., Wang, Y.Z., et al. (2007) Inhibition of hepatocarcinoma by systemic delivery of Apoptin gene via the hepatic asialoglycoprotein receptor. *Cancer Gene Ther,* 14**,** 66-73.

Pennarun, B., Meijer, A., de Vries, E.G., et al. (2010) Playing the DISC: turning on TRAIL death receptor-mediated apoptosis in cancer. *Biochim Biophys Acta,* 1805**,** 123-40.

Perkins, D.N., Pappin, D.J., Creasy, D.M., et al. (1999) Probability-based protein identification by searching sequence databases using mass spectrometry data. *Electrophoresis,* 20**,** 3551-67.

Petrache, I., Birukov, K., Zaiman, A.L., et al. (2003) Caspase-dependent cleavage of myosin light chain kinase (MLCK) is involved in TNF-alpha-mediated bovine pulmonary endothelial cell apoptosis. *FASEB J,* 17**,** 407-16.

Petrache, I., Verin, A.D., Crow, M.T., et al. (2001) Differential effect of MLC kinase in TNF-alpha-induced endothelial cell apoptosis and barrier dysfunction. *Am J Physiol Lung Cell Mol Physiol,* 280**,** L1168-78.

Petrovas, C., Mueller, Y.M., Yang, G., et al. (2007a) Actin integrity is indispensable for CD95/Fas-induced apoptosis of HIV-specific CD8+ T cells. *Apoptosis,* 12**,** 2175-86.

Phipps, L.E., Hino, S. & Muschel, R.J. (2011) Targeting cell spreading: a method of sensitizing metastatic tumor cells to TRAIL-induced apoptosis. *Mol Cancer Res,* 9**,** 249-58.

Piazzolla, D., Meissl, K., Kucerova, L., et al. (2005) Raf-1 sets the threshold of Fas sensitivity by modulating Rok-alpha signaling. *J Cell Biol,* 171**,** 1013-22.

Pitti, R.M., Marsters, S.A., Ruppert, S., et al. (1996) Induction of apoptosis by Apo-2 ligand, a new member of the tumor necrosis factor cytokine family. *J Biol Chem,* 271**,** 12687-90.

Plummer, R., Attard, G., Pacey, S., et al. (2007) Phase 1 and pharmacokinetic study of lexatumumab in patients with advanced cancers. *Clin Cancer Res,* 13**,** 6187-94.

Porras, A., Bennett, J., Howe, A., et al. (1996) A novel simian virus 40 early-region domain mediates transactivation of the cyclin A promoter by small-t antigen and is required for transformation in small-t antigen-dependent assays. *J Virol,* 70**,** 6902-8.

Poukkula, M., Kaunisto, A., Hietakangas, V., et al. (2005) Rapid turnover of c-FLIPshort is determined by its unique C-terminal tail. *J Biol Chem,* 280**,** 27345-55.

Prasad, K.V. & Prabhakar, B.S. (2003) Apoptosis and autoimmune disorders. *Autoimmunity,* 36**,** 323-30.

Pullikuth, A., McKinnon, E., Schaeffer, H.J., et al. (2005) The MEK1 scaffolding protein MP1 regulates cell spreading by integrating PAK1 and Rho signals. *Mol Cell Biol,* 25**,** 5119-33.

Puthalakath, H., Villunger, A., O'Reilly, L.A., et al. (2001) Bmf: a proapoptotic BH3-only protein regulated by interaction with the myosin V actin motor complex, activated by anoikis. *Science,* 293**,** 1829-32.

Putz, S.M., Boehm, A.M., Stiewe, T., et al. (2012) iTRAQ analysis of a cell culture model for malignant transformation, including comparison with 2D-PAGE and SILAC. *J Proteome Res,* 11**,** 2140-53.

Putz, S.M., Vogiatzi, F., Stiewe, T., et al. (2010) Malignant transformation in a defined genetic background: proteome changes displayed by 2D-PAGE. *Mol Cancer,* 9**,** 254.

Qiagen (2001) The QIAexpressionistT - A handbook for high-level expression and purification of 6xHis-tagged proteins.

Ramamurthy, B., Yengo, C.M., Straight, A.F., et al. (2004) Kinetic mechanism of blebbistatin inhibition of nonmuscle myosin IIb. *Biochemistry,* 43**,** 14832-9.

Ramaswamy, M., Dumont, C., Cruz, A.C., et al. (2007) Cutting edge: Rac GTPases sensitize activated T cells to die via Fas. *J Immunol,* 179**,** 6384-8.

Rangarajan, A., Hong, S.J., Gifford, A., et al. (2004) Species- and cell type-specific requirements for cellular transformation. *Cancer Cell,* 6**,** 171-83.

Rasper, D.M., Vaillancourt, J.P., Hadano, S., et al. (1998) Cell death attenuation by 'Usurpin', a mammalian DED-caspase homologue that precludes caspase-8 recruitment and activation by the CD-95 (Fas, APO-1) receptor complex. *Cell Death Differ,* 5**,** 271-88.

Rathmell, J.C. (2003) Bak-/- mouse: a model for apoptosis. IN YUFANG SHI, C. J. A., SCOTT DAVID, W JIA-RUI, SHI YUN-BO (Ed.) *Molecular Mechanisms of Programmed Cell Death.* New York, Kluwer Academic/Plenum Publishers.

Ravi, R. & Bedi, A. (2002) Sensitization of tumor cells to Apo2 ligand/TRAIL-induced apoptosis by inhibition of casein kinase II. *Cancer Res,* 62**,** 4180-5.

Ren, X.D., Wang, R., Li, Q., et al. (2004a) Disruption of Rho signal transduction upon cell detachment. *J Cell Sci,* 117**,** 3511-8.

Ren, Y.G., Wagner, K.W., Knee, D.A., et al. (2004b) Differential regulation of the TRAIL death receptors DR4 and DR5 by the signal recognition particle. *Mol Biol Cell,* 15**,** 5064-74.

Rey, M., Valenzuela-Fernandez, A., Urzainqui, A., et al. (2007) Myosin IIA is involved in the endocytosis of CXCR4 induced by SDF-1alpha. *J Cell Sci,* 120**,** 1126-33.

Rey, M., Vicente-Manzanares, M., Viedma, F., et al. (2002) Cutting edge: association of the motor protein nonmuscle myosin heavy chain-IIA with the C terminus of the chemokine receptor CXCR4 in T lymphocytes. *J Immunol,* 169**,** 5410-4.

Reynaert, H. (2005) Cytoskeleton and contractile apparatus of hepatic stellate cells IN BENHAGEN, E. F. (Ed.) *Hypertension: New Research.* Nova Science Pub Inc.

Rho, S.B., Chun, T., Lee, S.H., et al. (2004) The interaction between E-tropomodulin and thymosin beta-10 rescues tumor cells from thymosin beta-10 mediated apoptosis by restoring actin architecture. *FEBS Lett,* 557**,** 57-63.

Ricci, M.S., Jin, Z., Dews, M., et al. (2004) Direct repression of FLIP expression by c-myc is a major determinant of TRAIL sensitivity. *Mol Cell Biol,* 24**,** 8541-55.

Ridley, A.J. & Hall, A. (1992) The small GTP-binding protein rho regulates the assembly of focal adhesions and actin stress fibers in response to growth factors. *Cell,* 70**,** 389-99.

Ridley, A.J., Paterson, H.F., Johnston, C.L., et al. (1992) The small GTP-binding protein rac regulates growth factor-induced membrane ruffling. *Cell,* 70**,** 401-10.

Rieger, J., Ohgaki, H., Kleihues, P., et al. (1999) Human astrocytic brain tumors express AP02L/TRAIL. *Acta Neuropathol,* 97**,** 1-4.

Ripp, S.L., Falkner, K.C., Pendleton, M.L., et al. (2003) Regulation of CYP2C11 by dehydroepiandrosterone and peroxisome proliferators: identification of the negative regulatory region of the gene. *Mol Pharmacol,* 64**,** 113-22.

Rodriguez-Paredes, M. & Esteller, M. (2011) Cancer epigenetics reaches mainstream oncology. *Nat Med,* 17**,** 330-9.

Rohn, T.T., Head, E., Nesse, W.H., et al. (2001) Activation of caspase-8 in the Alzheimer's disease brain. *Neurobiol Dis,* 8**,** 1006-16.

Rosengart, M.R., Arbabi, S., Bauer, G.J., et al. (2002) The actin cytoskeleton: an essential component for enhanced TNFalpha production by adherent monocytes. *Shock,* 17**,** 109-13.

Rossin, A., Derouet, M., Abdel-Sater, F., et al. (2009) Palmitoylation of the TRAIL receptor DR4 confers an efficient TRAIL-induced cell death signalling. *Biochem J,* 419**,** 185-92, 2 p following 192.

Roth, W. (2009) Apoptoseresistenz in malignen Tumoren. *Der Pathologe,* 30**,** 113-116.

Rottner, K. & Stradal, T.E. (2011) Actin dynamics and turnover in cell motility. *Curr Opin Cell Biol,* 23**,** 569-78.

Sahai, E. & Marshall, C.J. (2003) Differing modes of tumour cell invasion have distinct requirements for Rho/ROCK signalling and extracellular proteolysis. *Nat Cell Biol,* 5**,** 711-9.

Saitoh, M., Ishikawa, T., Matsushima, S., et al. (1987) Selective inhibition of catalytic activity of smooth muscle myosin light chain kinase. *J Biol Chem,* 262**,** 7796-801.

Saitoh, T., Takemura, S., Ueda, K., et al. (2001) Differential localization of non-muscle myosin II isoforms and phosphorylated regulatory light chains in human MRC-5 fibroblasts. *FEBS Lett,* 509**,** 365-9.

Sanchez Mejia, R.O., Friedlander, R.M. (2001) Caspases in Huntington's disease. *Neuroscientist,* 7**,** 480-489.

Sanders, L.C., Matsumura, F., Bokoch, G.M., et al. (1999) Inhibition of myosin light chain kinase by p21-activated kinase. *Science,* 283**,** 2083-5.

Sandquist, J.C. & Means, A.R. (2008) The C-terminal tail region of nonmuscle myosin II directs isoform-specific distribution in migrating cells. *Mol Biol Cell,* 19**,** 5156-67.

Sato, K., Hida, S., Takayanagi, H., et al. (2001) Antiviral response by natural killer cells through TRAIL gene induction by IFN-alpha/beta. *Eur J Immunol,* 31**,** 3138-46.

Savill, J. & Fadok, V. (2000) Corpse clearance defines the meaning of cell death. *Nature,* 407**,** 784-8.

Scaffidi, C., Fulda, S., Srinivasan, A., et al. (1998) Two CD95 (APO-1/Fas) signaling pathways. *EMBO J,* 17**,** 1675-87.

Scaffidi, C., Schmitz, I., Krammer, P.H., et al. (1999) The role of c-FLIP in modulation of CD95-induced apoptosis. *J Biol Chem,* 274**,** 1541-8.

Schleich, K., Warnken, U., Fricker, N., et al. (2012) Stoichiometry of the CD95 Death-Inducing Signaling Complex: Experimental and Modeling Evidence for a Death Effector Domain Chain Model. *Mol Cell,* 47**,** 306-19.

Schneider, P., Holler, N., Bodmer, J.L., et al. (1998) Conversion of membrane-bound Fas(CD95) ligand to its soluble form is associated with downregulation of its proapoptotic activity and loss of liver toxicity. *J Exp Med,* 187**,** 1205-13.

Schneider, P., Thome, M., Burns, K., et al. (1997) TRAIL receptors 1 (DR4) and 2 (DR5) signal FADD-dependent apoptosis and activate NF-kappaB. *Immunity,* 7**,** 831-6.

Schneider, P. & Tschopp, J. (2000) Apoptosis induced by death receptors. *Pharm Acta Helv,* 74**,** 281-6.

Schneider-Brachert, W., Tchikov, V., Neumeyer, J., et al. (2004) Compartmentalization of TNF receptor 1 signaling: internalized TNF receptosomes as death signaling vesicles. *Immunity,* 21**,** 415-28.

Schoenwaelder, S.M. & Burridge, K. (1999) Bidirectional signaling between the cytoskeleton and integrins. *Curr Opin Cell Biol,* 11**,** 274-86.

Scholey, J.M., Taylor, K.A. & Kendrick-Jones, J. (1980) Regulation of non-muscle myosin assembly by calmodulin-dependent light chain kinase. *Nature,* 287**,** 233-5.

Scott, F.L., Stec, B., Pop, C., et al. (2009) The Fas-FADD death domain complex structure unravels signalling by receptor clustering. *Nature,* 457**,** 1019-22.

Sebbagh, M., Renvoize, C., Hamelin, J., et al. (2001) Caspase-3-mediated cleavage of ROCK I induces MLC phosphorylation and apoptotic membrane blebbing. *Nat Cell Biol,* 3**,** 346-52.

Secchiero, P., Gonelli, A., Carnevale, E., et al. (2004b) Evidence for a proangiogenic activity of TNF-related apoptosis-inducing ligand. *Neoplasia,* 6**,** 364-73.

Secchiero, P., Gonelli, A., Carnevale, E., et al. (2003) TRAIL promotes the survival and proliferation of primary human vascular endothelial cells by activating the Akt and ERK pathways. *Circulation,* 107**,** 2250-6.

Secchiero, P., Zerbinati, C., Rimondi, E., et al. (2004a) TRAIL promotes the survival, migration and proliferation of vascular smooth muscle cells. *Cell Mol Life Sci,* 61**,** 1965-74.

Sedger, L.M., Glaccum, M.B., Schuh, J.C., et al. (2002) Characterization of the in vivo function of TNF-alpha-related apoptosis-inducing ligand, TRAIL/Apo2L, using TRAIL/Apo2L gene-deficient mice. *Eur J Immunol,* 32**,** 2246-54.

Seki, N., Hayakawa, Y., Brooks, A.D., et al. (2003) Tumor necrosis factor-related apoptosis-inducing ligand-mediated apoptosis is an important endogenous mechanism for resistance to liver metastases in murine renal cancer. *Cancer Res,* 63**,** 207-13.

Sellers, J.R. (2000) Myosins: a diverse superfamily. *Biochim Biophys Acta,* 1496**,** 3-22.

Seol, D.W. & Billiar, T.R. (1999) A caspase-9 variant missing the catalytic site is an endogenous inhibitor of apoptosis. *J Biol Chem,* 274**,** 2072-6.

Serrano, M., Lin, A.W., McCurrach, M.E., et al. (1997) Oncogenic ras provokes premature cell senescence associated with accumulation of p53 and p16INK4a. *Cell,* 88**,** 593-602.

Shain, K.H., Landowski, T.H. & Dalton, W.S. (2002) Adhesion-mediated intracellular redistribution of c-Fas-associated death domain-like IL-1-converting enzyme-like inhibitory protein-long confers resistance to CD95-induced apoptosis in hematopoietic cancer cell lines. *J Immunol,* 168**,** 2544-53.

Sharma, P., Wagner, K., Wolchok, J.D., et al. (2011) Novel cancer immunotherapy agents with survival benefit: recent successes and next steps. *Nat Rev Cancer,* 11**,** 805-12.

Sharp, D.A., Lawrence, D.A. & Ashkenazi, A. (2005) Selective knockdown of the long variant of cellular FLICE inhibitory protein augments death receptor-mediated caspase-8 activation and apoptosis. *J Biol Chem,* 280**,** 19401-9.

Shawver, L.K., Slamon, D. & Ullrich, A. (2002) Smart drugs: tyrosine kinase inhibitors in cancer therapy. *Cancer Cell,* 1**,** 117-23.

Sheetz, M.P., Sable, J.E. & Dobereiner, H.G. (2006) Continuous membrane-cytoskeleton adhesion requires continuous accommodation to lipid and cytoskeleton dynamics. *Annu Rev Biophys Biomol Struct,* 35**,** 417-34.

Shepard, B.D. & Badley, A.D. (2009) The Biology of TRAIL and the Role of TRAIL-Based Therapeutics in Infectious Diseases. *Antiinfect Agents Med Chem,* 8**,** 87-101.

Shetty, S., Graham, B.A., Brown, J.G., et al. (2005) Transcription factor NF-kappaB differentially regulates death receptor 5 expression involving histone deacetylase 1. *Mol Cell Biol,* 25**,** 5404-16.

Shi, Y., Glynn, J.M., Guilbert, L.J., et al. (1992) Role for c-myc in activation-induced apoptotic cell death in T cell hybridomas. *Science,* 257**,** 212-4.

Shin, S., Lee, Y., Kim, W., et al. (2005) Caspase-2 primes cancer cells for TRAIL-mediated apoptosis by processing procaspase-8. *EMBO J,* 24**,** 3532-42.

Shirley, S., Morizot, A. & Micheau, O. (2011) Regulating TRAIL receptor-induced cell death at the membrane : a deadly discussion. *Recent Pat Anticancer Drug Discov,* 6**,** 311-23.

Siegel, R.M., Frederiksen, J.K., Zacharias, D.A., et al. (2000) Fas preassociation required for apoptosis signaling and dominant inhibition by pathogenic mutations. *Science,* 288**,** 2354-7.

Simon, A.K., Williams, O., Mongkolsapaya, J., et al. (2001) Tumor necrosis factor-related apoptosis-inducing ligand in T cell development: sensitivity of human thymocytes. *Proc Natl Acad Sci U S A,* 98**,** 5158-63.

Simpson, D.R., Yu, M., Zheng, S., et al. (2011) Epithelial cell organization suppresses Myc function by attenuating Myc expression. *Cancer Res,* 71**,** 3822-30.

Slee, E.A., Keogh, S.A. & Martin, S.J. (2000) Cleavage of BID during cytotoxic drug and UV radiation-induced apoptosis occurs downstream of the point of Bcl-2 action and is catalysed by caspase-3: a potential feedback loop for amplification of apoptosis-associated mitochondrial cytochrome c release. *Cell Death Differ,* 7**,** 556-65.

Smolewski, P. & Robak, T. (2011) Inhibitors of apoptosis proteins (IAPs) as potential molecular targets for therapy of hematological malignancies. *Curr Mol Med,* 11**,** 633-49.

Somlyo, A.P. & Somlyo, A.V. (2003) Ca2+ sensitivity of smooth muscle and nonmuscle myosin II: modulated by G proteins, kinases, and myosin phosphatase. *Physiol Rev,* 83**,** 1325-58.

Song, J.H., Tse, M.C., Bellail, A., et al. (2007) Lipid rafts and nonrafts mediate tumor necrosis factor related apoptosis-inducing ligand induced apoptotic and nonapoptotic signals in non small cell lung carcinoma cells. *Cancer Res,* 67**,** 6946-55.

Sontag, J.M. & Sontag, E. (2006) Regulation of cell adhesion by PP2A and SV40 small tumor antigen: an important link to cell transformation. *Cell Mol Life Sci,* 63**,** 2979-91.

Soria, J.C., Mark, Z., Zatloukal, P., et al. (2011) Randomized phase II study of dulanermin in combination with paclitaxel, carboplatin, and bevacizumab in advanced non-small-cell lung cancer. *J Clin Oncol,* 29**,** 4442-51.

Soria, J.C., Smit, E., Khayat, D., et al. (2010) Phase 1b study of dulanermin (recombinant human Apo2L/TRAIL) in combination with paclitaxel, carboplatin, and bevacizumab in patients with advanced non-squamous non-small-cell lung cancer. *J Clin Oncol,* 28**,** 1527-33.

Spiering, D. & Hodgson, L. (2011) Dynamics of the Rho-family small GTPases in actin regulation and motility. *Cell Adh Migr,* 5**,** 170-80.

Sprick, M.R., Rieser, E., Stahl, H., et al. (2002) Caspase-10 is recruited to and activated at the native TRAIL and CD95 death-inducing signalling complexes in a FADD-dependent manner but can not functionally substitute caspase-8. *EMBO J,* 21**,** 4520-30.

Sribenja, S., Li, M., Wongkham, S., et al. (2009) Advances in thymosin beta10 research: differential expression, molecular mechanisms, and clinical implications in cancer and other conditions. *Cancer Invest,* 27**,** 1016-22.

Steele, L.P., Georgopoulos, N.T., Southgate, J., et al. (2006) Differential susceptibility to TRAIL of normal versus malignant human urothelial cells. *Cell Death Differ,* 13**,** 1564-76.

Steelman, L.S., Franklin, R.A., Abrams, S.L., et al. (2011) Roles of the Ras/Raf/MEK/ERK pathway in leukemia therapy. *Leukemia,* 25**,** 1080-94.

Stow, J.L., Fath, K.R. & Burgess, D.R. (1998) Budding roles for myosin II on the Golgi. *Trends Cell Biol,* 8**,** 138-41.

Stuelsatz, P., Pouzoulet, F., Lamarre, Y., et al. (2010) Down-regulation of MyoD by calpain 3 promotes generation of reserve cells in C2C12 myoblasts. *J Biol Chem,* 285**,** 12670-83.

Sun, J., Yan, Y., Wang, X.T., et al. (2009) PTD4-apoptin protein therapy inhibits tumor growth in vivo. *Int J Cancer,* 124**,** 2973-81.

Suria, H., Chau, L.A., Negrou, E., et al. (1999) Cytoskeletal disruption induces T cell apoptosis by a caspase-3 mediated mechanism. *Life Sci,* 65**,** 2697-707.

Suzuki, Y., Imai, Y., Nakayama, H., et al. (2001) A serine protease, HtrA2, is released from the mitochondria and interacts with XIAP, inducing cell death. *Mol Cell,* 8**,** 613-21.

Suzuki, Y., Yamamoto, M., Wada, H., et al. (1999) Agonist-induced regulation of myosin phosphatase activity in human platelets through activation of Rho-kinase. *Blood,* 93**,** 3408-17.

Swailes, N.T., Colegrave, M., Knight, P.J., et al. (2006) Non-muscle myosins 2A and 2B drive changes in cell morphology that occur as myoblasts align and fuse. *J Cell Sci,* 119**,** 3561-70.

Takeda, K., Hayakawa, Y., Smyth, M.J., et al. (2001) Involvement of tumor necrosis factor-related apoptosis-inducing ligand in surveillance of tumor metastasis by liver natural killer cells. *Nat Med,* 7**,** 94-100.

Takeda, K., Smyth, M.J., Cretney, E., et al. (2002) Critical role for tumor necrosis factor-related apoptosis-inducing ligand in immune surveillance against tumor development. *J Exp Med,* 195**,** 161-9.

Takimoto, R. & El-Deiry, W.S. (2000) Wild-type p53 transactivates the KILLER/DR5 gene through an intronic sequence-specific DNA-binding site. *Oncogene,* 19**,** 1735-43.

Tan, I., Yong, J., Dong, J.M., et al. (2008) A tripartite complex containing MRCK modulates lamellar actomyosin retrograde flow. *Cell,* 135**,** 123-36.

Tanaka, S.S., Togooka, Y., Sato, H., et al. (1998) Expression and localization of membrane type matrix metalloproteinase-1 (MT1-MMP) in trophoblast cells of cultured mouse blastocysts and ectoplacental cones. *Placenta,* 19**,** 41-8.

Tang, Z., Bauer, J.A., Morrison, B., et al. (2006) Nitrosylcobalamin promotes cell death via S nitrosylation of Apo2L/TRAIL receptor DR4. *Mol Cell Biol,* 26**,** 5588-94.

Taylor, M.P., Koyuncu, O.O. & Enquist, L.W. (2011) Subversion of the actin cytoskeleton during viral infection. *Nat Rev Microbiol,* 9**,** 427-39.

Tecchio, C., Huber, V., Scapini, P., et al. (2004) IFNalpha-stimulated neutrophils and monocytes release a soluble form of TNF-related apoptosis-inducing ligand (TRAIL/Apo-2 ligand) displaying apoptotic activity on leukemic cells. *Blood,* 103**,** 3837-44.

Thomas, L.R., Henson, A., Reed, J.C., et al. (2004) Direct binding of Fas-associated death domain (FADD) to the tumor necrosis factor-related apoptosis-inducing ligand receptor DR5 is regulated by the death effector domain of FADD. *J Biol Chem,* 279**,** 32780-5.

Timmermann, M., Buck, F., Sorg, C., et al. (2004) Interaction of soluble CD163 with activated T lymphocytes involves its association with non-muscle myosin heavy chain type A. *Immunol Cell Biol,* 82**,** 479-87.

Todaro, M., Lombardo, Y., Francipane, M.G., et al. (2008) Apoptosis resistance in epithelial tumors is mediated by tumor-cell-derived interleukin-4. *Cell Death Differ,* 15**,** 762-72.

Tolcher, A.W., Mita, M., Meropol, N.J., et al. (2007) Phase I pharmacokinetic and biologic correlative study of mapatumumab, a fully human monoclonal antibody with agonist activity to tumor necrosis factor-related apoptosis-inducing ligand receptor-1. *J Clin Oncol,* 25**,** 1390-5.

Trabzuni, D., Famulski, K.S. & Ahmad, M. (2000) Functional analysis of tumour necrosis factor-alpha-related apoptosis-inducing ligand (TRAIL): cysteine-230 plays a critical role in the homotrimerization and biological activity of this novel tumoricidal cytokine. *Biochem J,* 350 Pt 2**,** 505-10.

Trarbach, T., Moehler, M., Heinemann, V., et al. (2010) Phase II trial of mapatumumab, a fully human agonistic monoclonal antibody that targets and activates the tumour necrosis factor apoptosis-inducing ligand receptor-1 (TRAIL-R1), in patients with refractory colorectal cancer. *Br J Cancer,* 102**,** 506-12.

Trinkaus, J.P. (1973) Modes of cell locomotion in vivo. *Ciba Found Symp,* 14**,** 233-49.

Truneh, A., Sharma, S., Silverman, C., et al. (2000) Temperature-sensitive differential affinity of TRAIL for its receptors. DR5 is the highest affinity receptor. *J Biol Chem,* 275**,** 23319-25.

Tse, W.T., Pendleton, J.D., Beyer, W.M., et al. (2003) Suppression of allogeneic T-cell proliferation by human marrow stromal cells: implications in transplantation. *Transplantation,* 75**,** 389-97.

Uberti, D., Cantarella, G., Facchetti, F., et al. (2004) TRAIL is expressed in the brain cells of Alzheimer's disease patients. *Neuroreport,* 15**,** 579-81.

Uchimura, T., Fumoto, K., Yamamoto, Y., et al. (2002) Spatial localization of mono-and diphosphorylated myosin II regulatory light chain at the leading edge of motile HeLa cells. *Cell Struct Funct,* 27**,** 479-86.

Ueda, H., Morishita, R., Itoh, H., et al. (2001) Galpha11 induces caspase-mediated proteolytic activation of Rho-associated kinase, ROCK-I, in HeLa cells. *J Biol Chem,* 276**,** 42527-33.

Ueda, K., Murata-Hori, M., Tatsuka, M., et al. (2002) Rho-kinase contributes to diphosphorylation of myosin II regulatory light chain in nonmuscle cells. *Oncogene,* 21**,** 5852-60.

Utsumi, T., Sakurai, N., Nakano, K., et al. (2003) C-terminal 15 kDa fragment of cytoskeletal actin is posttranslationally N-myristoylated upon caspase-mediated cleavage and targeted to mitochondria. *FEBS Lett,* 539**,** 37-44.

Van Damme, P., Martens, L., Van Damme, J., et al. (2005) Caspase-specific and nonspecific in vivo protein processing during Fas-induced apoptosis. *Nat Methods,* 2**,** 771-7.

van Leeuwen, H., Elliott, G. & O'Hare, P. (2002) Evidence of a role for nonmuscle myosin II in herpes simplex virus type 1 egress. *J Virol,* 76**,** 3471-81.

Varfolomeev, E., Alicke, B., Elliott, J.M., et al. (2009) X chromosome-linked inhibitor of apoptosis regulates cell death induction by proapoptotic receptor agonists. *J Biol Chem,* 284**,** 34553-60.

Varfolomeev, E., Maecker, H., Sharp, D., et al. (2005) Molecular determinants of kinase pathway activation by Apo2 ligand/tumor necrosis factor-related apoptosis-inducing ligand. *J Biol Chem,* 280**,** 40599-608.

Verhagen, A.M., Ekert, P.G., Pakusch, M., et al. (2000) Identification of DIABLO, a mammalian protein that promotes apoptosis by binding to and antagonizing IAP proteins. *Cell,* 102**,** 43-53.

Vicente-Manzanares, M., Webb, D.J. & Horwitz, A.R. (2005) Cell migration at a glance. *J Cell Sci,* 118**,** 4917-9.

Vicente-Manzanares, M., Koach, M.A., Whitmore, L., et al. (2008) Segregation and activation of myosin IIB creates a rear in migrating cells. *J Cell Biol,* 183**,** 543-54.

Vicente-Manzanares, M., Ma, X., Adelstein, R.S., et al. (2009) Non-muscle myosin II takes centre stage in cell adhesion and migration. *Nat Rev Mol Cell Biol,* 10**,** 778-90.

Vigneswaran, N., Wu, J., Nagaraj, N., et al. (2005) Differential susceptibility of metastatic and primary oral cancer cells to TRAIL-induced apoptosis. *Int J Oncol,* 26**,** 103-12.

Vilas, G.L., Corvi, M.M., Plummer, G.J., et al. (2006) Posttranslational myristoylation of caspase-activated p21-activated protein kinase 2 (PAK2) potentiates late apoptotic events. *Proc Natl Acad Sci U S A,* 103**,** 6542-7.

Virshup, D.M. & Shenolikar, S. (2009) From promiscuity to precision: protein phosphatases get a makeover. *Mol Cell,* 33**,** 537-45.

Vomastek, T., Iwanicki, M.P., Schaeffer, H.J., et al. (2007) RACK1 targets the extracellular signal-regulated kinase/mitogen-activated protein kinase pathway to link integrin engagement with focal adhesion disassembly and cell motility. *Mol Cell Biol,* 27**,** 8296-305.

Wagner, K.W., Punnoose, E.A., Januario, T., et al. (2007) Death-receptor O-glycosylation controls tumor-cell sensitivity to the proapoptotic ligand Apo2L/TRAIL. *Nat Med,* 13**,** 1070-7.

Wajant, H., Moosmayer, D., Wuest, T., et al. (2001) Differential activation of TRAIL-R1 and -2 by soluble and membrane TRAIL allows selective surface antigen-directed activation of TRAIL-R2 by a soluble TRAIL derivative. *Oncogene,* 20**,** 4101-6.

Walczak, H., Haas T.L. (2008) Biochemical analysis of the native TRAIL Death-Inducing Signaling Complex. IN MOR, G., ALVERO, A.B. (Ed.) *Apoptosis and Cancer - Methods in Molecular Biology.* Totowa, New Jersey, Humana Press.

Walczak, H., Miller, R.E., Ariail, K., et al. (1999) Tumoricidal activity of tumor necrosis factor-related apoptosis-inducing ligand in vivo. *Nat Med,* 5**,** 157-63.

Wandinger, K.P., Lunemann, J.D., Wengert, O., et al. (2003) TNF-related apoptosis inducing ligand (TRAIL) as a potential response marker for interferon-beta treatment in multiple sclerosis. *Lancet,* 361**,** 2036-43.

Wang, C.L. (2008) Caldesmon and the regulation of cytoskeletal functions. *Adv Exp Med Biol,* 644**,** 250-72.

Wang, C.L., Wang, L.W., Xu, S.A., et al. (1991) Localization of the calmodulin- and the actin-binding sites of caldesmon. *J Biol Chem,* 266**,** 9166-72.

Wang, F., Graham, W.V., Wang, Y., et al. (2005b) Interferon-gamma and tumor necrosis factor-alpha synergize to induce intestinal epithelial barrier dysfunction by up-regulating myosin light chain kinase expression. *Am J Pathol,* 166**,** 409-19.

Wang, G., Ahmad, K.A. & Ahmed, K. (2006) Role of protein kinase CK2 in the regulation of tumor necrosis factor-related apoptosis inducing ligand-induced apoptosis in prostate cancer cells. *Cancer Res,* 66**,** 2242-9.

Wang, J., Chun, H.J., Wong, W., et al. (2001) Caspase-10 is an initiator caspase in death receptor signaling. *Proc Natl Acad Sci U S A,* 98**,** 13884-8.

Wang, N., Tytell, J.D. & Ingber, D.E. (2009) Mechanotransduction at a distance: mechanically coupling the extracellular matrix with the nucleus. *Nat Rev Mol Cell Biol,* 10**,** 75-82.

Wang, S. & El-Deiry, W.S. (2003) TRAIL and apoptosis induction by TNF-family death receptors. *Oncogene,* 22**,** 8628-33.

Wang, Y., Engels, I.H., Knee, D.A., et al. (2004) Synthetic lethal targeting of MYC by activation of the DR5 death receptor pathway. *Cancer Cell,* 5**,** 501-12.

Wang, Y., Quon, K.C., Knee, D.A., et al. (2005) RAS, MYC, and sensitivity to tumor necrosis factor-alpha-related apoptosis-inducing ligand-induced apoptosis. *Cancer Res,* 65**,** 1615-6; author reply 1616-7.

Wang, Z., Yang, Z.Q. & Chacko, S. (1997) Functional and structural relationship between the calmodulin-binding, actin-binding, and actomyosin-ATPase inhibitory domains on the C terminus of smooth muscle caldesmon. *J Biol Chem,* 272**,** 16896-903.

Ware, C.F. (2003) The TNF superfamily. *Cytokine Growth Factor Rev,* 14**,** 181-4.
Washburn, M.P., Wolters, D. & Yates, J.R., 3rd (2001) Large-scale analysis of the yeast proteome by multidimensional protein identification technology. *Nat Biotechnol,* 19**,** 242-7.
Watanabe, T., Hosoya, H. & Yonemura, S. (2007) Regulation of myosin II dynamics by phosphorylation and dephosphorylation of its light chain in epithelial cells. *Mol Biol Cell,* 18**,** 605-16.
Webb, D.J., Donais, K., Whitmore, L.A., et al. (2004) FAK-Src signalling through paxillin, ERK and MLCK regulates adhesion disassembly. *Nat Cell Biol,* 6**,** 154-61.
Weber, K., Lazarides, E., Goldman, R.D. (1974) Localization and Distribution of Actin Fibers in Normal, Transformed and Revertant Cells. *Cold Spring Harbor Symposia on Quantitative Biology,* 39**,** 363-369.
Wei, Q. & Adelstein, R.S. (2000) Conditional expression of a truncated fragment of nonmuscle myosin II-A alters cell shape but not cytokinesis in HeLa cells. *Mol Biol Cell,* 11**,** 3617-27.
Wei, W., Wang, D., Shi, J., et al. (2010) Tumor necrosis factor (TNF)-related apoptosis-inducing ligand (TRAIL) induces chemotactic migration of monocytes via a death receptor 4-mediated RhoGTPase pathway. *Mol Immunol,* 47**,** 2475-84.
Weinlich, R., Brunner, T. & Amarante-Mendes, G.P. (2010) Control of death receptor ligand activity by posttranslational modifications. *Cell Mol Life Sci,* 67**,** 1631-42.
Westermarck, J. & Hahn, W.C. (2008) Multiple pathways regulated by the tumor suppressor PP2A in transformation. *Trends Mol Med,* 14**,** 152-60.
White, S.R., Williams, P., Wojcik, K.R., et al. (2001) Initiation of apoptosis by actin cytoskeletal derangement in human airway epithelial cells. *Am J Respir Cell Mol Biol,* 24**,** 282-94.
White-Gilbertson, S., Rubinchik, S. & Voelkel-Johnson, C. (2008) Transformation, translation and TRAIL: an unexpected intersection. *Cytokine Growth Factor Rev,* 19**,** 167-72.
Wiens, G.D. & Glenney, G.W. (2011) Origin and evolution of TNF and TNF receptor superfamilies. *Dev Comp Immunol,* 35**,** 1324-35.
Wiley, S.R., Schooley, K., Smolak, P.J., et al. (1995) Identification and characterization of a new member of the TNF family that induces apoptosis. *Immunity,* 3**,** 673-82.
Williams, C.J., Pendleton, A., Bonavita, G., et al. (2003) Mutations in the amino terminus of ANKH in two US families with calcium pyrophosphate dihydrate crystal deposition disease. *Arthritis Rheum,* 48**,** 2627-31.
Wu, G.S., Burns, T.F., Zhan, Y., et al. (1999) Molecular cloning and functional analysis of the mouse homologue of the KILLER/DR5 tumor necrosis factor-related apoptosis-inducing ligand (TRAIL) death receptor. *Cancer Res,* 59**,** 2770-5.
Wu, H., Lo, Y.C. (2009) *Structures, Domains and Functions in Cell Death (DD, DED, CARD, PYD),* Chichester, John Wiley & Sons.
Wu, X., Ahn, E.Y., McKenna, M.A., et al. (2005) Fas binding to calmodulin regulates apoptosis in osteoclasts. *J Biol Chem,* 280**,** 29964-70.
Wuchter, C., Krappmann, D., Cai, Z., et al. (2001) In vitro susceptibility to TRAIL-induced apoptosis of acute leukemia cells in the context of TRAIL receptor gene expression and constitutive NF-kappa B activity. *Leukemia,* 15**,** 921-8.
Yamaguchi, H. & Wang, H.G. (2004) CHOP is involved in endoplasmic reticulum stress-induced apoptosis by enhancing DR5 expression in human carcinoma cells. *J Biol Chem,* 279**,** 45495-502.

Yamashiro, S., Totsukawa, G., Yamakita, Y., et al. (2003) Citron kinase, a Rho-dependent kinase, induces di-phosphorylation of regulatory light chain of myosin II. *Mol Biol Cell,* 14**,** 1745-56.

Yang, L., Cao, Z., Yan, H., et al. (2003) Coexistence of high levels of apoptotic signaling and inhibitor of apoptosis proteins in human tumor cells: implication for cancer specific therapy. *Cancer Res,* 63**,** 6815-24.

Yeh, E., Cunningham, M., Arnold, H., et al. (2004) A signalling pathway controlling c-Myc degradation that impacts oncogenic transformation of human cells. *Nat Cell Biol,* 6**,** 308-18.

Yeh, W.C., Itie, A., Elia, A.J., et al. (2000) Requirement for Casper (c-FLIP) in regulation of death receptor-induced apoptosis and embryonic development. *Immunity,* 12**,** 633-42.

Yerbes, R., Palacios, C. & Lopez-Rivas, A. (2011) The therapeutic potential of TRAIL receptor signalling in cancer cells. *Clin Transl Oncol,* 13**,** 839-47.

Yin, X.M., Wang, K., Gross, A., et al. (1999) Bid-deficient mice are resistant to Fas-induced hepatocellular apoptosis. *Nature,* 400**,** 886-91.

Yoder, A., Yu, D., Dong, L., et al. (2008) HIV envelope-CXCR4 signaling activates cofilin to overcome cortical actin restriction in resting CD4 T cells. *Cell,* 134**,** 782-92.

Yokoyama, T., Arai, M., Sekiguchi, K., et al. (1999) Tumor necrosis factor-alpha decreases the phosphorylation levels of phospholamban and troponin I in spontaneously beating rat neonatal cardiac myocytes. *J Mol Cell Cardiol,* 31**,** 261-73.

Yoshida, T., Shiraishi, T., Nakata, S., et al. (2005) Proteasome inhibitor MG132 induces death receptor 5 through CCAAT/enhancer-binding protein homologous protein. *Cancer Res,* 65**,** 5662-7.

Yu, J., Boyapati, A. & Rundell, K. (2001) Critical role for SV40 small-t antigen in human cell transformation. *Virology,* 290**,** 192-8.

Yu, J., Boyapati, A. & Rundell, K. (2001) Critical role for SV40 small-t antigen in human cell transformation. *Virology,* 290**,** 192-8.

Yue, H.H., Diehl, G.E. & Winoto, A. (2005) Loss of TRAIL-R does not affect thymic or intestinal tumor development in p53 and adenomatous polyposis coli mutant mice. *Cell Death Differ,* 12**,** 94-7.

Zerafa, N., Westwood, J.A., Cretney, E., et al. (2005) Cutting edge: TRAIL deficiency accelerates hematological malignancies. *J Immunol,* 175**,** 5586-90.

Zhang, C., Ao, Z., Seth, A., et al. (1996) A mitochondrial membrane protein defined by a novel monoclonal antibody is preferentially detected in apoptotic cells. *J Immunol,* 157**,** 3980-7.

Zhang, C., Zhang, J., Niu, J., et al. (2008) Interleukin-12 improves cytotoxicity of natural killer cells via upregulated expression of NKG2D. *Hum Immunol,* 69**,** 490-500.

Zhang, D.W., Shao, J., Lin, J., et al. (2009) RIP3, an energy metabolism regulator that switches TNF-induced cell death from apoptosis to necrosis. *Science,* 325**,** 332-6.

Zhang, H., Landmann, F., Zahreddine, H., et al. (2011) A tension-induced mechanotransduction pathway promotes epithelial morphogenesis. *Nature,* 471**,** 99-103.

Zhang, L., Ren, X., Alt, E., et al. (2010) Chemoprevention of colorectal cancer by targeting APC-deficient cells for apoptosis. *Nature,* 464**,** 1058-61.

Zhang, M., Li, X., Pang, X., et al. (2001) Identification of a potential HIV-induced source of bystander-mediated apoptosis in T cells: upregulation of trail in primary human macrophages by HIV-1 tat. *J Biomed Sci,* 8**,** 290-6.

Zhang, Y. & Zhang, B. (2008) TRAIL resistance of breast cancer cells is associated with constitutive endocytosis of death receptors 4 and 5. *Mol Cancer Res,* 6**,** 1861-71.

Zhao, S., Asgary, Z., Wang, Y., et al. (1999) Functional expression of TRAIL by lymphoid and myeloid tumour cells. *Br J Haematol,* 106**,** 827-32.

Zhong, C., Kinch, M.S. & Burridge, K. (1997) Rho-stimulated contractility contributes to the fibroblastic phenotype of Ras-transformed epithelial cells. *Mol Biol Cell,* 8**,** 2329-44.

Zhou, L., Yan, C., Gieling, R.G., et al. (2009) Tumor necrosis factor-alpha induced expression of matrix metalloproteinase-9 through p21-activated kinase-1. *BMC Immunol,* 10**,** 15.

UNIVERSITÉ DE STRASBOURG

Cathrin SCHULZ

Ecole Doctorale des Sciences de la Vie et de la Santé STRASBOURG

Tumour-Selective Apoptosis
Identification of NMHCIIa as Novel Death Receptor Interactor
Regulating the Response to TRAIL

Résumé

La cytokine TRAIL est un candidat anticancéreux qui induit la mort spécifique de cellules tumorales. La liaison de TRAIL à ses récepteurs (DR) permet de former le complexe DISC qui induit la mort cellulaire. La raison de la mort sélective des cellules tumorales induite par TRAIL est inconnue. Nous avons découvert des partenaires de DR: chaînes lourdes de myosine IIa, IIb (NMHCIIa, NMHCIIb), chaîne légère régulatrice de myosine (MLC2) et ß-actine. Dans les cellules tumorales, la liaison de TRAIL abroge l'interaction NMHCII/DR, et DISC est activé. Au contraire, dans les cellules normales, l'interaction NMHCII/DR persiste et l'activation de DISC est incomplète. Affaiblir l'interaction NMHCII/DR par des inhibiteurs chimiques ou diminuer NMHCIIa permet d'augmenter l'apoptose liée à TRAIL. L'interaction réduite NMHCII/DR induit des niveaux altérés de phospho-MLC2 et de kinases régulant MLC2. Nous proposons que la résistance de cellules normales à TRAIL soit basée sur l'interaction DR/cytosquelette, déficiente dans des tumeurs. NMHCII étant aussi impliqué dans l'adhésion/migration cellulaire, il serait intéressant d'étudier les fonctions de NMHCII/DISC dans le détachement cellulaire, afin de mieux comprendre la résistance à TRAIL de certains cancers.

mots-clés: TRAIL, DISC, cellules normales, apoptose, spécifique de tumeur, cytosquelette, non-muscle myosin heavy chain IIa, NMHCIIa

Abstract

The cytokine TRAIL is a promising cancer therapeutic candidate as it induces apoptosis selectively in transformed cells. TRAIL-induced clustering of its receptors (DR) is essential for the formation of the DISC complex, which induces cell death. The mechanism for TRAIL's tumour selective effect is largely unknown. We identified the cytoskeleton proteins non-muscle myosin heavy chain IIa, IIb (NMHCIIa, NMHCIIb), myosin regulatory light chain (MLC2) and ß-actin as novel DR-interactors. An initially weak and TRAIL-induced abrogation of NMHCII/DR interaction correlated with efficient DISC formation in tumour cells. In contrast, a robust NMHCII/DR interaction that was sustained upon TRAIL stimulus was accompanied by incomplete DISC arrangement. Weakening the NMHCII/DR interaction in normal cells using chemical inhibitors enhanced TRAIL-induced apoptosis. Intriguingly, siRNA-mediated NMHCIIa- but not NMHCIIb depletion potently released the TRAIL resistance block in normal cells and influenced DISC composition. Reduced NMHCII/DR interaction in transformed cells was characterised by diminished MLC2 phosphorylation levels and altered protein expression levels of upstream regulatory kinases. Our results suggest that normal cell resistance to TRAIL-apoptosis is based on the interaction of cytoskeleton components with the DR that is impaired upon transformation. Since NMHCII function in cell adhesion and migration, it will be interesting to study possible roles of the NMHCII/DISC interaction in cell detachment in addition to modulating TRAIL sensitivity; moreover this link may provide clues as to the cause of TRAIL resistance in some cancers.

keywords: TRAIL, DISC, normal cells, apoptosis, tumour-selective, cytoskeleton, non-muscle myosin heavy chain IIa, NMHCIIa